UNIVERSITY OF BIRMINGHAM

THE ROLE OF NEUTROPHIL EXTRACELLULAR TRAPS IN THE PATHOGENESIS OF PERIODONTAL DISEASES

by

Phillipa Claire White

A thesis submitted to
The University of Birmingham
for the degree of
DOCTOR OF PHILOSOPHY

Department of Periodontology
School of Dentistry
College of Medical & Dental Sciences
The University of Birmingham
September 2015

ABSTRACT

This thesis investigated neutrophil extracellular traps (NETs) in the pathogenesis of periodontal diseases, including chronic periodontitis, experimental gingivitis and Papillon Lefèvre syndrome (PLS). *In vitro* assays investigated the interactions between periodontal bacteria and peripheral neutrophils isolated by discontinuous Percoll gradients, and demonstrated differential NET release in response to bacteria. Interestingly, NETs entrapped all periodontal bacteria assayed to some extent; however bacterial growth and survival were not impeded. A longitudinal intervention clinical study of chronic periodontitis patients and matched healthy controls revealed no differences in peripheral NET production; however NET production by patients decreased following non-surgical treatment. Furthermore, a subset of patients displayed impeded NET degradation by plasma that was restored following disease treatment; this may be the result of increased circulating immunoglobulins and free light chains (FLCs) pre-treatment. Peripheral NET production did not change throughout the experimental gingivitis model study; however NET release was impeded in PLS patients relative to healthy controls. Additional *in vitro* studies demonstrated that cigarette smoking had an inhibitory effect on NET release. Collectively, this thesis indicates that NETs contribute to innate immunity, however, given that periodontitis pathogenesis is characterised by aberrant neutrophil responses, NETs may also be involved in the progression of the disease.

ACKNOWLEDMENTS

I would like to begin by thanking my PhD supervisors Professor Iain Chapple, Professor Paul Cooper and Dr Mike Milward for their continued guidance and encouragement. I feel extremely lucky to have supervisors who care so much about my work and I am grateful for their support in response to my (endless) questions throughout my PhD. I want to express my gratitude to Dr Helen Wright, Dr Melissa Grant and Dr Naomi Hubber, all of whom have helped a great deal in the last few years. I would also like to thank Dr Adam Usher and Dr Iru Dias, who helped with the Dextran neutrophil isolation and flow cytometry, respectively. I would like to acknowledge the University of Birmingham Dental School, the Medical Research Council, the British Society of Periodontology and the Oral & Dental Research Trust for funding during my PhD. I am extremely grateful for the additional funding I benefitted from, which made it possible to go to several fascinating international conferences.

I wish to thank all of the postgraduate students at the Dental School, in particular those in the 7th floor post-graduate office, all of whom kept their sense of humour even on days when I had lost mine! I would also like to say a special thank you to Helen Roberts, who as well as being a great desk neighbour, will be a dear friend for life. In addition, I am very appreciative to all of those who repeatedly rolled up their sleeves to donate their blood in the name of science.

Most importantly, I would like to thank my family for their endless support throughout my PhD. In particular my husband, David White, who could no doubt write his own version of my thesis considering how much I've talked about my PhD.

TABLE OF CONTENTS

LIST OF FIGURES

LIST OF TABLES

ABBREVIATIONS

ACPA	Anti-citrullinated protein antibody
AFU	Arbitrary fluorescence units
AMP	Antimicrobial peptide
ANCA	Anti-neutrophil cytoplasmic antibodies
ANOVA	Analysis of variance
ATCC	American Type Culture Collection
ATP	Adenosine triphosphate
BAPTA	1,2-bis(o-aminophenoxy)ethane-N,N,N',N'-tetraacetic acid
BHI	Brain heart infusion
BOP	Bleeding on probing
BPI	Bactericidal/permeability-increasing
BSA	Bovine serum albumin
C	Complement
Ca^{2+}	Calcium ions
CAM	Cell adhesion molecule
cDNA	Complementary deoxyribonucleic acid
CF	Cystic fibrosis
CFTR	Cystic fibrosis transmembrane conductance regulator
CG	Cathepsin G
CGD	Chronic granulomatous disease
Cl^-	Chloride ions
CP	Crossing point
CRP	C-reactive protein
CSE	Cigarette smoke extract
DAG	Diacylglycerol
DEPC	Diethylpyrocarbonate
DMEM/F-12	Dulbecco's modified Eagle's medium:nutrient mixture F-12
DMSO	Dimethyl sulfoxide
DNA	Deoxyribonucleic acid
DNase	Deoxyribonuclease
DPI	Diphenylene iodonium
dsDNA	Double stranded DNA
dTNPmix	Deoxynucleotide mix
EGTA	Ethylene glycol tetraacetic acid
ELISA	Enzyme linked immunosorbent assay
FCγR	Fc-gamma receptor
Fiji	Fiji is just Image J
FLC	Free light chain
fMLP	*N*-formyl-methionyl-leucyl-phenylalanine

FS	Forward scatter
GAPDH	Glyceraldehyde-3-phosphate dehydrogenase
GAS	Group A streptococcal
GCF	Gingival crevicular fluid
GI	Gingival index
GM-CSF	Granulocyte-macrophage colony-stimulating factors
GO	Glucose oxidase
GPCR	G-protein-coupled receptor
GSH	Glutathione
GSSG	Oxidised glutathione
GTP	Guanosine triphosphate
H_2O_2	Hydrogen peroxide
HEPES	4-(2-Hydroxyethyl) piperazine-1-ethanesulfonic acid, N-(2-Hydroxyethyl) piperazine-N′-(2-ethanesulfonic acid)
HIV	Human immunodeficiency virus
HKG	Housekeeping gene
HMDS	Hexamethyldisilazane
HOCl	Hypochlorous acid
HOSCN	Hypothiocyanous acid
HPRT1	Hypoxanthine phosphoribosyltransferase 1
HRP	Horseradish peroxidase
HSP	Heat shock protein
HUVEC	Human umbilical vein endothelial cells
ICAM	Intercellular adhesion molecule
IgG	Immunoglobulin G
IL-	Interleukin-
K^+	Potassium ions
KO	Knock out
L	Litre
LAL	Limulus Amebocyte Lysate
LDH	Lactase dehydrogenase
LPS	Lipopolysaccharide
M	Molar
Mins	Minutes
MIP-1 alpha	Macrophage inflammatory protein-1 alpha
mm	Millimetre
MMP	Matrix metalloproteinase
MNase	Micrococcal nuclease
MOI	Multiplicity of infection
MPO	Myeloperoxidase
NAC	N-acetyl-cysteine

NADPH	Nicotinamide adenine dinucleotide phosphate
NE	Neutrophil elastase
NEi	Neutrophil elastase inhibitor
NETs	Neutrophil extracellular traps
NFκB	Nuclear factor kappa B
Nm	Nanometres
NO	Nitric oxide
NS	Not significant
O_2-	Superoxide
OCl-	Hypochlorite ions
OD_{600nm}	Optical density at 600 nanometres
OEC	Oral epithelium cell line
Oligo-dT	Oligonucleotide deoxy-thymine
OxPAPC	Oxidation of 1-palmitoyl-2-arachidonyl-sn- glycero-3-phosphorylcholine
PAD	Peptidyl arginine deiminase
PAF	Platelet activating factor
PAF	Platelet activating factor
PAMP	Pathogen-associated molecular patterns
PAR_2	Protease-activated receptor-2
PBN	Peripheral blood neutrophil
PBS	Phosphate Buffered Saline
PCR	Polymerase chain reaction
PI	Plaque index
PKC	Protein kinase C
PLS	Papillon Lefèvre syndrome
PMA	Phorbol 12-myristate 13-acetate
PMNL	Polymorphonuclear leukocytes
PPAD	*P. gingivalis* peptidyl arginine deiminase
PPD	Probing pocket depth
PR3	Proteinase 3
PRM	Pattern recognition molecule
PRR	Pattern recognition receptor
PVP	Polyvinylpyrrolidone
RA	Rheumatoid arthritis
rcf	Relative centrifugal force
RF	Rheumatoid factor
rhDNase	Recombinant deoxyribonuclease
RLU	Relative light units
RNA	Ribonucleic acid
RNase	Ribonuclease
ROS	Reactive oxygen species

RPL13	Ribosomal protein L13
RPMI	Roswell Park Memorial Institute
RT	Reverse transcriptase
SAP	Serum amyloid P
SCN-	Thiocyanate
SD	Standard deviation
Secs	Seconds
SEM	Scanning electron microscopy
SEM	Standard error of the mean
SIRS	Systemic inflammatory response syndrome
SLE	Systemic lupus erythematosus
SLPI	Serum leukocyte protease inhibitor
SOD	Superoxide dismutase
SS	Side scatter
T-EDTA	Trypsin ethylenediaminetetraacetic acid
TIMP	Tissue inhibitors of metalloproteinases
TLR	Toll like receptor
TMB	3,3',5,5'-Tetramethylbenzidine
TNF	Tumour necrosis factor
TSA	Tryptone soya agar
TSB	Tryptone soya broth
UC	Ulcerative colitis
WT	Wild type
YWHAZ	Tyrosine 3/tryptophan, 5-monooxygenase activation protein, zeta polypeptide

CHAPTER 1: INTRODUCTION

1.1 Neutrophilic polymorphonuclear leukocytes (PMNLs)

Neutrophilic polymorphonuclear leukocytes (PMNLs), otherwise known as neutrophils, are recognised for playing a critical role in both the innate and acquired (humoral) immune response. The name PMNLs derives from the cells' multi-lobed nucleus (Figure 1.1), which distinguishes the neutrophil from other granulocytes, such as eosinophils, basophils and mast cells (Kobayashi *et al.,* 2009). The innate immune system is characterised by a rapid, though poorly specific response to infection, which does not require previous exposure to microorganisms to be effective. This process is facilitated by pattern recognition receptors (PRR) on the PMNL membrane that recognise highly conserved pathogen-associated molecular patterns (PAMPs) from foreign species or "non-self". In contrast, the acquired (humoral) immune system specifically targets previously encountered pathogens and thus results in a delayed, but highly targeted and effective response (Kumar & Sharma 2010). In addition to the neutrophil's direct effector functions, such as phagocytosis and NETosis (see 1.1.4), they are able to modulate the activity of acquired immune cells by releasing signalling molecules, such as cytokines and by expressing humoral pattern recognition molecules (PRMs). Collectively, the diverse functions of neutrophils make them indispensable to both the cellular and humoral arms of the acquired immune response (Jaillon *et al.,* 2013).

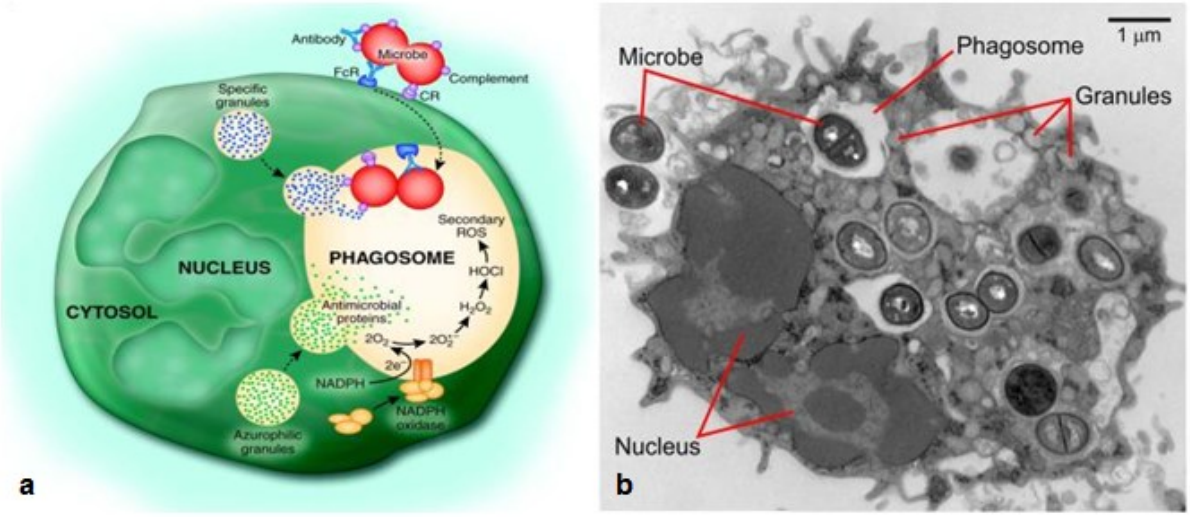

Figure 1.1: Microanatomy of the human neutrophil
(a) Schematic of neutrophil activation and the subsequent sequencing cascade in response to a microbe. (b) Transmission electron microscopy image of a neutrophil that has phagocytosed a microbe (red arrows indicate the microbe, phagosome, granules and nuclei) (Kobayashi *et al.,* 2009).

1.1.1 Neutrophil origin, maturation and longevity

Neutrophil production initiates in the bone marrow, with an estimated two thirds of haematopoiesis being assigned to the formation of myeloblasts (cells which are committed to becoming granulocytes). In a healthy individual, neutrophil production is maintained at a consistent level, with an estimated 1-2 x 10^{11} neutrophils being generated per day (Savil *et al.,* 1989). However, neutrophil release significantly increases up to 10 fold (Furze & Rankin 2008) during periods of infection and inflammation, and the transient increase in circulating neutrophils accommodates the heightened demands placed upon the immune system (Metcalf *et al.,* 1991). Whilst neutrophils were previously considered to be short-lived cells equipped with an estimated half-life of 8 hours in humans, a recent study demonstrated that neutrophils have a much longer circulatory lifespan of approximately 5.4 days (Pillay *et al.,* 2010). Precise adjustments of neutrophil levels are regulated by apoptosis pathways within the tissues, whereby increased neutrophil apoptosis signals a reduction in the number of stem

cells assigned to myeloblast formation within bone marrow (Michlewska *et al.,* 2009). Apoptotic neutrophils, along with the particles they have engulfed, are efficiently cleared by macrophages and dendritic cells, which recognise death signals on the neutrophil surface in the form of phosphatidylserine groups (Michlewska *et al.,* 2009, Hochreiter-Hufford & Ravichandran 2013).

1.1.2 The neutrophil extravasation cascade

Once released into the circulatory system, neutrophils resolutely survey for invading microorganisms. If pathogens are encountered the neutrophil transitions from a circulating non-activated cell, crosses the vascular endothelium and traverses the tissues for *in situ* eradication of the invading pathogen (Figure 1.2). This occurs as a result of the infection triggering the release of bacterial virulence factors, for example lipopolysaccharide (LPS) and *N*-formyl-methionyl-leucyl-phenylalanine (fMLP), as well as host derived inflammatory mediators such as interleukin-8 (IL-8) and macrophage inflammatory protein-1 alpha (MIP-1 alpha). The release of vascular peptides, such as histamine and complement (e.g. C5a and C3a) cause vasodilation within the capillary beds; this reduces flow rate and releases neutrophils from mid-stream flow, enabling neutrophil contact with the vascular endothelium (Muller *et al.,* 2013). The concomitant activation of the endothelium causes endothelial cells to up-regulate their expression of cell adhesion molecules (CAMs) on their luminal surfaces. Heightened expression of selectins (e.g. P- and E-selecins), a family of glycoproteins with an extracellular lectin-like domain, facilitates the adhesion between the endothelium and circulating leukocytes. Selectins bind to their corresponding ligand, causing the neutrophils to intermittently adhere to the vascular endothelium, which represents the initial stage of the cells' migration into the tissues. This transient adhesion causes the neutrophil to roll along the endothelium in the same direction as the vessel's blood flow, a process also referred to as

"leukocyte tethering". This further slows the cell and the contact with the endothelium induces neutrophil activation. Activation is postulated to be a synergistic process, instigated by a combination of several pro-inflammatory cytokines, (e.g. tumour necrosis factors-α [TNFα] and IL-1) and contact with the activated endothelial cells. The expression of immunoglobulin-superfamily cell adhesion molecules, such as platelet endothelial cell adhesion molecule-1 (PECAM-1), are also thought to facilitate transmigration (Christofidou-Solomidou *et al.,* 1997). Neutrophil diapedesis through the endothelium is believed to occur either between endothelial cells (paracellularly) or via a single endothelial cell (transcellularly) (Wagner *et al.,* 2000).

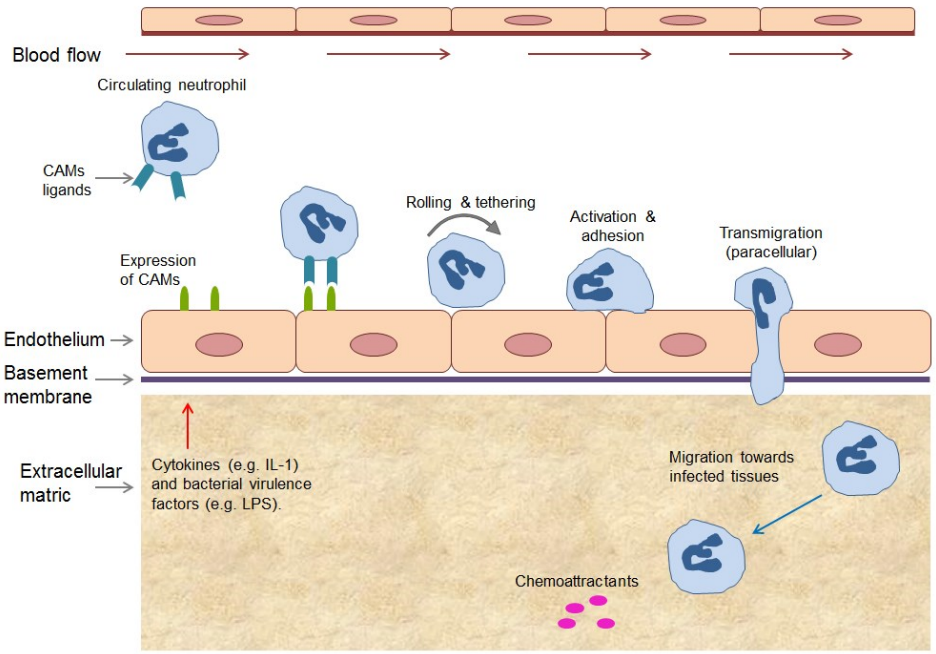

Figure 1.2: Neutrophil extravasation cascade
Tissue infection triggers the release of cytokines and bacterial virulence factors that activate the vascular endothelium. This causes the expression of cell adhesion molecules (CAMs), such as selectins and integrins, which bind to their corresponding ligand on the neutrophil and cause the cells to roll along the endothelium. Interaction with the endothelium induces neutrophil activation and subsequent adhesion, which results in neutrophil transmigration. Once the endothelium and basement membrane is traversed, neutrophils follow a chemotactic gradient, e.g. complement or bacterial components that emanate from the infected tissue. (Image produced by P. White).

1.1.3 Chemotaxis

Chemotaxis describes the directional movement of neutrophils in response to a chemotactic gradient, enabling the cells to migrate through the infected tissues. Once leaving the bloodstream and entering the tissue, neutrophils no longer rely on chemokines produced by the endothelium, but follow a new chemotactic gradient emanating from the site of infection. It is hypothesised that this occurs as a result of a hierarchy of chemotactic molecules that overrides the endothelial chemoattractants (Kim & Haynes 2012). Chemoattactants can be categorised into endogenous factors, such as platelet activating factor (PAF), complement components (e.g. C5a) and cytokines/chemokines (e.g. IL-8); or exogenous factors, which include bacterial components such as fMLP and endotoxins (e.g. LPS). Chemoattractants provide a chemical hierarchy due to differences in concentrations and potencies, which orchestrate the recruitment of neutrophils towards the site of infection. Typically neutrophils are the first immune cells to arrive at the site of infection and are present in abundance (Swirski *et al.,* 2013). Neutrophil activation triggers a downstream signalling cascade leading to the activation of their cytoskeleton to facilitate cell movement (Samanta *et al.,* 1990). The highly sequential migration of cells occurs by polymerisation of F-actin, which brings about cytoskeletal changes and the protrusion of pseudopods in the direction of the gradient enabling the motile behaviour seen in neutrophil chemotaxis (Andrew & Insall 2007). The chemotactic gradient also activates neutrophils via the complementary neutrophil receptors of the transmembrane G-protein-coupled receptor (GPCR) family.

1.1.4 Neutrophil killing

In order to fulfil their primary role of eliminating invading pathogens, neutrophils rely on the release of granule proteins and the generation of ROS. Research suggests that a combination of both granule proteins and oxidase activity are required for the most efficient microbial killing. This is evidenced in knockout (KO) mice deficient in either ROS or neutrophil proteases (e.g. neutrophil elastase [NE]), in which both strains of mice were susceptible to infection compared with wild type (WT) mice (Papayannopoulos *et al.,* 2010).

1.1.4.1 Neutrophil cytoplasmic granules

One of the neutrophils' defining features is their granules, which are organelles assigned to housing a variety of antimicrobial molecules and deploying them into either the phagosome or extracellularly via secretory vesicles. Dependent upon their contents and the time at which they are produced during haematopoeisis, granules are subdivided into 3 principal types (as described below); however there is significant overlap between granule content (Faurschou & Borregaard 2003).

Peroxide positive granules (azurophilic) were named on the basis of their uptake of the dye "azure A"; they are the largest of the three granules and the first to be produced in the cell. Azurophilic granules contain multiple proteins and peptides that function to aid the neutrophil in eliminating microbes. Myeloperoxidase (MPO), NE, cathepsin G (CG) and proteinase 3 (PR3) are all contained in azurophilic granules (Faurschou & Borregaard 2003). Azurophilic granules also provide a rich source of defensins, which are cationic peptides that possess the ability to kill a wide variety of microbes (Ganz *et al.,* 1985).

Peroxide-negative granules can be categorised into "specific" and "gelatinase" granules (Kjeldsen *et al.,* 1992). There are significant differences between the granule content;

whereas the specific granules are a reservoir of proteins targeted to microbial killing, gelatinase granules are involved in other neutrophilic processes.

Specific granules provide a rich source of lactoferrin, which upon release, has the ability to sequester bacterial iron and bind to the bacterial membranes. This enables lactoferrin to elicit antimicrobial activity against a range of both Gram-positive and Gram-negative bacteria by causing membrane disruption and subsequent cell death (Yamauchi *et al.,* 1993).

Gelatinase-containing granules facilitate neutrophil extravasation, providing the enzymes necessary to digest the extracellular matrix. Typically, gelatinase granules are assigned based on these granules lacking lactoferrin, whereas many lactoferrin-containing specific granules will also contain gelatinase. Both specific and gelatinase granules contain flavocytochrome $b_{558,}$ which is a heterodimer membrane component of nicotinamide adenine dinucleotide phosphate (NADPH)-oxidase and composed of cytochrome P-22^{phox} and GP-91^{phox} subunits (Yu *et al.,* 1999, Borregaard & Cowland 1997).

1.1.4.2 Neutrophil oxidative killing

The generation of ROS via the NADPH-oxidase pathway is critical to the neutrophil's ability to kill invading pathogens. The significance of this process is exemplified in chronic granulomatous disease (CGD) patients, in whom a mutation in any of the four genes encoding the NADPH-oxidase complex proteins causes impaired ROS generation and thus defective microbial killing (Bianchi *et al.,* 2011). Oxidative killing relies on the assembly of the NADPH-oxidase, resulting in the non-mitochondrial generation of ROS and increased oxygen uptake via the "respiratory burst". Flavocytochrome b_{558} plays a pivotal role in sequentially transporting electrons from NADPH-oxidase, residing in the neutrophil cytoplasm, across the phagosome membrane. In order for electron transfer to occur,

NADPH-oxidase needs to bind with an assembled form of flavocytochrome b_{558}. Following neutrophil stimulation, second messengers such as protein kinase C (PKC), activate the assembly of the cytosolic oxidase components, P-47^{phox}, P-67^{phox} and P40^{phox}, which translocate to join flavocytochrome b_{558} on the phagosome membrane and activate the subsequent electron transfer within the completely assembled oxidase complex. Electron transfer results in molecular oxygen being reduced to form superoxide ($O_2^{\cdot}$-), which is pumped into the vacuole where it is believed to produce active forms of pro-active enzymes. The $O_2^{\cdot}$- is then converted to hydrogen peroxide (H_2O_2), either spontaneously or following superoxide dismutase-2 (SOD-2) enzyme activity. Finally, catalysed by MPO, H_2O_2 combines with chloride ions (Cl^-) to form HOCl (Robinson 2008, Chapple 1996) (Figure 1.3). HOCl plays a vital role in bacterial killing; despite not being well characterised, HOCl has been suggested to elicit its bactericidal activity by chlorinating bacteria (Chapman *et al.,* 2002). In addition to killing bacteria directly, the generation of ROS via the NADPH-oxidase cascade also activates granule proteins. This involves an elevation in pH and potassium ions (K^+) to compensate for the charge difference created by the movement of electrons into the vacuole. Increased K^+ causes the cationic contents of the granules to lose their charge interaction with negatively charged proteoglycans and triggers the release of granule proteins (Reeves *et al.,* 2002).

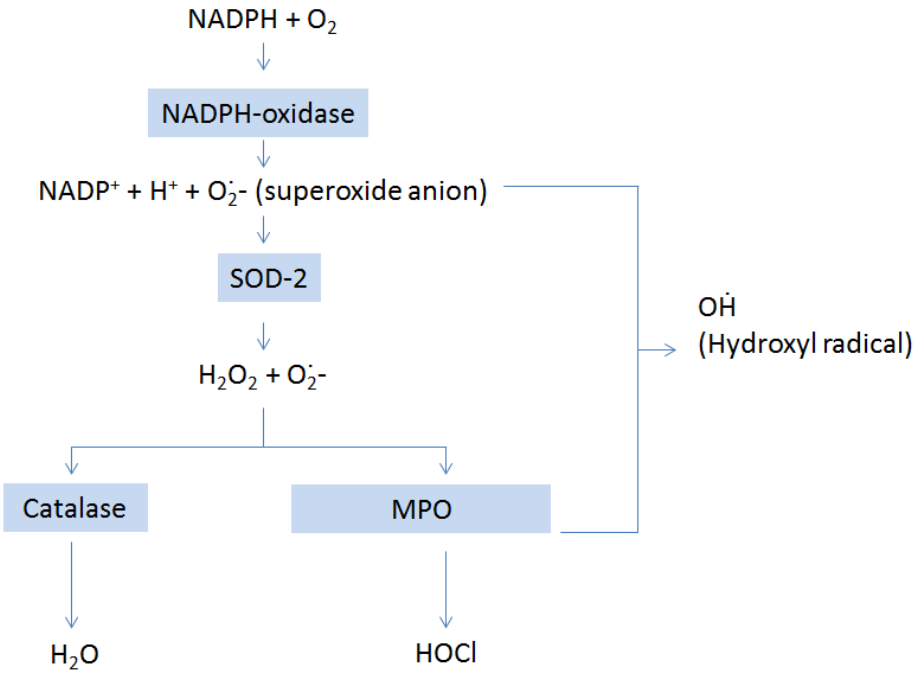

Figure 1.3: NADPH-oxidase pathway for the generation of ROS
Neutrophil activation stimulates the assembly of the NADPH-oxidase complex. This results in molecular oxygen being reduced to superoxide (O_2^-), which is subsequently converted to hydrogen peroxide (H_2O_2), either spontaneously or catalysed by superoxide dismutase (SOD-2). Finally, catalysed by myeloperoxidase (MPO), H_2O_2 combines with chloride ions (Cl^-) to produce hypochlorous acid (HOCl) (Chapple 1996).

1.1.4.3 Intracellular killing: phagocytosis

Phagocytosis is the intracellular microbicidal mechanism of neutrophils thought to represent "safe" killing through containment of cytotoxic molecules within a membrane bound phagosome. Neutrophils are equipped to recognise unopsonised pathogens, as well as opsonised pathogens. Phagocytosis of opsonised pathogens, either with immunoglobulins or complement components, relies primarily on Fc-gamma receptors (FcγR) or integrins, respectively (Nordenfelt & Tapper 2011). Neutrophils are also capable of recognising pathogens directly by their expression of Toll-like receptors (TLR), which are type-1 transmembrane PRRs that have the capacity to recognise invading microbes. For example,

TLR2 allows the neutrophil to detect peptidoglycans of Gram-positive bacteria and TLR4 detects LPS present from Gram-negative bacteria (Takeuchi *et al.,* 1999). Following recognition of invading pathogens by neutrophils, the microorganism is internalised into the neutrophil phagocytic vacuole, and the maturation of the phagosome follows. This is characterised by the activation of NADPH-oxidase and the fusion of granules within the phagosome, thus delivering proteins derived from azurophilic granules into the phagosome, which destroy the engulfed pathogen (Nunes *et al.,* 2013). Following bacterial phagocytosis, neutrophils undergo apoptosis to prevent the release of cytotoxic substances derived from necrosing phagocytic neutrophils, such as oxygen radicals, which are reported to cause collateral tissue host damage and further propagate the immune response into a chronic state (Henson & Johnston 1987).

1.1.4.4 Extracellular killing: degranulation

In addition to the granule contents being released into the phagosome, neutrophil activation can also trigger the extracellular expulsion of granule proteins. The initial step in exocytosis is the acquisition of granules from the neutrophil cytoplasm to the plasma membrane. Following translocation, the granules tether along the cell membrane surface, which promotes granule fusion with the target membrane and the release of the granule contents. The process relies on elevations of intracellular calcium ions (Ca^{2+}) and the hydrolysis of adenosine triphosphate (ATP) and guanosine triphosphate (GTP) (Lacy *et al.,* 2006).

1.1.4.5 Extracellular killing: Neutrophil extracellular traps (NETs)

A relatively novel neutrophil-mediated defence mechanism, termed neutrophil extracellular traps (NETs), was recently reported (Brinkmann *et al.,* 2004). NETs are highly conserved extracellular mesh-like structures of decondensed nuclear chromatin (Figure 1.4). The DNA backbone is associated with antimicrobial peptides (AMPs) derived from the azurophilic,

specific and gelatinase granules. The DNA component is essential for extracellular fibres to maintain their structure. Indeed analysis of the nuclear and granular NET components revealed that deoxyribonuclease (DNase) treatment, which degrades DNA, resulted in NET digestion, whilst protease treatment did not (Brinkmann *et al.,* 2004). NETs are believed to function by containing and subsequently destroying pathogenic microbes following their immobilisation within the "DNA" traps, thus preventing bacterial dissemination into underlying tissues.

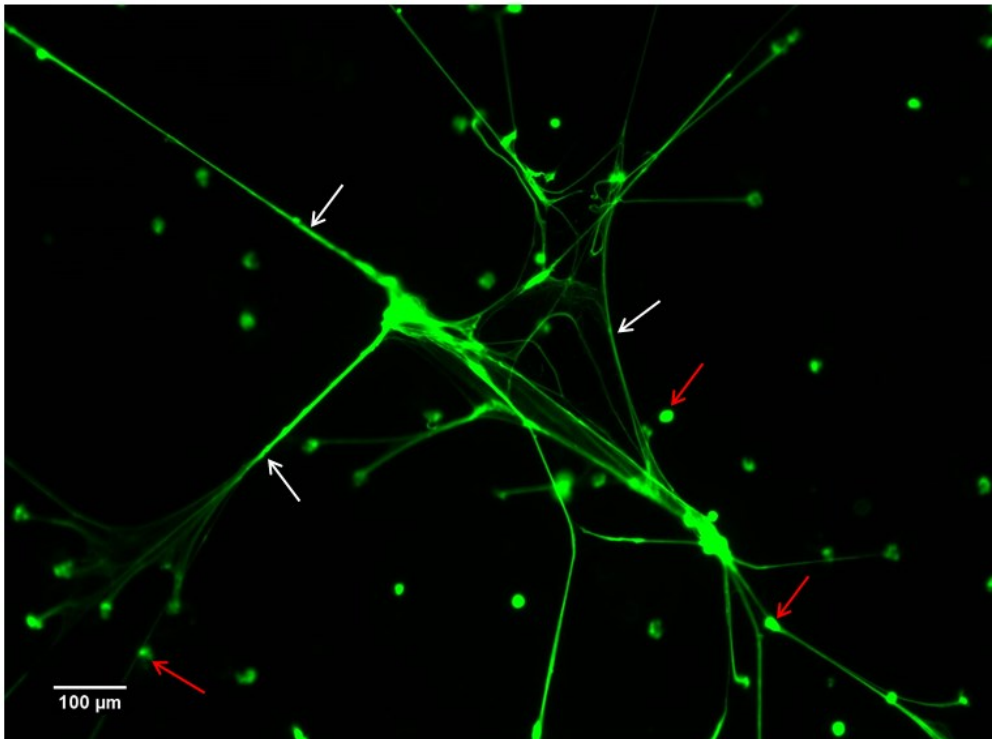

Figure 1.4: Photomicrograph illustrating fluorescence microscopy of NETs
Image captured by fluorescence microscopy (x10 magnification) using a Sytox green stain for DNA on 50nM phorbol 12-myristate 13-acetate (PMA)-stimulated neutrophils (10^5) after 4 hours. Red arrows indicate neutrophils and white arrows show NET strands, scale bar represents 100µm. (Image produced by P. White).

NETs are only released by mature neutrophils, endowed with the molecular equipment to trigger receptor signalling and the subsequent enzyme activation necessary for NET extrusion (Martinelli *et al.,* 2004). Live image microscopy by Fuchs *et al.,* (2007) demonstrated that

NETs are produced during a unique and active form of programmed cell death (termed NETosis), which is distinct from apoptosis and necrosis. A range of stains were employed to unravel the sequential events of NET formation and data indicated that neutrophils treated with phorbol 12-myristate 13-acetate (PMA), a commonly utilised stimulus for *in vitro* NET production, exhibited nuclear DNA decondensation and subsequent release into the cytoplasm following plasma membrane rupture, leading to chromatin and granular protein expulsion (Figure 1.5). This process was in agreement with previous findings by Brinkmann *et al.,* (2004), who demonstrated that NET formation was indeed distinct from necrosis as lactate dehydrogenase (a marker of cell necrosis) was not simultaneously released with NETs. NETs have also been shown to be released by viable neutrophils in response to priming with granulocyte-macrophage colony-stimulating factors (GM-CSF) and subsequent stimulation with LPS or complement (C5a), a process referred to as vital NET release. This requires a much shorter stimulation period of as little as 15 mins. Interestingly, polymerase-chain reaction (PCR) analysis demonstrated that the extracellular DNA sequences in vital NET release were derived from mitochondrial DNA, rather than nuclear DNA. Mitochondrial NETs are distinct from nuclear DNA derived NETs, as they lack nuclear proteins, such as lamin B and nuclear matrix protein-45 (Yousefi *et al.,* 2009). It is therefore possible that nuclear and mitochondrial NETs have different extracellular effects.

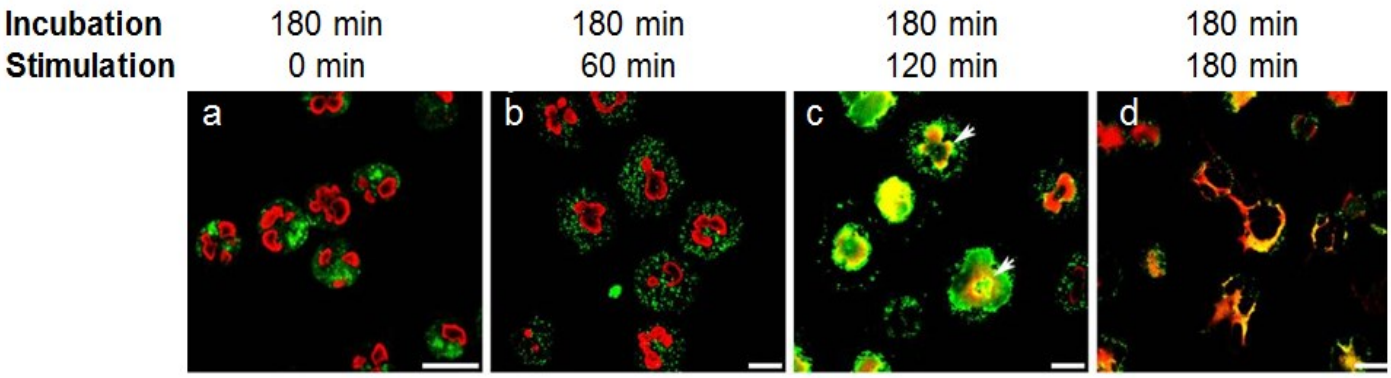

Figure 1.5: Confocal immunofluorescensce images of NET release
(a) 180 min incubation period without stimulation: neutrophil chromatin and granules are distinctly separate. (b) 60 min incubation period with 20nM phorbol 12-myristate 13-acetate (PMA) stimulation: neutrophils flatten to show clear nuclei and granules. (c) 120 min incubation period with 20nM PMA: co-localisation of nuclei and granules (arrows show intense yellow staining at nuclear borders). (d) 180 min incubation period with 20nM PMA: some cells are releasing NETs. Immunofluorescence stains: Red (histone-DNA), green (neutrophil elastase), yellow (co-localisation of chromatin and NE). Scale bar represents 10μm (Fuchs *et al.,* 2007).

1.2 The process of NET release

The initial step in the production of NETs by activated and NETosing neutrophils is the generation of ROS via the NADPH-oxidase complex. As previously described, this results in the production of H_2O_2, which is catalysed by MPO to produce HOCl. Subsequent to the production of ROS, arginine and methylarginine residues are citrullined by peptidyl arginine deiminase 4 (PAD4), causing the nuclear chromatin to decondense (Wang *et al.,* 2009). Chromatin decondensation promotes the formation of vesicles between the inner and outer nuclear membranes, and neutrophil granule proteins are released and co-localise with the chromatin (Figure 1.6). Nuclear membrane integrity is lost and this enables the DNA to combine with AMPs. Indeed, proteins such as elastase and MPO have all been found to associate with the NET complex. Subsequently, the decondensed DNA, now decorated with AMPs, occupies the intracellular cytoplasmic space before rupturing the neutrophil cell

membrane. Active expulsion of the NET web-like structure requires the activation of the neutrophil actin cytoskeleton and microtubular systems (Neeli *et al.,* 2009). Finally, the DNA/histone complex is released into the extracellular space.

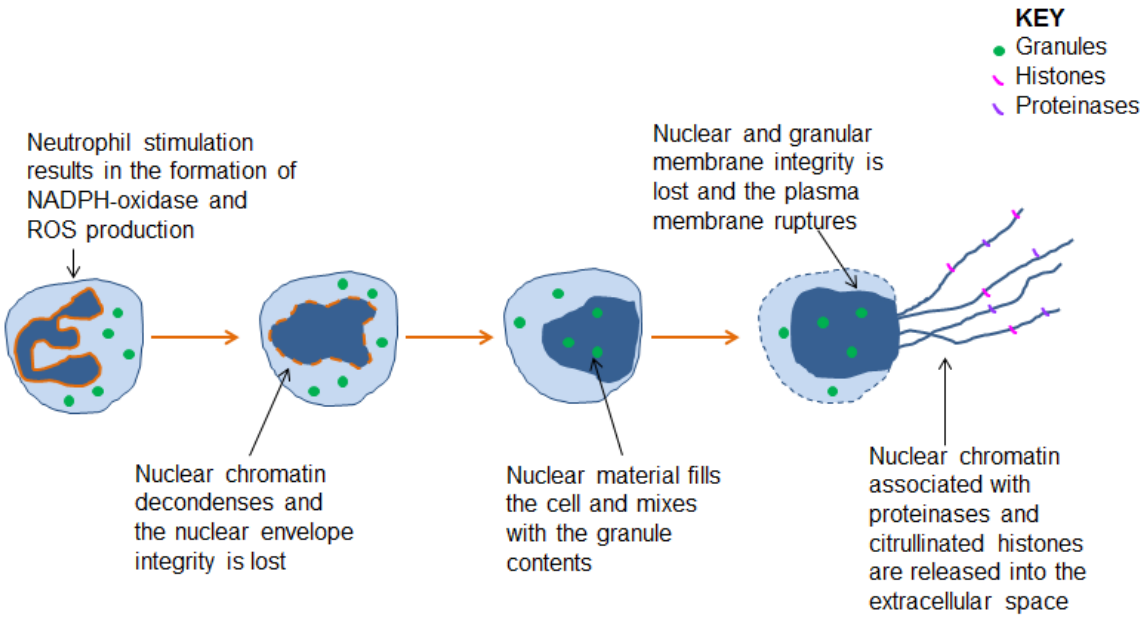

Figure 1.6: Schematic representation of the steps involved in nuclear NET release (Adapted from Brinkmann & Zychlinsky 2007).

1.2.1 Requirements for NET release

The role of the NADPH-oxidase was confirmed by Fuchs *et al.,* (2007), who demonstrated that neutrophils subjected to PMA, alongside diphenylene iodonium (DPI) treatment (an NADPH-oxidase inhibitor), produced fewer NETs. Subsequent findings from patients with CGD showed these individuals also lacked the ability to produce NETs. However the phagocytosis of glucose oxidase (GO) coated latex spherules, which circumvents the mutation by producing a H_2O_2 generating system (Baehner *et al.,* 1970), restored NET production. Recent findings by Bianchi *et al.,* (2011) have confirmed the importance of NETs in the immune response in CGD patients suffering from pulmonary aspergillosis, where the restoration of NET formation using gene therapy was correlated with the

eradication of the *Aspergillus* infection. These results lend further support for the importance of NADPH-oxidase activity in NET production and immune defence. NET release is also reported to require PAD4, an enzyme which converts arginine and methylarginine residues to citrulline. Hypercitrullination of condensed nuclear chromatin causes chromatin decondensation/unfolding, which is crucial for extracellular NET formation and subsequent NET extrusion (Wang *et al.,* 2009). Mice deficient in PAD4 do not citrullinate histones, which subsequently results in no unfolding of the nuclear chromatin and an inability to produce NETs. Abrogated NET production in these mice has been associated with a susceptibility to bacterial infections (Li *et al.,* 2010). It has also been reported that azurophil-derived NE necessitates chromatin decondensation prior to NET extrusion. Papayannopoulos *et al.,* (2010) demonstrated that NE inhibitors caused attenuated NET release, as a result of inhibited nuclear decondensation. NE has been proposed to play a key role in determining whether neutrophils are assigned to phagocytosis or NETosis in response to invading pathogens. It has been suggested that the acquisition of NE to the phagosome concomitantly sequesters NE from the nucleus, which inhibits chromatin decondensation and NET release (Branzk *et al.,* 2014). Use of additional specific inhibitors revealed that MPO and other serine proteases, including CG and PR3, were not essential for NET release. Active expulsion of the NET web-like structure also relies on the actions of the neutrophil actin cytoskeleton and microtubular systems. Inhibition of either of these mechanisms, for example with cytochalasin D and nocodazole, considerably reduced NET formation in response to LPS from 30% to 5% (Neeli *et al.,* 2009). Whilst it is believed that the actin cytoskeleton is essential for signal transmission involved in histone deamination (Neeli *et al.,* 2009), microtubules have been suggested to transport other components that are vital for NET release, such as NE and PAD4 (Cooper *et al.,* 2013). Furthermore, intracellular calcium has been found to play a role in NET release. In response to PMA, neutrophils pre-treated with

2-bis(o-aminophenoxy)ethane-N,N,N',N'-tetraacetic acid (BAPTA; which chelates intracellular calcium) exhibited significantly reduced NET production. Notably, NET production was not inhibited to the same extent in response to bacterial stimulation of NETs, thus the exact contribution of calcium to this process is difficult to delineate (Parker *et al.,* 2012). These requirements for NET release further support the contention that their expulsion involves a highly sequential and orchestrated series of events.

1.2.2 Stimuli that induce NET release

Neutrophils release NETs in response to multiple stimuli including bacteria and their components, viruses, fungi and protozoa/parasites (Table 1.1). Interestingly, host derived components, such as cytokines and activated platelets, can also potentiate NET production.

Table 1.1: All previously reported NET stimuli

Bacterial	Parasites/protozoa and fungi
Streptococcus pneumonia[1]	*Candida albicans*[18]
Staphyloccus aureus[2]	*Aspergillus funigatus*[19]
Shigella flexneri[3]	*Cryptococcus gattii*[20]
Escherichia coli[4]	*Leishmania amazonensis*[21], *chagasi*[21], *donovani*[15], *major*[15]
Mycobacterium tuberculosis[5]	*Eimeria bovis*[22]
Listeria monocytogenes[6]	*Plasmodium falciparum*[23]
Klebsiella pneumonia[7]	
Mannheimia haemolytica[8]	**Viruses**
Serratia marcescens[9]	
Yersinia pseudotuberculosis[10]	Influenza A[24]
Porphyromonas gingivalis[11]	HIV-1[25]
	Feline leukaemia virus[26]

Bacteria-derived components	Host/Inflammatory mediators
Glucose oxidase[12]	Platelets & platelet activating factor (PAF)[27]
Lipopolysaccharide (LPS)[13]	Nitric oxide[28]
fMLP[14]	Antibodies[29]
Lipophosphoglycan[15]	TNF-α[30]
Leukotoxin GH (*S. aureus*)[16]	IL-1β[30], 8[30]
Panton-Valentine leukocidin (*S. aureus*)[16]	GM-CSF+C5a, LPS[31]
Streptococcal surface enolase[17]	LL-37[32]
Adhesive protein invasin (*Y. enterocolitica)*[10]	
	Non-physiological
	Phorbol 12-myristate *13*-acetate (PMA)[13]
	Hypochlorous acid (HOCl)[33]
	Statins[34]

References: (1) Beiter *et al.,* 2006. (2) Pilsczek *et al.,* 2010. (3) Brinkmann *et al.,* 2004. (4) Grinberg *et al.,* 2008. (5) Ramos-Kichik *et al.,* 2009. (6) Munafo *et al.,* 2009. (7) Papayannopoulos *et al.,* 2010. (8) Aulik *et al.,* 2010. (9) González-Juarbe *et al.,* 2015. (10) Gillenius & Urban 2015. (11) Delbosc *et al.,* 2011. (12) Yost *et al.,* 2009. (13) Fuchs *et al.,* 2007. (14) Neeli *et al.,* 2009. (15) Gabriel *et al.,* 2010). (16) Malachowa *et al.,* 2013. (17) Mori *et al.,* 2012. (18) Byrd *et al.,* 2013. (19) Urban *et al.,* 2006. (20) Springer *et al.,* 2010. (21) Guimarães-Costa *et al.,* 2009. (22) Behrendt *et al.,* 2010. (23) Baker *et al.,* 2008. (24) Narasaraju *et al.,* 2011. (25) Saitoh *et al.,* 2012. (26) Wardini *et al.,* 2010. (27) Clark *et al.,* 2007. (28) Patel *et al.,* 2010. (29) Short *et al.,* 2014. (30) Keshari *et al.,* 2012. (31) Yousefi *et al.,* 2009. (32) Neumann *et al.,* 2014. (33) Palmer *et al.,* 2012. (34) Chow *et al.,* 2010.

1.2.2.1 *Ex vivo* stimuli

PMA is structurally and functionally analogous to diacylglycerol (DAG), an intracellular second-messenger lipid and an agonist for PKC. PMA exposure triggers NET production as it bypasses neutrophil surface receptors and the activation of phagocytosis. Fuchs *et al.,* (2007) reported that *in vitro* stimulation neutrophils with PMA caused one third of cells to release NETs. HOCl is also known to be required for NET release *in vivo* and using relevant concentrations of sodium hypochlorite as a stimulus can replicate this in *ex vivo* assays. HOCl is usually produced by activated neutrophils following NADPH-oxidase assembly. This is followed by the production of H_2O_2, which is converted to HOCl by the enzymatic activity of MPO. HOCl as an *ex vivo* stimulant negates the requirement for receptor-ligand binding and the activation of the NADPH-oxidase, and has been reported to produce NETs in as little as 30 mins (Palmer *et al.,* 2012).

1.2.2.2 Bacteria-derived stimuli

Live bacteria, such as *Staphylococcus aureus (S. aureus)* (Fuchs *et al.,* 2007) and *Shigella flexneri (S. flexneri)* (Brinkmann *et al.,* 2004), which are Gram-positive and Gram-negative bacteria, respectively, have been found to stimulate NET production. As previously mentioned (section 1.2.1), bacteria-induced NET production is dependent upon the activation of NADPH-oxidase as DPI treatment (an NADPH-oxidase inhibitor) attenuates NET production. Intriguingly, it has been reported that NETs can be produced in an oxidant-independent manner in as little as 10 mins in response to *S. aureus*. Unlike the typical 4 hour release that results in nuclear DNA NETs, this rapid mechanism is thought to also involve the expulsion of intact secretory vesicles without nuclear and plasma membrane fusion. The authors hypothesise that this rapid NET release may be critical to contain bacterial infections

and the mechanism is dependent on vesicular exocytosis, rather than activation of NADPH-oxidase (Pilsczek *et al.,* 2010).

LPS is a key component of Gram-negative bacterial cell walls, where it maintains the structural integrity, stability and negative charge of the bacteria. LPS does not have the capacity to directly induce neutrophils to release NETs, however, there is growing evidence that LPS can activate platelets, which subsequently initiates NET release. TLR4 has recently been reported to be present on platelets, which is indicative of platelets having the capacity to recognise and respond to LPS from Gram-negative bacteria (Andonegui *et al.,* 2005). TLR4 positive platelets have also been found to sequester in infectious tissues as a result of bacterial LPS release. Activation of platelet TLR4 receptors by LPS causes binding of platelets to neutrophils, which has been found to trigger NET release and is believed to enable the ensnaring of invading microbes (Clark *et al.,* 2007).

Streptococcus pneumoniae (*S. pneumoniae*) is reported to associate with plasmin(ogen), an enzyme that may facilitate bacterial dissemination via increased proteolytic activity. *S. pyogenes,* and other group A streptococcal species (GAS), possess a plasmin(ogen) receptor, known as streptococcal surface enolase (Bergmann *et al.,* 2001). Streptococcal surface enolase expressed by *S. pneumoniae* was found to stimulate NET release by human peripheral blood neutrophils (PBN). However, the mechanisms pertaining to the production of surface enolase-mediated NET release remains to be elucidated (Mori *et al.,* 2012).

1.2.2.3 Protozoan/parasitic and fungal-derived stimuli

Neutrophils also produce NETs in response to a range of protozoan parasites, including *Apicomplexan* and *Trypanosomatid* species (Behrendt *et al.,* 2010, Guimarães-Costa *et al.,* 2009, respectively). These parasites are intracellular, however the putative function of NET

release in this context is to prevent the dissemination and invasion of protozoa into other cells. Fungi also possess the requisite signals to trigger NET release, including *Aspergillus fumigatus (A. fumigatus)* (Urban *et al.,* 2006) and *Candida albicans (C. albicans)* (Byrd *et al.,* 2013). *C. albicans* can be found in both cellular and hyphal forms. Similar to protozoan parasites, NET activation by the cellular form is limited to when *C. albicans* is emerging from cells to invade other cells. Hyphal forms are extracellular and are likely to be too large to phagocytose; thus NETs may represent a critical extracellular defence mechanism (Branzk *et al*., 2014). Interestingly, *C. albicans'* β-glucan, a pathogen associated molecule pattern (PAMP), can also stimulate for NET release. β-glucan is present in the cell walls of fungi and enables neutrophils to recognise the invading fungus. In the presence of fibronectin, an extracellular matrix glycoprotein, β-glucan reportedly stimulated neutrophils to release NETs in as little as 30 mins (Byrd *et al.,* 2013). The authors postulate that neutrophil activation and downstream NET release is likely due to fibronectin binding with integrins, which causes an oxidant-independent mechanism via homotypic aggregration.

1.2.2.4 Host-derived NET stimuli

Host-derived inflammatory mediators involved in neutrophil recruitment and activation have recently been reported to induce NET production. Systemic inflammatory response syndrome (SIRS) is a disease characterised by a dysregulated inflammatory response to non-infectious insults, such as surgery and trauma (Drifte *et al.,* 2013, Nystrom *et al.,* 1998). SIRS patients are known to have high circulating levels of cytokines, including IL-8, IL-1β and TNFα and reported to release elevated levels of NETs. This knowledge prompted the investigation into the contribution of circulating cytokines to NET release, which revealed that the addition of SIRS patients' plasma to healthy neutrophils resulted in NET production. The neutralisation of patient plasma cytokines prior to incubation with neutrophils

normalised NET release, confirming the contribution of cytokines to NET production (Keshari *et al.,* 2012).

Another known stimulus for NETs is LL-37, a member of the cathelicidin family. Cathelicidins are AMPs that bind to cholesterol deficient membranes to elicit antibacterial (Gennaro & Zanetti 2000), antiviral (Takiguchi *et al.,* 2014) and antifungal (Lopez-Garcia *et al.,* 2005) activity. Neutrophil production of LL-37 is considerably increased when the cell is challenged with an infectious agent. *Ex vivo* experiments with PBNs have shown that physiologically relevant concentrations of LL-37 can cause the production of NETs. It was found that LL-37 could trigger NET release directly, but also confer increased NET production in response to *S. aureus*. Subsequent immunostaining studies suggested that LL-37 translocates to the nucleus, which then ruptures the nuclear membrane and facilitates the extrusion of nuclear chromatin-derived NETs (Neumann *et al.,* 2014).

1.3 Microbial virulence factors used to bypass NET effects

Bacteria are known to possess virulence factors that enable them to evade host-defence mechanisms, thereby increasing the likelihood of bacterial survival and dissemination. Some bacterial evasion strategies are believed to target the NET response with the aim of escaping this form of extracellular entrapment and killing.

1.3.1 Formation of a bacterial capsule

The expression of a bacterial capsule comprising a layer of polysaccharides can mimic the host's sialic acids. This allows bacteria to conceal their antigenic molecules, which would otherwise be recognised by the host's immune cells and trigger innate and acquired immune responses (Moxon & Kroll 1990). Capsule expression has recently been shown to allow the fungal pathogen, *Cryptococcus neoformans* (*C. neoformans*), to evade NET production. It

was discovered that compared with a mutant strain, the WT capsular fungus inhibited neutrophil ROS production in PMA-stimulated neutrophils. Considering NET production is largely ROS-dependent, dampened ROS responses may be responsible for the attenuated NET production observed (Rocha *et al.,* 2015). In addition, Wartha *et al.,* (2007) observed that *S. pneumonia* trapped in NET structures were resistant to killing compared with the non-capsulated serotype of the same organism. The evasion mechanism appears to be the result of a polysaccharide capsule and the incorporation of a positive surface charge, which repels the positively charged AMPs within the NETs. Conversely, some bacteria do not attempt to prevent recognition by immune cells, but rely on exaggerated responses to bring about pro-inflammatory activity. Lauth *et al.,* (2009) demonstrated that GAS express a crucial virulence factor, M1 protein, which causes the production of excessive NETs relative to M1 KOs. Subsequent to increased NET production, M1 also promoted GAS survival by conferring a resistance to AMPs and thus inhibiting NET-mediated killing.

1.3.2 Bacterial surface charge modifications

Bacterial surface charge modifications can also facilitate bacterial survival in the host. By altering their usual anionic (negative) surface charge, bacteria are thought to bypass specific innate responses (Ernst *et al.,* 1999). AMPs harbour positive cations, which allow them to electrostatically bind to bacterial surfaces. NETs provide a high local concentration of AMPs in the extracellular milieu, however if the bacterial surface charge is altered, the AMPs can be repelled rendering NETs ineffective. Surface modifications employed by the Gram-negative bacteria*, S. flexneri,* allow it to escape neutrophil killing. *S. flexneri* were found to utilise their negatively charged surface to bind AMPs derived from neutrophil degranulation. This enhanced bacterial adherence resulted in hyper-invasion into epithelial cells and the authors postulated that *S. flexneri* rely on its adherence to AMPs to disseminate into epithelial cells

and escape neutrophil killing. However this appears to be counter-intuitive, as whilst the bacteria may be conferred with enhanced invasion capabilities allowing dissemination into epithelial tissues, they would also surely be susceptible to AMP killing (Eilers *et al.,* 2010).

1.3.3 Deoxyribonucleases (DNases)

One virulence strategy that appears to be specifically directed at NET structures involves the release of bacterial DNases. DNases target the DNA backbone of NETs, thus disassembling the network of AMPs. DNase production by Gram-negative bacteria, and to a lesser extent, Gram-positive bacteria, has been recognised for many years (Porschen & Sandra 1974), but has lacked a logical explanation. However, the discovery of NETs provides a rationale for bacterial DNase release and it seems logical to hypothesise that invading bacteria may promote their survival by degrading NETs. A recent study in mice revealed that treatment with human recombinant deoxyribonuclease (rhDNase) results in decreased NET-derived antimicrobial activity. Notably, rhDNase treatment during polymicrobial sepsis facilitates sepsis progression, increased murine mortality and perturbed neutrophil function. Increased neutrophil infiltration was also observed in the lungs and liver of mice treated with rhDNase, and was associated with severe tissue damage. It is possible that the increased neutrophil recruitment is a compensation strategy for attenuated NET bactericidal activity. These findings suggest that NETs play a pivotal role in the elimination of bacteria *in vivo* (Meng *et al.,* 2012). Similar findings have been observed in mono-microbial infections with *S. aureus.* Berends *et al.,* (2010) investigated the ability of NETs to kill a WT *S. aureus* strain and a nuclease deficient mutant strain. The nuclease deficient strain of *S. aureus* was susceptible to entrapment and killing by NETs, while the WT organism exhibited resistance.

1.4 The role of NETs in the immune response

NETs may be fundamental to containing sizeable pathogens in a plaque biofilm, which may be too large to remove by phagocytosis, such as fungal hyphae (Branzk *et al.,* 2014). The nuclear chromatin backbone is negatively charged and it is likely that the charge interactions between NETs and the pathogens' cell surface cause microbial immobilisation (Figure 1.7). Indeed, NETs have been found to trap a significant majority of microorganisms, including Gram-positive and Gram-negative bacteria (Brinkmann *et al.,* 2004).

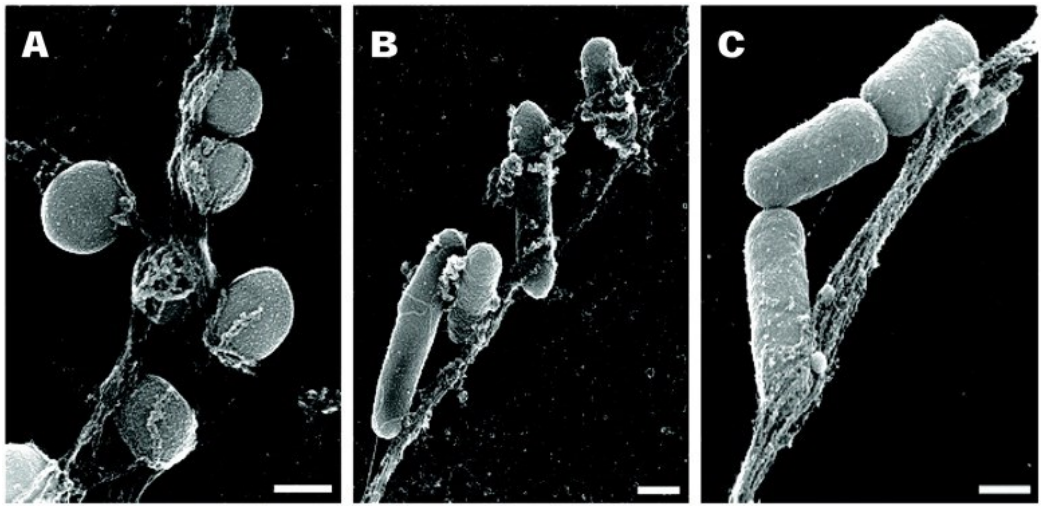

Figure 1.7: NETs associated with bacteria
Scanning electron micrographs illustrating (a) *Staphylococcus aureus* (Gram-positive), (b) *Salmonella typhimurium* (Gram-negative) and (c) *Shigella flexneri* (Gram-negative) interaction with NET structures. Neutrophils were primed with 100ng of IL-8 for 40 mins prior to infection. (Scale bar represents 500nm) (Adapted from Brinkmann *et al.,* 2004).

NET-associated proteases, such as NE, can elicit bactericidal activity against Gram-positive and Gram-negative bacteria by degrading bacterial virulence factors (Brinkman *et al.,* 2004). MPO is also reported to be involved in NET-mediated microbial killing. In a recent study where *S. aureus* were incubated with NETs, the growth of colonies following incubation indicated that NETs did not affect bacterial viability. However the addition of H_2O_2, which

functions as a substrate for MPO in the generation of HOCl, led to the killing of the bacteria. It is possible that in inflamed tissues, there is a continued recruitment of neutrophils, which provides a source of H_2O_2 to enable the production of HOCl by NET-bound MPO, resulting in a lethal environment in the extracellular space (Parker *et al.,* 2012).

As well as acting as a trigger for NET release, the presence of NET-bound LL-37 has been strongly correlated with NET antimicrobial activity (Kaplan & Radic 2012). This fortuitous association inferred that a high local concentration of LL-37 in the extracellular milieu may have bactericidal properties. However, earlier studies by Weiner *et al.,* (2003) showed that the interaction between LL-37 with DNA resulted in LL-37 losing its antimicrobial activity against *Pseudomonas spp* bacteria. This considered; a recent publication by Neumann *et al.,* (2014) sought to characterise the exact contribution of NET-bound LL-37 to bacterial killing. The authors found that LL-37 is a cationic molecule that can bind to extracellular DNA and prevent the action of bacteria-derived nucleases. Virulent nucleases released by invading bacteria, such as *S. aureus* and *S. pneumoniae,* allow them to degrade NETs and thus evade this immune killing mechanism. Subsequently the association of LL-37 with NET-DNA is postulated to promote NET longevity during their encounter with nuclease-producing bacterial species (Neumann *et al.,* 2014).

Histones are also proposed to elicit antimicrobial properties against Gram-positive and Gram-negative bacteria, including *S. flexneri* and *S. aureus* respectively (Brinkmann *et al.,* 2004). Antibody neutralisation of histones, both NET-bound and purified histones, causes increased bacterial viability, indicating that histones do participate in NET-mediated killing. However, it is likely that histone antimicrobial activity is pathogen specific, as *C. albicans,* in both fungal and hyphal forms, appears to demonstrate resistance to histone treatment and remains viable (Urban *et al.,* 2006).

In addition to fighting bacterial pathogens, NETs are equipped to defend against viral challenge. The role of NETs in viral infections is less well understood than in bacterial infections, however recent findings by Jenne *et al.,* (2013) demonstrated that NETs are produced following the systemic administration of poxvirus in a mouse model. This is believed to be the result of the concurrent recruitment of neutrophils and platelets, as already alluded to, platelets are capable of activating NET release. The importance of extracellular DNA was evident following DNase degradation, which led to increased viral survival and dissemination. Supporting the contribution of NETs to the host's response to viral infections, NET release is also believed to be important in human immunodeficiency virus (HIV)-1 infection. The interactions of the NET-bound components, MPO and α-defensin, have been reported to inactivate HIV-1 (Saitoh *et al.,* 2012).

A further consideration is the participation of NETs in facilitating the acquired immune response. NET production may provide a link between the innate and acquired immune responses. NETs can directly prime helper T-cells ($CD4^+$) and cytotoxic T-cells ($CD8^+$), which has been shown to elevate T-cell responses by decreasing their activation threshold. NET-mediated activation of T-cells resulted in increased cytokine release, proliferation and surface marker expression. Collectively, the presence of NETs can bridge the gap between the innate and acquired immune systems, providing for a more efficient activation of specific immune responses (Tillack *et al.,* 2012). NETs can also interact with the classical pathway of the host's complement system. The classical pathway plays a key role in the humoral branch of the immune response, and involves opsonising foreign microorganisms to facilitate the lysis of the target pathogen. Binding of C1q to NET DNA initiates the activation of the classical pathway (Leffler *et al.,* 2012).

1.5 NET degradation and removal

Following the discovery of NETs in 2004, investigations into NET removal have only been performed recently. Whilst it is appreciated that the appropriate removal of NETs is essential for tissue homeostasis, the time scale and processes involved in this are not yet fully understood. In 2010 it was reported NETs produced *in vitro* are stable for over 90 hours. However NET treatment with human sera results in the degradation of extracellular NET-DNA. The authors deduced that it was the acquisition of serum-derived DNase 1 that was responsible for deconstructing the NETs, as specifically chelating calcium impeded NET degradation (Hakkim *et al.,* 2010) (Figure 1.8). NET degradation by DNase 1 is believed to represent the initial stage in NET clearance, which facilitates their subsequent removal by macrophages. Following disassembly, NET histones and DNA are opsonised by complement component C1q, which causes phagocytosis of NET debris by macrophages. It is postulated that NETs are then degraded in the lysosomal compartment of the macrophage; however the specific nucleases involved in this process remain elusive. Key to this process is that NET clearance resembles a mechanism similar to that of apoptosis, whereby macrophages appear non-phlogistic and do not release pro-inflammatory cytokines (Farrera & Fadeel 2013).

1.5.1 Host-derived DNase

DNases may also be necessary to maintain a normal tissue homeostasis, such as in fertilisation, where NETs are produced by "sperm-activated neutrophils", which may entrap and immobilise spermatozoa. Artificial insemination of spermatozoa alongside seminal plasma was found to increase the chance of fertilisation, which is believed to be due to the presence of DNase in the seminal plasma preventing NET entrapment and facilitating motility of the spermatozoa (Alghamdi *et al.,* 2005). The importance of host DNase production is also evident in cystic fibrosis (CF) (see section 1.6.3), where it has been proposed that not only are NETs detrimental to the host, evidenced by the fact that NET

production is positively correlated with impaired obstructive lung function (Marcos *et al.,* 2010), but DNase may have utility in CF treatment. The administration of DNase as an adjuvant therapy alongside current anti-proteases facilitates NET degradation and thus the removal of potentially immunogenic structures (Papayannopoulos *et al.,* 2011).

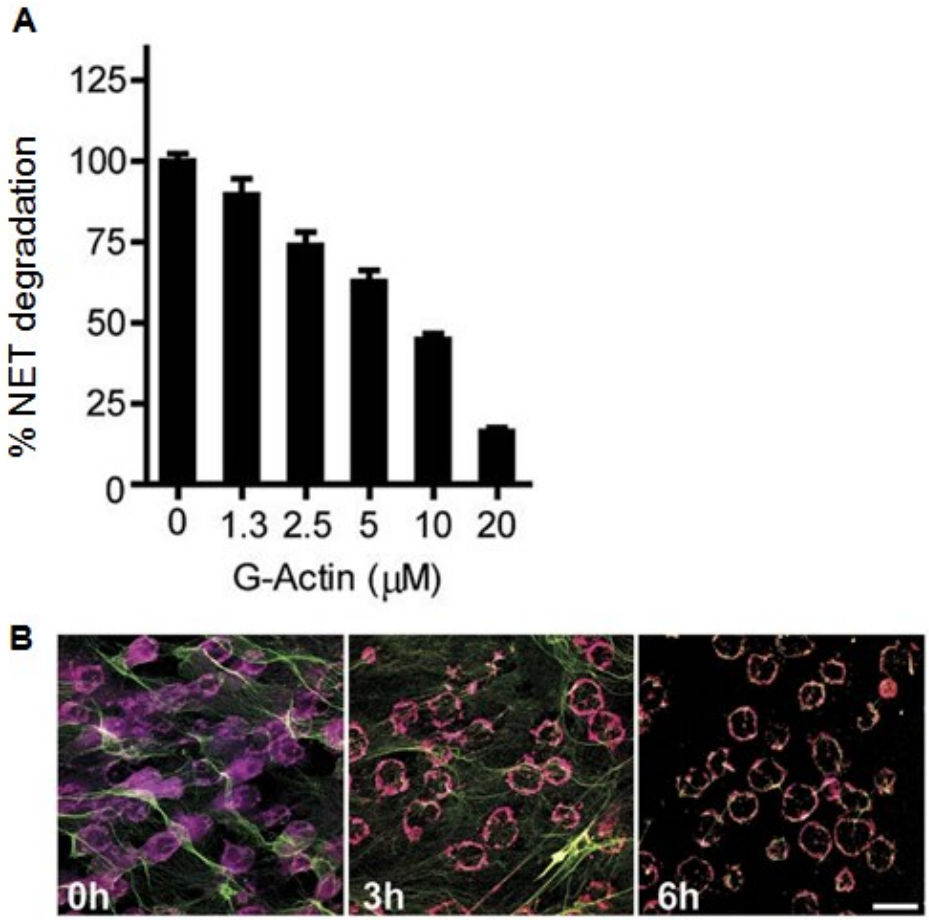

Figure 1.8: NET degradation by DNase 1
(a) NETs were incubated with healthy DNase-containing serum (10%) for 6 hours in the presence of G-actin. NET degradation was inhibited in a concentration-dependent matter following treatment with G-actin, a specific DNase 1 inhibitor. (b) Neutrophils were stimulated to produce NETs and were subsequently incubated with 10% serum for 0, 3 or 6 hours. The cells were fixed and immunostained for histones (red), DNA (blue) and MPO (green). There were considerably fewer NETs following incubation with serum. Scale bar represents 10μm (Hakkim *et al.,* 2010).

1.6 NETs and autoimmune processes

In contrast to the proposed beneficial anti-infectious role of NETs, excess NET formation has been associated with deleterious effects in a range of pathologies. Whilst the extracellular DNA and high localised concentrations of AMPs function to remove invading pathogens, they concomitantly provide a source of cytotoxicity; therefore perturbed NET release or delayed NET clearance may initiate undesirable immune processes.

1.6.1 Rheumatoid arthritis (RA)

Rheumatoid arthritis (RA) is a chronic systemic inflammatory disease that causes inflammation of joints, causing pain, swelling and restricted movement. Neutrophils play an active role in RA, by processes such as the release of cytokines and interacting with other immune cells. RA patient neutrophils exhibit hyperactivity in terms of ROS generation and have elevated concentrations of granule proteins in the synovial fluid, which have been linked to collateral tissue damage (Wright *et al.,* 2014). RA patients are known to release autoantibodies, namely rheumatoid factor (RF) and anti-citrullinated protein antibodies (ACPA). RA patients also exhibit higher levels of circulating pro-inflammatory cytokines, including TNFα (Wright *et al.,* 2014). Neutrophils from RA patients reportedly have a greater propensity to produce NETs compared with healthy controls. Notably, patient derived RF, ACPAs and higher levels of pro-inflammatory cytokines reportedly stimulate healthy neutrophils to release NETs. RA patients are therefore susceptible to excessive NET production in both circulating and RA synovial fluid neutrophils (Khandpur *et al.,* 2013). As previously discussed (section 1.2.1), NETs are dependent on the enzymatic actions of PAD4 (Wang *et al.,* 2009), which is essential for NET release, as NETs have been found to harbour citrullinated proteins in their extracellular structures. Interestingly, ACPAs react with citrullinated histone H4, indicating that NETs may provide a source of autoantigenic histones

that enhance ACPA formation (Pratesi *et al.,* 2014). This may bring about a vicious cycle characterised by increased NETs and subsequent increased ACPA levels. The authors also demonstrated that elevated levels of NETs were associated with more severe clinical endpoints, such as increased joint destruction. Moreover, there is significant interest in the association between RA and periodontitis, with NET production in periodontal tissues serving as a plausible mechanism for ACPA generation following a break in immune tolerance to citrullinated proteins released by neutrophils (dePablo *et al.,* 2009). In addition the periodontal pathogen, *P. gingivalis,* possesses a unique PAD enzyme that functions similarly to that of the mammalian isoform (Wegner *et al.,* 2010). *P. gingivalis* PAD (PPAD) may citrullinate *P. gingivalis* proteins in a form of molecular mimicry or may citrullinate host proteins, thus generating ACPAs.

1.6.2 Systemic lupus erythematosus (SLE)

Systemic lupus erythematosus (SLE) is an autoimmune disease caused by a loss of tolerance to self-antigens that results in autoantibody production against nuclear antigens including double-stranded DNA (dsDNA) and histones. Neutrophils are understood to play a predominant role in disease mechanisms that contribute to the pathogenesis of SLE (Yu & Su 2013). In addition to exaggerated neutrophil activation, SLE neutrophils reportedly display abnormal phagocytosis, increased aggregation and elevated apoptosis (Abramson *et al.,* 1983; Courtney *et al.,* 1999). Anti-neutrophil cytoplasmic antibodies (ANCAs) are present in 25%-56% of SLE patients (Fauzi *et al.,* 2004) and NETs may therefore perpetuate SLE, as they contain multiple neutrophil-derived granular proteins that act as immunogens. Notably, it has recently been reported that NET clearance by sera is impeded in a subset of SLE patients. To establish the mechanisms preventing NET disassembly by DNase 1, Hakkim *et al.,* (2010) identified two processes that resulted in reduced NET removal. In one group of "poor

degraders", DNase 1 inhibitors were believed to be responsible. However, some individuals exhibited elevated levels of anti-NET antibodies, which were thought to provide a physical barrier that blocked enzymatic NET degradation by host DNases. Abrogated NET clearance in some SLE patients was also confirmed by Leffler *et al.,* (2012) in a different patient cohort. However Leffler *et al.,* (2012) found that DNase 1 treatment could augment NET degradation in all "poorly degrading" patients, indicating the absence of DNase inhibitors. Conversely, it was found that NETs could bind C1q, a component of the classical complement pathway. Whilst the deposition of C1q is believed to facilitate NET phagocytosis by macrophages (Farrera & Fadeel 2013), Leffler *et al.,* (2012) proposed that C1q may concomitantly provide a physical barrier preventing enzymatic disassembly by DNase 1. The delayed removal of NETs may provide a source of citrullinated autoantigens in the extracellular space, such as nuclear chromatin and AMPs, which may indeed promote anti-dsDNA titres and therefore contribute to SLE pathogenesis (Khandpur *et al.,* 2013).

1.6.3 Cystic fibrosis (CF)

Cystic fibrosis (CF) is an autosomal recessive disease caused by a mutation in the cystic fibrosis transmembrane conductance regulator (CFTR) gene, which is associated with mucocilary dysfunction characterised by excess amounts of abnormal mucus. Despite an excessive inflammatory response, patients are unable to effectively eradicate bacteria inhaled into the lungs, such as *Pseudomonas aeruginosa* (Gifford & Chalmers *et al.,* 2014, Lyczak *et al.,* 2002). The neutrophil is the predominant immune cell in CF; however whilst their recruitment facilitates defence against the bacterial challenge, neutrophil accumulation and their compromised clearance concomitantly fuels the inflammatory response associated with disease progression. In addition, CF neutrophils are believed to be less responsive to anti-inflammatory signals released by IL-10, which perpetuates the inflammatory response (Petit-

Bertron *et al.,* 2008). Following this, the excessive production and accumulation of NETs in CF patients is reported to exacerbate disease development. Recent findings have identified a specific chemokine receptor, CXCR2, believed to facilitate NADPH-oxidase independent NET release in CF patients. This was confirmed by CXCR2 inhibitors that negated NET production and may represent a therapeutic target in CF patients, as interestingly, inhibited NET production was not reported to affect antimicrobial defence (Marcos *et al.,* 2010). It is likely that exaggerated NET production in CF produces NET-bacteria complexes, which if not removed efficiently, provide a source of autoantigens that trigger further inflammatory episodes. As previously discussed (1.5.1), DNase inhalation therapy has been found to improve lung function in CF by digesting NET structures within the mucous (Saffarzadeh *et al.,* 2013).

1.7 Periodontitis

Periodontitis is the most prevalent chronic inflammatory disease of humans, and severe periodontitis represents the sixth most common disease worldwide (Kassebaum *et al.,* 2014). In the UK, 45% of all adults have periodontitis, defined by periodontal pockets measuring ≥4mm (Adult Dental Health Survey 2009, White *et al.,* 2012). Periodontitis is believed to be the leading cause of tooth loss worldwide, but also impacts upon speech, function, nutrition and quality of life. Moreover, periodontitis has far reaching consequences for general health contributing to elevations in the systemic inflammatory burden, which is associated with increased risk of age-related conditions including cerebrovascular accident (CVA) (Grau *et al.,* 2004), atherosclerosis (Pinho *et al.,* 2013) and RA (Smit *et al.,* 2012). It is well recognised that periodontitis is the result of a bacterially evoked inflammatory response in susceptible individuals, which leads to tissue destruction and disease progression (Figure 1.9). This results in periodontal pocket formation, gingival bleeding and alveolar bone

destruction (Bascones-Martínez *et al.,* 2009). Periodontitis and gingivitis represent two inflammatory processes affecting the tissues surrounding the teeth (the periodontium), in response to bacterial accumulation in the form of a plaque biofilm.

Figure 1.9: Clinical symptoms of chronic periodontitis
Image from a 50 year old female patient with chronic periodontitis illustrating inflammation, calculus formation and recession with drifting of upper left central incisor due to bone loss (courtesy of Professor I. Chapple).

Gingivitis is a reversible inflammatory condition limited to the gingival tissues and unlike periodontitis; the inflammatory response does not ultimately result in connective tissue attachment loss and alveolar bone destruction. Periodontitis is believed to be preceded by gingivitis. Progression to periodontitis arises when inflammation is not limited to the gingiva but spreads to the deeper periodontal tissues, causing a deep gingival crevice (known as the periodontal pocket) between the tooth and lining epithelial surface (Kinane 2001). However, the transition from gingivitis to periodontitis only arises in susceptible individuals, which may be as a result of exposure to a variety of risk factors, e.g. smoking, plaque accumulation, diabetes or genetic predisposition (section 1.7.3). Notably according to Löe *et al.*, (1986) approximately 10% of the population is completely resistant to the disease.

1.7.1 Role of the microbial biofilm in periodontitis

Periodontitis is initiated by the accumulation of bacterial plaque at, and below, the gingival margin (Figure 1.10). Indeed it has been estimated that ~500 oral bacterial species and ~1200 predominant phylotypes exist (Paster & Dewhirst 2009, Dewhirst *et al.,* 2010). Of these bacterial species, 5 major bacterial complexes (red, orange, yellow, green and purple) have been identified by Socransky *et al.,* (1988). The clustering and ordination analysis allowed Socransky to assign microbial species to a colour complex dependent upon the strength of association with each other and the clinical staging of periodontitis (Figure 1.11). For example, bacteria assigned to orange and red complexes denote late stage colonisers associated with the subgingival plaque. Bacteria have also been categorised according to their location in relation to the gingival margin: supragingival or subgingival. Whereas the supragingival plaque contains facultative species (such as *Streptococcus* species), the subgingival plaque is dominated by a Gram-negative anaerobic motile microbiota (Loesche *et al.,* 1982). The role of bacteria in periodontitis has historically been encapsulated in two different hypotheses, describing how microflora may contribute to the host response and disease pathogenesis. The "non-specific hypothesis" (Loesche 1976) proposes that the entire microbial flora contribute to the disease and once a threshold quantity is reached, periodontitis will occur. Alternatively, the "specific hypothesis" (Theilade 1986) proposes that the presence of particular pathogenic bacterial species is necessary for the diseased state (Loesche & Grossman 2001). A third model was introduced by Marsh (1994), the "ecological hypothesis", which encompasses both previous hypotheses. This model proposes that an inflammatory response is initiated as a direct result of the accumulation of a pathogenic subgingival microbiota, which triggers a shift away from microbial homeostasis, encouraging the growth of proteolytic and anaerobic bacterial species. The colonisation of multiple bacteria in the generation of a mature plaque biofilm is a highly organised sequential

process. The biofilm is orchestrated to maximise adherence, communication, survival and the accumulation of other bacterial species. Oxygen levels, environmental exposures and competing commensal bacteria will all determine microbial growth and govern the locality of where each bacterial species will thrive (Feng & Weinberg 2006). The biofilm encloses the bacterial community and protects it from mechanical and chemical disruption; however a synergistic and antagonistic relationship exists between bacteria (Koll-Klais *et al.,* 2005). Development of the plaque biofilm is initiated by deposition of salivary components, such as glycoproteins (termed the acquired pellicle), onto the tooth surface prior to deposition of early colonising bacteria. The acquired pellicle provides receptors on the tooth surface for microorganisms to adhere to; routinely *Streptococci* species are the first to adhere, representing 60-90% of the initial colonisers (Nyvad & Kilian 1987). Subsequent to initial colonisation, secondary colonisers adhere via co-adhesion and co-aggregation, increasing the biofilm size and complexity. Particular bacterial species appear to play a more dynamic role. For example *Fusobacterium nucleatum* (*F. nucleatum*), a Gram-negative anaerobe that is present in periodontally diseased sites, is not generally classified as an early or late coloniser, but is a quorum sensing organism believed to facilitate biofilm formation (Kolenbrander *et al.,* 2009, 2010). A health promoting biofilm is essential for periodontal health, as bacteria exist symbiotically with each other and the host. However, if the biofilm is allowed to mature and is not frequently disrupted, then pathogenic species emerge. Dysbiosis results in susceptible individuals and the host-microbial equilibrium is lost, which can result in the onset of disease (Hajishengallis 2014).

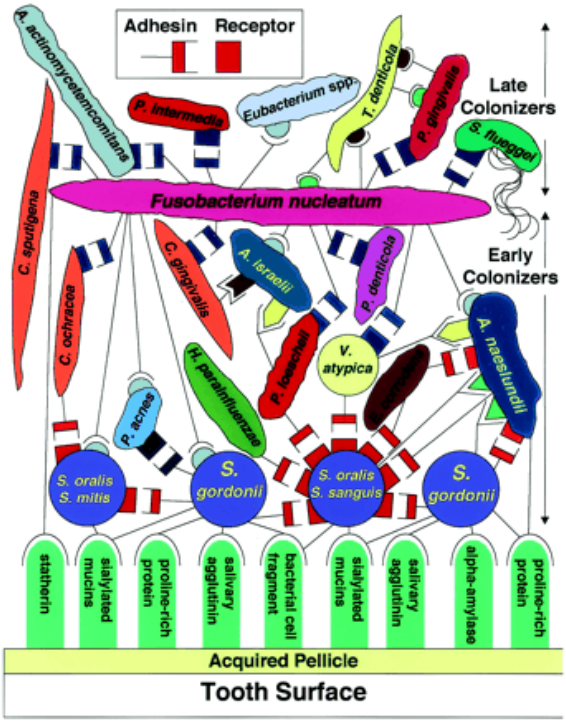

Figure 1.10: Sequential bacterial colonisation which results in the formation of a plaque biofilm

The acquired pellicle (yellow), containing receptors (green), is deposited onto the tooth surface. Early colonisers (blue) bind to their complementary receptors (black lines), followed by the adherence of secondary colonisers. Sequential binding enables co-aggregation between different species, which bridges the gap between bacteria. *F. nucleatum* (pink) bridges early and late colonisers, allowing interaction between the two groups. Co-aggregation is represented by complementary shapes, for example the top left depicts adhesion (red and white, with stem) and it's receptor (red, no stem) (Kolenbrander *et al.,* 2002).

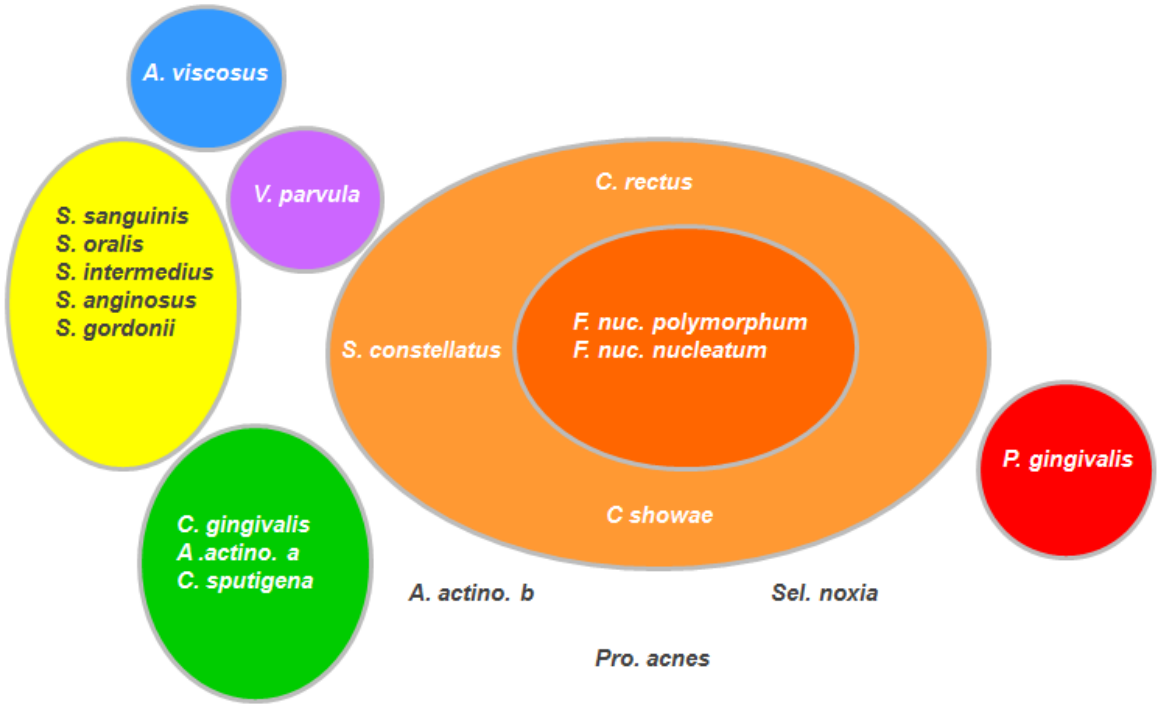

Figure 1.11: Periodontal bacteria assigned to the Socransky colour complexes
Diagrammatic representation indicates the relationships between specific bacterial species within the colour complexes. The complexes also provide a possible sequence of colonisation in the biofilm and the associations with the clinical parameters of periodontitis. The bacteria listed above represent the panel of bacterial species employed in this thesis (adapted from Socransky *et al.,* 1998).

1.7.2 The contribution of the immune response to host periodontal tissue damage

Periodontitis occurs as a result of dysbiosis, which involves an increase in harmful periodontal bacteria that become established in the host (Hajishengallis 2014) (Figure 1.12). However, the microbial biofilm thrives by exploiting the host response, in particular the neutrophil-mediated inflammatory response in susceptible individuals. This fuels a vicious cycle of bacterial accumulation, inflammation and subsequent tissue destruction. The acute inflammatory response is initially protective, providing the recruitment of neutrophils, the activation of innate neutrophil-derived defence mechanisms and the activation of the acquired cellular and humoral immune response. However in periodontitis, the neutrophil response is reputed to unintentionally contribute to the progression of periodontitis causing collateral

tissue damage, which perpetuates the inflammation leading to chronicity and providing nutrients for pathogenic bacteria like *P. gingivalis* to survive and proliferate (Scott & Krauss 2012). A common hypothesis for the involvement of the host in periodontitis pathogenesis is that neutrophils exhibit hyperactivity and hyper-reactivity in response to the biofilm. This exaggerated immune response is exemplified in the systemic neutrophils derived from chronic periodontitis patients. PBNs are reportedly hyper-reactive in response to a microbial challenge, but also hyperactive in the absence of an exogenous stimulus (Matthews *et al.,* 2007a, 2007b). In addition, excessive proteolytic activity has been observed in periodontitis patients, which normalised following successful treatment. This is thought to be partly attributed to the increased intensity of protease-activated receptor-2 (PAR_2) expression in chronic periodontitis. PAR_2 is a receptor present on multiple cells, including neutrophils, and is involved in the initiation of an inflammatory response via interactions with bacterial proteases (Lourbakos *et al.,* 1998). Increased PAR_2 expression can promote the production of cytokines and proteolytic enzymes, such as IL-6, IL-8 and matrix metalloproteinase (MMP)-9 (Holzhausen *et al.,* 2006). MMPs are a family of proteolytic enzymes that function to degrade extracellular matrix molecules during physiological and pathophysiological tissue remodeling. However these proteolytic agents are also thought to be key proteinases involved in periodontal tissue destruction. Periodontal bacteria, including *F. nucleatum* and *P. gingivalis,* trigger the extracellular release of MMPs. MMP release is regulated by endogenous inhibitors, such as the tissue inhibitors of metalloproteinases (TIMPs), however neutrophils do not produce this inhibitor *de novo* (Masure *et al.,* 1991) and it is thought this inhibitory mechanism is overwhelmed in periodontitis (Romanelli *et al.,* 1999). The elevated release of MMPs facilitates tissue degradation, which is likely to be exacerbated by the heightened recruitment of neutrophils in periodontitis. Other neutrophil serine proteases also associated with tissue degradation include NE and CG. NE can contribute to tissue

destruction by degrading molecules such as collagen and fibronectin and has been positively correlated with periodontal attachment loss (Armitage *et al.,* 1996). Interestingly, CG can activate MMP-8 (Ding *et al.,* 2005) and has been found to be higher in periodontitis patients (Tervahartiala *et al.,* 1996). It has been proposed that the elevated release of NE is the result of a genetic polymorphism that leads to neutrophils with an intrinsically elevated function. For example neutrophils from individuals with a (131 H/H) polymorphism of the Fcγ-receptor are associated with more severe periodontitis. These individuals also overexpress degranulation markers, CD63 and CD66b, resulting in increased NE release when challenged with an infectious agent (Nicu *et al.,* 2007).

Periodontitis is also associated with increased levels of cytokines, as a result of plaque bacteria initiating the recruitment of neutrophils. As already discussed, chemokines orchestrate the directional movement of neutrophils to the infected periodontal tissues (see section 1.1.3). Chemokines have been suggested to be involved in bone resorption, as they play a role in maintaining the equilibrium between osteoblastogenesis (bone formation) and osteoclastogenesis (bone resorption) (Silva *et al.,* 2007), a loss of which may associate with alveolar bone resorption in periodontitis. Chemokines have been reported to be involved in multiple steps of the signalling cascade resulting in osteoclastogenesis. For example CXCR4 expressed on osteoclast precursor cells is involved in their chemotaxis and differentiation into osteoclasts (Wright *et al.,* 2005). Furthermore, chemokines can indirectly modulate osteoclastogenesis by possessing ligands that can increase MMP-9 activity, which in turn facilitates tissue destruction and bone resorption (Grassi *et al.,* 2004). Cytokines are also deemed partly responsible for promoting bone resorption in periodontitis. This is evident in periodontitis patients, in whom IL-1β was found to be elevated at sites of recent bone and attachment loss (Lee *et al.,* 1995).

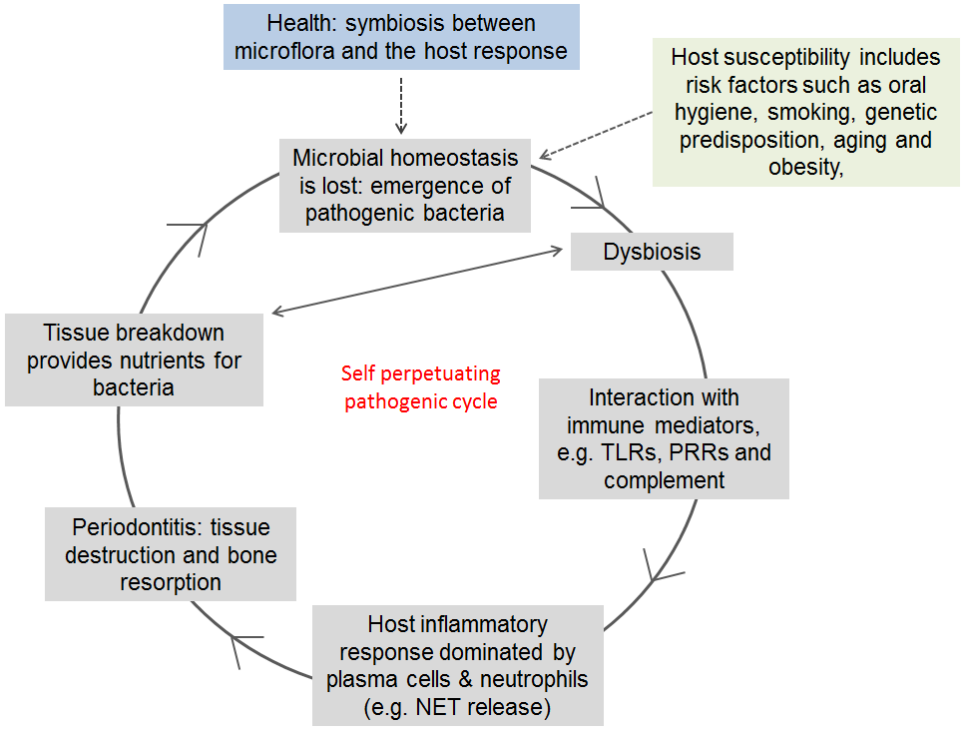

Figure 1.12: The pathogenic model of periodontitis
In susceptible individuals, the equilibrium between commensal and periodontal bacteria is lost; giving rise to polymicrobial dysbiosis. This triggers activation of immune cells, for example by toll-like receptors (TLRs), pattern recognition receptors (PRRs) and complement. This triggers an inflammatory response, in which neutrophils are the predominant immune cell. Whilst aiming to contain the bacteria attempting to colonise the epithelium, neutrophil immune responses concurrently cause tissue damage. This provides nutrients which bacteria utilise to proliferate, which promotes further dysbiosis (adapted from Hajishengallis 2014).

However, it is noteworthy that whilst neutrophil hyperactivity likely exacerbates periodontal tissue destruction, impaired neutrophil activity can also increase disease severity. Multiple diseases characterised by a deficient immune response are also correlated with severe periodontitis. For example Papillon Lefèvre syndrome (PLS) is an autosomal recessive disease in which a mutation in the cathepsin C gene (*CTSC*) results in a failure to encode lysosomal cysteine protease, cathepsin C. Disease is characterised by palmoplantar hyperkeratosis (abnormal thickening of the skin on the palms of the hands and soles of the feet), significant pre-pubertal periodontal attachment loss, alveolar bone destruction, and the

subsequent loss of primary and permanent dentition (Singh *et al.,* 2011). *CTSC* is essential for post-translational trimming of serine proteases, e.g. granule-associated neutrophil serine proteases (NSP) including NE, CG, PR3 and the recently described neutrophil serine protease 4 (Perera *et al.,* 2013). *CTSC* removes N-terminal amino acids that block the active site of the proteases and is thus necessary for activation of these proteases. These proteases are stored as active enzymes in neutrophil granules, and localise to primary granules (azurophilic) (Figure 1.13). NET production has recently been found to be impeded in a female PLS patient (homozygous missense mutation in the *CTSC* gene) and the authors report that this is due to decreased NE, which necessitates NET release (Sorensen *et al.,* 2014). As ROS is not inhibited in PLS patients, it is unlikely that reduced NET production is due to aberrant NADPH-oxidase production (as in CGD). Whilst CGD patients also fail to generate NETs, there are contradictory findings as to whether these individuals suffer from rapidly progressing periodontitis (Budeneli *et al.,* 2001, Cohen *et al.,* 1985). Notably, the mild immunodeficiency in PLS patients indicates that NET formation is not a major antimicrobial defence mechanism, however the exact process that leads to such aggressive periodontitis with clinically severe inflammation in PLS remains elusive. Furthermore, patients with cyclic neutropenia who have considerably fewer neutrophil numbers are susceptible to severe periodontitis (Matarasso *et al.,* 2009).

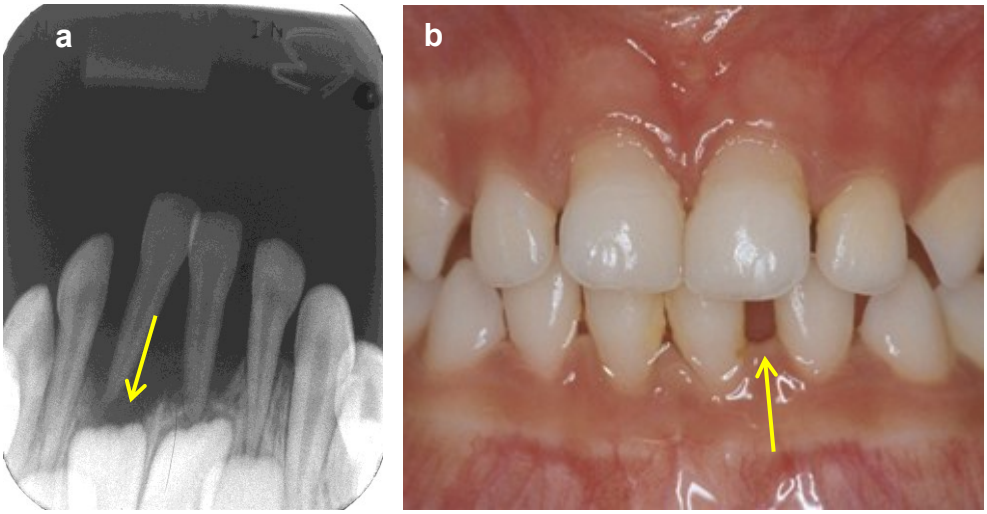

Figure 1.13: Clinical signs and symptoms in a PLS case study
Intraoral periapical radiograph (a) and clinical photograph (b) from a 4 year old male with PLS. The images show generalised gingival recession and severe periodontal destruction, indicated by the yellow arrows (courtesy of Professor I. Chapple).

The importance of the host response is also evident in KO mice deficient in the chemokine, CXCR2. Upon infection with *P. gingivalis,* CXCR2 KO mice had elevated periodontal bone destruction compared with WT mice (Jeffrey *et al.,* 2007). Interestingly, as previously discussed (1.6.3) CXCR2 is also postulated to be required for NET release in an NADPH-oxidase independent mechanism (Marcos *et al.,* 2010). Collectively these results highlight that both a hyperactive and deficient neutrophil response are associated with increased disease. It is therefore likely that a homeostatic imbalance in the immune response contributes to the initiation and development of disease in susceptible individuals.

1.7.3 Risk factors for periodontitis

Substantial epidemiological data exists which have identified the risk factors contributing to the initiation and progression of periodontal disease. These include poor oral hygiene (Kakudate *et al.,* 2008), smoking (Bergstrom *et al.,* 2000), obesity (Gocke *et al.,* 2014),

poorly controlled diabetes (Demmer *et al.*, 2012), genetic predisposition (Divaris *et al.,* 2013), stress (MousaviJazi *et al.,* 2013) and osteoporosis (Esfahanian *et al.,* 2012). The understanding that periodontitis only affects a proportion of the population who exhibit atypical susceptibility has fuelled further research to understand the importance of specific risk factors. Cigarette smoking is considered to be a major risk factor in the development of periodontitis (Grossi *et al.,* 1994, 1995). Tobacco smoking causes the inhalation of over 4000 toxins and is associated with many diseases, including cardiovascular disease (Burns 1991, Ambrose *et al.,* 2004). Ragghianti *et al.,* (2004) reported an association between smoking and the clinical manifestations of periodontitis (Table 1.2). Worthy of note is that numerous studies have shown that smoking is positively correlated with poor oral hygiene; however even after adjustment for oral hygiene as a cofactor, smoking still appears to be a primary independent risk factor (Tonetti *et al.,* 1998). There is also a body of evidence suggesting that smoking adversely affects treatment responses, indeed considerably more smokers require additional treatment after the initial periodontal therapy (Delima *et al.,* 2010). These findings are supported by individuals who showed improved treatment outcomes following smoking cessation. A possible explanation for the increased prevalence of periodontitis amongst smokers is that smoking was found to select for specific periodontal bacteria, including *P. gingivalis, Treponema denticola* (*T.* denticola) and *Tannerella forsythia* (*T. forsythia*) (Zambon *et al.,* 1996). These are all bacterial species assigned to the red Sokransky complexes and are associated with severe disease. Smoking has also been found to adversely affect neutrophil function, indeed nicotine has been shown to promote neutrophil degranulation, which can cause an exaggerated response to the invading bacteria and induce local tissue damage (Soder *et al.,* 1999).

It has been reported that smoking can affect neutrophil total, extracellular and superoxide ROS production (Matthews *et al.,* 2011, 2012). High concentrations of cigarette smoke

extract (CSE) resulted in increased ROS production; however pre-treatment of neutrophils with lower concentrations of CSE had an inhibitory effect on subsequent ROS production in response to FcγR and TLR stimulation. In periodontitis, reduced ROS production in smokers may impede the elimination of periodontal bacteria; however in heavy smokers increased ROS production may facilitate oxidative stress and tissue damage. Intriguingly, neither nicotine nor cotinine were deemed responsible for the observed effects, as these did not directly alter ROS production. Notably, CSE was not found to be cytotoxic towards neutrophils, but did have an inhibitory effect on apoptosis. It is possible that transient exposure to cigarette smoke components may perturb the neutrophil response to bacterial infection if ROS species are not being generated accordingly. However in the absence of an exogenous stimulus, such as a bacterial biofilm, smokers may elicit excessive background ROS production, which could associate with collateral tissue damage. Abnormal neutrophil responses may therefore represent a crucial link between smoking and periodontitis.

Table 1.2: Effect of smoking status on periodontal health
Mean pocket depth (mm) and clinical attachment loss (mm) were measured in 380 periodontitis patients in Brazil. Smoking status (self-reported smoking habits: current smoker or non-smoker) was significantly correlated with disease severity (ANOVA and Tukey test: $p \leq 0.05$). Data expressed ± standard deviation (SD) (adapted from Ragghianti *et al.,* 2004).

Age (years)	Pocket depth (mm)		Clinical attachment loss (mm)	
	Non-smoker	Smoker	Non-smoker	Smoker
20-29	2.56 ± 0.54	2.80 ± 0.63	2.63 ± 0.57	2.91 ± 0.65
30-39	2.64 ± 0.51	3.09 ± 0.74	2.87 ± 0.58	2.52 ± 0.95
40-49	2.85 ± 0.72	3.02 ± 0.62	3.29 ± 0.81	3.81 ± 1.33
≥50	2.81± 0.69	3.37 ± 0.86	3.59 ± 1.02	4.25 ± 0.96

1.8 The role of NETs in periodontitis

Currently there is a paucity of literature investigating the role of NETs in the pathogenesis of periodontitis. As already discussed, chronic periodontitis patients elicit hyperactivity and hyper-reactivity in terms of ROS release (Matthews *et al.,* 2007a, 2007b) (section 1.7.2). This may represent a constitutive mechanism, in which increased baseline ROS production is involved in the onset of disease. Conversely, this could be a reactive mechanism as a result of a pathogenic biofilm and the development of periodontitis. It is possible that, given NET release is reliant on ROS generation; periodontitis may associate with exaggerated NET production. Recent evidence from our group suggests that neutrophil hyperactivity/hyper-reactivity may result from an altered intracellular ratio of reduced glutathione (GSH) to oxidised glutathione (GSSG), as well as defective GSH synthesis in periodontal patient neutrophils (Grant *et al.,* 2010, Dias *et al.,* 2013). Perturbed antioxidant functioning in chronic periodontitis may thus affect NADPH-oxidase dependent NET release. High concentrations of NET-associated cytotoxic components in the tissues may provide a source of autoantigens. This could be exacerbated if NETs are produced in excess or are not cleared

efficiently, which may result in further periodontal tissue damage. Vitkov *et al.,* (2009) employed microscopy to visualise NETs, which appeared abundant in gingival pocket epithelium, the gingival exudate and in the gingival crevicular fluid (GCF) of chronic periodontitis patients (Vitkov *et al.,* 2010) (Figure 1.14). The authors postulated that during the bacteria's attempt to migrate and adhere to the gingival surface, they encounter NETs which shield the epithelium and prevent adhesion. Interestingly, the bacterial counts in the purulent GCF exudate were relatively inconsistent, which led to the theory that if phagocytosis is overwhelmed, for example due to large numbers of colonising bacteria, NETs may compensate for the increased demand on the immune system by providing an additional neutrophil-defence mechanism. Further observations, such as the lack of neutrophils containing engulfed bacteria and the large quantities of NETs in the GCF suggest NETosis is the predominant defence mechanism employed by neutrophils in the GCF at periodontally diseased sites (Vitkov *et al.,* 2010). Worthy of note is that this research did not include healthy matched controls and that NETs were not quantified in the periodontal tissues. Indeed it would be interesting to compare GCF and periodontal tissue samples from periodontitis patients and matched controls to determine if any disparity exists in NET formation and accumulation. Preliminary findings presented in Cooper *et al.,* (2013) employed confocal microscopy and immunofluorescence staining to identify increased levels of NET-like structures in inflamed gingival tissues, compared with healthy control tissues (Figure 1.15). Supporting the theory of increased NETosis in periodontitis is that a range of molecules that are elevated in periodontitis, such as nitric oxide and interferon-α (IFNα), can also stimulate for NET release (Reher *et al.,* 2007, Wright *et al.,* 2008).

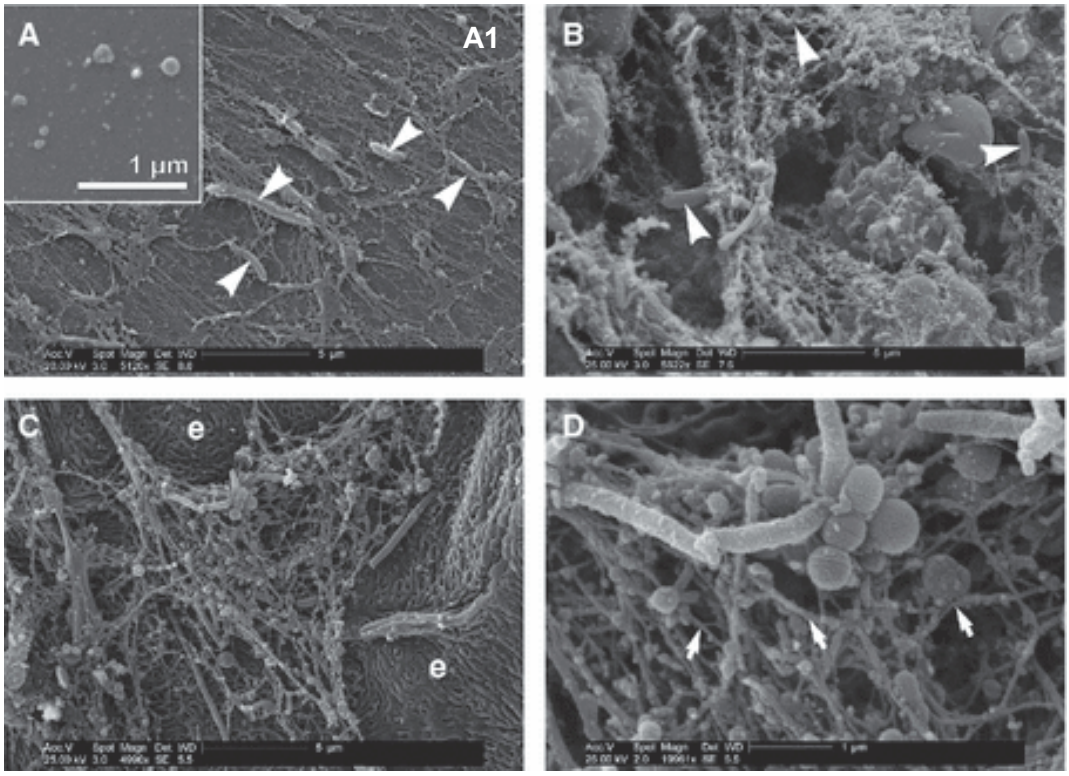

Figure 1.14: NET entrapment of periodontal bacteria
Scanning electron micrographs illustrating: (a1) Crevicular exudate containing bacteria (white arrowheads), contrast with (a), which has received DNase treatment (degrading NETs) and shows no entrapped bacteria. (b) Crevicular exudate with multiple large NETs entrapping bacteria (white arrowheads). (c) Pocket epithelium with entrapped bacteria, (e) denotes epithelium surface. (d) enlarged version of (c), showing NET fibres (small white arrowheads). Scale bar represents 5µm (a1, b, c), 1µm (a, d) (Vitkov *et al.,* 2009).

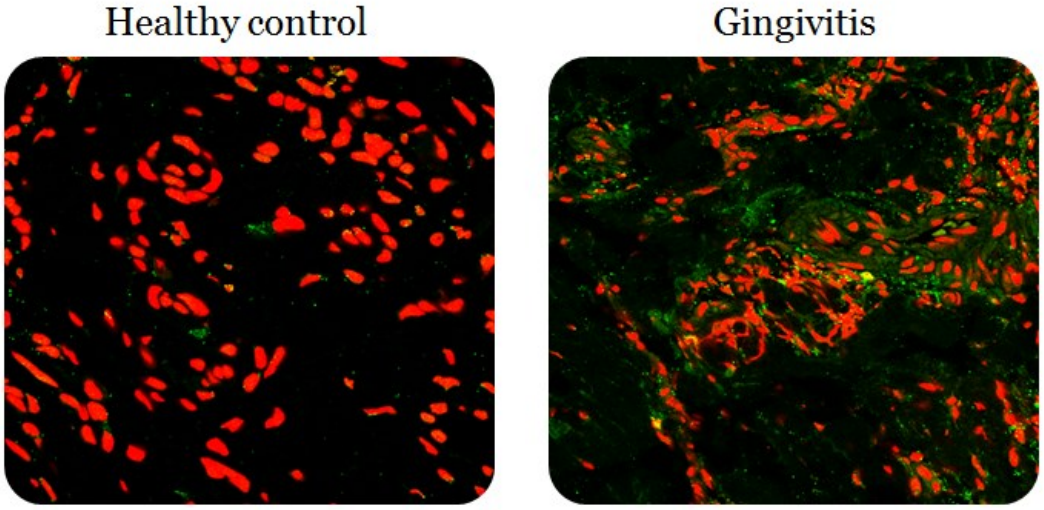

Figure 1.15: NETs in human gingival tissues
Confocal microscopy where DNA is stained red and MPO is stained green in gingival tissues in health and disease. Considerably more NET-like structures were observed in gingivitis compared with health (Cooper *et al.,* 2013, courtesy of Dr Yousefi University of Berne, Switzerland).

The timely removal of NETs may represent an important mechanism in periodontitis. As previously mentioned, the removal of NETs in SLE patients is impeded, compared with healthy controls (see section 1.6.2) and the delayed removal of NETs provides a high concentration of NET-associated molecules that may drive the autoimmune response. Indeed, de Pablo *et al.,* 2013) reported an increased prevalence of ACPAs and raised ACPA titres within the serum of non-RA patients with periodontitis, relative to non-periodontitis controls (see section 1.6.1).

Conversely, decreased levels of NETs in periodontitis may enhance patient susceptibility to increased periodontal bacterial colonisation. DNases released by bacteria can degrade the DNA backbone, which disassembles the NET structure (see 1.3.3). This is thought to enable invading bacteria to circumvent NET defences and allow bacterial dissemination into the surrounding tissues (Berends *et al.,* 2010). Notably, several periodontal bacteria, including *P.*

gingivalis and *F. nucleatum*, have been found to express membrane-bound and secreted DNases (Palmer *et al.,* 2012). DNase release will enable bacterial infiltration and their establishment within the biofilm. NET production has also been reported to be reduced in older (over 50 years) periodontitis patients compared with younger patients (under 50) in response to HOCl. This implies the neutrophil responses in periodontitis may deteriorate with age, which may be associated with periodontitis being an age related disease (Grossi *et al.,* 1995), however in this cohort (n=19 pairs) no differences in NET production were observed between periodontitis patients and their healthy controls (Hazeldine *et al.,* 2014). Reduced levels of NETs have been associated with increased susceptibility to infections, for example in neonates (Yost *et al.,* 2009) and CGD (Bianchi *et al.,* 2011). It is possible that decreased NETs in periodontitis would impair the elimination of pathogenic species; facilitating persistent dysbiosis. This would likely result in further neutrophil recruitment and activation, such as extracellular degranulation, which may result in further tissue damage.

1.9 Neutrophil isolation and *ex vivo* handling

To characterise neutrophils in periodontitis, as well as other inflammatory diseases, cells are often isolated from the peripheral blood of volunteers and investigated *ex vivo*. Indeed there are neutrophil-like cells, such as the HL60 human promyelocytic cell line, which can be employed within the laboratory to circumvent problems of inter-individual variations between neutrophil donors (Martin *et al.,* 1990). Nevertheless, these immortalised cell lines do not fully reflect primary neutrophils in their behaviour or in their intricate biological functions (Hallett 1990). In addition, despite 99% of murine genes having an equivalent human counterpart, murine disease models also do not fully replicate the human situation. Exemplifying the limitations of such murine models is the fact that while human neutrophils represent 50-70% of circulating PBNs, mouse neutrophils make up only 10-25% of cells

(Doeing *et al.,* 2003). Isolation from human blood requires an efficient, aseptic and reproducible method to obtain non-activated and viable cells. A further consideration is the effect of the isolation and purification method on neutrophil behaviour; in particular neutrophils may become activated as a result of *ex vivo* manipulation (Oh *et al.,* 2008). Therefore, research investigating neutrophil function needs to consider whether *ex vivo* purification techniques influence neutrophil activation status. Methods of neutrophil isolation from whole blood can differ between research groups, creating potential phenotypic differences in neutrophils even if retrieved from the same volunteer.

1.9.1 Neutrophil isolation: density gradient materials

There are currently several materials employed for the isolation and purification of neutrophils from whole blood; including Percoll™ (GE Healthcare), Dextran (Sigma) and Histopaque™ (Sigma). Neutrophil isolation aims to provide an appropriate separation range at a high purity from other blood cells, whilst at the same time, not stimulating or activating the cells.

1. Percoll is comprised of colloidal silica and coated with non-dialyzable polyvinylpyrrolidone (PVP), and is used in conjunction with NaCl and water to produce a gradient to isolate neutrophils by differences in density.
2. An alternative density gradient material is Histopaque, which is a polysucrose and sodium diatrizoate solution that also enables the isolation of neutrophils at a density gradient interface.
3. A third method involves layering the blood on Dextran, which results in the sedimentation of a neutrophil layer above the aggregated erythrocytes. The neutrophil layer is then collected by aspiration and centrifuged on layered Percoll gradients to isolate the neutrophils further.

1.10 Aims of this study

Background: The pathogenic biofilm that initiates periodontitis has previously been characterised with respect to the sequence of microbial colonisation and associations with disease manifestations (Socransky *et al.,* 1998). However, the interactions between periodontal bacteria and NET release are less well understood. Specifically, whether bacterial species stimulate for increased or decreased NET release, and whether NETs have the capacity to entrap and kill periodontal microbes remains to be elucidated.

Aim 1: To investigate the interactions between NETs and a range of periodontal bacteria.

Background: NET release represents a novel neutrophilic defence mechanism; however the exact role of NETs in the pathogenesis of periodontitis remains unclear. Periodontitis is driven by a dysfunctional inflammatory response towards a pathogenic biofilm, in which the neutrophil is a key effector cell and patients' neutrophils are hyperactive and hyper-reactive in terms of ROS production (Matthews *et al.,* 2007a, 2007b). It is likely that NETs are also employed by the neutrophil in periodontitis pathogenesis, and given that NETs are largely dependent on ROS generation (Fuchs *et al.,* 2007), it is possible that NET release is also perturbed in periodontitis.

Aim 2: To investigate NET production by PBNs from periodontitis patients and in patients with PLS in comparison with healthy control groups.

Background: The importance of NET clearance has recently received substantial attention in studies of disease pathogenesis, such as in CF and SLE. As with periodontitis, both CF and SLE are characterised by a dysfunctional host immune response. NET clearance is reportedly impeded in SLE patients (Hakkim *et al.,* 2010); however the clearance of NETs in periodontitis has not been studied. Therefore, the ability of periodontitis patients to degrade

NETs and the nature of the mechanisms involved is of interest. An accumulation of NETs in certain tissues has been associated with disease severity via autoimmune mechanisms, for example in RA (Khandpur *et al.,* 2013). Indeed our own group have reported significantly elevated levels of autoantibodies to NET-related antigens in the serum of periodontitis patients (dePablo *et al.,* 2013).

Aim 3: To investigate NET degradation by periodontitis patients' plasma and the effect of NETs on neutrophil function.

Background: Cigarette smoking is a major risk factor in the development of periodontitis (Grossi *et al.,* 1995), and it has previously been reported that smoking has a range of effects upon neutrophil ROS production (Matthews *et al,.* 2011, 2012).

Aim 4: To determine the impact of CSE upon NET production, neutrophil chemotaxis and the expression of key genes involved in neutrophil activation.

CHAPTER 2: MATERIALS AND METHODS

2.1 MATERIALS

2.1.1 GENERAL BUFFERS

2.1.1.1 Phosphate Buffered Saline (PBS)

A 1L bottle of PBS was prepared by adding 7.75g NaCl (Sigma S9625), 0.2g KH_2PO_4 (Sigma P5379) and 1.5g K_2HPO_4 (Sigma P8281) to 1L of sterile distilled water. This was autoclaved (121°C for 15 mins) and stored at 4°C for up to 1 month prior to use.

2.1.1.2 PBS supplemented with glucose and cations (gPBS)

A 1L bottle of gPBS was prepared by adding 1.8g glucose (Sigma G8270), 0.15g $CaCl_2$ (BDH 10070), 1.5ml 1M $MgCl_2$ (BDH 22093) to 1L of PBS. This solution was made up in order with each component mixed before adding the next. This was stored at 4°C for up to 1 month prior to use.

2.1.1.3 Blocking buffer: 1% bovine serum albumin (BSA)

A 1L bottle of BSA was produced by adding 10g BSA (Sigma A2153) to 1L of PBS. The resulting solution was filter-sterilised (pore size 0.22 μm), added to 25ml universal containers and frozen at -20°C until needed.

2.1.1.4 4-(2-Hydroxyethyl) piperazine-1-ethanesulfonic acid, N-(2-Hydroxyethyl) piperazine-N′-(2-ethanesulfonic acid) (HEPES) buffer

HEPES (0.1M) (Sigma H3375) was prepared by adding 2.38g HEPES to 100ml of distilled water. This was adjusted to a pH of 7.5 (Beckman 40 pH meter, pH adjusted with HCl or NaOH) and stored at 4°C prior to use.

2.1.1.5 0.9% saline solution

A 1L bottle of 0.9% saline solution was prepared by adding 9g of NaCl (Sigma S9625) to 1L of distilled water and autoclaving (121°C for 15 mins).

2.1.2 NEUTROPHIL PREPARATION AND ASSAYS

2.1.2.1.1 Preparation of Percoll gradients

Percoll densities composed of 1.13g/ml Percoll, distilled water and 1.5M NaCl (Sigma S9625) were prepared according to Table 2.1.

Table 2.1: Preparation of Percoll density gradients

Density	1.079	1.098
Percoll	19.708ml	24.823ml
Water	11.792ml	6.677ml
NaCl (1.5M)	3.5ml	3.5ml

2.1.2.1.2 Lysis Buffer

A 1L bottle of lysis buffer was prepared by adding 8.3g NH_4Cl (A9434 Sigma), 1g $KHCO_3$ (Sigma P9144), 0.04g Na_2 EDTA $2H_2O$ (E5134 Sigma) and 2.5g BSA (Sigma A2153) to 1L of sterile distilled water. This was stored at 4°C for up to 1 month prior to use.

2.1.2.1.3 Preparation of Dextran and Percoll gradients

Dextran-isolation of neutrophils involves layering the blood onto Dextran (see 2.2.1.1.4), which results in the sedimentation of a neutrophil layer above the aggregated erythrocytes. The neutrophil layer is then collected with a Pasteur pipette and centrifuged on layered Percoll gradients to separate the neutrophils further.

2.1.2.1.4 2% Dextran

A 2% Dextran solution was prepared by adding 1g Dextran (Sigma 31392) to 50ml of 0.9% NaCl (saline). This was mixed by vortexing prior to being syringe-filter sterilised (pore size 0.22μm).

2.1.2.1.5 90% isotonic stock Percoll

Percoll for use in the preparation of 80% and 56% gradients (see Table 2.2) was prepared by combining 5ml of 9% NaCl with 45ml of Percoll (17-0891-01 GE Healthcare).

Table 2.2: Preparation of Percoll density gradients following Dextran sedimentation

Density	80%	56%
90% Percoll	40ml	28ml
0.9% NaCl (saline)	10ml	22ml

2.1.2.1.6 Luminol

A 30mM stock solution was prepared by dissolving 0.5g luminol (Sigma A8511) in 94.05ml of 1mM NaOH. The stock solution was foil-wrapped and stored for up to 6 months at 4°C prior to use. The working solution was prepared on the day by diluting 1ml of stock solution with 9ml of PBS and the pH adjusted to 7.3 (Beckman 40 pH meter, pH adjusted with HCl or NaOH).

2.1.2.1.7 Isoluminol

A 30mM stock solution was prepared by dissolving 0.5g isoluminol (Sigma A8264) in 94.05ml of 1mM NaOH. The stock solution was foil-wrapped and stored for up to 6 months at 4°C. The working solution was prepared on the day by diluting 1ml of stock solution with

9ml PBS and the pH adjusted to 7.3 (Beckman 40 pH meter, pH adjusted with HCl or NaOH).

2.1.2.1.8 Lucigenin

A 1mg/ml stock solution of Lucigenin was prepared by dissolving 0.005g lucigenin (Sigma B49203) in 5ml of PBS. The stock solution was foil-wrapped and stored for up to 6 months at 4°C prior to use. The working solution was made up on the day prior to use by diluting 1:3 with PBS.

2.1.2.2 Micrococcal nuclease (MNase)

MNase (Worthington 4789) was diluted to a 13.3U/ml working solution and stored at -20°C in 1ml aliquots. MNase was used at a final concentration of 1U/ml in 15µl aliquots unless otherwise stated.

2.1.2.3 Sytox green

Sytox green (Invitrogen S7020) was diluted 1:500 in RPMI (Roswell Park Memorial Institute)-1640 (Sigma R7509) to obtain a 10µM working solution. This solution was foil wrapped and stored at -20°C in 1ml aliquots.

2.1.2.4 Fluorescein-5-isothiocyanate (FITC)

FITC (isomer I, Invitrogen F-1906) was diluted to a working concentration of 6mg/ml in 1.5ml Eppendorfs, which were foil wrapped and stored at -20°C prior to use. When needed, FITC was defrosted at room temperature and used at a final concentration of 0.3mg/ml by adding 50µl to 1ml of bacterial suspension in a 1.5ml Eppendorf.

2.1.2.5 Cytochalasin B

Cytochalasin B (Sigma C6762), which blocks phagocytosis (Densen & Mandell 1978), was used at a final concentration of 10μg/ml by adding 166.5μl cytochalasin B (2mg/ml stock in DMSO, Sigma D8418) to 4.833ml of PBS. This was stored at -20°C.

2.1.3 BACTERIAL CULTURE

2.1.3.1 Bacterial stimuli

A panel of 19 bacteria (see Tables 2.5 & 2.6), plus opsonised *S. aureus,* was employed to stimulate neutrophils via TLR and FcγR, respectively. Bacterial stocks were provided by Dr. Mike Milward, originally obtained from the Forsyth Institute (Boston, US) or purchased from the American Type Culture Collection (ATCC).

2.1.3.2 Blood agar plates

Pre-prepared blood agar plates (Base no. 2 with 7% horse blood) were purchased from Oxoid (PB0114). Plates were stored at 4°C and allowed to equilibrate to room temperature for an hour prior to use. All plates were used before the manufacturer's expiry date.

2.1.3.3 Fastidious plates

P. gingivalis (strain W83) was cultured on pre-prepared anaerobic 20% blood agar plates (Wilkins Chalgren) purchased from Oxoid (PB0112). This is a medium enriched with neomycin that is specific for the growth of fastidious anaerobes. Plates were stored at 4°C and allowed to equilibrate to room temperature for an hour prior to use. All plates were used before the manufacturer's expiry date.

2.1.3.4 Tryptone soya agar (TSA) plates

S. aureus was cultured on tryptone soya agar (TSA) plates. Plates were made according to the manufacturer's instructions by adding 40g TSA (Oxoid CM0131) to 1L of distilled water. This was autoclaved (121°C for 15 mins) and cooled to 50°C, prior to pouring the agar into Petri dishes (Sterilin 101VR20). Plates were inverted and incubated at room temperature to solidify. Plates were subsequently stored at 4°C until needed, at which point they were equilibrated to room temperature for an hour prior to use.

2.1.3.5 Brain heart infusion (BHI) broth

BHI broth was made according to the manufacturer's instructions (Oxoid CM1135); 37g dehydrated culture medium were dissolved in 1L of distilled water. The BHI broth was mixed, autoclaved (121°C for 15 mins) and stored at 4°C until needed.

2.1.3.6 Fastidious anaerobe broth

Fastidious anaerobe broth was used to culture *P. gingivalis*. This dehydrated medium enriched with vitamin K, haemin and L-cysteine was purchased from Lab M (LAB071). Fastidious anaerobe broth was made according to the manufacturer's instructions by adding 29.7g to 1L of distilled water. This mixture was autoclaved (121°C for 15 mins) and stored at 4°C until needed.

2.1.3.7 Typtone soya broth (TSB)

TSB (Oxoid CM0876) was made by adding 30g of dehydrated culture medium to 1L of distilled water. This was mixed, autoclaved (121°C for 15 mins) and stored at 4°C until needed.

2.1.3.8 Crystal violet

Crystal violet solution was prepared by adding 2g crystal violet (Sigma C0775) to 20ml of 95% ethanol (Sigma E7023). 0.8g ammonium oxalate (Sigma A8545) was dissolved in 80ml of distilled water to produce 1% ammonium oxalate. The crystal violet solution was mixed with 1% ammonium oxalate in a 1:1 dilution and allowed to stand at room temperature for several days prior to use.

2.1.3.9 Carbon fuchsin

A 1ml stock of carbol fuchsin solution (BDH 351874U) was mixed with 9ml of distilled water and kept at room temperature.

2.1.3.10 Glutaraldehyde in sodium cacodylate buffer

A 100ml of 0.1M sodium cacodylate buffer were prepared by adding 4.28g sodium cacodylate trihydrate (Sigma CO250) to 100ml of distilled water, and adjusted to pH 7.4 (Beckman 40 pH meter, pH adjusted with HCl or NaOH). 2.5% glutaraldehyde was made by combining 7.5ml of sodium cacodylate buffer, 6ml of distilled water and 1.5ml of glutaraldehyde solution (Sigma G5882).

2.1.4 CIGARETTE SMOKING REAGENTS

2.1.4.1 Nicotine

Liquid nicotine was purchased (Sigma N3876) and diluted to final concentrations of 1µg/ml, 5µg/ml and 10µg/ml in PBS (section 2.2.4.1.1) and stored at -20°C.

2.1.4.2 Cotinine

Cotinine was purchased from Sigma (C5923) and used at the same final concentrations as nicotine (see 2.2.4.1.1); 1µg/ml, 5µg/ml and 10µg/ml in PBS and stored at -20°C. Cotinine is the principal stable metabolite of nicotine and it has been demonstrated that 70-80% of absorbed nicotine is subsequently metabolised to produce cotinine (Yuki *et al.,* 2013, Hukkanen et al., 2005). Concentrations in the saliva of smokers are reportedly 0.23 ± 0.17 µg/ml, ranging from 0.003µg/ml to 0.733µg/ml (Etter & Perneger 2001).

2.1.4.3 Thiocyanate (SCN-)

Thiocyanate (SCN-) levels are significantly elevated in the plasma of smokers, as it in an end product of detoxification of hydrogen cyanide, which is inhaled in cigarette smoke. SCN- is present in the plasma of smokers at levels of 131.4 ± 30.8µM (Morgan *et al.,* 2011). SCN- functions as a substrate for neutrophil derived MPO in the generation of hypothiocyanous acid (HOSCN-). Sodium thiocyanate was purchased from Sigma (251410) and diluted to final concentrations of 50µM, 100µM and 150µM in PBS and stored at -20°C.

2.1.5 PCR STUDIES

2.1.5.1 The synthesis of complementary DNA (cDNA)

Ribonucleic acid (RNA) was reverse transcribed to produce cDNA from pooled RNA using a cDNA synthesis kit (Tetro Bioline 65042) (Table 2.3).

Table 2.3: Components and quantities used for cDNA synthesis
All components were provided in the cDNA synthesis kit (Tetro Bioline 65042).
Abbreviations: Oligo-dT (oligonucleotide deoxy-thymine) dNTP mix (deoxynucleotide mix), RT (reverse transcriptase), RNase (ribonuclease), DEPC (diethylpyrocarbonate).

cDNA Kit components	1 x Eppendorf
Pooled RNA (0.5-0.6µg)	8µl
Oligo-dT primer mix	1µl
dNTP mix 10mM total	1µl
5x RT Buffer	4µl
RNase inhibitor (10u/µl)	1µl
Reverse transcriptase (200u/µl)	1µl
DEPC-treated water	4µl

2.1.5.2 Design and validation of PCR primers

Housekeeping and target gene primer sequences were selected from the literature (Table 2.4) and purchased from Invitrogen, UK.

Table 2.4: Primers employed to quantify gene expression in CSE and SCN- treated neutrophils using real time PCR

Abbreviations: YWHAZ (tyrosine 3/tryptophan, 5-monooxygenase activation protein, zeta polypeptide); GAPDH (glyceraldehyde-3-phosphate dehydrogenase); RPL13 (ribosomal protein L13); HPRT1 (hypoxanthine phosphoribosyltransferase 1); NFκB epsilon (nuclear factor kappa B); HSP40 (heat shock protein 40); IL-8 (interleukin-8). Efficiency refers to the amplification of the targer molecule, where an efficiency of 2.0 is considered 100% efficient and means the target molecule doubles every PCR cycle (LightCycler®).

Gene	Primer sequence (5'-3')	Amplicon size (bp)	Efficiency
Housekeeping genes			
YWHAZ	(f) ACTTTTGGTACATTGTGGCTTCAA (r) CCGCCAGGACAAACCAGTAT	94	1.93
GAPDH	(f) CTCCTGTTCGACAGTCAG (r) GCCCAATACGACCAAATC	111	1.83
RPL13	(f) CCTGGAGGAGAAGAGGAAAGAGA (r) TTGAGGACCTCTGTGTATTTGTCAA	126	1.86
HPRT1	(f) GACCAGTCAACAGGGGACAT (r) AACACTTCGTGGGGTCCTTTTC	195	1.97
Target genes			
NFκB epsilon	(f) GTGAAGCCTGTTTGCCTCTC (r) AGGGTCCTCAACAGCAAGAA	172	2.07
HSP40	(f) TACAGGAGCACTGTGGAAACG (r) AGGTCTGAGCACTGGACTGG	192	1.83
IL-8	(f) TAGCAAAATTGAGGCCAAGG (r) GGACTTGTGGATCCTGGCTA	204	1.75
P-47^{phox}	(f) ACCCAGCCAGCACTATGTGT (r) AGTAGCCTGTGACGTCGTCT	767	1.89
P-67^{phox}	(f) CGAGGGAACCAGCTGATAGA (r) CATGGGAACACTGAGCTTCA	726	1.78
GP-91^{phox}	(f) GCTGTTCAATGCTTGTGGCT (r) TCTCCTCATCATGGTGCACA	403	1.93

2.1.6 CELL CULTURE

2.1.6.1 Culture of an oral epithelium cell line

A human oral epithelium cell line (OEC), H400, was kindly donated by Dr S. Prime from University of Bristol, UK. The cell line was derived from a squamous cell carcimona of the alveolar process from a 55 year old female. The carcinoma was at stage 2, node negative, moderately differentiated and measured 20-40mm in size. Prime *et al.,* (1990) demonstrated close similarities to gingival epithelium and therefore H400s represent a suitable cell line for use as a model system.

2.1.6.2 Supplemented Dulbecco's Modified Eagle's Medium:nutrient mixture F-12 (DMEM/F-12)

DMEM/F-12 (Invitrogen 21331-020 500ml) is a commonly used medium for the growth of human endothelial cells, which is a 1:1 solution of DMEM and Ham's F-12. The media was supplemented with heat-inactivated foetal calf serum (FCS, 10% v/v), L-glutamine (2% v/v, Sigma G7513) and 10mg/ml hydrocortisone (0.005% v/v, Sigma H0888). Supplemented growth media was stored at 4°C prior to use.

2.1.6.3 Trypsin Ethylenediaminetetraacetic Acid (T-EDTA)

T-EDTA (Invitrogen R-001-100), comprising 0.0025% trypsin and 0.01% EDTA, was used to release adherent cells to produce a cell suspension. This solution was divided and frozen at -20°C in 4ml aliquots until needed.

2.2 METHODS

2.2.1 ISOLATION OF NEUTROPHILS FROM PERIPHERAL BLOOD

2.2.1.1 Percoll components

2.2.1.1.1 Preparation of Percoll gradients

PMNLs were isolated from whole blood using discontinuous Percoll gradients (17-0891-01 GE Healthcare). The discontinuous gradients were generated by carefully layering 8ml of 1.079 density gradient over 8ml of 1.098 (see 2.1.2.1.1) in a 25ml centrifuge tube (Fisher Scientific).

2.2.1.1.2 Neutrophil isolation with Percoll

Blood was collected in 6ml lithium heparin vacutainers (Greiner Bio-One) and inverted to ensure the mixing of the anticoagulant. Post-collection, 6ml of blood were layered over the Percoll density gradients and centrifuged (Hettich Universal 320R) for 8 mins at 150 relative centrifugal force (rcf), followed by 10 mins at 1200rcf (both with a ramp and brake of 1 and at 4°C). Plasma, monocytes, lymphocytes and density gradient material were aspirated off and discarded, allowing for the transfer of the neutrophil layer to 30ml of lysis buffer (see 2.1.2.1.2) in a 50ml centrifuge tube (Fisher Scientific), which was then made up to a total volume of 50ml with lysis buffer. Following gentle inversion, the centrifuge tube was incubated for 15 mins at room temperature to lyse any remaining erythrocytes. Subsequently, the tube was centrifuged for 6 mins at 500rcf (4°C) to pellet the neutrophils. The supernatant was aspirated off, whilst the pellet was re-suspended in 2ml of lysis buffer and incubated for 5 mins at room temperature, prior to centrifugation for 6 mins at 500rcf (4°C). The supernatant was again aspirated off and the neutrophil pellet washed in 2ml of PBS, followed by re-centrifugation (6 mins at 500rcf, 4°C). The supernatant was discarded, cells re-

suspended in 2ml of PBS (see 2.1.1.1) and counted by light microscopy (Leitz Laborlux s) (2.2.1.1.5).

2.2.1.1.3 Isolation of neutrophils by Histopaque gradients

H1077 (Sigma) density Histopaque (3ml) were layered over H1119 (Sigma) (3ml) in a 15ml tube (Fisher Scientific). 6ml of blood were carefully layered over the gradients using a Pasteur pipette, prior to centrifugation (Hettich Universal 320R) for 50 mins at 800rcf (at 4°C). Plasma, monocytes, lymphocytes and density gradient material were aspirated and discarded, allowing for the retrieval of the neutrophil layer from the H1077/H1119 interface. Neutrophils were transferred to 5ml of Dulbecco's PBS (Sigma D8537) in a fresh 15ml centrifuge tube and centrifuged for 6 mins at 400rcf, followed by manual aspiration of the supernatant. The neutrophil pellet was re-suspended in 10ml of Dulbecco's PBS, prior to re-centrifugation for 6 mins at 400rcf (4°C). The supernatant was again aspirated off and cells re-suspended in 1ml of Dulbecco's PBS prior to erythrocyte lysis, where 5ml of distilled ice cold water were added, followed by the immediate addition of 2ml 4x PBS after 30 secs. Neutrophils were then centrifuged for 8 mins at 450rcf (4°C), finally re-suspended in 2ml Dulbecco's PBS and cells were counted by light microscopy (Leitz Laborlux s) (2.2.1.1.5).

2.2.1.1.4 Isolation of neutrophils using Dextran

Blood (approximately 6ml) was added to a 50ml tube containing 1ml of 2% Dextran (see 2.1.2.1.3); this was incubated for 40 mins at room temperature to sediment erythrocytes. Post-incubation, the neutrophil "buffy coat" was collected from the blood and carefully layered over the Percoll density gradients using a Pasteur pipette (2.1.2.1.4). This was centrifuged (Hettich Universal 320R) for 20 mins at 220rcf (4°C) and post-incubation the neutrophils were added to a falcon tube (Fisher Scientific) containing 5ml PBS. This was re-centrifuged (10 mins at 250rcf, 4°C) and the supernatant discarded. The cells were then re-

suspended in 5ml of RPMI-1640 (Sigma R7509) and counted by light microscopy (Leitz Laborlux s) (2.2.1.1.5).

2.2.1.1.5 Neutrophil cell counting

Cells (10µl of isolated cell suspension) were counted using a haemocytometer (Neubauer, Reichert) on a light microscope at x20 magnification (Leitz Laborlux s). The central area of the haemocytometer ($1mm^2$) is sub-divided into 25 smaller squares ($0.04mm^2$). Cells were counted in 9 of the $0.04mm^2$ squares and calculations were subsequently performed according to the equation below, where 25 refers to the number of squares, $1x10^4$ denotes the haemocytometer dimensions and 9 is the number of squares counted.

$$\frac{(\text{Cell count} \times 25 \times 1x10^4)}{9} = \text{number of cells/ml stock cell suspension}$$

2.2.1.2 NEUTROPHIL VIABILITY AND METABOLIC ACTIVITY

2.2.1.2.1 Confirmation of neutrophil isolation by cytospin

Neutrophils were re-suspended in PBS (see 2.1.1.1) at $2x10^6$ cells/ml, added to a cytospin funnel and centrifuged for 5 mins at 300rcf (Shandon cytospin). The resultant smears on glass slides were allowed to air dry for 20 mins. Neutrophils were stained with Diff-Quick, which is a Romanowski stain, in which slides are submerged in a methanol fixative, followed by staining with eosin and methylene blue. Slides were then rinsed in distilled water and allowed to air dry, this was followed by visualisation and differential cell counts using light microscopy (x20 magnification) (Leitz Laborlux s). The nuclei of neutrophils stain a dark blue, whilst the cytoplasms appear pink.

2.2.1.2.2 Confirmation of neutrophil isolation by flow cytometry

Flow cytometry was employed to determine the isolation and purity of neutrophils. Percoll-isolated cells were diluted to $1x10^6$ in 100µl of PBS (see 2.1.1.1) and combined with 1µl of CD66b with an anti-human phycoerythrin tag (eBioscience, clone G10F5) and incubated for 30 mins on ice. Erythrocytes were lysed by adding 50µl of whole blood to 450µl OptiLyse C (Beckman Coulter A11895) and 500µl of PBS, and incubated for 30 mins on ice. To serve as a negative control, whole blood was also assayed. Post-incubation, whole blood or isolated cells were transferred to a flow cytometry tube and analysed (300 secs or 50,000 parts) on a Cytomics FC 500 flow cytometer (Beckman Coulter, CXP software, FL3 wavelength).

2.2.1.2.3 Trypan blue exclusion

Cell viability was confirmed by trypan blue dye (Sigma T8154) exclusion staining using a 1:1 dilution of cells with trypan blue. Cells were visualised with a haemocytometer (Neubauer, Reichert) and light microscopy (x20 magnification) (Leitz Laborlux s). Tyrpan blue is not absorbed by viable cells, however if the neutrophil cell membrane is damaged, the dye will be absorbed and stain the cell blue. A calculation was employed to determine the percentage of viable cells: number of viable cells/ total number of cells x 100.

2.2.1.2.4 Quantification of neutrophil caspase-3 and 7 activity

Neutrophil apoptosis was measured by quantifying caspase-3 and 7 activities using the Caspase-Glo® 3/7 assay (Promega G8091). Following isolation, $1x10^5$ neutrophils were re-suspended in 100µl of gPBS (see 2.1.1.2). 50µl of Caspase-Glo® 3/7 substrate, containing a tetrapeptide sequence (DEVD), were added to each well. Caspase activity results in the cleavage of the caspase-substrate to release aminoluciferin generating light, which was measured by chemiluminescence (Berthold Tristar^2 LB942, MikroWin2000) for 10 mins. The light production is directly proportional to apoptotic activity.

2.2.1.2.5 Quantification of neutrophil adenosine triphosphate (ATP) activity

The amount of ATP released by neutrophils is indicative of the metabolic activity and therefore proportional to the number of viable cells (Crouch *et al.,* 1993). ATP was measured using CellTiter-Glo® (Promega G7570), which utilises the luminescence produced by luciferase in the presence of ATP. Following isolation, $1x10^5$ neutrophils were re-suspended in 100µl of gPBS (see 2.1.1.2). 50µl of CellTiter-Glo® were added to each well. ATP production is proportional to light production, which was measured by chemiluminescence (Berthold Tristar^2 LB942, MikroWin2000) for 10 mins.

2.2.2 NEUTROPHIL ACTIVATION

2.2.2.1 Stimuli employed to activate neutrophils

Neutrophils were stimulated using a range of stimuli. Phorbol 12-myristate 13-acetate (PMA) targets NET production via the activation of PKC. Previous findings (Palmer 2010), demonstrated that double the concentration of PMA is required for NET release (50nM) compared with what is needed to stimulate ROS production (25nM) by neutrophils. HOCl is usually produced from H_2O_2, in a reaction catalysed by MPO. HOCl stimulation therefore avoids the requirement for receptor-ligand binding and the activation of NADPH-oxidase, and thus avoids the upstream signalling of the NET production pathway (Palmer *et al.,* 2012). Gram-positive and -negative bacteria activate neutrophils via TLR-2 and -4 and were employed as a stimulus for ROS (2.2.3.2) and NET (2.2.3.3) release. In addition, ROS and NETs were produced in response to stimulation with opsonised *S. aureus* (2.2.2.2.5), which activates neutrophils via FcγR.

2.2.2.2 Determination of the concentration of HOCl

Sodium hypochlorite was purchased from Sigma (425044), which contains 10-15% available chlorine. The concentration of hypochlorite ions (OCl-) was determined previously (Palmer *et al.,* 2012) by measuring the optical density of solutions at pH 12 (OD_{290nm}, extinction coefficient of 350M/cm). HOCl used in experimentation had approximately the same pH and acid dissociation constant (pKa) of 7.5. Therefore it was assumed that 50% of the solution existed as HOCl and 50% as OCl-. HOCl was used at a final concentration of 0.75mM for all neutrophil assays.

2.2.2.2.1 Culture of periodontal bacteria

Bacterial suspensions (2.1.3.1) in cryotubes containing tryptone soya broth (TSB, Oxoid CM0876) and 10% dimethyl sulfoxide (DMSO, Sigma D8418) were stored at -80°C. When required, they were resuscitated by defrosting at room temperature. Inocula were established by pipetting 100µl of bacterial suspension onto agar plates (sections 2.1.3.2, 2.1.3.3 & 2.1.3.4) and spread with disposable pre-sterilised loops. Plates were loosely wrapped in Clingfilm to prevent desiccation of agar following prolonged incubation, inverted and incubated in the appropriate chamber (Tables 2.5 & 2.6) for at least 3 days. Cultures were grown planktonically by inoculating a single representative colony into the appropriate growth broth (sections 2.1.3.5, 2.1.3.6 & 2.1.3.7).

2.2.2.2.2 Determination of bacterial growth

Bacterial cell suspensions were measured spectrophotometrically (Jenway 6300) at an optical density of 600nm (OD_{600nm}). Non-inoculated media was used to calibrate the spectrophotometer. The OD_{600nm} values used to estimate bacterial numbers were calculated by the Forsyth Institute (Boston) and have been previously reported by Roberts *et al.,* (2005).

2.2.2.2.3 Heat-killing of bacteria

Following planktonic growth in broth, the bacterial suspension was centrifuged (Harrier 18/80, 15 mins, 1800rcf, 4°C). The supernatant was discarded and the bacterial pellet re-suspended in sterile PBS (see 2.1.1.1), this step was repeated a total of 3 times to wash the bacteria. The bacterial concentration was determined by spectrophotometry (section 2.2.2.2.2) and then diluted to the desired bacterial concentration in PBS (2.1.1.1). The bacteria were heat-killed by incubating at 80°C for 30 mins (microbiology oven, LTE OP30).

2.2.2.2.4 Comparison of live and heat-killed bacteria

Experiments were conducted to compare live and heat-killed bacterial stimuli. A panel of 4 bacteria was cultured on agar plates (2.1.3.2, 2.1.3.4), followed by inoculation of broth (2.1.3.5, 2.1.3.7), and incubation for a further 48 hours. Once turbid due to bacterial growth, the bacteria were subjected to 3 PBS (2.1.1.1) wash steps as described above. Each bacterial species suspension was divided into 2 tubes and bacterial concentrations determined by spectrophotometry (section 2.2.2.2.2). All bacteria were diluted to $5x10^7$ (multiplicity of infection [MOI] of 500) and whilst 1 tube of each species was placed in an oven (microbiology oven, LTE OP30) at 80°C for heat-killing, the second tube was maintained at 4°C. Neutrophil ROS and NET production was determined following stimulation with live or dead bacteria in parallel.

2.2.2.2.5 Opsonisation of *S. aureus*

*S. aureus (*ATCC 9144) was grown on TSA plates (2.1.3.4) prior to planktonic growth in TSB (2.1.3.7). Following a 48 hour growth in the aerobic chamber (Swallow), the bacteria were pelleted by centrifugation (Harrier 18/80, 15 mins, 1800rcf, 4°C). The supernatant was discarded and the pellet re-suspended in sterile PBS (see 2.1.1.1); this was repeated a total of 3 times to remove any remaining broth. Bacterial concentration was determined by

spectrophotometry and diluted as necessary for subsequent assays (2.2.2.2.2). Bacteria were heat-killed by incubating at 80°C for 30 mins (2.2.2.2.3) prior to opsonisation with Vigam liquid (5mg/ml IgG, Bio Products Laboratory), which was used at 33µl per ml of bacterial suspension (Bergstrom & Åsman 1993). This mixture was agitated (Luckham R11/TW, speed 2) overnight at room temperature to enable thorough opsonisation of the bacteria. Following this, the bacteria were subjected to 2 wash steps in PBS (2.1.1.1) and stored at -20°C until needed.

2.2.2.2.6 Gram-stain protocol

To identify bacterial species, colonies were visualised microscopically to determine their colour, size and morphology. Gram-stains were also utilised to determine whether the bacteria were Gram-positive or Gram-negative. Gram-staining differentiates positive and negative bacteria by detecting peptidoglycan, which whilst present as a thick outer layer in Gram-positive cell walls, is thinner and surrounded by an outer lipid membrane in Gram-negative species. These characteristic cell wall properties enable species distinction between Gram-positive bacteria (appear purple or blue) and Gram-negative bacteria (appear red or pink) (McClelland 2001). A drop of saline was deposited onto a microscope slide, prior to the addition of a bacterial colony sample, forming an emulsion, which was heat fixed using a Bunsen burner. Crystal violet (see 2.1.3.8) was added to the slide for 30 secs, rinsed with water, followed by the addition of Lugol's iodine (Sigma L6146) for a further 30 secs prior to rinsing with distilled water. Acetone was then added and immediately rinsed with water; finally the slide was flooded with carbol fuchsin (see 2.1.3.9) for 30 secs and rinsed with distilled water. The slide was blotted dry and visualised under oil immersion microscopy at x100 magnification (Leitz Dialux 22) and digital images captured (Nikon Coolpix 1990). Images were subsequently analysed in Fiji Is Just ImageJ (Fiji) (http://fiji.sc/Fiji).

Table 2.5: Characterisation of periodontal bacterial species
The Socransky complex indicates the colour complex the bacteria are assigned to (Socransky *et al.,* 1998). Abbreviations: ATCC (American type culture collection)

Bacteria Strain	ATCC number	Socransky complex	Gram-stain
Actinomyces viscosus (naeslundii genospecies 2)	43146	Blue	Positive
Aggregatibacter actinomycetemcomitans serotype b	43718	White	Negative
Propionybacterium acnes	11827	White	Positive
Selenomonas noxia	43541	White	Negative
Veillonella parvula	10790	Purple	Negative
Streptococcus sanguinis	10556	Yellow	Positive
Streptococcus oralis	35037	Yellow	Positive
Streptococcus intermedius	27335	Yellow	Positive
Streptococcus anginosus	33397	Yellow	Positive
Streptococcus gordonii	10558	Yellow	Positive
Capnocytophagia gingivalis	33624(27)	Green	Negative
Aggregatibacter actinomycetemcomitans serotype a	29523	Green	Negative
Capnocytophaga sputigena	33612(4)	Green	Negative
Streptococcus constellatus	27823(M32b)	Orange	Positive
Camylobacter rectus	33238(371)	Orange	Negative
Campylobacter showae	51146	Orange	Negative
Fusobacterium nucleatum sp. Nucleatum	25586	Orange	Negative
Fusobacterium nucleatum sp. Polymorphum	10953	Orange	Negative
Porphyromonas gingivalis	W83	Red	Negative
Staphyloccus aureus (opsonised)	9144	N/A	Positive

Table 2.6: Culture conditions of periodontal bacterial species
Abbreviations: BHI (brain heart infusion), TSA (tryptone soya agar), TSB (tryptone soya broth). Bacteria were incubated at 37°C in an aerobic incubator (Swallow), a 5% CO_2 incubator (Napco 6500) or under anaerobic conditions (Don Whitley Scientific, Modular Atmosphere Controlled System, CAL-3200).

Bacteria Strain	Culture medium	Growing conditions	Bacteria per ml if OD_{600nm} =1
Actinomyces viscosus (naeslundii genospecies 2)	Plate: Blood Broth: BHI	Anaerobic	$8.3x10^8$
Aggregatibacter actinomycetemcomitans serotype b	Plate: Blood Broth: BHI	Anaerobic	$6.8x10^9$
Propionybacterium acnes	Plate: Blood Broth: BHI	Anaerobic	$1.69x10^9$
Selenomonas noxia	Plate: Blood Broth: BHI	Anaerobic	$1.69x10^9$
Veillonella parvula	Plate: Blood Broth: BHI	Anaerobic	$6.8x10^9$
Streptococcus sanguinis	Plate: Blood Broth: BHI	5% CO_2	$1.69x10^9$
Streptococcus oralis	Plate: Blood Broth: BHI	5% CO_2	$1.69x10^9$
Streptococcus intermedius	Plate: Blood Broth: BHI	5% CO_2	$1.69x10^9$
Streptococcus anginosus	Plate: Blood Broth: BHI	5% CO_2	$1.69x10^9$
Streptococcus gordonii	Plate: Blood Broth: BHI	5% CO_2	$1.69x10^9$
Capnocytophagia gingivalis	Plate: Blood Broth: BHI	Anaerobic	$1.62x10^9$
Aggregatibacter actinomycetemcomitans serotype a	Plate: Blood Broth: BHI	Anaerobic	$6.8x10^9$
Capnocytophaga sputigena	Plate: Blood Broth: BHI	Anaerobic	$1.62x10^9$
Streptococcus constellatus	Plate: Blood Broth: BHI	5% CO_2	$1.69x10^9$
Camylobacter rectus	Plate: Blood Broth: BHI	Anaerobic	$6.8x10^9$
Campylobacter showae	Plate: Blood Broth: BHI	Anaerobic	$6.8x10^9$
Fusobacterium nucleatum sp. Nucleatum	Plate: Blood Broth: BHI	Anaerobic	$1.62x10^9$
Fusobacterium nucleatum sp. Polymorphum	Plate: Blood Broth: BHI	Anaerobic	$1.62x10^9$
Porphyromonas gingivalis	Plate: Fastidious blood with neomycin Broth: Fastidious	Anaerobic	$1.69x10^9$
Staphyloccus aureus (opsonised)	Plate: TSA Broth: TSB	Aerobic	$1.69x10^9$

2.2.2.3 Modulators of neutrophil activation

To further characterise the activation of neutrophils, specific components of the neutrophil activation cascade were targeted (Table 2.7) to determine their effect on ROS (2.2.3.2) and NET (2.2.3.3) release in response to a range of stimuli. All modulating agents were added to wells in 50µl aliquots prior to the addition of $1x10^5$ neutrophils (2.2.1.1.2), incubated for 30 mins (Galaxy S, 37°C, 5% CO_2) and subsequently stimulated. Neutrophil total ROS and NET production with and without the addition of modulating agents was quantified in response to a panel of bacterial species ($1x10^8$, MOI of 1000) and PMA (50nM).

Table 2.7: Modulators of neutrophil activation
Abbreviations: TLR (toll like receptors), NADPH-oxidase (nicotinamide adenine dinucleotide phosphate-oxidase), H_2O_2 (hydrogen peroxide), HOCl (hypochlorous acid).

Modulating agent	Concentration	Neutrophil activation cascade target
OxPAPC (Invivogen tlrl-oxp1)	Working: 120µg/ml Final: 30µg/ml	Interacts with bacterial lipids, which prevents bacterial signalling and blocks TLR2 and TLR4 activation.
Chloroquine (Invivogen tlrl-chq)	Working: 400µM Final: 100µM	Inhibits endosomal TLRs 3, 7 and 9 by preventing endosomal acidification.
Diphenyleneiodonium chloride (DPI) (Sigma D2926)	Working: 100µM Final: 25µM	Inhibitor of flavoenzymes such as neutrophil NADPH-oxidase.
N-acetyl-cysteine (NAC) (Sigma A7250)	Working: 40mM Final: 10mM	Glutathione peroxidase precursor substrate, causing the removal of H_2O_2.
Taurine (Sigma T0625)	Working: 400mM Final: 100mM	Scavenges HOCl by reacting with it to produce taurine chloramine.

2.2.3 NEUTROPHIL ASSAYS

2.2.3.1 Treatment of neutrophil assay plastic-ware

All plastic-ware was coated with filter-sterilised 1% BSA (2.1.1.3) and incubated at 4°C overnight, as the addition of BSA "blocks" assay plates to prevent neutrophil adhesion and inadvertent activation (Palmer 2010, Steinckwich *et al.,* 2007). Following incubation, un-adhered BSA was removed by washing 5 times in PBS (2.1.1.1) with a plate washer (assay plates, BioTek ELx50) or using a Pasteur pipette (coverslips).

2.2.3.2 Chemiluminescence protocol for ROS assay

Neutrophils ($1x10^5$ in 100µl gPBS, 2.1.1.2) were added to a white flat bottom non-treated 96-well plate (Costar 3912) previously coated with 200µl filter-sterilised 1% BSA (2.2.3.1). To measure total ROS, 30µl luminol (2.1.2.1.6) was added, and to identify extracellular radical generation 60µl of isoluminol (2.1.2.1.7) and 15µl of 1.5 units of horseradish peroxidase (HRP, Sigma P8415) were added. To selectively measure superoxide production, 30µl of lucigenin (2.1.2.1.8) was added. The plate was placed in the luminometer (Berthold Tristar^2 LB942) and after a 30 mins, selected wells were stimulated with PMA (25nM), bacteria ($1x10^8$, MOI of 1000, see section 2.2.2) or opsonised *S. aureus* (5×10^7, MOI of 500, see section 2.2.2.2.5). Light output was read for a further 120 mins. All readings were expressed as relative light units (RLUs) and read at 37°C in MikroWin2000.

2.2.3.3 Quantification of NET-DNA

Neutrophils ($1x10^5$ in 175µl RPMI-1640, Sigma R7509) were added to a white flat bottom non-treated 96-well plate (Costar 3912) previously coated with 200µl filter-sterilised 1% BSA (2.2.3.1). After a 30 min incubation period (Galaxy S, 37°C, 5% CO_2), selected wells were stimulated with either PMA (50nM), heat-killed bacteria ($1x10^8$, MOI of 1000) or

opsonised *S. aureus* ($5x10^7$, MOI of 500) (see 2.2.2), and incubated for 4 hours (Galaxy S, 37°C, 5% CO_2). Post-incubation, 15µl of 1U/ml micrococcal nuclease (MNase, Worthington, 2.1.2.2) were added to each well and incubated at room temperature for 15 mins, prior to centrifugation (Hettich Universal 320R, 10 mins at 1800rcf). Subsequently, 150µl of the supernatant were transferred to a black flat bottom non-treated 96-well plate (Costar 3915), with the addition of 15µl of 10µM Sytox green (Invitrogen S7020, 2.1.2.3) to quantify free DNA within the supernatant. Fluorescence was read in arbitrary fluorescence units (AFU) using a fluorometer (Twinkle LB970, Berthold Technologies; MikroWin2000, excitation filter F485, emission filter F535, lamp energy 2000) 10 times at 37°C. Bacteria-derived DNA was also quantified in a neutrophil-free 96-well plate and these values were subtracted from the final NET quantification readings.

2.2.3.4 Quantification of NET-bound components

Quantifying neutrophil granule components associated with NETs is a DNA-independent measure of NET production. Neutrophils ($1x10^6$ in 800µl RPMI-1640, Sigma R7509) were added to a clear non-treated 24-well plate (Costar 3526) previously coated with 200µl filter-sterilised 1% BSA (2.2.3.1). After a 30 min incubation period (Galaxy S, 37°C, 5% CO_2), selected wells were stimulated with PMA (50nM), heat-killed bacteria ($1x10^8$, MOI of 1000) or opsonised *S. aureus* ($5x10^7$, MOI of 500) (see 2.2.2). The plate was incubated for 4 hours (Galaxy S, 37°C, 5% CO_2). Post incubation, the supernatant was gently aspirated and the NETs were subjected to 2 x 1ml wash steps with RPMI-1640. This approach removes non NET-bound components concurrently released during neutrophil activation. 75µl of 1U/ml MNase (2.1.2.2) were added to the well and incubated at room temperature for 15 mins, followed by centrifugation (Hettich Universal 320R, 10 mins at 1800rcf). The supernatants were then transferred to fresh cryotubes and stored at -20°C. To quantify NE, MPO or CG,

the samples were defrosted at room temperature and centrifuged (Geneflow micro, 10 mins at 1800rcf).

2.2.3.4.1 Neutrophil elastase (NE)

NET-bound NE was quantified by adding 100µl of sample to a clear non-treated 96-well plate (Costar 3370) in duplicate. 100µl of 0.5mM N-Methoxysuccinyl-Ala-Ala-Pro-Val p-nitroanilide (Sigma M4765) was added to each well and the plate was covered and incubated for 2 hours (Galaxy S, 37°C, 5% CO_2). Post incubation, the optical density was determined at 405nm (OD_{405nm}) (ELx800, Bio-Tek Instruments Inc. Gen 5 1.11) (Figure 2.1). A standard curve was generated by serially diluting a human NE standard solution (Caymann chemical 601014).

2.2.3.4.2 Myeloperoxidase (MPO)

NET-bound MPO was quantified by adding 50µl of sample to a clear non-treated 96-well plate (Costar 3370) in duplicate. 50µl of 3,3',5,5'-Tetramethylbenzidine (TMB) substrate (Cayman chemical 400074) was added to each well and the plate covered and incubated for 20 mins at room temperature. Post-incubation, 50µl of 1M sodium phosphate was added to stop the reaction. The optical density was immediately read at 450nm (OD_{450nm}) (ELx800, Bio-Tek Instruments Inc. Gen 5 1.11). A standard curve was generated by serially diluting the MPO standard derived from human leukocytes (Sigma M6908).

2.2.3.4.3 Cathepsin G (CG)

NET-bound CG was quantified by adding 50µl of sample to a clear non-treated 96-well plate (Costar 3370) in duplicate. 50µl of 1mM N-Succinyl-Ala-Ala-Pro-Phe p-nitroanilide (Sigma S7388) in 0.1M HEPES (see 2.1.1.4) was added to each well and the plate covered and incubated for 2 hours (Galaxy S, 37°C, 5% CO_2). Post incubation, the absorbance was read

at 405nm (OD_{405nm}) (ELx800, Bio-Tek Instruments Inc. Gen 5 1.11). A standard curve was generated by serially diluting CG from human leukocytes (Sigma 4428).

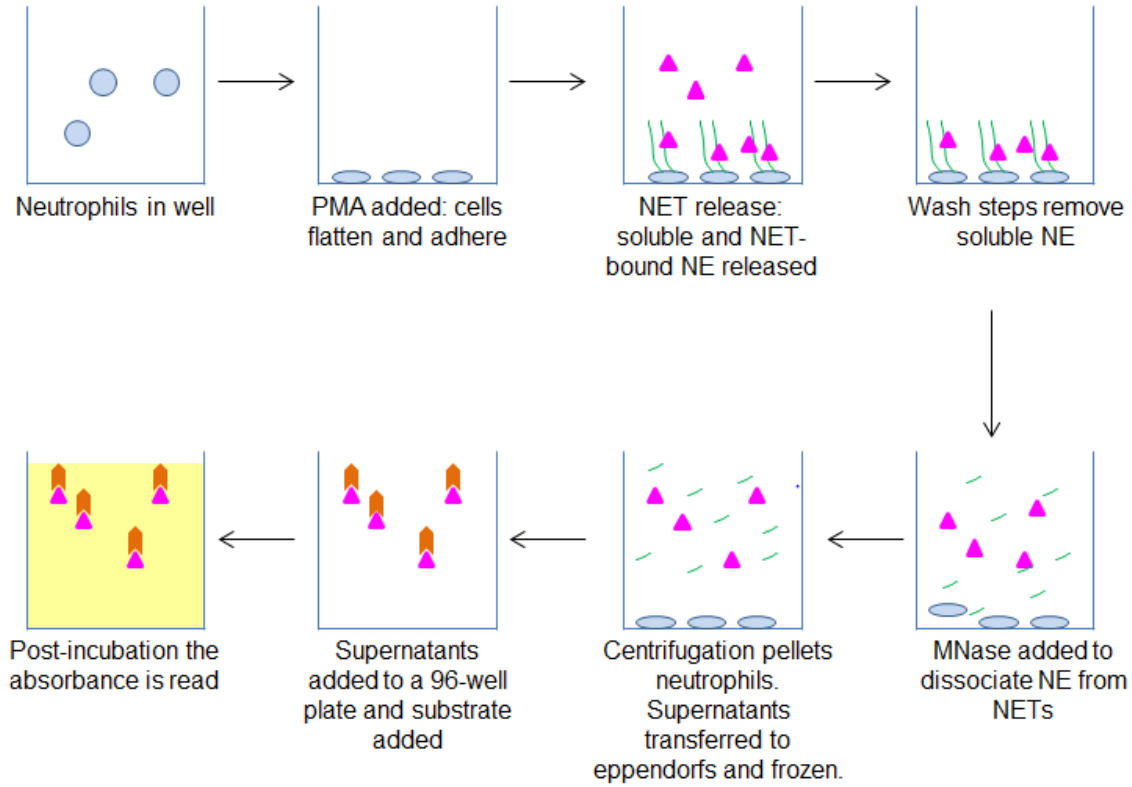

Figure 2.1: Diagrammatic representation of the quantification of NET-bound NE
PMA-activated neutrophils are incubated for 4 hours (37°C, 5% CO_2) to produce NETs (green strands) and allow for NE release (purple triangles). Following multiple wash steps and freeze storage, NET-bound NE is quantified in the supernatants by the addition of 0.5mM N-Methoxysuccinyl-Ala-Ala-Pro-Val p-nitroanilide substrate (Sigma M4765, orange chevrons) and incubated for 2 hours. The optical density is read at 405nm (OD_{405nm}). Schematic based on Cayman Chemical kit (601010). Abbreviations: NE (neutrophil elastase); PMA (phorbol 12-myristate 13-acetate); MNase (micrococcal nuclease).

2.2.3.5 NET entrapment of bacteria

Neutrophils ($1x10^5$ in 175µl RPMI-1640, Sigma R7509) were added to a black flat bottom non-treated 96-well plate (Costar 3915) previously coated with 200µl filter-sterilised 1% BSA (2.2.3.1). After a 30 min incubation period (Galaxy S, 37°C, 5% CO_2), selected wells were stimulated with 25µl of 0.75mM HOCl (Palmer *et al.,* 2012) and incubated for 3 hours

(Galaxy S, 37°C, 5% CO_2). Bacteria were measured by spectroscopy (section 2.2.2.2.2) and diluted to $1x10^7$ per 50µl (MOI of 100) prior to incubation with 0.3mg/ml fluorescein-5-isothiocyanate (FITC isomer I, Invitrogen F-1906) (see 0) with continuous agitation (Luckham R11/TW, speed 2) for 30 mins on ice. The bacteria were centrifuged (Geneflow micro, 10 mins at 5000rpm) to precipitate FITC-stained live bacteria, which were then re-suspended in 1ml PBS (see 2.1.1.1) and added to the NETs suspensions in 50µl aliquots and incubated for 1 hour (Napco 6500, 37°C, 5% CO_2). Post-incubation, the supernatant was carefully aspirated and replaced with 200µl fresh, pre-warmed (20°C) PBS (2.1.1.1). This washing procedure was repeated to ensure bacteria not actively bound within NETs were removed. Fluorescence was read in AFU on a fluorometer (2.2.3.3).

2.2.3.6 NET killing of bacteria

Neutrophils ($1x10^5$ in 440µl RPMI-1640, Sigma R7509) were added to a clear non-treated 24-well plate (Costar 3526) previously coated with 500µl filter-sterilised 1% BSA (2.2.3.1). After a 30 min incubation period (Galaxy S, 37°C, 5% CO_2), selected wells were stimulated with 60µl of 0.75mM HOCl (section 2.2.2.2, Palmer *et al.,* 2012) and incubated for 3 hours (Galaxy S, 37°C, 5% CO_2). Post-incubation, the supernatant was carefully removed from each well and replaced with fresh 500µl RPMI-1640 with or without 10µg/ml cytochalasin B (to prevent phagocytosis, see 2.1.2.5) or 100U/ml MNase (2.1.2.2) and incubated for 15 mins at room temperature. Live bacteria were added to each well at $1x10^7$ in 50µl aliquots (MOI of 100), determined by OD measurements (2.2.2.2.2). The plate was centrifuged (10 mins at 700rcf) and incubated for 1 hour (Napco 6500, 37°C, 5% CO_2). Post-incubation, selected wells were subjected to MNase digestion (100U/ml, 2.1.2.2) for 15 mins at room temperature, to degrade NETs. The well contents were aliquoted, diluted in broth and 50µl of this

suspension, sub-cultured onto blood agar plates and incubated for 24 hours in the appropriate atmospheric incubator for subsequent colony counting.

2.2.3.7 NET fluorescence visualisation

Neutrophils ($1x10^5$ in 260µl RPMI-1640, Sigma R7509) were added to a clear non-treated 24-well plate (Costar 3526) previously coated with 300µl filter-sterilised 1% BSA (2.2.3.1). After a 30 min incubation period (Galaxy S, 37°C, 5% CO_2), selected wells were stimulated with PMA (50nM) and the plate covered and incubated for 4 hours (Galaxy S, 37°C, 5% CO2). Post-incubation, 30µl of 10µM Sytox green (Invitrogen S7020, 2.1.2.3) were added to each well. NETs were visualised with an epi-fluorescence microscope (Nikon Eclipse TE300) with excitation and emission fluorescence filters of 472nm and 520nm, respectively. Images were captured with a QImaging camera (Retiga 2000R) in Micro-Manager and analysed in Fiji.

2.2.3.8 Scanning electron microscopy (SEM) of NETs

Round 11mm glass coverslips were sterilised in 0.2M HCl, followed by 2 wash steps in distilled water. After which, coverslips were coated in 100µl filter-sterilised 1% BSA and stored at 4°C overnight (2.2.3.1). Neutrophils ($1x10^5$ in 100µl) were seeded onto the coverslips, and after a 30 min period (Napco 6500, 37°C, 5% CO_2) stimulated with either 50nM PMA or $1x10^7$ previously cultured live bacteria (MOI of 100) (section 2.2.2.2.1). After 4 hours of incubation (Napco 6500, 37°C, 5% CO_2), samples were fixed in 2.5% glutaraldehyde in 0.1M sodium cacodylate buffer (pH 7.3) (see 2.1.3.10) for 30 mins at room temperature. The samples were dehydrated through a graded ethanol (Sigma E7023) series diluted in distilled water (20%, 30%, 40%, 50%, 60%, 70%, 90%, 100% x2 for 10 mins each). Samples were then dried with hexamethyldisilazane (HMDS, Sigma 440191), which

was allowed to evaporate in a fume hood overnight. Dried samples were mounted onto 25mm aluminium stubs (G3024 Agar Scientific) with carbon conductive tabs and coated in gold for 90 secs (Denton Vacuum Desk II). The samples were analysed using a Zeiss EVO MA10 scanning electron microscope at an accelerating voltage of 5 kilovolts (kV). Images were captured in SmartSEM software and analysed in Fiji.

2.2.4 CIGARETTE SMOKING AND NEUTROPHIL RESPONSES

2.2.4.1 Extraction and preparation of cigarette smoke extract (CSE)

To mimic the *in vivo* inhalation of cigarette constituents, cigarettes were attached to automatic smoking apparatus and lit (Matthews *et al.,* 2011, Figure 2.2). The cigarette smoke extract (CSE) was collected by drawing the smoke through a cigarette filter and bubbled through 30ml of PBS (see 2.1.1.1) (pH 7.4, 37°C) via a peristaltic pump. The cigarettes employed (Superkings Black) were commercially available filter cigarettes (10mg tar, 0.9mg nicotine, 10mg CO) and measured 100mm in length, including a 30mm filter. The CSE was collected over a 5 min period and stopped after 65mm of the cigarette had burnt. Three cigarettes were consumed for every 30ml PBS, and this process was repeated 10 times to produce 300ml of pooled CSE. This was divided into 1ml aliquots and stored under liquid nitrogen until needed; the resultant extract represented 100% CSE. For use in neutrophil assays, CSE was defrosted at room temperature and used immediately (Matthews *et al.,* 2011, 2012).

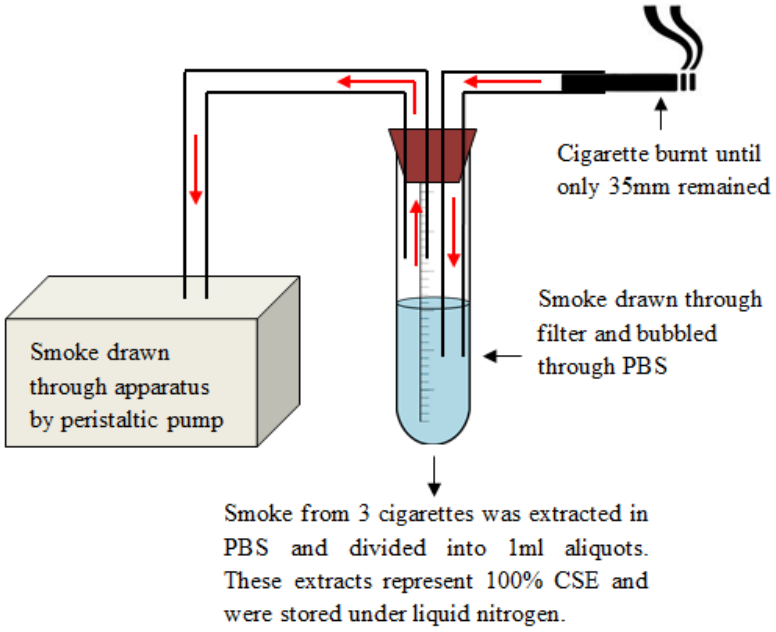

Figure 2.2: Schematic representation showing the collection of CSE
Cigarettes were burnt until 65mm were consumed (5 mins) and the smoke was drawn through PBS by a peristaltic pump to collect 100% CSE (image produced by P. White).

2.2.4.1.1 Estimation of CSE concentration

The concentration of CSE was determined based on the assumption that all available nicotine was collected during 65mm burning to produce the 100% CSE solution (Matthews *et al.,* 2011). The stored CSE aliquots would thus constitute an estimated 83.6µg/ml of nicotine (Matthews *et al.,* 2011). Reported levels of nicotine in saliva and GCF after smoking one cigarette are 1.82 ± 0.61*µ*g/ml and 5.96 ± 0.77µg/ml respectively (mean ± SE) (Ryder *et al.,* 1998). 100% CSE was diluted with PBS to final concentrations of 1%, 5% and 10%, which is equivalent to 0.84µg/ml, 4.2µg/ml and 8.4µg/ml of nicotine (2.1.4.1), respectively.

2.2.4.2 Cigarette components

In addition to looking at the impact of CSE on neutrophil activity, specific cigarette constituents were also assayed, including nicotine (section 2.1.4.1), cotinine (section 2.1.4.2) and thiocyanate (SCN-) (section 2.1.4.3).

2.2.4.2.1 Impact of CSE and CSE components on NET production

The impact of CSE and CSE components on NET production was determined by quantifying NET-DNA (section 2.2.3.3). In brief, neutrophils were exposed to CSE (1%, 5% or 10%), nicotine (1µg/ml, 5µg/ml or 10µg/ml), cotinine (1µg/ml, 5µg/ml or 10µg/ml) or SCN- (50µM, 100µM or 150µM) priming, followed by subsequent stimulation with PMA (50nM) or HOCl (0.75mM). Alternatively, neutrophils did not receive priming, but were stimulated with CSE or CSE components. Both primed and stimulated neutrophils were incubated for 4 hours prior to quantification of NET-DNA with Sytox green (2.2.3.3).

2.2.4.2.2 NET visualisation of CSE and CSE component-treated neutrophils

NETs were also visualised in response to CSE (1%, 5% or 10%), nicotine (1µg/ml, 5µg/ml or 10µg/ml), cotinine (1µg/ml, 5µg/ml or 10µg/ml) or SCN- (50µM, 100µM or 150µM). NET-DNA was visualised by fluorescence microscopy by staining extracellular DNA with Sytox green 4 hours post-stimulation (see 2.2.3.7).

2.2.4.2.3 Neutrophil Chemotaxis assay

To determine the effect of CSE on neutrophil chemotaxis, cells were incubated with PBS (2.1.1.1) or CSE (1%, 5% or 10%) (2.2.4.1.1) for 30 mins, prior to washing by centrifugation (6 mins at 500rcf) and re-suspending in RPMI-1640 (Sigma R7509). To visualise and quantify neutrophil chemotaxis (speed, velocity, and resultant vector length) in response to chemoattractants, an assay was developed in house (Roberts *et al.,* 2015) using the Insall

chamber (Muinonen-Martin *et al.,* 2010, Figure 2.3). Isolated neutrophils were diluted to $1x10^6$/ml in RPMI-1640 (Sigma R7509), plus 1.5µl of 7.5% BSA (Sigma A2153, 2.1.1.3) per ml of cell suspension. Coverslips (square 22ml, VWR international) were washed by submerging in 0.2M HCl, followed by 2 wash steps in distilled water. After air drying (approximately 30 mins), 400µl of 7.5% filter-sterilised BSA (2.1.1.3) was added to each coverslip and this was incubated at room temperature for 20 mins to facilitate neutrophil adhesion. During this time, the Insall chamber was washed 3 times in RPMI-1640. Post-incubation, the coverslip was inverted onto the washed chamber, ensuring the chemoattractant loading bays were still exposed. Excess fluid was aspirated from the chamber with filter paper to create a seal between the coverslip and chamber. 80µl of the chemoattractant was pipetted into the loading bay, which included RPMI-1640 (negative control), 10nM N-Formyl-Met-Leu-Phe (fMLP, Sigma F3506) or 200ng/ml IL-8 (Sigma, SRP3098). Neutrophil migration was visualised by microscopy (x20 magnification) (Zeiss Primovert, Carl Zeiss Imaging Thornwood) and time-lapse images captured every 30 secs for 40 frames over 20 mins (Q Imaging Retiga 2000R).

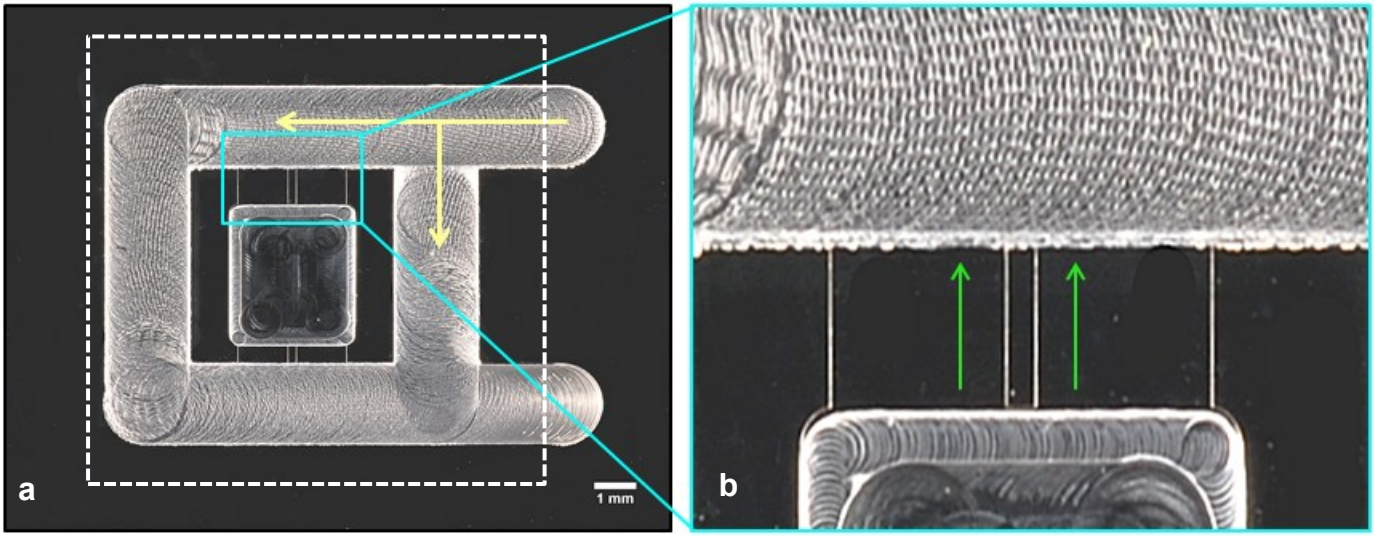

Figure 2.3: Photograph of Insall chemotaxis chamber
To visualise neutrophil chemotaxis, neutrophils on a coverslip were placed over the Insall chamber, as shown by the white dotted square in Figure (a). The yellow arrows indicate the addition of the chemoattractant via the loading bays. Figure (b) shows a magnified image of the area visualised by time-lapse microscopy, indicated by the blue square. Neutrophil chemotaxis in response to the chemoattractant is recorded every 30 secs for 40 frames (20 mins), typical migration towards the chemoattractant is illustrated by the green arrows. Scale bar represents 1mm (image produced by P. White).

2.2.4.2.4 Neutrophil chemotaxis analysis

The 40 time-lapse images produced for each condition were processed with Q pro-imaging software, followed by analysis in Fiji. The movement of 15 mobile cells (selection of cells validated by Helen Roberts) was tracked through each frame with a manual tracking plug-in (MtrackJ). The quantitative data generated was used to calculate neutrophil speed, velocity and chemotactic index, see Table 2.8 for definitions.

Table 2.8: Neutrophil chemotaxis measurements

Chemotaxis measure	Description
Speed	Average speed of neutrophil movement in any direction over 40 frames (20 mins).
Velocity	Average speed of neutrophil directional movement over 40 frames.
Chemotactic index	Measure of directional accuracy of neutrophil chemotaxis calculated by the angle of cell movement along the Y-axis (Andrew & Insall 2007).

2.2.4.3 Gene expression of CSE and SCN- treated neutrophils

Quantitative real time polymerase chain reaction (RT-PCR) was employed to compare the expression profile of neutrophil gene transcripts in response to CSE and SCN- treatment.

2.2.4.3.1 Storage of neutrophils for subsequent RNA isolation

Following isolation (2.2.1.1.2), neutrophils were re-suspended at $1x10^6$ in 1ml of RPMI-1640 (Sigma R7509) in a 1.5ml Eppendorf. Cells were incubated (Galaxy S, 37°C, 5% CO_2) with CSE (1%, 5% or 10%, see 2.2.4.1) or SCN- (50µM, 100µM or 150µM, see 2.1.4.3) for 4 hours, then centrifuged for 6 mins at 500rcf, after which the supernatant was carefully removed and discarded. 1ml of Tri-reagent (Sigma T9424) was added to each Eppendorf, the pellet re-suspended by pipetting and the sample frozen at -20°C until needed.

2.2.4.3.2 Isolation of RNA

RNA was isolated from neutrophils using a Qiagen RNeasy Minikit (74104) according to the manufacturer's instructions. Neutrophils previously stored in tri-reagent were defrosted and 200µl of chloroform (Sigma 34854) added to each Eppendorf prior to mixing and centrifugation (Eppendorf 5415D) for 15 mins at 800rcf. Following centrifugation, 450µl (clear section) from each tube were transferred to a fresh 1.5ml Eppendorf, followed by the

addition of 450µl 70% ethanol (Sigma E7023). The mixture was gently combined by pipetting, before being transferred to a spin column assembly and centrifuged (30 secs at 3500rcf). The collection tube was emptied to discard the flow through fluid. 700µl of wash buffer were added to the spin column to wash the membrane, this was then centrifuged (30 secs at 3500rcf). The collection tube contents were discarded and 500µl of RPE buffer (provided in kit and prepared by adding 44ml 100% ethanol prior to use) were added to the spin column. This was centrifuged for 30 secs at 3500rcf, this step was repeated, however with a centrifugation step of 2 mins at 3500rcf to dry the membrane and to ensure that all the ethanol was removed. The flow through fluid and collection tube were discarded and the spin column membrane was placed in a fresh Eppendorf. 50µl RNase free water was added and this was centrifuged for 1 min at 3500rcf. This results in the RNA being eluted from the membrane into the Eppendorf collection tube. The spin column was discarded and the samples were stored at -80°C until needed.

2.2.4.3.3 Quantification of RNA

The amount and purity of neutrophil RNA isolated was determined by measuring the optical density and the ratio of absorbance at 260/280nm ($OD_{260/280nm}$). Pure RNA has a 260/280nm absorbance of 2.1, thus a value between 1.8-2.0nm is considered to be pure (Sambrook *et al.,* 1989; Manchester 1996). RNA samples were diluted in RNase free water (2µl sample plus 68µl diluent). Based on the amount of RNA in each sample, samples were equally pooled across the treatment conditions (n=10 biological repeats).

2.2.4.3.4 The synthesis of complementary DNA (cDNA)

RNA was reverse transcribed to produce complementary DNA (cDNA) from pooled RNA with a cDNA synthesis kit (Tetro Bioline 65042). Pooled RNA samples were defrosted, gently mixed and kept on ice until needed. The primer mix was made up in an RNase free

reaction tube as described in section 2.1.5.1. Samples were heated to 45°C for 40 mins and the reaction terminated by incubating the samples for 5 mins at 85°C (Eppendorf Mastercycler Gradient). Samples were made up to a final volume of 500µl with RNase free water and the sample was transferred to a Microcon® tube (Millipore 42410). This was centrifuged for 2 mins at 100rcf, prior to inverting the column into a new tube to collect approximately 50µl of clean cDNA. This was centrifuged for 1 min at 3500rcf and the cDNA samples were stored at -20°C until needed for real time PCR.

2.2.4.3.5 Quantitative real time PCR analysis

A white 96-well multi-well plate (LightCycler® 480, 04729692001) was prepared by combining 2µl of cDNA (2.2.4.3.4), 10µl LightCycler® 480 SYBR green PCR mix (04707516001), 0.5µM of forward and reverse primers and RNase-free water to give a final volume of 20µl per well. The plate was covered and centrifuged (3 mins at 1500rcf) and PCR was performed by placing the plate in the Roche LightCycler® 480 PCR system. All samples were amplified in duplicate and 2 "no-template" controls per primer pair were included in every run (Table 2.9 and Figure 2.4). Gene expression levels were measured by following the manufacturer's instructions from crossing point (Cp) values by fit points methods programmed on the LightCycler® 480 software (Roche diagnostics version 1.5).

2.2.4.3.6 Validation of PCR primers and assays

Preliminary experiments were used to determine the PCR amplification and efficiency for each primer pair (see 2.1.5.2) for reference genes and target genes), to indicate the amount of amplicon being amplified each cycle. An efficiency of 2.0 is considered 100% efficient, and means the target molecule doubles every PCR cycle (LightCycler®). Pooled cDNA was serially diluted (1, 1:1, 1:10, 1:100, 1:1000) with RNase free water using the LightCycler®

480 software. Melt curves were also produced for each primer to ensure primers were only amplifying a single amplicon, which is the housekeeper or target gene (Figure 2.5).

2.2.4.3.7 Analysis of gene expression levels

Target gene expression was determined using LightCycler® 480 software by calculating fold-changes in gene expression as a ratio of a housekeeping gene. The most appropriate housekeeper was determined by analysis with the statistical algorithm "BestKeeper" (Pfaffl *et al.*, 2004). The BestKeeper program index was created using the geometric mean of each candidate gene's Cp values. The variation of the housekeeping gene is calculated according to the Cp values, standard deviation (SD) and coefficient of variance. Reference genes with a SD of >1 are considered inconsistent, whilst the lowest SD is considered the most stable (Piehler *et al.*, 2010, Radonic *et al.,* 2004). Based on these results, the YWHAZ housekeeper was considered the most consistent and subsequently used as a reference to quantify the expression of the genes of interest.

	Temperature	Time	Cycles
Pre-incubation	98°C	5 mins	1
Denaturation	98°C	20 secs	60
Annealing	60°C	20 secs	
Extension	72°C	30 secs	
Melting	98°C	-	1
Cooling	4°C	Hold	1

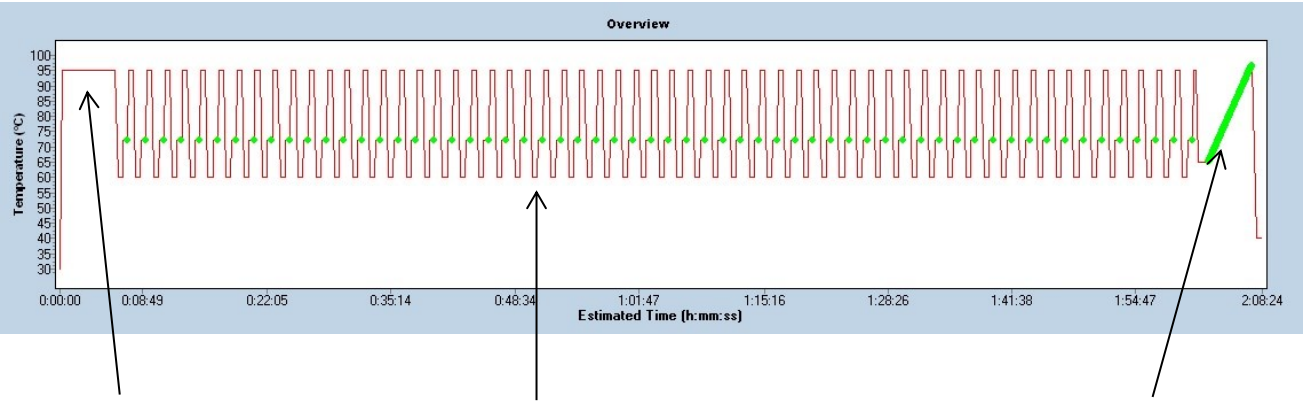

Denaturation of DNA at 98°C

Primers anneal at 60°C and extend at 72°C. Green indicates the point at which the product is quantified.

Product melts at 98°C

Table 2.9 and Figure 2.4: PCR cycling protocol

Amplification of the neutrophil housekeepering and target genes was performed according to the temperatures and times outlined in the graph and table. Graph shows the representative cycling conditions for reference gene, YWHAZ.

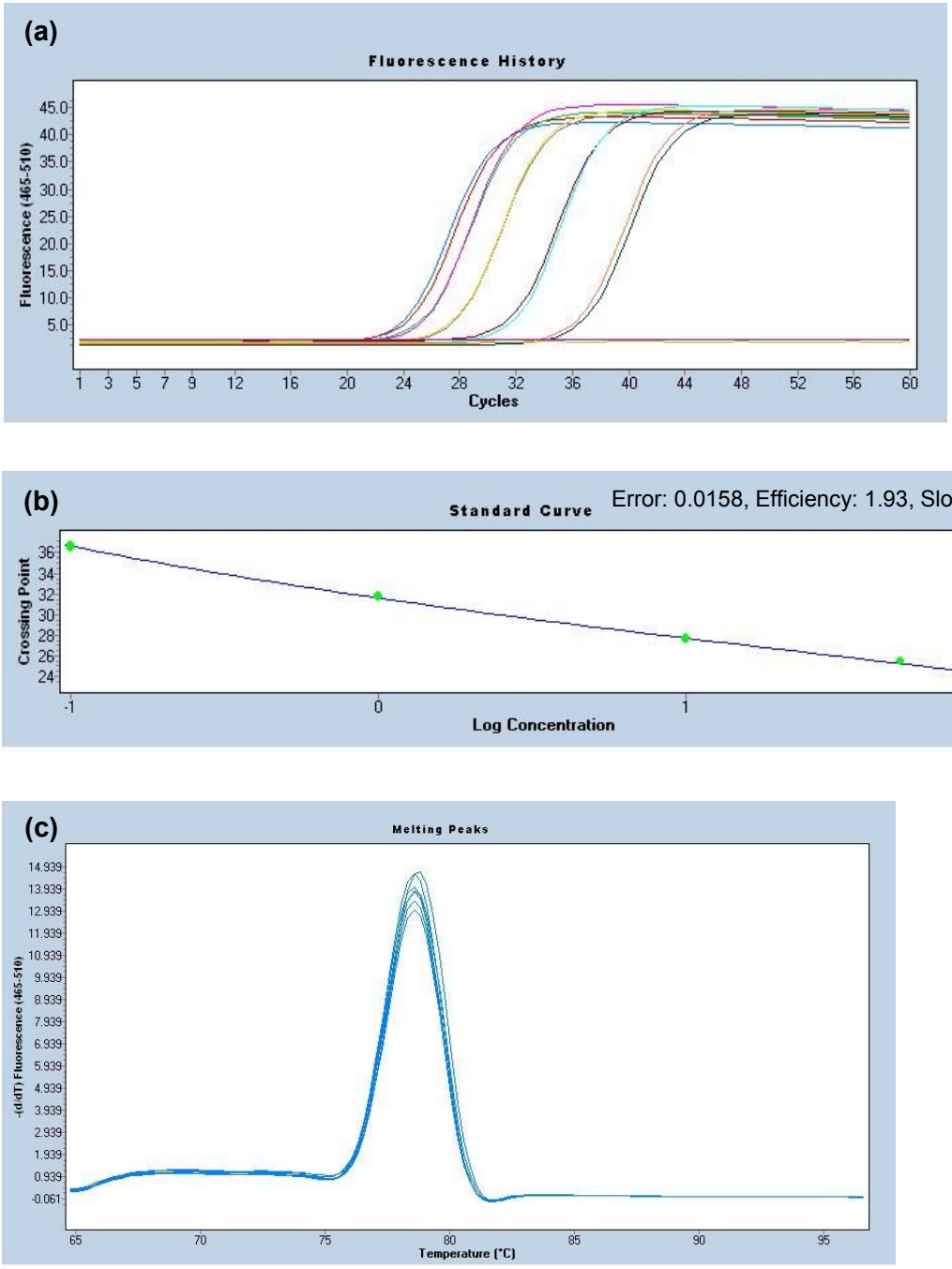

Figure 2.5: Amplification curve, efficiency standard curve and melt curve for the YWHAZ assay

(a) Representative amplification curve of serially diluted reference gene YWHAZ, including 2 no-template controls. This enabled the generation of a YWHAZ standard efficiency curve by the LightCycler® 480 software, (b), which is indicative of the amount of amplicon being amplified each cycle. An efficiency of 2.0 is considered 100% efficient. (c) YWHAZ melt curve was assessed to ensure primers are only amplifying a single amplicon (i.e. the product of interest), as shown by the single peak. Amplification curves, standard efficiency curves and melt curves were produced for all references and targets genes.

2.2.5 NET DEGRADATION AND THE EFFECT OF DELAYED NET REMOVAL

2.2.5.1 NET degradation with plasma

Neutrophils were isolated (2.2.1.1.2) and stimulated for NET production in a 96-well plate (Corning) (section 2.2.3.3). Following NET release, previously isolated plasma samples (section 2.2.6.2.3) were defrosted and diluted to 10% in PBS (2.1.1.1). Plasma was added to wells in 50µl aliquots and incubated for 3 hours (Galaxy S, 37°C, 5% CO_2). Selected wells containing NETs were treated with 1U/ml MNase (2.1.2.2) for 15 mins to act as a positive control for NET degradation, and were considered "100% NET degradation" (Hakkim *et al.,* 2010). After 3 hours incubation, the plate was centrifuged (Hettich Universal 320R, 10 mins at 1800rcf). Next, 150µl of the supernatant were transferred to a a black flat bottom non-treated 96-well plate (Costar 3915), with the addition of 15µl of 10µM Sytox green (Invitrogen S7020) to quantify any free DNA within the supernatant. Controls included the addition of 1U/ml Mnase to the plasma sample prior to incubation with NETs. Fluorescence was read in AFU on a fluorometer (2.2.3.3).

2.2.5.2 Quantification of immunoglobulin G (IgG), free light chains (FLCs), and cystatin C

Plasma samples (500µl aliquots, 2.2.6.2.3) from chronic periodontitis patients and healthy controls were processed for the quantification of IgG subclasses (1-4), FLCs and cystatin C. All plasma samples were analysed by The Binding Site Group Ltd (Birmingham, UK). IgG subclasses were quantified using the SPAPLUS® analyser and the reference ranges used for IgG subclasses were: IgG1: 3.824-9.286g/L, IgG2: 2.418-7.003g/L, IgG3: 0.218-1.761g/L, IgG4 0.039-0.864 (Schauer *et al.,* 2003). Samples were analysed for FLC kappa and FLC lambda on the SPAPLUS® turbidimeter (Freelite, The Binding Site Group Ltd, Bradwell *et al.,* 2001). The reference ranges employed for FLC analyses were: FLC kappa: 3.3-19.4mg/L, FLC lambda: 5.71-26.3mg/L, FLC kappa/lambda ratio: 0.26-1.65, summated FLC:

9.01-45.7 (Katzmann *et al.,* 2002). Plasma cystatin C levels were quantified using the SPAPLUS® assay, the reference range was 0.51-0.98 mg/L (Finney *et al.,* 2000).

2.2.5.3 Collection of NET supernatants

Isolated neutrophils ($1x10^5$, 2.2.1.1.2) were stimulated to produce NETs using 0.75mM HOCl in a clear non-treated 24-well plate (Costar 3526) (section 2.2.3.3). Following a 4-hour incubation (Galaxy S, 37°C, 5% CO_2), the supernatant was gently aspirated and the NETs washed by adding 1ml of pre-warmed (20°C) RPMI-1640 (Sigma R7509). This process removes components that are not NET bound and also any remaining HOCl (Appendix III). NETs were digested by adding 75µl MNase (1U/ml, 2.1.2.2) and the plate was incubated for 15 mins at room temperature. Post incubation, the plate was centrifuged (Hettich Universal 320R, 10 mins at 1800rcf). The supernatants were then transferred to fresh 2mL cryotubes and frozen under liquid nitrogen prior to storage at -80°C. Preliminary experiments revealed that snap freezing produced NET supernatants most representative of fresh NETs, compared with -20°C, -80°C and slow freezing (1°/min, Mr Frosty^{TM}) (Appendix VI).

2.2.5.4 NET supernatant concentration

To determine the concentration of NET supernatants, the amount of DNA in each pooled sample (from 5 volunteers) were quantified fluorometrically with Sytox green (2.2.3.3). 50µl of 25%, 50% or 100% of NET supernatants were added to a black flat bottom non-treated 96-well plate (Costar 3915), 125µl of RPMI-1640 (Sigma R7509) added, plus 15µl of 10µM Sytox green. A standard curve was produced by serially diluting calf thymus DNA (Sigma D4522). Fluorescence was read in AFU using a fluorometer (2.2.3.3). To determine whether NET supernatants stimulate neutrophil responses, pooled samples were employed as total ROS stimuli (2.2.3.2), NET stimuli (2.2.3.3) and chemoattractants (2.2.4.2.3).

2.2.5.5 NET supernatants effects on oral epithelial cells (OECs)

To determine whether NET supernatants affect the growth of OECs, H400s were cultured (see section 2.1.6) in a 96-well plate and incubated with NET supernatants (25%, 50%, 100%, 2.2.5.3). At 4 and 24 hours, the impact of NET supernatants on H400 cell apoptosis, metabolic activity and necrosis was determined by quantifying caspase activity (see 2.2.1.2.4), ATP activity (see section 2.2.1.2.5) and lactase dehydrogenase (LDH) release (see 2.2.5.7).

2.2.5.5.1 H400 oral epithelial cell storage and recovery

Preservation of H400 oral epithelial cells for future use was achieved by storing cells at -80°C. Cells in supplemented Dulbecco's Modified Eagle's Medium:nutrient mixture F-12 (DMEM/F-12) were divided into 1ml cryotubes containing $1x10^6$ cells in 20% (v/v) heat inactivated FCS (Labtech) and 10% (v/v) DMSO (Sigma D8418) (see 2.1.6.2). When required, cell suspensions were rapidly defrosted in a water bath (37°C) and transferred to 9ml of pre-warmed (37^oC) DMEM/F-12 and gently mixed. This mix was centrifuged (10 mins at 150rcf) and the supernatant removed prior to the pellet being re-suspended in 10ml of fresh warmed (37^oC) DMEM/F-12. This was then transferred to a sterile cell $75cm^2$ culture flask (Thermo Scientific) and incubated for 3-4 days (Galaxy S, 37°C, 5% CO_2). Cell growth was observed microscopically (Leitz Laborlux s), after which the media was removed and replaced with 10ml of fresh pre-warmed (37^oC) DMEM/F-12. The flask was re-incubated (Galaxy S, 37°C, 5% CO_2) for an additional 2-3 days and cells were passaged when the monolayer was nearing confluence with a neutral pH. This was indicated by the phenol red present in DMEM/F-12, where if the cells are left too long and the nutrients in the media are exhausted, the media solution will turn yellow due to increased acidity (The Merck Index 1996).

2.2.5.5.2 Cell passage

H400 oral epithelial cells were passaged when they reached 90-100% confluence. This process dissociates the monolayer of adherent cells to produce a cell suspension for re-seeding into a new flask. Growth media was removed and the adherent cells were washed with pre-warmed (37^{o}C) Dulbecco's PBS (Invitrogen 14190). This was then removed and 4ml of T-EDTA added (see 2.1.6.3), and the flask then incubated for 10 mins (Galaxy S, 37°C, 5% CO_2). Microscopy was employed to confirm cells were released from the monolayer. The resultant single cell suspension was transferred to a universal container with 4ml of pre-warmed (37^{o}C) DMEM/F-12, in order to terminate the action of T-EDTA. The cells were centrifuged (IEC Centra CL2, 10 mins at 150rcf) and the supernatant removed. Pelleted cells were re-suspended in 5ml of pre-warmed (37^{o}C) DMEM/F-12, counted with a haemocytometer (Neubauer, Reichert) (2.2.5.5.3) and seeded accordingly in a sterile flask (75cm^2, Thermo Scientific). All experiments were undertaken between 4 and 10 passages.

2.2.5.5.3 Determination of cell concentrations and viability

Trypsinised cells were counted under a light microscope at x20 magnification (Leitz Laborlux s) on each of the 4 quadrants of a haemocytometer (Neubauer, Reichert). This count was divided by 4 to yield a cell count of 1x10^4 per ml of cell suspension. This stock of cells was diluted appropriately in DMEM/F-12 (2.1.6.2). Cell viability was confirmed by trypan blue exclusion (Sigma T8154, 2.2.1.2.3). Tyrpan blue is not absorbed by viable cells, however if the neutrophil cell membrane is damaged, the dye will be absorbed and stain the cell blue. A calculation was employed to determine the percentage of viable cells: number of viable cells/ total number of cells x 100. Preliminary experiments compared trypsinised cells and *in situ* cell counts (Appendix VII), and based on these results all subsequent experiments relied on trypsinised cell counts.

2.2.5.6 Culture of H400 oral epithelial cells in a 96-well format

To determine the effect of NETs on H400 oral epithelial cell growth, cultures were maintained in a white walled tissue culture grade 96-well plate with clear bottoms (Costar 3610). Following cell passage, $1x10^4$ cells in 100µl of DMEM/F-12 (2.1.6.2) were seeded into each well of a 96-well plate. Cells were cultured until 90% confluent prior to addition of NET supernatants (25%, 50% and 100%) in 50µl aliquots (2.2.5.3). Treatment with 0.1% triton (Sigma T8787) was also employed to act as a positive control for cell death.

2.2.5.7 Determination of H400 oral epithelial cell lactate dehydrogenase release

The CytoTox-ONE™ (Promega G7890) homogenous membrane integrity assay was employed to determine H400 cell viability, by fluorometrically quantifying lactate dehydrogenase (LDH), which is released when cell membrane integrity is lost. Cell culture supernatants (50µl) were transferred to a black flat bottom non-treated 96-well plate (Costar 3915) and an equal volume of CytoTOx-ONE reagent was added. The plate was covered and incubated at room temperature for 10 mins. 25µl of stop solution (kit reagent) was added to each well and the fluorescence was read at an excitation of 560nm and an emission of 590nm (Berthold Tristar^2 LB942, ICE).

2.2.6 NEUTROPHIL RESPONSES IN PERIODONTAL HEALTH AND DISEASE

2.2.6.1 NEUTROPHIL RESPONSES IN GINGIVITIS

2.2.6.2 21-day gingivitis model

An experimental model of gingivitis in 10 systemically and periodontally healthy undergraduate dental students from the University of Birmingham was employed (Loe *et al.,* 1965). Ethical approval was obtained from South Birmingham Research Ethics Committee

(2004/074) and all volunteers gave informed consent. A split mouth model was used, in which volunteers were required to wear a soft vinyl mouth guard that covers the maxillary left 4-6 teeth (the right side was used in left handed individuals) during brushing for 21 days (Table 2.10). This prevents mechanical or chemical cleaning of these teeth, allowing for the accumulation of plaque and the development of inflammatory responses characteristic of gingivitis. The maxillary right 4-6 teeth were used as control teeth, as these teeth were subjected to normal oral hygiene, comprised of brushing twice a day. All volunteers were non-smokers (for at least 5 years), had not been prescribed antibiotics or anti-inflammatories in the past 3-months and were not diabetic or pregnant. Volunteers also refrained from using mouth wash and chewing gum for the entirety of the study period.

2.2.6.2.1 Clinical measures of gingival inflammation

Plaque accumulation was determined using the Quigley & Hein, Turesky & Lobene modified (1982) plaque index (PI; Quigley & Hein 1962, Turesky *et al.,* 1970, Lobene *et al.,* 1982). Gingival inflammation was measured using the Löe (1967) gingival index (GI; Löe 1967) and the volume of GCF was also measured using a pre-calibrated Periotron 8000^{TM} (Chapple *et al.,* 1999). GCF was collected over a 30 sec period by inserting Periopaper strips (OraFlow) into the mesio-buccal gingival crevices of test and control sites. Clinical parameters were measured immediately prior to blood collection for neutrophil assays. All volunteers were assessed and indices performed at days 0, 7, 14 and 21 of plaque accumulation (Table 2.10). At day 21 all plaque was removed by prophylaxis and volunteers recommenced normal brushing prior to final assessment at day 35 (designated as return to health). All clinical parameters were measured immediately prior to blood collection for neutrophil assays by a single experienced examiner.

2.2.6.2.2 Plaque sampling

Plaque samples were collected from the palatal test and control teeth at each time point outlined in Table 2.10, using a size 30 finger spreader (25mm, Claudius Ash). Plaque was re-suspended in 200µl PBS (2.1.1.1) and vortexed until the plaque was homogenised and samples were stored at -20°C within 1 hour of collection. Collection of plaque at each time point was from different teeth to ensure plaque accumulation was assessed after 0, 7, 14 and 21 days of build-up, and final samples were obtained at day 35 (return to health).

2.2.6.2.3 Collection of plasma

Plasma was isolated from blood collected into 6ml lithium heparin anticoagulant tubes by centrifuging for 30 mins at 1000rcf (4°C). Following centrifugation, plasma was transferred to cryotubes in 500µl aliquots and stored at -80°C.

Table 2.10: Outline of the 21-day gingivitis model study
Pink background denotes the 21-day study period and ticks indicate the time points at which clinical indices and bloods were collected. Abbreviations: GCF (gingival crevicular fluid).

Time (Days)	Gingivitis model study design	Measurement of gingivitis and plaque & GCF collection	Blood collection for plasma/neutrophil assays
-14	Volunteers were introduced to the study and those who consented were assessed, their teeth professionally cleaned and impressions taken for the construction of an occlusal guard.		
0	Volunteers were fitted with a guard to commence 21 days of no brushing of the maxillary left 4-6 teeth.	✓	✓
7	Volunteers were examined and clinical indices measured.	✓	
14	Volunteers were examined and clinical indices measured.	✓	
21	Volunteers no longer have to wear the mouth guard and their teeth are professionally cleaned.	✓	✓
35	Volunteers were examined to ensure they have returned to gingival health.	✓	✓

2.2.6.2.4 Plaque as a neutrophil stimulus

The ability of plaque to stimulate neutrophils for ROS (2.2.3.2) and NET production (2.2.3.3) was assayed. Preliminary experiments sought to determine the concentrations of plaque required to evoke ROS and NET production; plaque was initially derived from a healthy volunteer who had not brushed for 24 hours. Preliminary experiments were conducted to determine the concentration of plaque required to stimulate neutrophils, and based on these resutls all further assays employed plaque as a neutrophil stimulus at 25% in 25µl aliquots.

Plaque was pooled across the 10 volunteers at each time point, providing 1 control and 1 test plaque suspension at days 0, 7, 14, 21 and 35.

2.2.6.2.5 Characterisation of plaque samples

Pooled plaque samples were characterised in order to normalise ROS and NET production in response to a plaque stimulus. Endotoxin, DNA and protein content were quantified for pooled plaque sample at each time-point.

2.2.6.2.5.1 Quantification of endotoxin

Gram-negative bacterial endotoxins present within plaque were characterised using the Pierce® Kit Limulus Amebocyte Lysate (LAL) Chromogenic Endotoxin Quantitation Kit (88282). A clear non-treated 24-well plate (Costar 3526) was equilibrated to 37°C for 10 mins, followed by the addition of 25µl of 50% plaque sample. A standard curve was produced by serially diluting an *Escherichia coli* endotoxin standard (011:B4, provided in kit). The plate was covered and incubated for 5 mins (Galaxy S, 37°C, 5% CO_2). 50µl LAL reagent were added to each well, the plate was again covered and incubated for 10 mins (Galaxy S, 37°C, 5% CO_2). Post-incubation, 100µl of substrate solution was added to each well, this was then incubated for a further 6 mins (Galaxy S, 37°C, 5% CO_2). Finally, 50µl of stop reagent (25% acetic acid) were added to each well. The optical density was read on a plate reader at 405nm (OD_{405nm}) (ELx800, Bio-Tek Instruments Inc. Gen 5 1.11). Plaque samples and standards were assayed in duplicate.

2.2.6.2.5.2 Quantification of DNA

The amount of plaque DNA within plaque samples was quantified fluorometrically with Sytox green. 25µl of 50% plaque samples was added to a black flat bottom non-treated 96-well plate (Costar 3915). 125µl of RPMI-1640 (Sigma R7509) was added, plus 15µl of

10μM Sytox green (2.1.2.3). A standard curve was produced by serially diluting calf thymus DNA (D4522). Fluorescence was read in AFU on a fluorometer (2.2.3.3).

2.2.6.2.5.3 Quantification of protein

Plaque protein content was measured using a Pierce™ bicinchoninic acid (BCA) Protein Assay Kit (23227), which enables colorimetric detection of total protein content. 25μl of a 50% plaque sample were added to a clear non-treated 96-well plate (Costar 3370), followed by the addition of 200μl working reagent. A standard curve was produced by serially diluting BSA (Sigma A2153, 2.1.1.3). The plate was covered and incubated for 30 mins (Galaxy S, 37°C, 5% CO_2). Post-incubation the plate was cooled at room temperature for 5 mins and the optical density read at 562nm (OD_{562nm}) on a plate reader (ELx800, Bio-Tek Instruments Inc. Gen 5 1.11)

2.2.6.3 NEUTROPHIL RESPONSES IN CHRONIC PERIODONTITIS

2.2.6.3.1 Chronic periodontitis clinical study volunteers

NET production (2.2.3.3) by neutrophils derived from the peripheral blood of chronic periodontitis patients pre- and post-treatment was investigated. All volunteers provided written informed consent, and ethical approval for the study was obtained from the West Midlands Research Ethics Committee (10/H1208/48). Chronic periodontitis was defined by a minimum of 2 non-adjacent sites per quadrant with probing pocket depth >4mm, which bled upon probing and displayed radiographic bone loss >30% of the root length, as defined by the European Federation of Periodontology (Tonetti & Claffey 2005). All patients were non-smokers (for at least 5 years), had not been prescribed antibiotics or anti-inflammatories in the past 3-months and were not diabetic or pregnant. The study group age ranged from 33 to 63, however age was accounted for by recruiting age and gender-matched healthy controls.

The patients received tailored oral hygiene instruction and non-surgical periodontal treatment that involved scaling and root surface debridement of periodontal pockets >4mm. The periodontally healthy control group showed no interproximal attachment loss, no probing pocket depths >3mm and whole mouth bleeding scores were <10%. These volunteers were also subjected to the same exclusion criteria as the chronic periodontitis patients. All NET assays were carried out on patients and their healthy counterpart in parallel on the same day. Plasma (2.2.6.2.3) and neutrophils (2.2.1.1.2) were isolated from peripheral venous blood pre-treatment and 3 months post-therapy.

2.2.6.3.2 Clinical measures of gingival inflammation

To determine the severity of periodontitis and the response to treatment, several parameters were measured. These included clinical attachment loss (CAL) probing pocket depth (PDD) and bleeding on probing (BOP). CAL was calculated by summation of periodontal pocket depth and gingival recession measurements in accordance with Haffajee & Socransky (1986). In addition, Plaque accumulation was determined using the Quigley & Hein, Turesky & Lobene modified (1982) PI (Quigley & Hein 1962, Turesky *et al.,* 1970, Lobene *et al.,* 1982). Gingival inflammation was measured using the Löe (1967) GI (Löe 1967) and the volume of GCF was also measured using a pre-calibrated Periotron 8000^{TM} (Chapple *et al.,* 1999). All clinical parameters were measured immediately prior to blood collection for neutrophil assays by a single experienced examiner, who also confirmed periodontal health in the healthy controls.

2.2.6.4 NEUTROPHIL RESPONSES IN PAPILLON LEFÈVRE SYNDROME (PLS)

2.2.6.4.1 PLS study volunteers

PLS patients ranging from 9-14 years old (n=3 males, n=2 females) were enrolled into the study by the University of Birmingham Dental School following a specialised clinic at the Birmingham Children's Hospital. All volunteers provided written informed consent, and ethical approval for the study was obtained from the West Midlands Research Ethics Committee (14/WM/1175). Prior to the study, all volunteers had been genotyped, assessed for comorbidities and their dermatological and periodontal health was determined by Birmingham Children's Hospital. Plasma (2.2.6.2.3) and neutrophils (2.2.1.1.2) from the peripheral blood of patients and healthy gender-matched controls were isolated in parallel for subsequent NET assays (2.2.3.3). Healthy volunteers were periodontally and systemically healthy, non-smokers (for at least 5 years), had not been prescribed antibiotics or anti-inflammatories in the past 3-months and were not diabetic or pregnant.

2.2.6.4.2 Quantification of NE and LL-37 in plasma samples

Commercially available sandwich ELISA kits were employed to quantify NE (eBioscience BMS269) and LL-37 (Hycult biotech HK321) in PLS patient and control plasma samples (2.2.6.2.3). To analyse the previously stored (-80°C) patient and control plasma samples, samples were defrosted, centrifuged (6 mins at 500rcf to pellet any cell debris), and the supernatants transferred to a fresh cryotube. All reagents were provided in the kit were equilibrated to room temperature and diluted according to the manufacturer's instructions prior to use.

2.2.6.4.2.1 Quantification of NE

Samples were diluted 1:100 with sample diluent (provided in kit) and 100µl added to each well (samples assayed in duplicate). The standard (human NE) was serially diluted from 10ng/ml to achieve a suitable standard dilution range and also added to the plate in 100µl aliquots. The plate was covered and incubated at room temperature for 1 hour on a shaker (Luckham R11/TW, speed 2). Post incubation, wells were washed 4 times by emptying wells, adding 400µl wash buffer (incubate for 15 secs at room temperature) followed by aspiration. 150µl of HRP was added to each well and the plate covered and incubated at room temperature for 1 hour on a shaker (Luckham R11/TW, speed 2). The wells were again washed 4 times (as before with 400µl wash buffer), followed by the addition of 200µl TMB substrate and incubation at room temperature in the dark for 20 mins. The reaction was subsequently stopped by the addition of 50µl of stop solution (2M HCl) and the absorbance read at 450nm (OD_{450nm}) (ELx800, Bio-Tek Instruments Inc. Gen 5 1.11). The standard curve was used to determine sample concentrations and expressed in ng/ml.

2.2.6.4.2.2 Quantification of LL-37

Samples were diluted 1:20 with sample diluent (provided in kit) and 100µl added to each well (samples assayed in duplicate). The standard (human LL-37) was serially diluted from 100ng/ml to achieve a suitable standard dilution range and also added to the plate in 100µl aliquots. The plate was covered and incubated at room temperature for 1 hour on a shaker (Luckham R11/TW, speed 2). Post incubation, wells were washed 4 times by emptying wells, adding 400µl wash buffer (incubate for 15 secs at room temperature) followed by aspiration. 100µl of biotinylated tracer antibody was added to each well and the plate covered and incubated at room temperature for 1 hour on a shaker (Luckham R11/TW, speed 2). The wells were again washed 4 times (as before with 400µl wash buffer), followed by the

addition of 100µl of streptavidin peroxidase and incubation at room temperature for 1 hour on a shaker (Luckham R11/TW, speed 2). The 4 wash steps were repeated, prior to the addition of 100µl of TMB solution and incubation at room temperature in the dark for 30 mins. The reaction was subsequently stopped by the addition of 100µl of stop solution (2% oxalic acid) and the absorbance read at 450nm (OD_{450nm}) (ELx800, Bio-Tek Instruments Inc. Gen 5 1.11). The standard curve was used to determine sample concentrations and expressed in ng/ml.

2.2.7 STATISTICAL ANALYSIS

Unless otherwise stated, all statistical analyses were performed in GraphPad Prism 5 software package. The distribution of data, and thus whether data was considered parametric or non-parametric, was determined by Kolmogorov-Smirnov tests. Statistical tests employed for the purpose of this study were at a significance of 0.05. The level of significance is indicated as follows: *, **, *** and **** denotes <0.05, <0.01, <0.001 and <0.0001 respectively, ns means the results are >0.05 and therefore not significant.

CHAPTER 3: NEUTROPHIL ISOLATION TECHNIQUES AND THEIR EFFECTS UPON *EX VIVO* NEUTROPHIL BEHAVIOUR

3.1 Introduction

This chapter reports on the preparation technique of neutrophils upon *ex vivo* neutrophil behaviour using a variety of assays to determine neutrophil function and viability. Isolation aims to separate neutrophils from other blood cells, whilst at the same time not causing inadvertent cell activation, which may affect subsequent *ex vivo* neutrophil analysis (1.9). There are a number of neutrophil isolation methods reported in the literature, including use of different density gradient materials, such as Percoll, Histopaque and Dextran sedimentation followed by Percoll centrifugation (2.2.1). This work aims to determine whether the method of isolation affects *ex vivo* neutrophil activation levels and to identify the most appropriate technique prior to application of a range of *ex vivo* neutrophil assays used in this thesis. Initially, neutrophils were isolated from healthy volunteers (University of Birmingham Ethics Reference ERN_13-0325) using Percoll or Histopaque density centrifugation. Subsequent experiments compared cell isolation by Percoll density centrifugation and Dextran sedimentation (Dextran neutrophils were kindly isolated by Dr Adam Usher, University of Birmingham). Comparisons between isolation techniques were performed in parallel from the same individual.

3.2 Comparisons between isolation techniques

It is worthy of note that Percoll-Histopaque comparisons were undertaken at a different time and in a different research laboratory to the Percoll-Dextran comparisons. Therefore differences in blood donors, laboratory equipment and the neutrophil stimuli employed only allow for these direct comparisons, and not comparisons between Dextran and Histopaque isolation procedures.

3.2.1 Cell yield: Percoll vs Histopaque

Following neutrophil isolation from whole blood, cells were counted to ensure the appropriate numbers of re-suspended cells were employed in subsequent assays (2.2.1.1.5), and also to provide relative yields following Percoll, Histopaque or Dextran isolation procedures (Figure 3.1). Comparisons between Percoll and Histopaque demonstrated that across 10 paired isolations neutrophil yield was significantly higher for the Percoll gradient isolation procedure (Mann-Whitney $^{**}p=0.0014$, n=10) (Figure 3.1a).

3.2.2 Cell yield: Percoll vs Dextran

Across 5 paired isolations with Percoll or Dextran isolation gradients, there was no significant difference in the cell yield isolated per ml of blood. Percoll and Dextran isolation approaches resulted in a mean cell yield of 8.9×10^6 and 9.7×10^6, respectively (Mann-Whitney $p=0.467$, n=5) (Figure 3.1b).

a) Cell yield: Percoll vs Histopaque

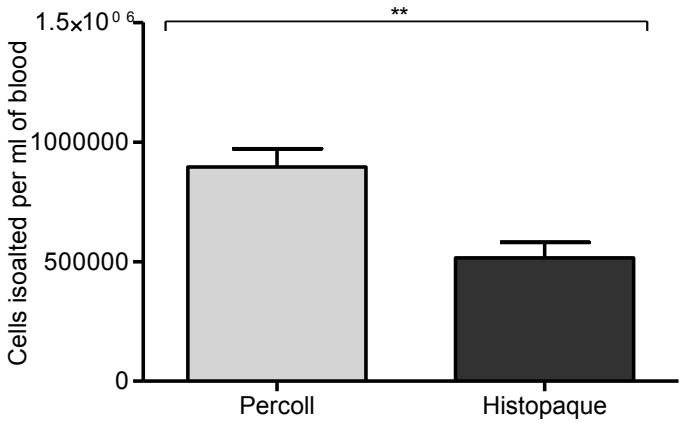

b) Cell yield: Percoll vs Dextran

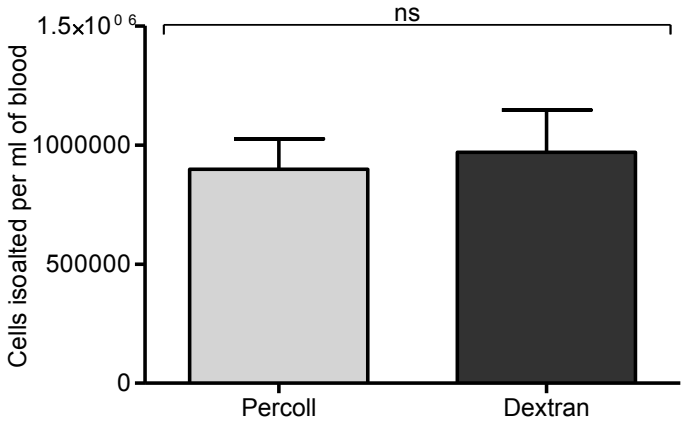

Figure 3.1: The effect of neutrophil preparation techniques on cell numbers
Cell yield (per ml of blood) was compared between (a) Percoll- and Histopaque-isolated neutrophils (n=10 in triplicate), and (b) Percoll- and Dextran- isolated neutrophils (n=5 in triplicate). Statistical significance calculated using Mann-Whitney tests (**$p<0.01$, ns=not significant) n=10 in triplicate. Data expressed as mean ± SEM (n=5 in triplicate).

3.2.3 Total peak ROS production: Percoll vs Histopaque isolation procedures

Subsequent to isolation, Percoll and Histopaque separated neutrophils were assessed for ROS generation (total ROS was measured with luminol, section 2.2.3.2) (Figure 3.2). Histopaque-isolated neutrophils demonstrated higher peak ROS production in response to PBS (unstimulated control); however this did not reach statistical significance. Percoll-isolated cells stimulated with opsonised *S. aureus* ($5x10^7$ and MOI of 500) produced significantly more ROS compared with Histopaque-isolated neutrophils (2 way ANOVA and Bonferroni post-hoc tests ***$p<0.001$, n=10), however there was no significant difference in total ROS production between *F. nucleatum poly*-stimulated ($1x10^8$ and MOI of 1000) Histopaque- and Percoll-isolated neutrophils (Figure 3.2a).

3.2.4 Total peak ROS production: Percoll vs Dextran isolation procedures

Following isolation, both Percoll and Dextran separated neutrophils were assessed for ROS generation (total ROS measured with luminol) in response to PBS (unstimulated control), *F. nucleatum poly* ($1x10^8$ and MOI of 1000) or PMA (25nM). There was no significant difference in ROS generation by untreated cells (PBS) or cells stimulated with *F. nucleatum poly* or PMA between Percoll and Dextran isolated neutrophils (2way ANOVA $p=0.0762$, n=5) (Figure 3.2b).

a) Total peak ROS production: Percoll vs Histopaque

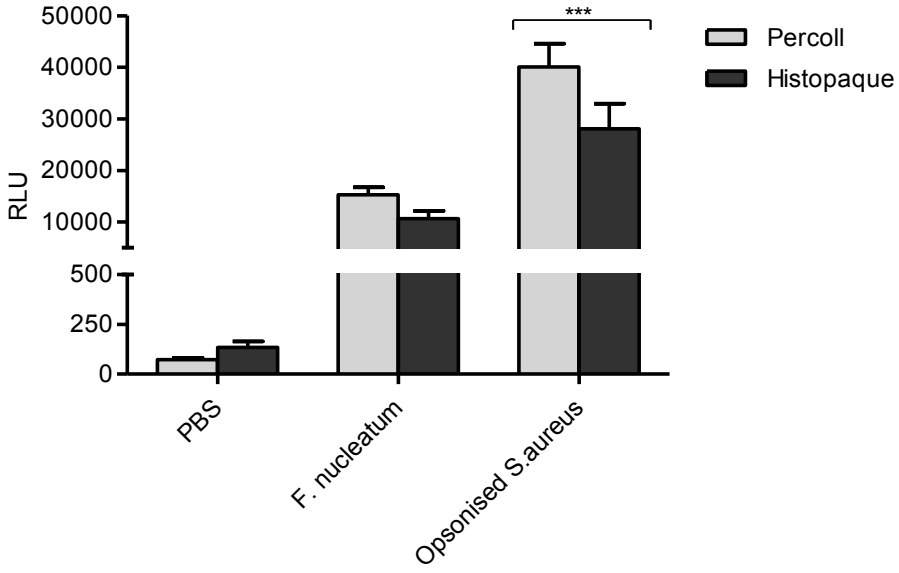

b) Total peak ROS production: Percoll vs Dextran

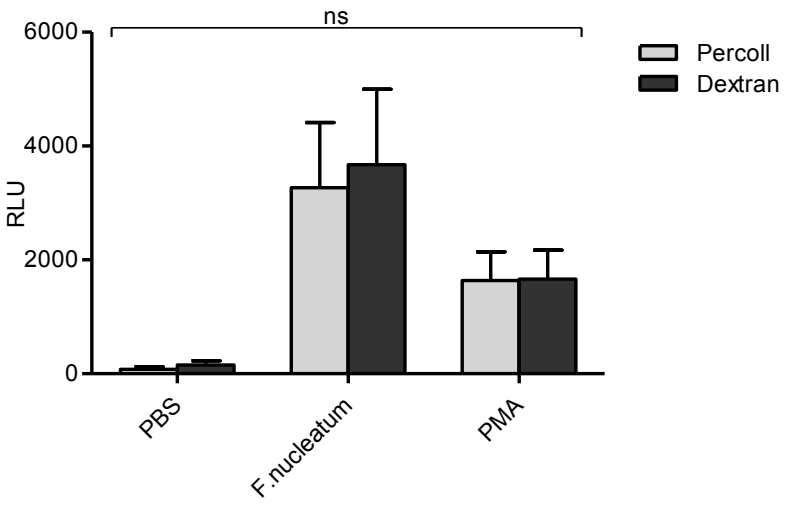

Figure 3.2: The effect of neutrophil preparation technique on peak total ROS production

Total ROS production (quantified with luminol) was compared between (a) Percoll- and Histopaque-isolated neutrophils in response to *F. nucleatum poly* ($1x10^8$, MOI of 1000) and opsonised *S. aureus* ($5x10^7$, MOI of 500) (n=10 in triplicate), or (b) Percoll- and Dextran-isolated neutrophils in response to *F. nucleatum poly* ($1x10^8$, MOI of 1000) and PMA (25nM) (n=5 in triplicate). Statistical significance calculated using 2way ANOVA and Bonferroni post-tests (***$p<0.001$, ns=not significant). Data expressed as the peak RLU (relative light units) and mean ± SEM.

3.2.5 Total ROS production over stimulation period: Percoll vs Histopaque isolation procedures

Consistent with the total peak ROS results, ROS production expressed as "area under the curve" over a 175 min time-course revealed that Histopaque-isolated cells produced marginally higher levels of ROS in response to PBS (unstimulated control), compared with Percoll, implying greater background activation of the isolated neutrophils (Figure 3.3a). No differences were observed between Percoll and Histopaque cells in response to *F. nucleatum poly* ($1x10^8$ and MOI of 1000) (Figure 3.3b), however higher levels of total ROS were produced following opsonised *S. aureus* stimulation ($5x10^7$ and MOI of 500) in Percoll-isolated cells (Figure 3.3c). Following stimulation at 30 mins, levels of total ROS considerably increased in both *F. nucleatum poly* and opsonised *S. aureus*-stimulated cells at approximately 60 mins, and peaked at approximately 80 mins.

3.2.6 Total ROS production over stimulation period: Percoll vs Dextran isolation procedures

Consistent with the total peak ROS results, time-course ROS production expressed as "area under the curve" over 250 mins revealed no observable differences in ROS production between Percoll and Dextran cells in response to PBS (unstimulated control) (Figure 3.4a), *F. nucleatum poly* ($1x10^8$ and MOI of 1000) (Figure 3.4b) and PMA (25nM) (Figure 3.4c). Following stimulation at 30 mins, ROS production in response to *F. nucleatum poly* and PMA steadily increased at approximately 125 mins.

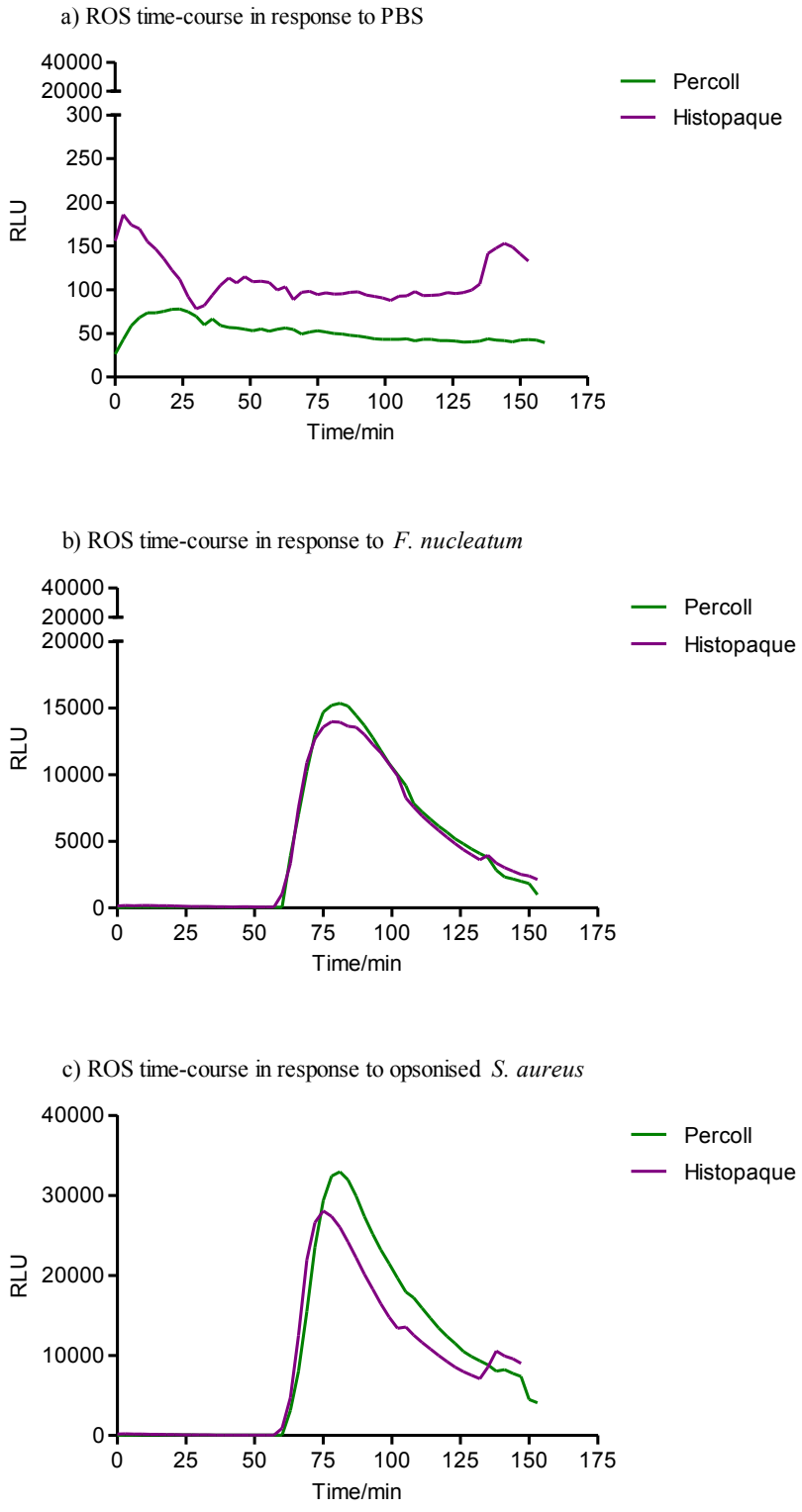

Figure 3.3: Neutrophil isolation time-course analysis of ROS production
Time-course total ROS production over 175 mins by cells isolated with Percoll (green) or Histopaque (purple). (a) ROS production by cells treated with PBS (unstimulated), (b) *F. nucleatum poly* ($1x10^8$, MOI of 1000) or (c) opsonised *S. aureus* ($5x10^7$, MOI of 500). Data presented as mean RLU (relative light units) (n=10 in triplicate).

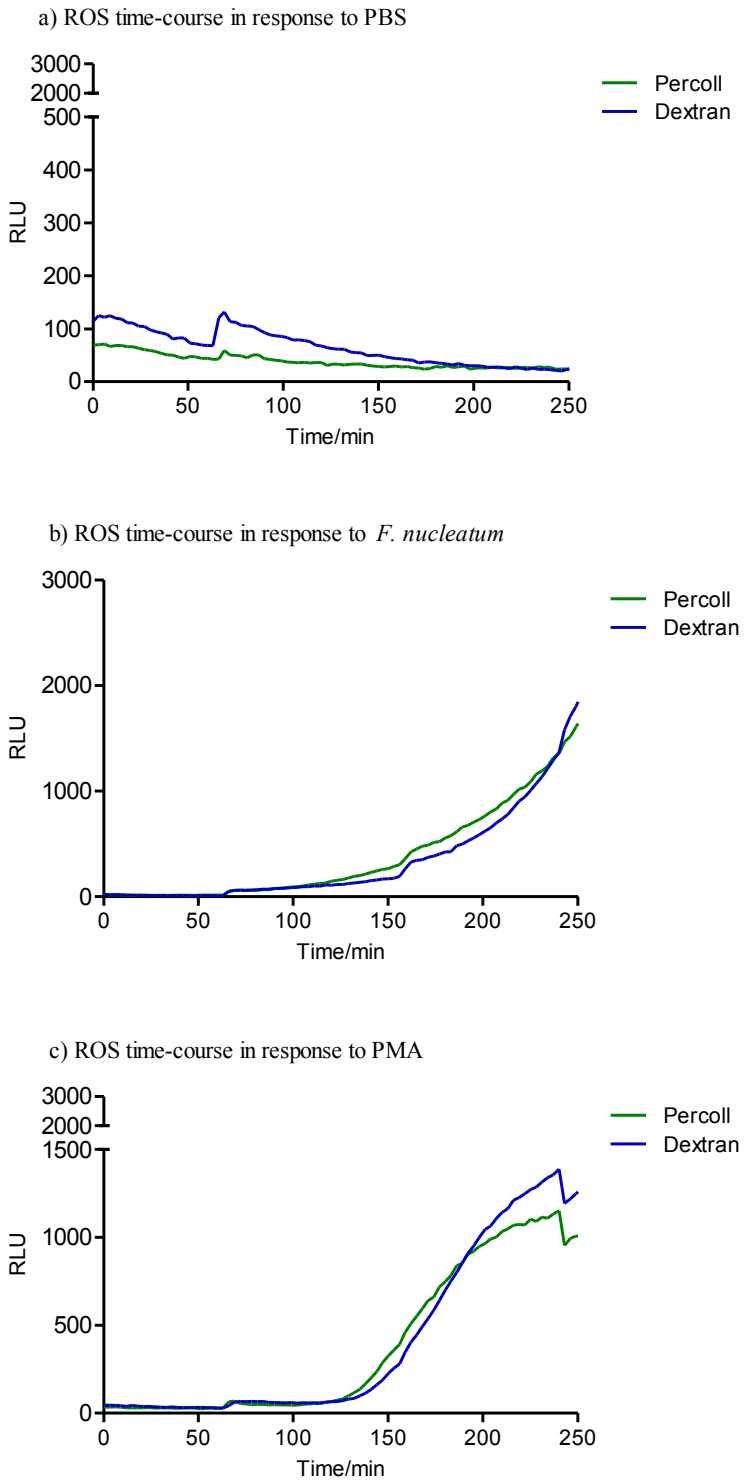

Figure 3.4: Neutrophil isolation time-course analysis of ROS production

Time-course total ROS production over 250 mins by cells isolated with Percoll (green) or Dextran (blue). (a) ROS production by cells treated with PBS (unstimulated), (b) *F. nucleatum poly* ($1x10^8$, MOI of 1000) or (c) PMA (25nM). Data presented as mean RLU (relative light units) (n=5 in triplicate).

3.2.7 NET production: Percoll vs Histopaque isolation procedures

NET production (NET-DNA quantified with Sytox green, section 2.2.3.3) was considerably higher in Percoll-isolated unstimulated cells (PBS); however this did not reach statistical significance. Neutrophils stimulated with *F. nucleatum poly* ($1x10^8$ and MOI of 1000) or opsonised *S. aureus* ($5x10^7$ and MOI of 500) also exhibited increased NET release when isolated with Percoll (2way ANOVA and Bonferroni post-tests ***$p<0.001$* and *$p<0.05$* for *F. nucleatum poly* and opsonised *S. aureus,* respectively, n=10) (Figure 3.5a).

3.2.8 NET production: Percoll vs Dextran isolation procedures

Dextran-prepared neutrophils produced significantly fewer NETs in response to stimulation with PMA (50nM) and HOCl (0.75mM) relative to cells isolated with Percoll gradients (2way ANOVA and Bonferroni post-tests **$p<0.01$* and ***$p<0.001$, for PMA and HOCl, respectively, n=5). Higher NET release in unstimulated Percoll-isolated cells was also observed, however this difference was not statistically significant (Figure 3.5b).

a) NET production: Percoll vs Histopaque

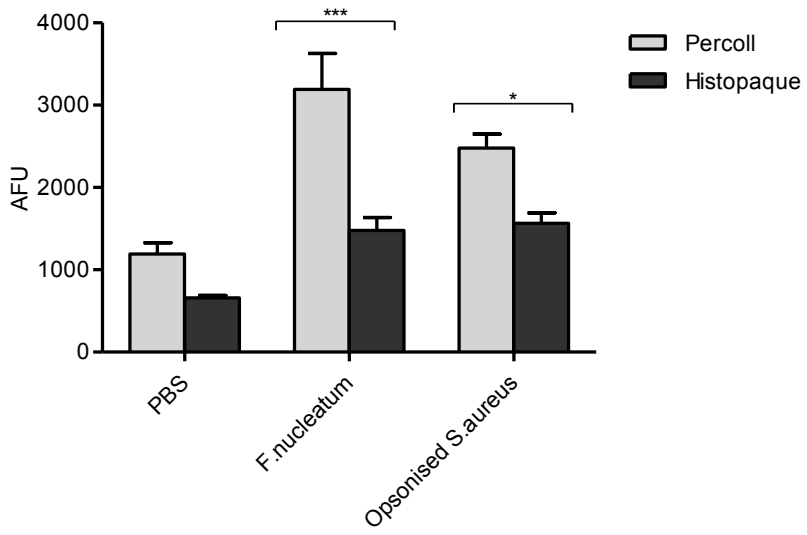

b) NET production: Percoll vs Dextran

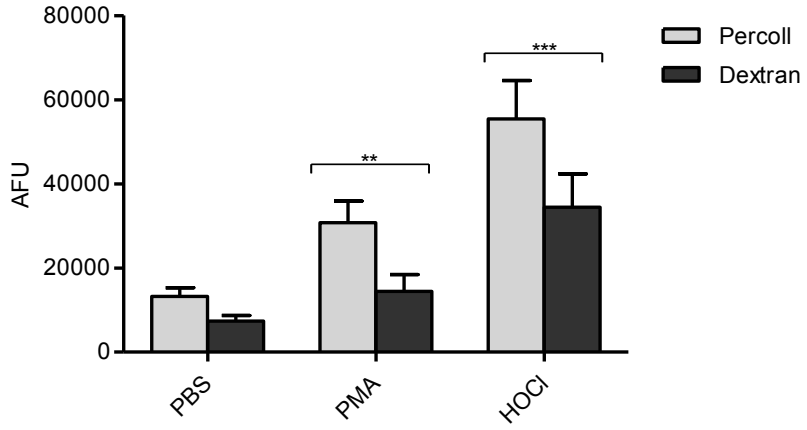

Figure 3.5: The effect of neutrophil preparation techniques on subsequent NET production

NET production (quantified with Sytox green) was compared between (a) Percoll- and Histopaque-isolated neutrophils in response to *F. nucleatum poly* ($1x10^8$, MOI of 1000) and opsonised *S. aureus* ($5x10^7$, MOI of 500) (n=10 in triplicate), or (b) Percoll- and Dextran-isolated neutrophils in response to PMA (50nM) and HOCl (0.75mM) (n=5 in triplicate). Statistical significance calculated using 2way ANOVA and Bonferroni post-tests (*$p<0.05$, **$p<0.01$, ***$p<0.001$). Data expressed as AFU (arbitrary fluorescence units) and mean ± SEM.

3.2.9 Metabolic activity: Percoll vs Histopaque

To investigate neutrophil metabolic activity, ATP production by isolated neutrophils was measured at 30 min intervals over a 60 min period (section 2.2.1.2.5). ATP generation was initially higher in Histopaque-isolated neutrophils compared with Percoll-isolated neutrophils (2way ANOVA and Bonferroni post-tests $*p<0.05$, n=10). However over the 60 min period, ATP production by Histopaque-isolated neutrophils decreased. The metabolic activity of Percoll-isolated neutrophils was lower at the onset of the ROS assay and despite also decreasing with time, the reduction in ATP activity did not reach the level of that of Histopaque-isolated neutrophils. Therefore the difference between Percoll- and Histopaque-isolated cell activity at 30 and 60 mins was not statistically significantly different (Figure 3.6a).

3.2.10 Metabolic activity: Percoll vs Dextran

ATP production by isolated neutrophils was measured at 30 min intervals over a 60 min period. ATP generation was significantly higher in Dextran-isolated neutrophils compared with Percoll-isolated cells at all 3 time-points assayed (2way ANOVA and Bonferroni post-tests $***p<0.001$, $***p<0.001$ and $**p<0.01$ at time-points 0, 30 and 60 mins, respectively, n=5). The metabolic activity of both Percoll and Dextran-isolated cells remained relatively consistent over the 60 min period (Figure 3.6b).

a) Metabolic activity: Percoll vs Histopaque

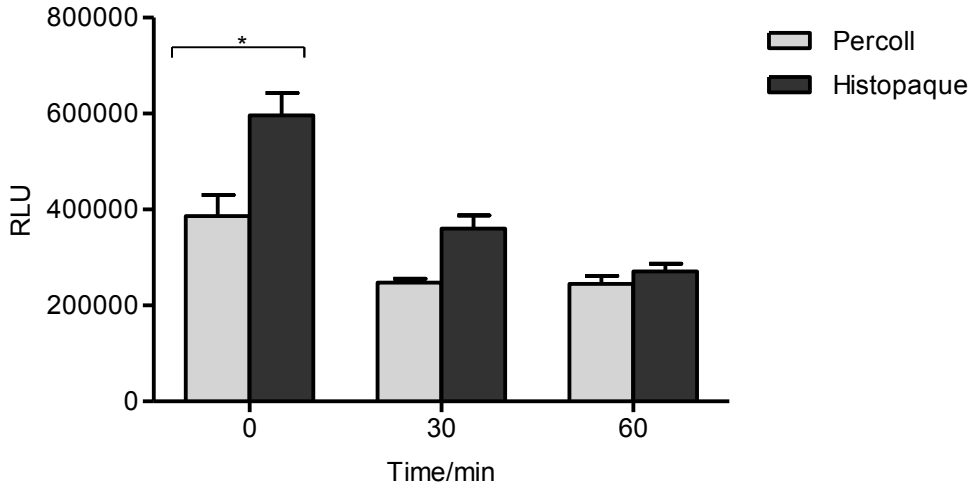

b) Metabolic activity: Percoll vs Dextran

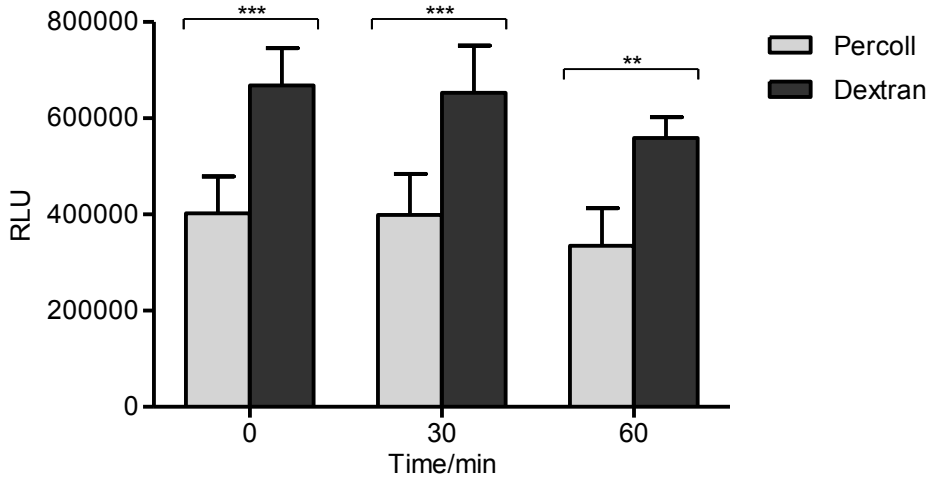

Figure 3.6: The effect of the neutrophil preparation technique on neutrophil metabolic activity

ATP production (indicative of metabolic activity) was compared between (a) Percoll- and Histopaque-isolated neutrophils (n=10 in triplicate) and (b) Percoll- and Dextran- isolated neutrophils (n=5 in triplicate) following isolation. Statistical significance calculated using 2way ANOVA and Bonferroni post-tests (*$p<0.05$, **$p<0.01$, ***$p<0.001$). Data expressed as RLU (relative light units) and mean ± SEM.

3.2.11 Caspase activity: Percoll vs Histopaque

To investigate the effect of neutrophil preparation methods upon apoptosis, caspase-3 and -7 activity was assayed in isolated neutrophils at 30 min intervals over a 60 min period (section 2.2.1.2.4). Caspase activity was initially higher in Histopaque-isolated neutrophils compared with Percoll-isolated neutrophils (0mins, 2way ANOVA and Bonferroni post-tests $*p<0.05$, n=10). Over the 60 min period, caspase activity in Histopaque-isolated neutrophils gradually decreased. The apoptotic activity of Percoll-isolated neutrophils remained consistent over the 60 min measurement period. There was no significant difference in caspase-3 and -7 activity between Percoll and Histopaque isolated cells at 30 or 60 mins (Figure 3.7a).

3.2.12 Caspase activity: Percoll vs Dextran

Caspase activity in Percoll and Dextran isolated neutrophils was measured at 30 min intervals over a 60 min period. Caspase-3 and -7 production was marginally higher at each time-point (0, 30 and 60 mins) in cells isolated by Dextran sedimentation, however this difference was not statistically significant (2way ANOVA $p=0.0855$, n=5) (Figure 3.7b).

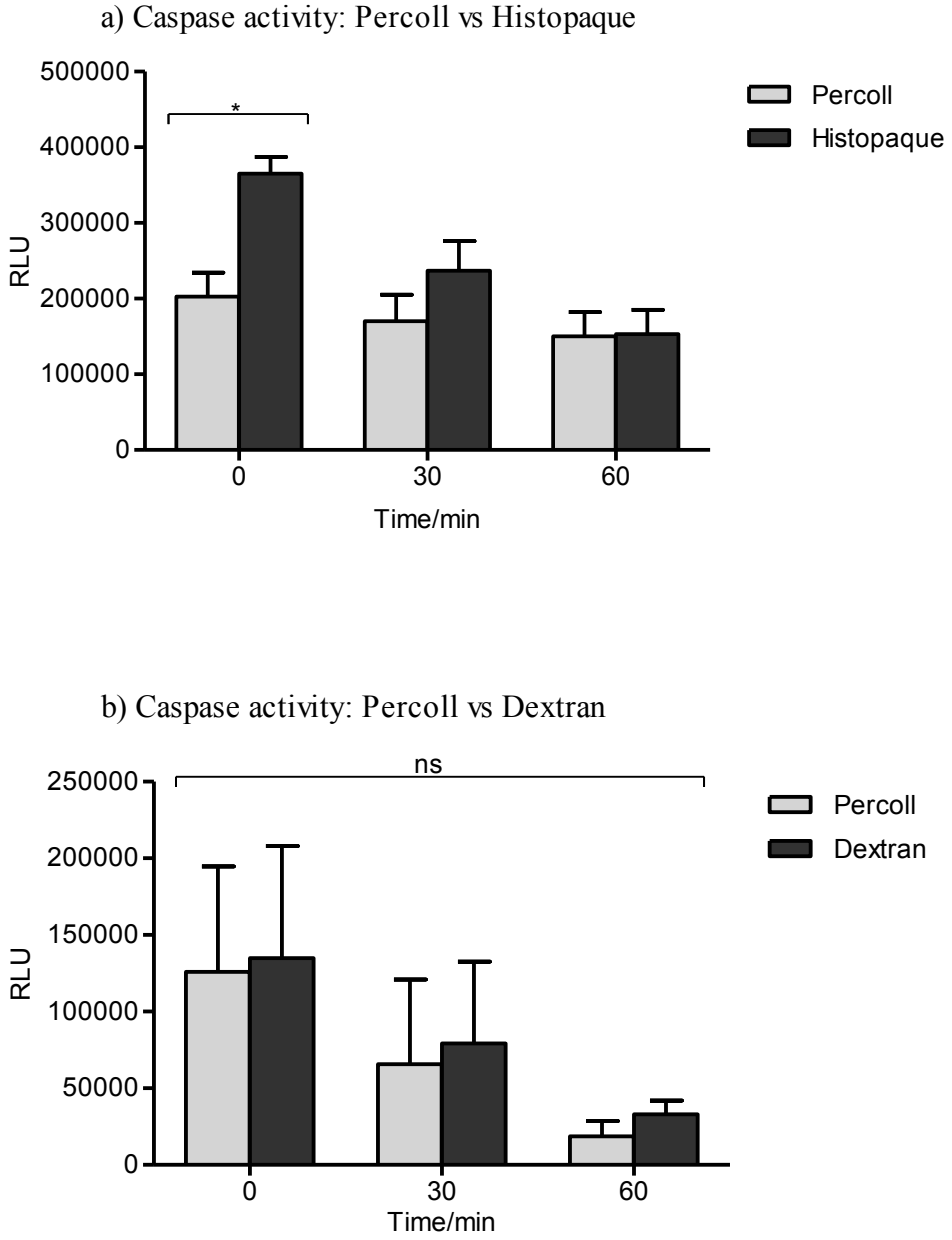

Figure 3.7: The effect of the neutrophil preparation technique on caspase activity
Caspase-3 and -7 activity (indicative of apoptotic activity) was compared between (a) Percoll- and Histopaque-isolated neutrophils (n=10 in triplicate) and (b) Percoll- and Dextran- isolated neutrophils (n=5 in triplicate) following isolation. Statistical significance calculated using 2way ANOVA and Bonferroni post-tests (*$p<0.05$, ns=not significant). Data expressed as RLU (relative light units) and mean ± SEM.

3.3 Efficiency of neutrophil preparation using Percoll

3.3.1 Validation of chosen neutrophil preparation technique using Percoll gradients

The isolation and purity of neutrophils obtained from peripheral venous blood by discontinuous Percoll gradients was determined by nuclear morphological analysis using a cytospin technique, and the expression of the CD66 surface marker (Carlos *et al.,* 1994) by fluorescence microscopy and flow cytometry.

3.3.1.1 Cytospin of Percoll-isolated neutrophils

Representative cytospins from 3 separate experiments demonstrated that Percoll-isolated neutrophils display the characteristic multi-lobed nuclei of neutrophils stained blue (indicated by yellow arrows), whilst the cytoplasm stained pink, following staining with Diff-Quick (Figure 3.8).

3.3.1.2 CD66 staining of neutrophil preparations

Neutrophil isolation using Percoll gradients was confirmed by staining for surface marker activation antigen, CD66, which is specific to granulocytes (Carlos *et al.,* 1994). Fluorescence microscopy demonstrated that the cells isolated by Percoll density gradient centrifugation expressed the surface marker CD66 (Figure 3.9).

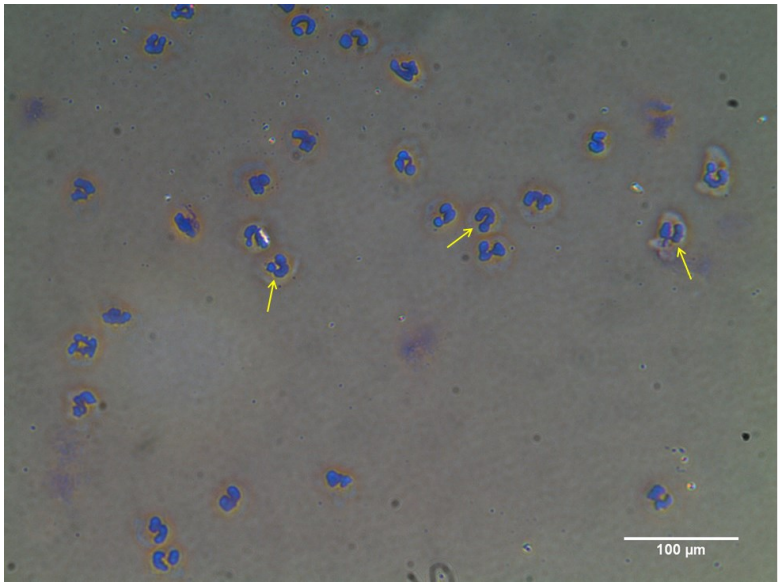

Figure 3.8: Cytospin of Percoll-isolated neutrophils
Following neutrophil isolation using a Percoll gradient, cells were stained with Diff-Quick and visualised using light microscopy (x10 magnification). Multi-lobed nuclei characteristic of neutrophils stained dark blue and the cytoplasms stained pink. Representative image from 3 separate experiments is shown. Scale bar represents 100µm.

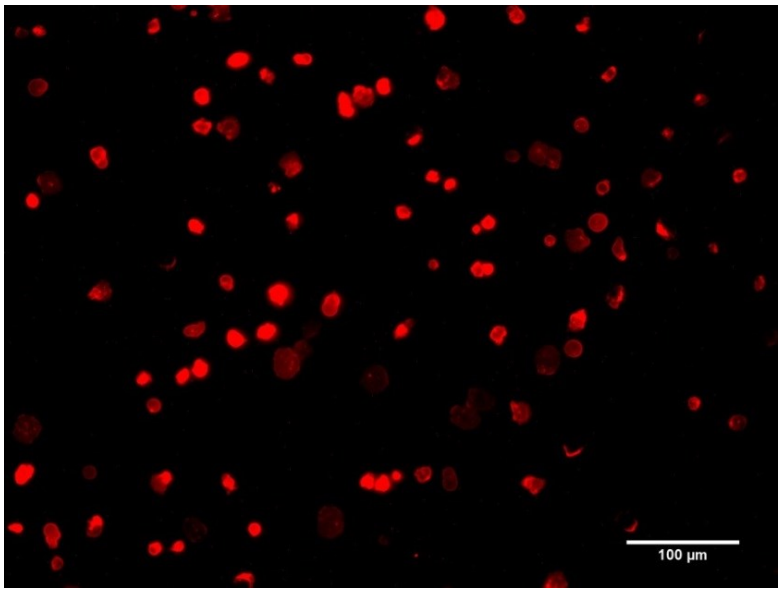

Figure 3.9: Fluorescence microscopy of surface marker CD66
Following neutrophil isolation, cells were stained for CD66 expression and visualised using fluorescence microscopy (x10 magnification). The expression of CD66 on neutrophils was indicated by the red staining. Representative image from 3 separate experiments is shown. Scale bar represents 100µm.

3.3.1.3 Flow cytometric identification of neutrophils.

Flow cytometry was employed to determine the isolation efficiency and purity of neutrophils in Percoll-derived cell suspensions (section 2.2.1.2.2). Neutrophils were quantified in whole peripheral blood prior to isolation by measuring their auto-fluorescence in the blood sample, which indicated that neutrophils represent 40.21% of the cells (representative results from 2 separate isolations) (Figure 3.10a). Following isolation with Percoll gradients, levels of the surface marker CD66b was quantified. Flow cytometry data indicated that Percoll gradients resulted in a cell suspension comprising 97.3% neutrophils (Figure 3.10b). Representative results from 2 separate isolations.

a) Flow cytometric analysis of whole blood

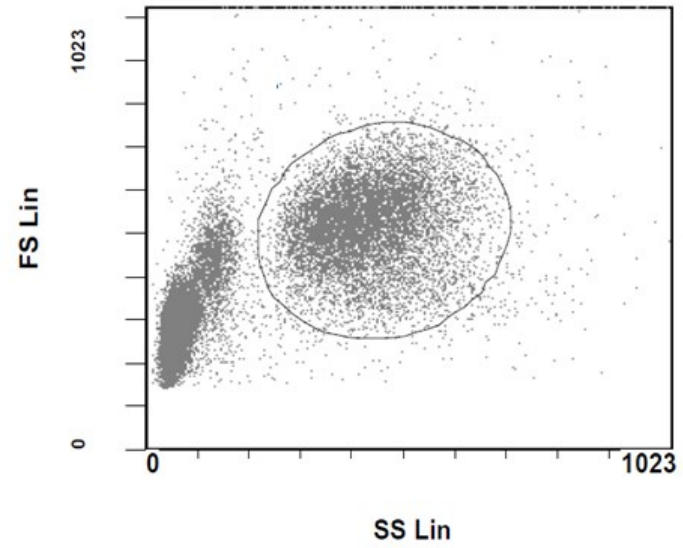

b) Flow cytometric analysis of Percoll-isolated neutrophils

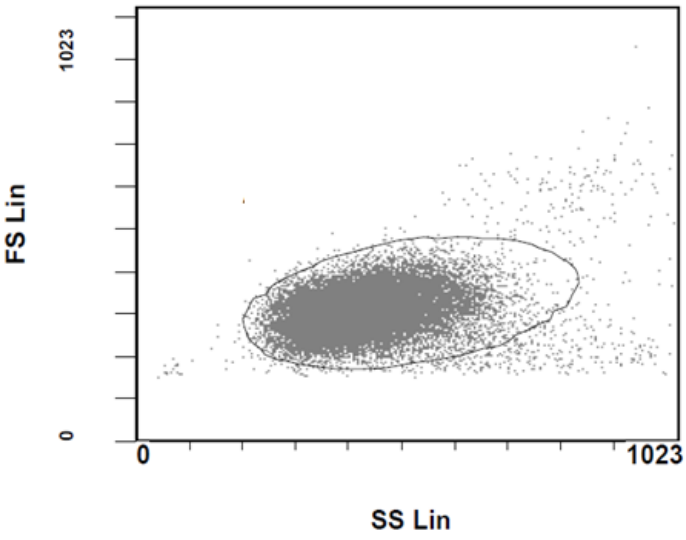

Figure 3.10: Flow cytometric characterisation of neutrophils
(a) Flow cytometry analysis of unstained whole blood (relies on autofluorescence of cells) demonstrated that prior to any neutrophil preparation, whole blood contains 40.21% neutrophils. (b) The enumeration of CD66b on Percoll-isolated neutrophils demonstrated that the isolation of neutrophils from whole blood resulted in a cell suspension containing 97.3% neutrophils. The gating identifies the neutrophil population. Representative results from 2 separate isolations. Abbreviations: FS Lin (forward scatter linear), SS Lin (side scatter linear).

3.4 Discussion

The aim of this work was to determine the most suitable method for peripheral blood neutrophil isolation by comparing Percoll isolation with two additional neutrophil isolation approaches with respect to *ex vivo* neutrophil responses. Parameters investigated included cell yield, ROS release (luminol chemiluminescence), NET production (quantification of NET-DNA with Sytox green), apoptotic activity (caspase-3 and -7 production) and metabolic status (ATP production). Overall, results revealed that there were indeed differences in cellular responses generated following the various neutrophil isolation techniques.

The numbers of neutrophils obtained from the same individual were significantly higher when a Percoll gradient was used for purification (section 3.2.1, 3.2.2). This is consistent with the findings of Grisham (1985), who reported that the use of two discontinuous Percoll gradients produced a higher cell yield than Histopaque gradients. However no difference in cell yield was observed between Percoll and Dextran gradient isolated neutrophils. Whilst recent *in vivo* analyses have demonstrated neutrophil longevity within the blood stream of 5.4 days (Pillay *et al.,* 2010), neutrophils are terminally differentiated cells, meaning they cannot be passaged in tissue culture without undergoing apoptosis (Gottlieb *et al.,* 1995). Therefore, despite the fact that this difference in yield is corrected for in subsequent neutrophil assays, yield is an important variable as the number of cells attainable from a limited amount of venous blood governs the number of subsequent experiments that can be conducted.

To determine whether the isolation method activated neutrophils, baseline ROS production over a 30 min period was measured (section 3.2.3, 3.2.4). At this point, cells were unstimulated and the method of neutrophil isolation represented the only variable between these cells. Although no statistical difference in ROS production was measured between Percoll and Histopaque-isolated cells, there was a general trend towards higher ROS

production in neutrophils isolated with Histopaque. It is possible that the Histopaque isolation method activates the neutrophils, resulting in inadvertent ROS production immediately after isolation. ROS release is known to be a causative agent in neutrophil death, as co-incubation of neutrophils with glutathione, which scavenges H_2O_2 and other ROS, has been found to decrease neutrophil death (Yamamoto *et al.,* 2002). These findings infer that upon exposure to a threshold level of ROS, as a result of activation, neutrophils will enter into apoptosis (Scheel-Toellner *et al.,* 2004). Conversely, high levels of ROS can also inhibit caspase activity, suggesting that caspase-independent pathways may be involved in ROS-dependent cell death (Fadeel *et al.,* 1998). However it is noteworthy that apoptosing neutrophils are still capable of producing substantial amounts of ROS in response to exogenous stimulation (Xu *et al.,* 2009), thus baseline ROS may be derived from a combination of activated and/or apoptosing neutrophils.

Caspase activity was determined by quantifying effector caspases-3 and -7 over a 60 min period post-isolation (section 3.2.11, 3.2.12). Caspase activity was higher in Histopaque-isolated cells immediately following isolation; however less caspase activity was evident over time. In response to stimulation, Percoll-isolated cells produced higher levels of ROS than Histopaque-isolated cells. This could be due to the Histopaque-prepared cells being less responsive to exogenous stimulation, or the possibility that initially apoptotic neutrophils are no longer viable and thus less ROS is produced in response to stimulation. No differences were observed between Percoll and Dextran isolation with respect to baseline total ROS release, as well as in response to stimulation. Furthermore, no significant differences were found between Percoll and Dextran isolation techniques with regard to neutrophil apoptosis, which lends further support for the association of caspase activity with ROS production.

Percoll, Histopaque and Dextan-purified neutrophils were also compared in terms of their ability to produce NETs (3.2.7, 3.2.8). Percoll-isolated neutrophils were found to produce consistently more NETs following stimulation with *F. nucleatum poly* and opsonised *S. aureus*. This was also observed following Dextran isolation, with Percoll-isolated cells producing significantly higher levels of NETs in response to PMA and HOCl. Collectively, these findings suggest that Percoll isolated neutrophils are more sensitive to NET production following stimulation. The differences between Percoll and Histopaque cell NET production may be explained by the total ROS results being lower in Histopaque isolated cells following stimulation, as ROS is known to be vital for NET release (Kirchner *et al.,* 2011, Nishinaka *et al.,* 2011); in support of this is treatment of neutrophils with NADPH-oxidase inhibitor (DPI), which abolishes NET release. Whilst it is recognised that NADPH-oxidase independent NETs may occur, and could therefore provide an explanation for the reduced NET release in Dextran cells (as decreased ROS was not observed in these cells), this seems unlikely as NADPH-oxidase independent NET release is reported in response to specific stimuli such as uric acid (Arai *et al.,* 2014) and soluble immune complexes (Chen *et al.,* 2012). It is also a possibility that a higher proportion of Histopaque- and Dextran-isolated neutrophils are no longer viable 3 hours following isolation, which is the time at which NETs are quantified and may explain the lower number of NETs quantified.

Consistent with the hypothesis that Histopaque isolation causes activation of neutrophils, ATP quantification (indicative of metabolic activity) revealed that Histopaque isolated cells were metabolically active initially, however less ATP was produced over time, indicating either that negative internal feedback mechanisms switch neutrophils to a less active state, or potentially that apoptosis was indeed being induced (Scheel-Toellner *et al* 2004) (section 3.2.9). Metabolic activity was significantly higher in Dextran-isolated cells at each time points, relative to Percoll cells (section 3.2.10). Physiologically relevant concentrations of

ATP are correlated with a concentration dependent delay in neutrophil apoptosis (Vaughan *et al.,* 2007). Although NETosis is distinct from apoptosis (Fuchs *et al.,* 2007); it is possible that increases in ATP may also be associated with delayed or decreased NET release, which was observed in both Histopaque- and Dextran-prepared cells. To the best of my knowledge, the effect of neutrophil isolation technique upon NET responses has not previously been investigated.

A further consideration is that neutrophils isolated with Percoll were subjected to multiple centrifugation and wash steps, whereas isolation with Histopaque and Dextran required less handling and transfers between tubes; suggesting Histopaque and Dextran neutrophils should be less activated. All three gradient protocols take approximately 90 mins, and following several reports demonstrating that delays prior to isolation can trigger neutrophil activation (Ferrante & Thong 1980, Maqbool *et al.,* 2011), isolation was started immediately following blood collection. Thus with regard to neutrophils' relatively short life span, no gradient is superior in terms of isolation time. Whilst erythrocyte lysis produces a cleaner cell suspension, it has been reported that repeated or extended lysis can damage neutrophils (Nauseef *et al.,* 2007). Dextran isolation did not employ a lysis step, however the Histopaque protocol relied on a 30 sec erythrocyte lysis with distilled water, as initial experiments demonstrated erythrocyte contamination. This is distinct from Percoll-isolated neutrophils, which are subjected to an ammonium chloride (NH_4Cl) lysis. Although it has been suggested that distilled water-induced erythrocyte lysis causes less neutrophil activation, the ROS results in this particular study indicate this may not be the case under these particular assay conditions. This is also supported by Vuorte *et al.,* (2001), who reported that neither hypotonic shock with distilled water or NH_4Cl lysis influenced neutrophil integrity or activation. In addition the choice of anticoagulant blood collection tube may also influence neutrophil isolation and effector functions. All blood for the current study was collected in

lithium heparin tubes, acting as an anticoagulant by activating anti-thrombin. However, another commonly used collection tube is ethylenediamine tetraacetic acid (EDTA), which chelates free calcium ions. Calcium ions play a vital role in the activation of the neutrophil respiratory burst, and are the likely explanation for reports demonstrating reduced Histopaque-isolated neutrophil ROS release from blood collected into EDTA tubes, compared with heparin (Freitas *et al.,* 2008).

Visualisation of Percoll-isolated neutrophils by cytospin identified neutrophils in the cell suspension, evidenced by the characteristic multi-lobed nuclei observed that stained dark blue (section 3.3.1.1). Fluorescence microscopy of the neutrophil surface marker CD66 also confirmed the isolation of neutrophils (section 3.3.1.2). To determine the purity of Percoll-isolated cells, neutrophil marker CD66b was quantified by flow cytometry; this demonstrated that the cell suspension contained 97.3% neutrophils (section 3.3.1.3), which is in line with other reports that obtain >95% purity following the isolation of human neutrophils (Kirchner *et al.,* 2011, Maqbool *et al.,* 2011). The remaining 2.7% of cells are likely to include eosinophils and monoculear cells (Dorward *et al.,* 2013). In addition, neutrophils were quantified in lysed whole peripheral blood prior to Percoll-isolation by measuring the auto-fluorescence in the blood sample, which demonstrated that neutrophils comprised 40.21% of whole blood prior to isolation. Optimisation of the Percoll-isolation protocol and meticulous technique can reduce the number of contaminating mononuclear cells in the neutrophil cell suspension. However it is noteworthy that density gradient centrifugation techniques cannot prevent the complete exclusion of contaminating cells, for example, it is reported that in blood derived from individuals with atopic conditions, such as asthma, eosinophils may represent 5-10% of the granulocyte population isolated (Dorward *et al.,* 2013).

In conclusion, when analysing the impact of isolation technique on neutrophil cell yield, function and activation, Percoll appears to be the most appropriate method, evidenced by the lower metabolic activation and higher NET release by Percoll-isolated cells. Percoll was subsequently selected as the isolation technique for all *ex vivo* neutrophil assays in this thesis.

CHAPTER 4: INTERACTIONS BETWEEN PERIODONTAL BACTERIA AND PERIPHERAL BLOOD NEUTROPHILS

4.1 Introduction

Given that NET release is reported to be predominantly ROS dependent (Fuchs *et al.,* 2007), various neutrophil responses to heat-killed periodontal bacteria were investigated (Appendices I, IV), including total, extracellular and superoxide ROS production (section 2.2.3.2). NET production was determined by quantifying the amount of DNA released (2.2.3.3) alongside the NET-bound components, neutrophil elastase (NE), myeloperoxidase (MPO) and cathepsin G (CG) (2.2.3.4, Appendix III). The ability of NETs to entrap bacteria was also qualitatively determined by visualising interactions using SEM (2.2.3.8), and by quantifying the number of viable bacteria entrapped within NET structures (2.2.3.5, 2.2.3.6, Appendix II). All neutrophils were from periodontally and systemically healthy volunteers (University of Birmingham Ethics Reference ERN_13-0325) and neutrophil assays employed a panel of bacteria associated with periodontitis. For clinical relevance, data are presented by grouping periodontal bacteria according to the Socransky complexes (Socransky *et al.,* 1998). The ROS-dependent activation and signalling cascades for NET release in response to heat-killed periodontal bacteria were also investigated by determining the effects of modulators of neutrophil activation (2.2.2.3).

4.2 Neutrophil ROS release in response to periodontal bacteria

ROS production in response to a panel of 19 heat-killed periodontal bacteria ($1x10^8$ and MOI of 1000) was determined using enhanced chemiluminescence (2.2.3.2). ROS release following exposure to PBS (unstimulated negative control), PMA (25nM, positive control) and opsonised *S. aureus* ($5x10^7$ and MOI of 500, positive control) was also quantified. Neutrophils were stimulated after being equilibrate for a 30 min baseline period and then ROS measured over the subsequent 100 mins. Total neutrophil ROS release was determined using luminol chemiluminescence. Opsonised *S.aureus* induced significantly higher ROS

production than the PBS control (Kruskal-Wallis and Dunn's multiple comparison post-tests ***$p<0.001$, n=5). Certain periodontal bacteria elicited higher total ROS production, which was statistically significant for *P. acnes, S. anginosus* and *C. rectus* (Kruskal-Wallis and Dunn's multiple comparison post-tests **$p<0.01$, **$p<0.01$, *$p<0.05$, respectively, n=5) (Figure 4.1a).

Neutrophil extracellular ROS production was subsequently analysed by isoluminol chemiluminescence. PMA induced significantly higher ROS production than PBS treatment (Kruskal-Wallis and Dunn's multiple comparison post-tests **$p<0.01$, n=5). *S. gordonii* also elicited significantly higher total ROS production (Kruskal-Wallis and Dunn's multiple comparison post-tests *$p<0.05$, n=5) (Figure 4.1b).

Neutrophil superoxide production was measured with lucigenin. PMA and opsonised *S. aureus* did not induce significantly higher superoxide production relative to the PBS control. However, some periodontal bacterial species elicited higher superoxide production, which was statistically significant for *S. anginosus*, *C. suptigena,* and *F. nucleatum nuc* (Kruskal-Wallis and Dunn's multiple comparison post-tests **$p<0.01$, *$p<0.05$, *$p<0.05$, respectively, n=5) (Figure 4.1c).

a) Neutrophil total ROS production

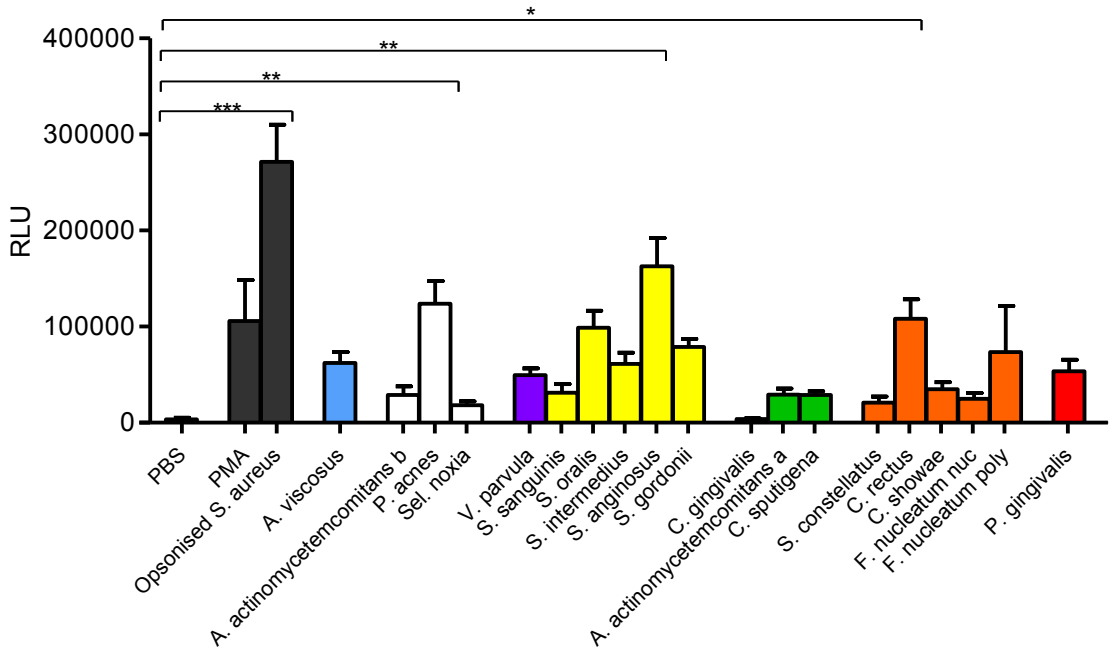

b) Neutrophil extracellular ROS production

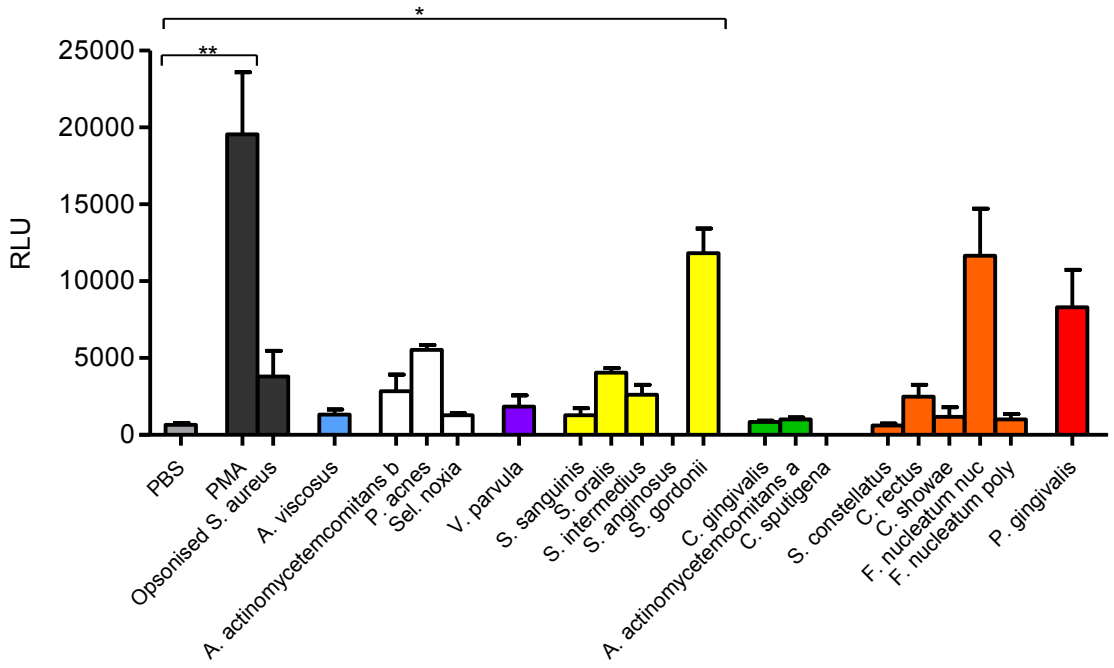

c) Neutrophil superoxide production

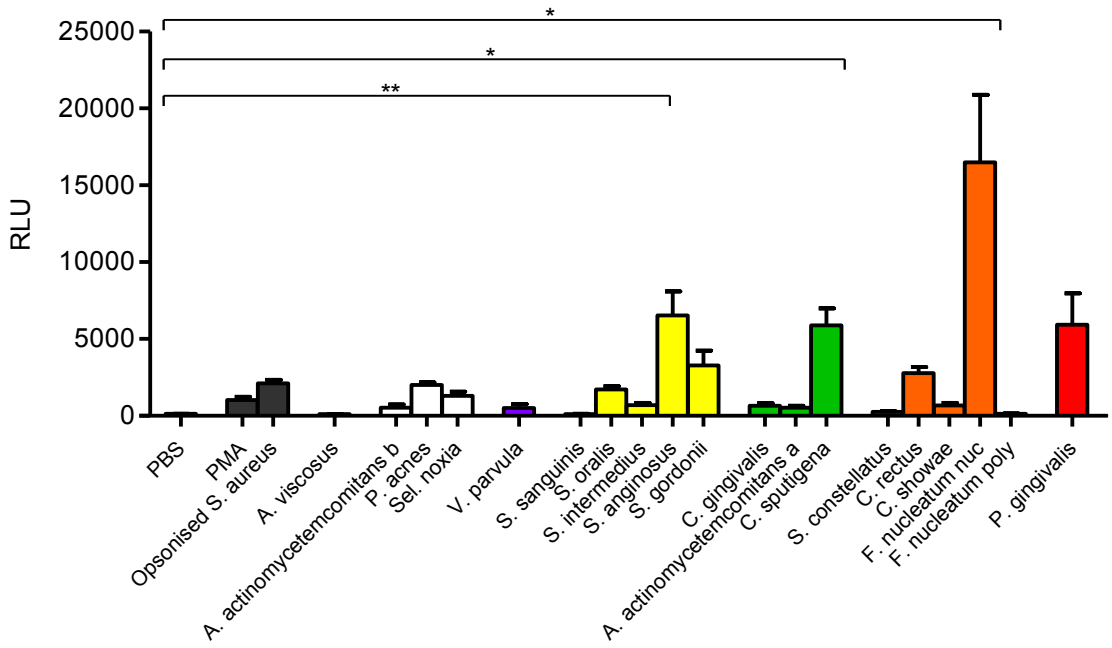

Figure 4.1: Neutrophil ROS production in response to periodontal bacteria
Neutrophil (a) total ROS, (b) extracellular ROS and (c) superoxide production were quantified in response to a panel of periodontal bacteria ($1x10^8$ and MOI of 1000) using luminol, isoluminol and lucigenin enhanced chemiluminescence, respectively. ROS release in response to PBS (unstimulated negative control), PMA (25nM, positive control) and opsonised *S. aureus* ($5x10^7$ and MOI of 500, positive control) was also quantified. Statistical significance calculated using Kruskal-Wallis and Dunn's multiple comparison post-tests (*$p<0.05$, **$p<0.01$, ***$p<0.001$). Data presented as RLU (relative light units) and expressed as mean ± SEM (n=5 in triplicate).

4.2.1 Time-course of neutrophil ROS production in response to periodontal bacteria

The time-course of ROS production was analysed following stimulation with heat-killed periodontal bacteria, as previously described. Consistent with the data expressed as total peak ROS production, time-course ROS production expressed as "area under the curve" demonstrated that total ROS production (luminol) was highest in response to opsonised *S. aureus* ($5x10^7$ and MOI of 500), followed by *S. anginosus* ($1x10^8$ and MOI of 1000). Notably, the increase in total ROS following stimulation with opsonised *S. aureus* was more rapid than following bacterial stimulation, as illustrated by the sharp increase in ROS levels following stimulation. Total ROS release following opsonised *S. aureus*-stimulation peaked at approximately 20 mins post stimulation, which was followed by a steady decrease in total ROS production (Figure 4.2a). Extracellular ROS production measured using isoluminol demonstrated that PMA (25nM) stimulation induced the highest ROS signal. The steep time-course curve in response to PMA suggests a rapid neutrophil response to PMA. PMA-induced extracellular ROS release peaked approximately 20 mins post stimulation, followed by a steady decrease in total ROS. *S. gordonii* ($1x10^8$ and MOI of 1000) also produced elevated levels of extracellular ROS in comparison with other periodontal bacteria (Figure 4.2b). The quantification of superoxide production (lucigenin) in response to periodontal bacteria demonstrated that *F. nucleatum nuc* ($1x10^8$ and MOI of 1000) generated the highest levels of superoxide, relative to other periodontal bacteria. *F. nucleatum nuc*-induced superoxide release peaked approximately 30 mins post-stimulation, followed by a steady decrease in total ROS. PMA and opsonised *S. aureus* did not generate detectable elevations in superoxide production (Figure 4.2c).

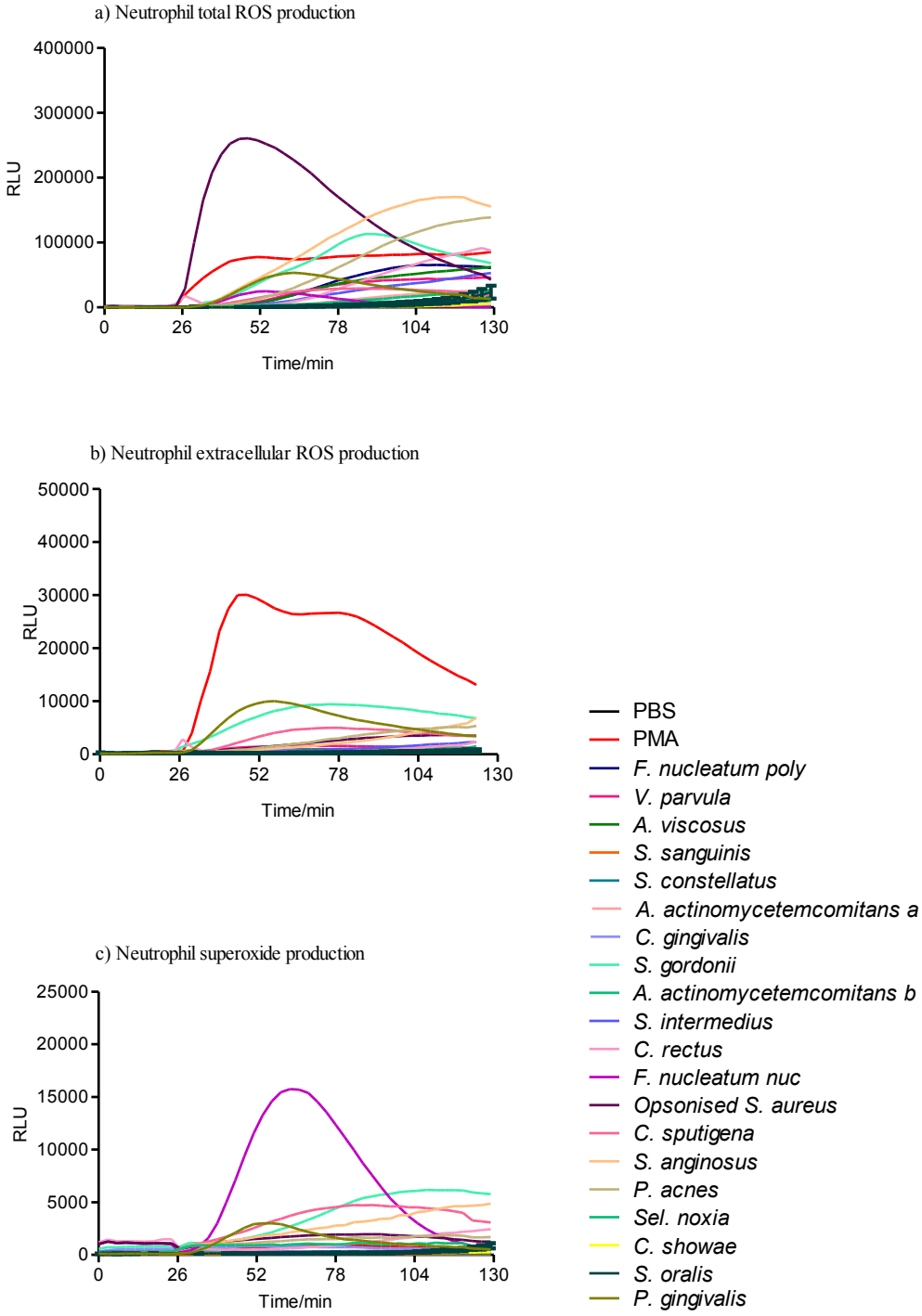

Figure 4.2: Time-course of neutrophil ROS production in response to periodontal bacteria

Time-course for ROS production assayed over 130 mins by neutrophils stimulated with PMA (25nM), opsonised *S. aureus* ($5x10^7$ and MOI of 500) or periodontal bacteria ($1x10^8$ and MOI of 1000). (a) Total ROS production (luminol), (b) extracellular ROS production (isoluminol), (c) superoxide production (lucigenin). Data presented as mean RLU (relative light units) (n=5 in triplicate).

4.3 Quantification of NET production in response to periodontal bacteria exposure

NET production in response to a panel of 19 heat-killed periodontal bacteria ($1x10^8$ and MOI of 1000) was determined by quantifying NET-DNA (2.2.3.3) and NET bound components (2.2.3.4). NET release following exposure to PBS (unstimulated negative control), PMA (50nM, positive control) and opsonised *S. aureus* ($5x10^7$ and MOI of 500, positive control) was also quantified. Neutrophils were stimulated after being equilibrate for a 30 min baseline period and then NET production measured after a 4 hour incubation period. NET-DNA measured with Sytox green demonstrated that PMA stimulated significantly higher NET production compared with PBS (Kruskal-Wallis and Dunn's multiple comparison post-tests $*p<0.05$, n=5). Certain periodontal bacteria elicited higher NET-DNA production and this was statistically significant compared with PBS for *P. acnes*, *V. parvula,* and *S. gordonii* (Kruskal-Wallis and Dunn's multiple comparison post-tests $*p<0.05$, $*p<0.05$, $*p<0.05$, respectively, n=5) (Figure 4.3a).

NET-bound NE was quantified colorimetrically (2.2.3.4.1) and demonstrated that certain periodontal bacteria elicited higher NET-bound NE production relative to PBS, however this was not statistically significant. Similarly, stimulation with PMA and opsonised *S. aureus* (positive controls) stimulation did not reach statistical significance (Kruskal-Wallis $p>0.05$, n=3) (Figure 4.3b).

NET-bound MPO was quantified colorimetrically (2.2.3.4.2) and demonstrated that PMA stimulated significantly higher NET-bound MPO production (Kruskal-Wallis and Dunn's multiple comparison post-tests $*p<0.05$, n=3). Certain periodontal bacterial species elicited higher NET-bound MPO production relative to PBS; however this did not reach statistical significance (Kruskal-Wallis and Dunn's multiple comparison post-tests $p>0.05$, n=3) (Figure 4.3c).

NET-bound CG was quantified colorimetrically (2.2.3.4.3) and demonstrated that opsonised *S. aureus* stimulated for significantly higher NET-bound CG production (Kruskal-Wallis and Dunn's multiple comparison post-tests *$p<0.05$, n=3*).* Certain periodontal bacterial species elicited higher NET-bound CG production, which was statistically significant for *A. viscosus* and *C. gingivalis* (Kruskal-Wallis and Dunn's multiple comparison post-tests *$p<0.05$ for both, n=3) (Figure 4.3d).

a) NET-DNA

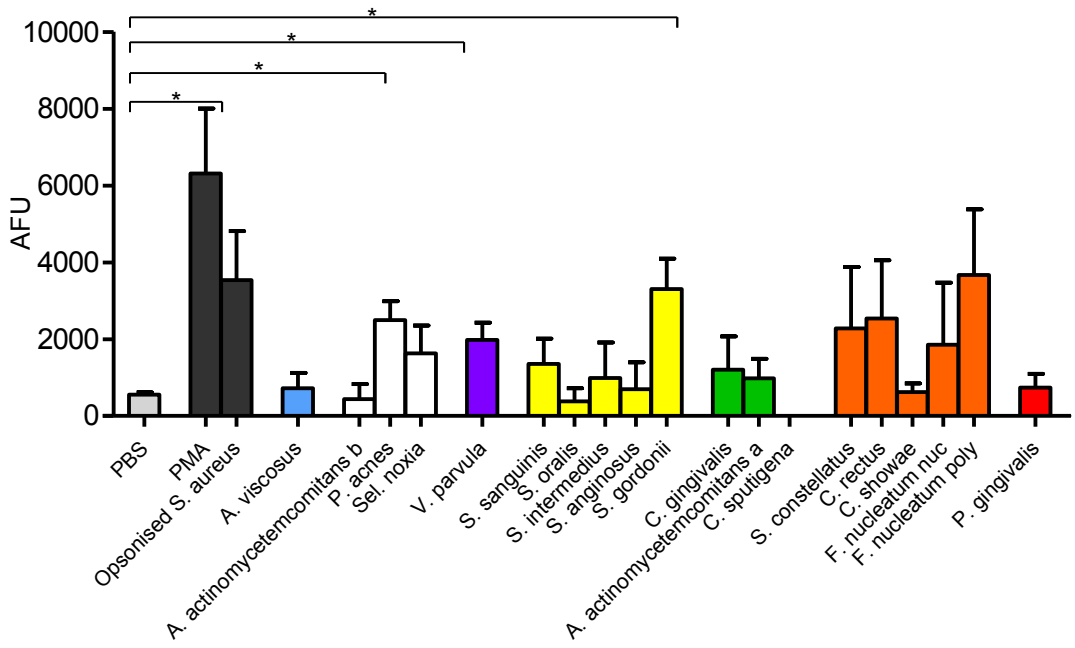

b) NET-bound neutrophil elastase

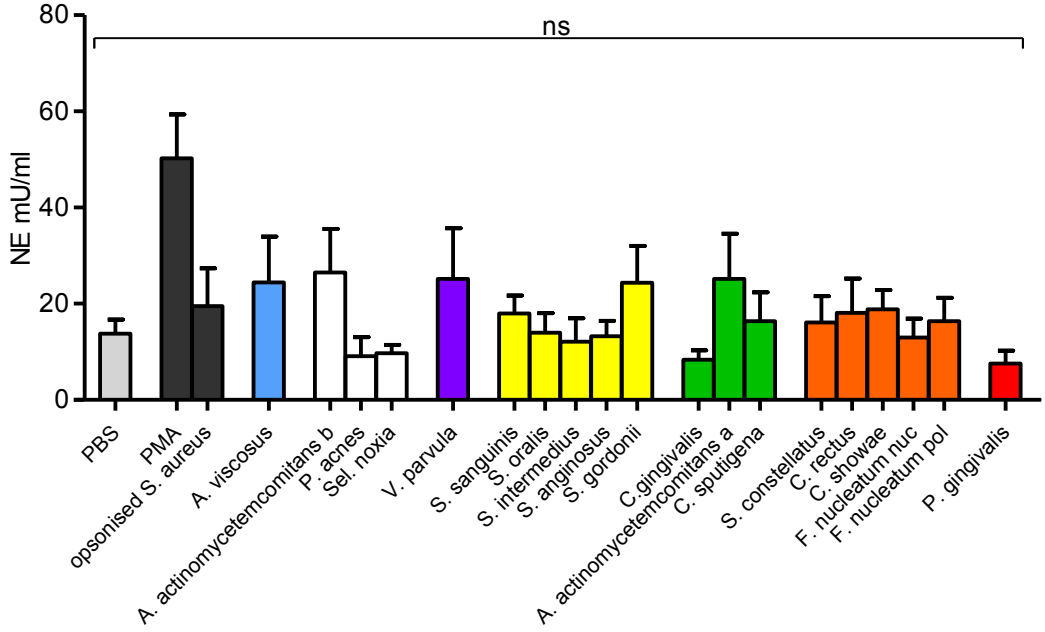

c) NET-bound myeloperoxidase

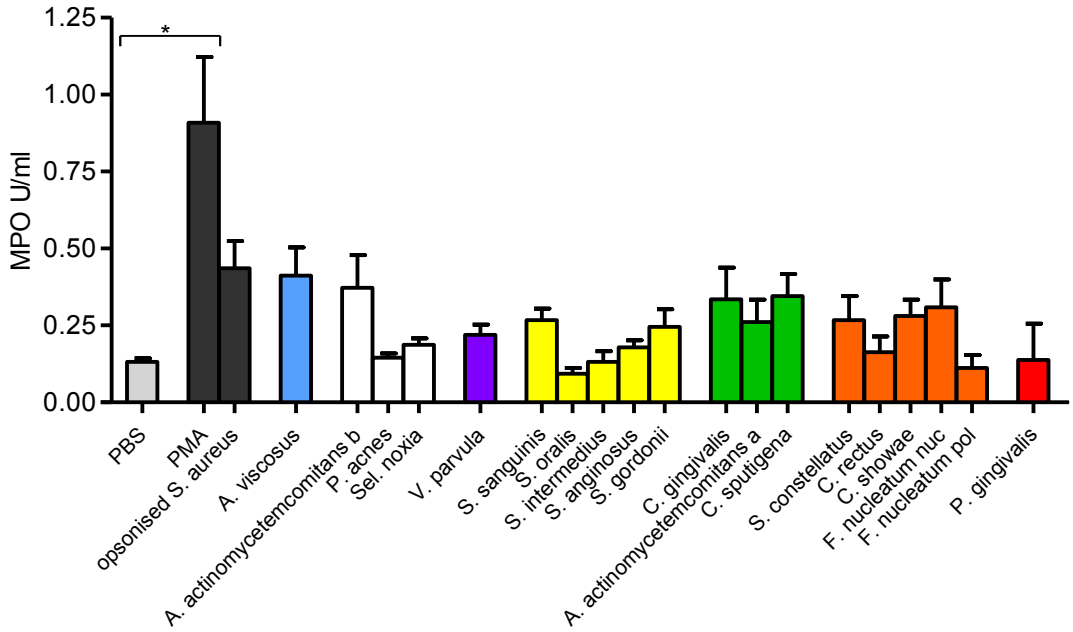

d) NET-bound cathepsin G

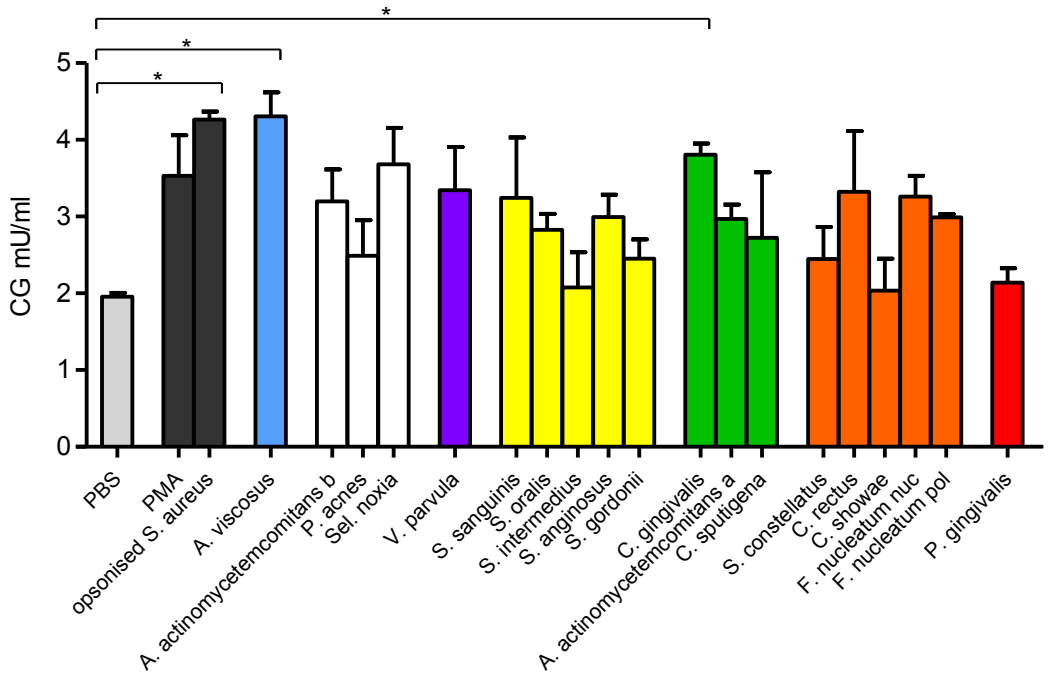

Figure 4.3: Quantification of NET production in response to periodontal bacteria exposure

NET production was quantified in response to a panel of periodontal bacteria ($1x10^8$ and MOI of 1000). NET release in response to PBS (unstimulated negative control), PMA (50nM, positive control) and opsonised *S. aureus* ($5x10^7$ and MOI of 500, positive control) was also quantified. (a) NET-DNA was quantified with Sytox green and NET-bound (b) neutrophil elastase, (c) myeloperoxidase and (d) cathepsin G were quantified colorimetrically. Statistical significance was calculated using Kruskal-Wallis and Dunn's multiple comparison post-tests (*$p<0.05$, ns=not significant). Data is presented as (a) AFU (arbitrary fluorescence units), (c) U/ml or (d, e) mU/ml and expressed as mean ± SEM (n=5 in triplicate).

4.4 NET entrapment of bacteria

To assess the ability of NETs to immobilise periodontal bacteria, FITC-stained live bacteria ($1x10^7$ and MOI of 100) were incubated for 1 hour with either unstimulated neutrophils, intact NETs (produced by 0.75mM HOCl stimulation) or NET structures following degradation with MNase (section 2.2.3.5). Following multiple wash steps to remove any unbound bacteria the amount of bacteria entrapped was fluorometrically quantified and normalised to FITC-stained bacteria incubated with PBS (cell-free control). For clinical relevance, data are presented by grouping periodontal bacteria according to the Socransky complexes (Socransky *et al.,* 1998).

NET entrapment of bacteria not assigned to a Socransky complex

Sel. noxia appeared to be entrapped within NET structures relative to bacteria entrapped within neutrophils or degraded NETs (negative controls) (1way ANOVA *$p=0.0111$, n=5). However, neither *A. actinomycetemcomitans* (serotype b) nor *P. acnes* were significantly entrapped within NETs (1way ANOVA $p>0.05$, n=5) (Figure 4.5a).

NET entrapment of blue complex bacteria

A. viscosus appeared to evade entrapment within NET, compared with bacteria entrapped within neutrophils or degraded NETs (negative controls) (1way ANOVA $p=0.1169$, n=5) (Figure 4.5b).

NET entrapment of purple complex bacteria

V. parvula was found to be significantly entrapped within NETs compared with bacteria incubated with unstimulated neutrophils or degraded NET structures (1way ANOVA *$p=0.0129$, n=5) (Figure 4.5c).

NET entrapment of yellow complex bacteria

S. anginosus and *S. gordonii* were significantly entrapped within NETs, relative to bacteria entrapped within neutrophils or degraded NETs (1way ANOVA **p=0.0216* and **p=0.0305,* respectively, n=5). However the other yellow complex bacteria assayed, *S. sanguinis, S. oralis* and *S. intermedius,* appeared to evade entrapment within NET structures in this assay system (1way ANOVA *p>0.05,* n=5) (Figure 4.5d).

NET entrapment of green complex bacteria

No green complex bacteria assayed appeared significantly entrapped within NETs relative to bacteria entrapped within neutrophils or degraded NETs (negative controls) according to the assay conditions employed (1way ANOVA *p=0.1135,* n=5) (Figure 4.5e).

NET entrapment of orange complex bacteria

C. rectus, C. showae and *F. nucleatum poly* were significantly entrapped within NETs relative to bacteria entrapped within neutrophils or degraded NETs (negative controls) (1way ANOVA ****p=0.0004, ****p=0.0002, **p=0.0079,* respectively, n=5). However the other orange complex bacteria assayed, *S. constellatus* and *F. nucleatum nuc*, were not significantly entrapped within NET structures (1way ANOVA *p>0.05*, n=5) (Figure 4.5f).

NET entrapment of red complex bacteria

P. gingivalis was significantly entrapped within NET structures compared with bacteria incubated with unstimulated neutrophils or degraded NET structures (1way ANOVA **p=0.027,* n=5) (Figure 4.5g).

a) Bacteria not assigned to a Socransky complex

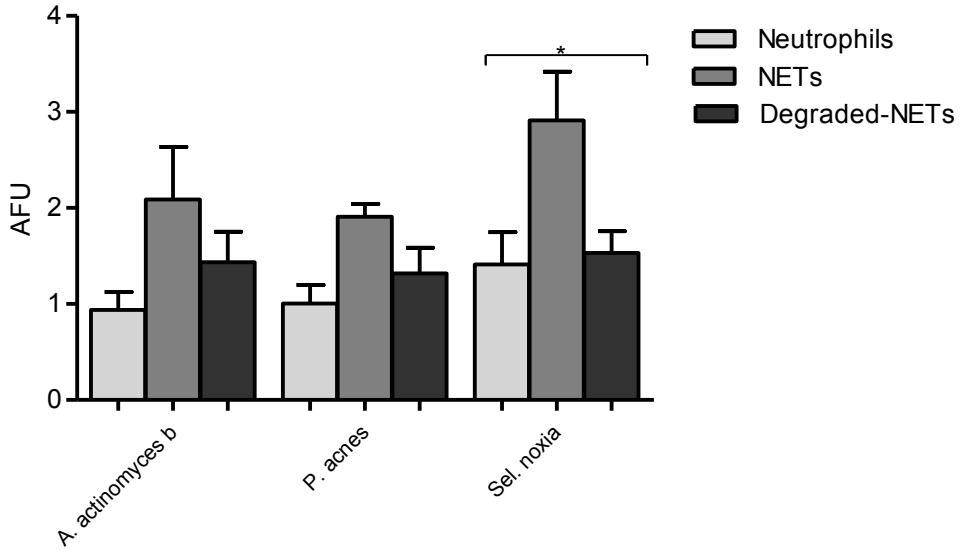

b) Blue complex bacteria

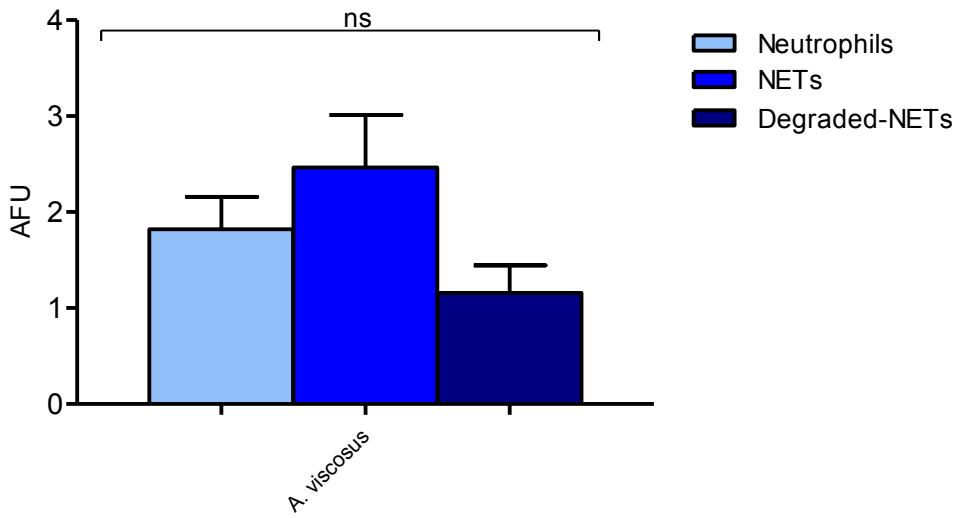

c) Purple complex bacteria

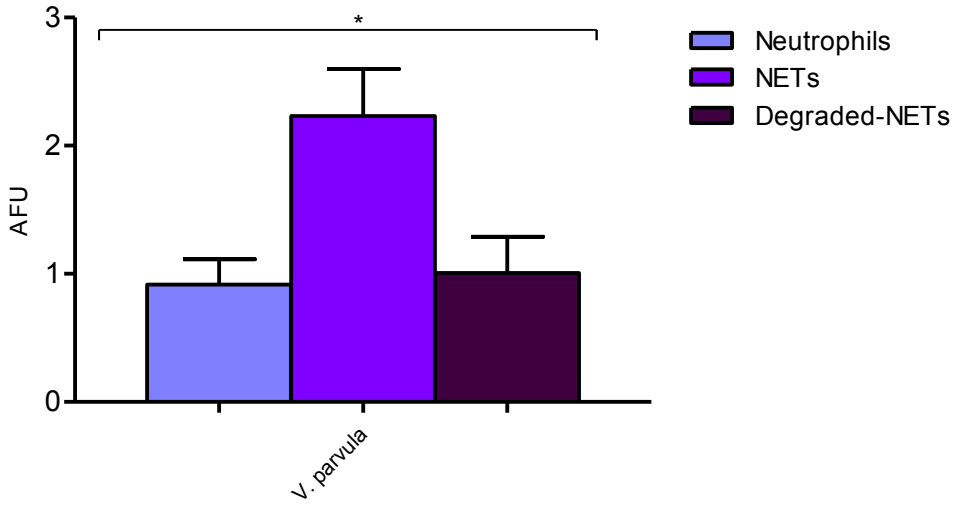

d) Yellow complex bacteria

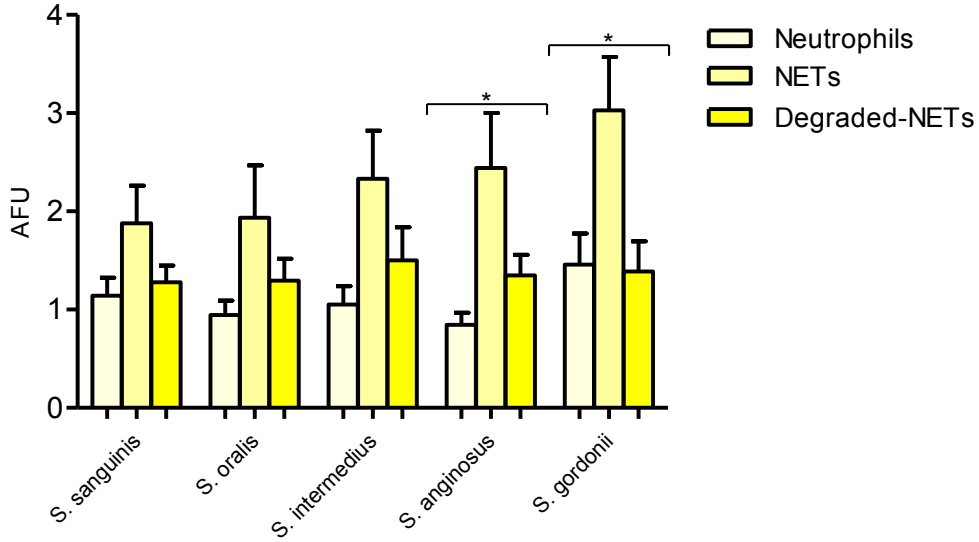

(e) Green complex bacteria

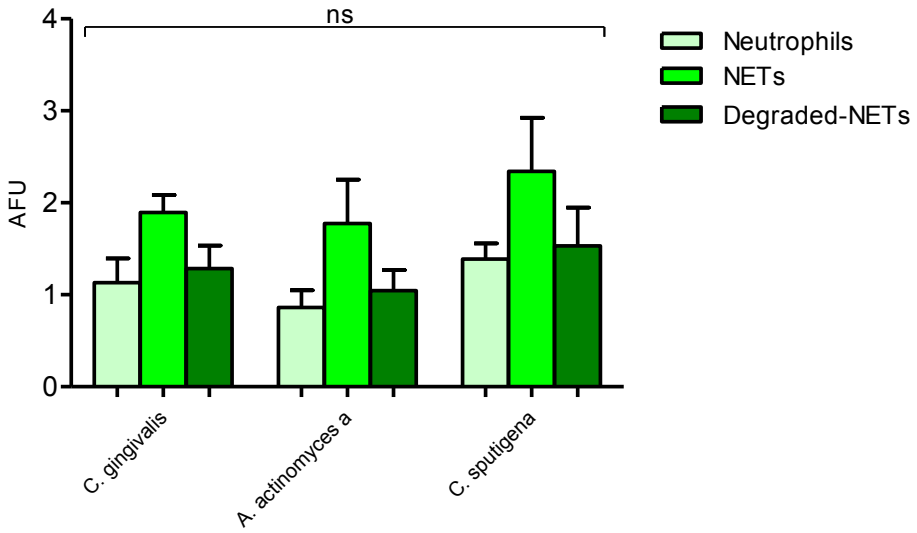

f) Orange complex bacteria

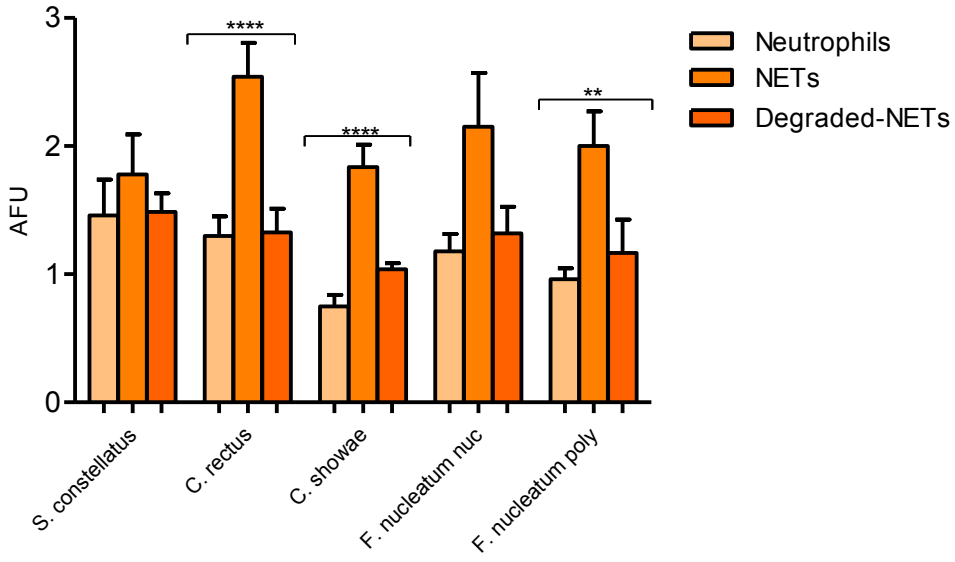

g) Red complex bacteria

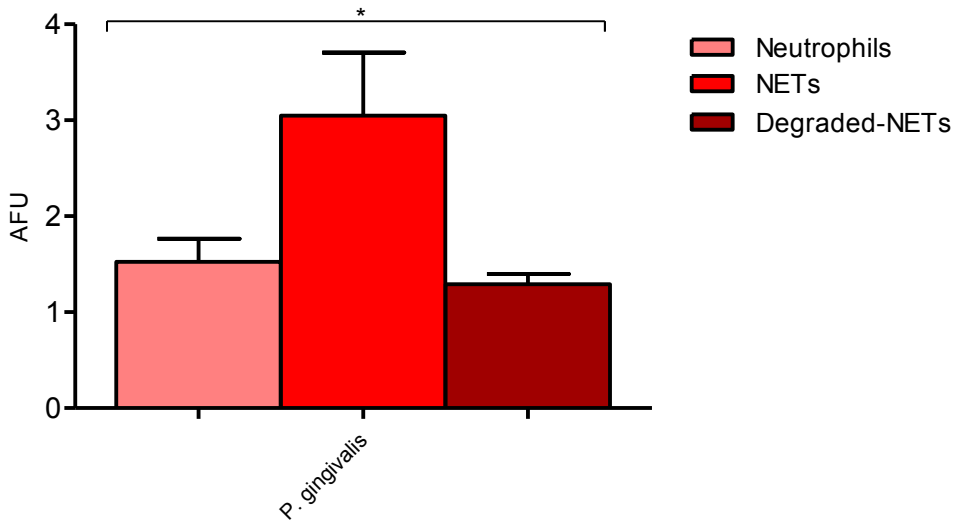

Figure 4.4: NET entrapment of periodontal bacteria
NET entrapment of (a) bacteria not assigned to a Socransky complex, (b) blue complex bacteria, (c) purple complex bacteria, (d) yellow complex bacteria, (e) green complex bacteria, (f) orange complex bacteria and (g) red complex bacteria was determined by quantifying FITC-stained bacteria immobilised in NET structures. Results are normalised to FITC-stained bacteria entrapped in PBS. Statistical significance (1way ANOVA) of NET-derived bacterial entrapment is relative to bacteria entrapped within neutrophils and degraded NETs (*$p<0.05$, **$p<0.01$, ***$p<0.001$, ****$p<0.0001$, ns=not significant). Data presented as AFU (arbitrary fluorescence units) and expressed as mean ± SEM (n=5 in triplicate).

4.5 Scanning electron microscopy of NET-bacteria interactions

To visualise the interactions between NETs and bacteria, NET structures were visualised by SEM following incubation with PBS (negative control) and selected live periodontal bacteria ($1x10^7$ MOI of 100) (2.2.3.8). As expected, SEM images of unstimulated neutrophils demonstrated spherical cells with no NET structures evident (Figure 4.5). The visualisation of neutrophils following incubation with bacteria; *A. actinomycetemcomitans* serotype a (Figure 4.6a), *V. parvula* (Figure 4.6b) and *A. viscosus* (Figure 4.6c), revealed the release of NET structures from neutrophils. The strand-like filaments between the neutrophils appeared to associate with bacteria, for example *A. actinomycetemcomitans* (serotype a) appear to cluster along the length of the NET structure (Figure 4.6a). SEM analysis also enabled detailed visualisation of bacteria at a high magnification, which consistent with Gram stains (Appendix IV), confirmed bacterial morphology.

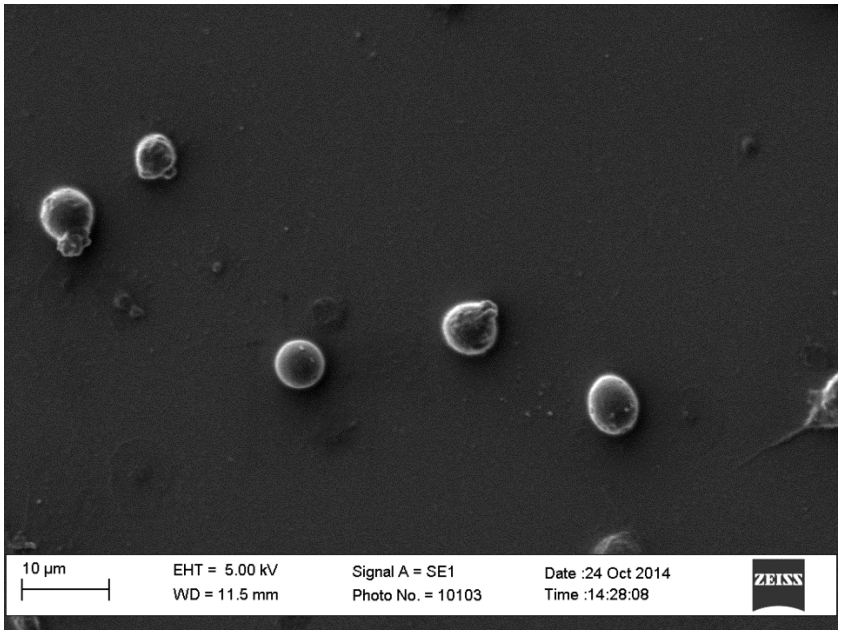

Figure 4.5: Scanning electron microscopy of resting neutrophils
Resting neutrophils ($1x10^5$) were visualised by SEM. Representative image of 3 experiments, scale bar represents 10µm.

a) *A. actinomycetemcomitans* serotype a

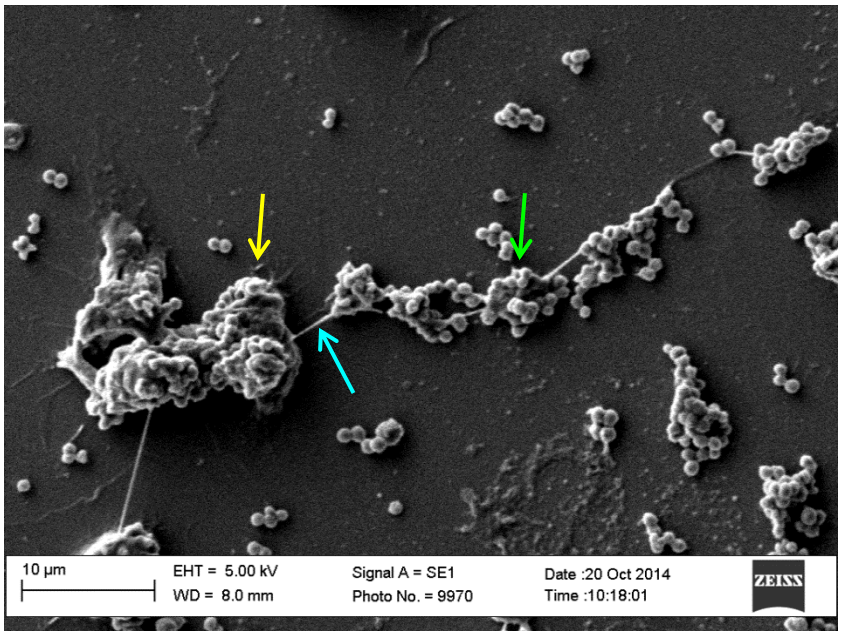

b) *V. parvula*

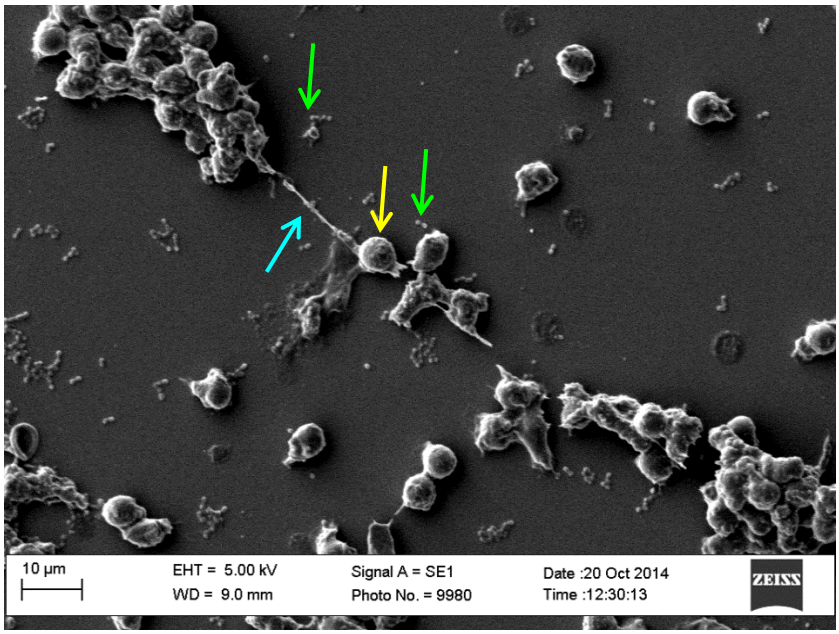

c) *A. viscosus*

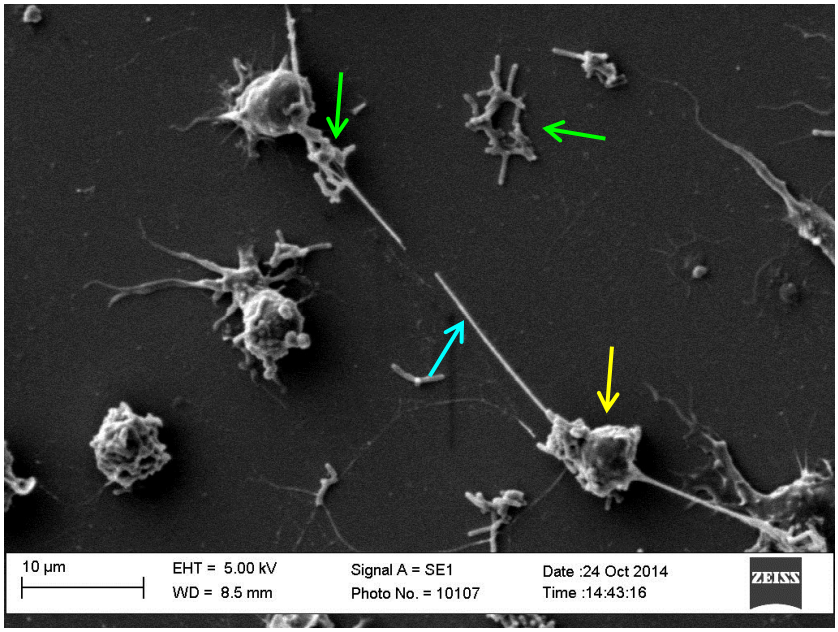

Figure 4.6: Scanning electron microscopy of neutrophils stimulated with periodontal bacteria

Neutrophils (yellow arrow) ($1x10^5$) incubated with live (a) *A. actinomycetemcomitans* serotype a, (b) *V. parvula* or (c) *A. viscosus* ($1x10^7$ and MOI of 100) were visualised by SEM. Blue arrow indicates NET strand structures and bacteria are indicated with green arrows. Representative image of 3 experiments, scale bar represents 10µm.

4.6 Quantification of NET-mediated killing of periodontal bacteria

To determine whether NETs are capable of killing entrapped bacteria, periodontal bacteria ($1x10^7$ and MOI of 100) were incubated with PBS (negative control), unstimulated neutrophils, intact NETs (produced by 0.75mM HOCl), degraded NETs (by MNase digestion), unseparated NETs (NETs not degraded with MNase prior to bacteria subculture) or with cytochalasin B-treated NETs (to block neutrophil phagocytosis) (section 2.2.3.6, Appendix II). Following 1 hour incubation bacteria were released from NETs by MNase digestion, diluted and inoculated onto agar plates and cultured for 24 hours prior to performing colony counts. Of the 6 periodontal bacteria assayed, no significant NET-mediated killing of periodontal bacteria was observed (all analysed by 2way ANOVA, n=5) *F. nucleatum poly* (*p=0.5873), S. intermedius* (*p=0.6007*), *S. sanguinis* (*p=0.8977*), *A. viscosus* (*p=0.9573*), *V. parvula* (*p=0.9239*) and *C. gingivalis* (*p=0.9787*) (Figures 4.7a-f).

a) *F. nucleatum polymorphum*

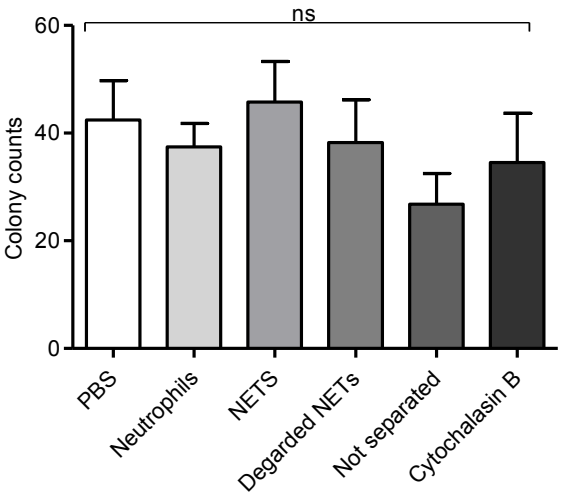

b) *S. intermedius*

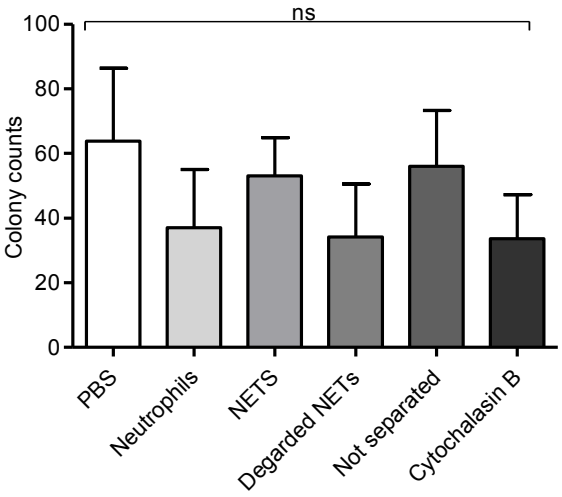

c) *S. sanguinis*

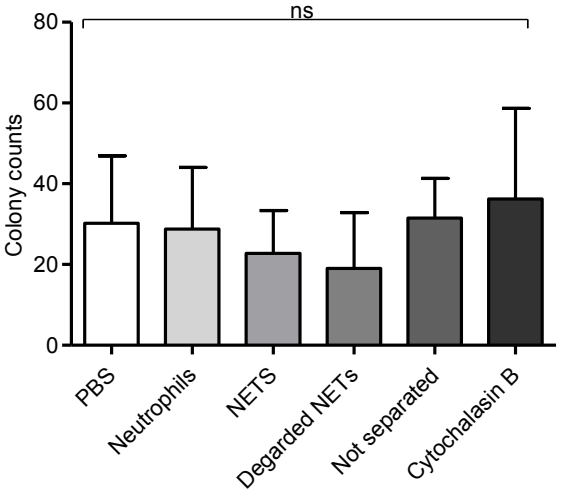

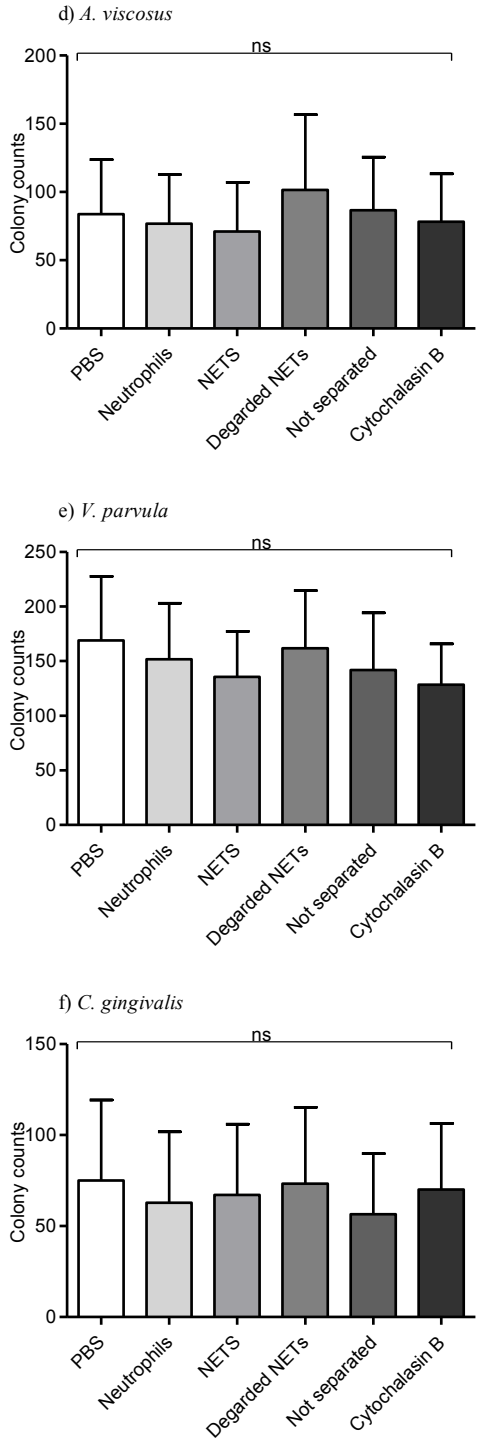

Figure 4.7: Quantification of NET-mediated killing of periodontal bacteria
Bacterial colonies were counted following incubation with PBS (negative control), neutrophils, intact NETs (0.75mM HOCl), degraded NETs (100U/ml MNase), unseparated NETs (NETs not degraded with MNase prior to bacteria subculture) or with cytochalasin B-treated NETs (to block neutrophil phagocytosis). No significant NET-mediated killing of periodontal bacteria was observed (1way ANOVA $p>0.05$). Data presented as total colony counts and expressed as mean ± SEM (n=5).

4.7 Effect of NADPH-oxidase pathway modulating agents on ROS and NET production

To further understand the importance of NADPH-oxidase and downstream products in bacteria-induced ROS and NET production, specific components of the NADPH-oxidase signalling pathway were targeted (section 2.2.2.3). Isolated neutrophils were incubated with diphenyleneiodonium (DPI) (25μM), an inhibitor of NADPH-oxidase, N-acetyl-cysteine (NAC) (10mM), a synthetic glutathione precursor that scavenges H_2O_2, or taurine (100mM), which scavenges HOCl to produce taurine chloramine. Neutrophil total ROS and NET production were measured following pre-incubation with the modulating agent for 30 mins prior to stimulation with PMA (50nM), opsonised *S. aureus* ($5x10^7$ and MOI of 500) and a panel of 9 selected heat-killed periodontal bacteria ($1x10^8$ and MOI of 1000).

DPI pre-treatment resulted in a reduction in total ROS release in response to all stimuli, relative to non-DPI treated cells. This was statistically significant for PMA (*$p<0.05$*), as well as following stimulation with opsonised *S. aureus* (*****p<0.0001), S. gordonii* (*****p<0.0001), F. nucleatum poly* (**p<0.05)* and *Sel. noxia* (**p<0.05)* (2way ANOVA and Bonferroni post-tests, n=3) (Figure 4.8a). NET-DNA was quantified with Sytox green following enzymatic degradation of NET structures with MNase. DPI pre-treatment also significantly reduced NET release in response to all stimuli relative to cells that did not receive DPI pre-treatment. This was statistically significant in response to PMA (*****p<0.0001*), but not for *S. aureus*-induced NET production or the periodontal bacteria assayed (2way ANOVA and Bonferroni post-tests, n=3) (Figure 4.8b).

NAC treatment significantly reduced total ROS release in response to all stimuli relative to cells that did not receive NAC pre-treatment. This was statistically significant for PMA (**p<0.05*) and opsonised *S. aureus* (*****p<0.0001)*, as well as following bacterial stimulation with *S. gordonii* (*****p<0.0001)* and *Sel. noxia* (**p<0.05)* (2way ANOVA and Bonferroni post-tests, n=3) (Figure 4.8c). NET-DNA was quantified with Sytox green following

enzymatic degradation of NET structures with MNase. NAC treatment reduced NET release in response to all stimuli relative to cells that did not receive NAC pre-treatment. This was statistically significant for to PMA (****$p<0.0001$) and *Sel. noxia* (*$p<0.05$), but not for opsonised *S. aureus* or the other periodontal bacteria assayed (analysed by 2way ANOVA and Bonferroni post-tests, n=3) (Figure 4.8d).

Taurine treatment significantly reduced total ROS release in response to all stimuli relative to cells that did not receive taurine; however this was to a lesser extent than that observed with DPI and NAC. Decreased ROS release following taurine pre-treatment was significant for opsonised *S. aureus* (****$p<0.0001$), *S. gordonii* (***$p<0.001$) and *Sel. noxia* (*$p<0.05$) (2way ANOVA and Bonferroni post-tests, n=3) (Figure 4.8e). Taurine pre-treatment had a differential effect on neutrophil NET production, relative to untreated cells. Taurine significantly reduced NET production following stimulation with PMA (2way ANOVA and Bonferroni post-test ****$p<0.0001$, n=3), but did not significantly reduce NET production in response to opsonised *S. aureus* or bacterial stimulation (Figure 4.8f).

a) ROS release (luminol) and DPI

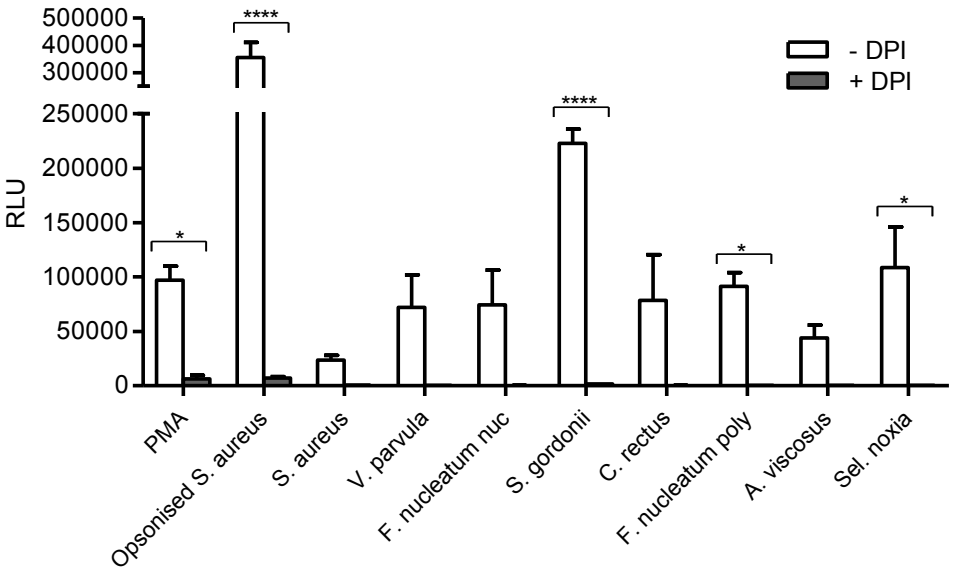

b) NET-DNA release and DPI

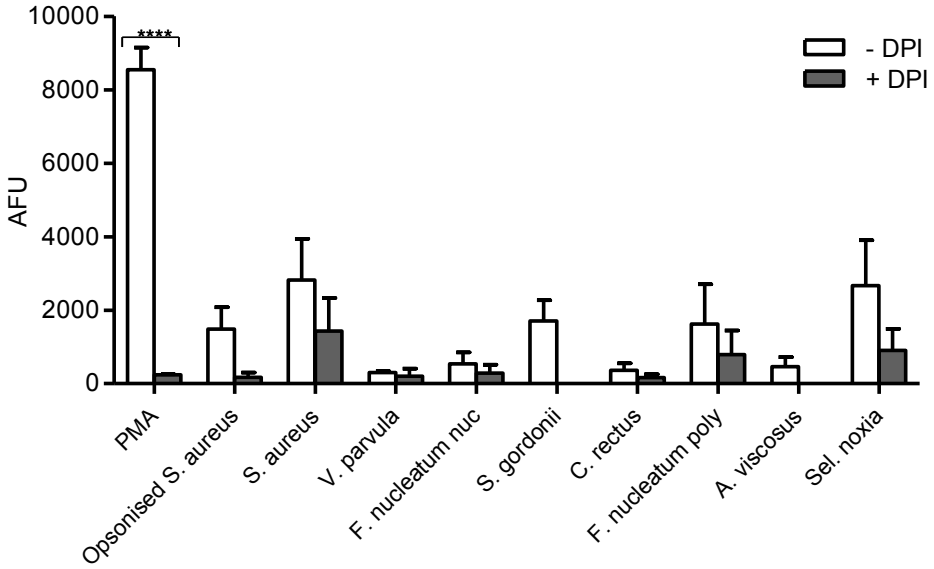

c) ROS release (luminol) and NAC

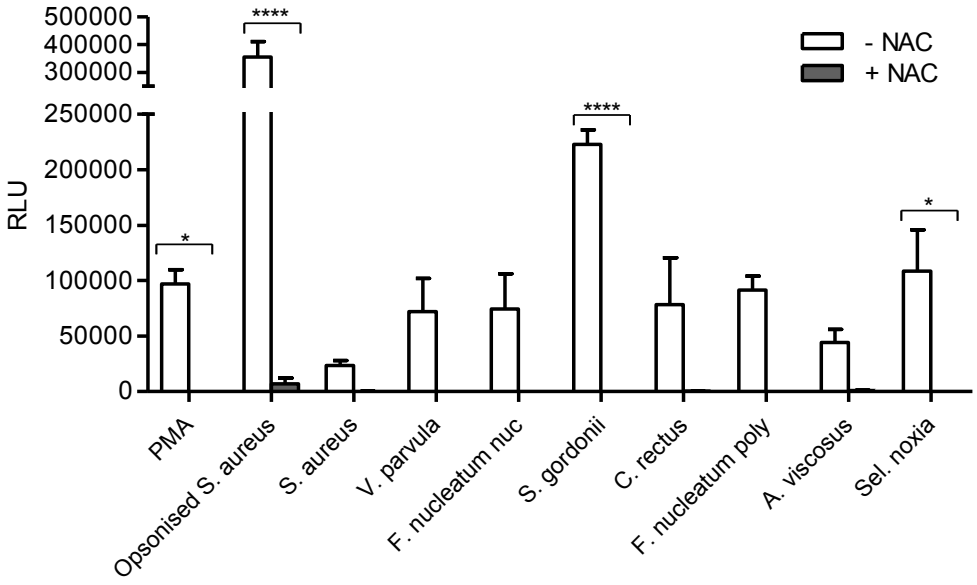

d) NET-DNA release and NAC

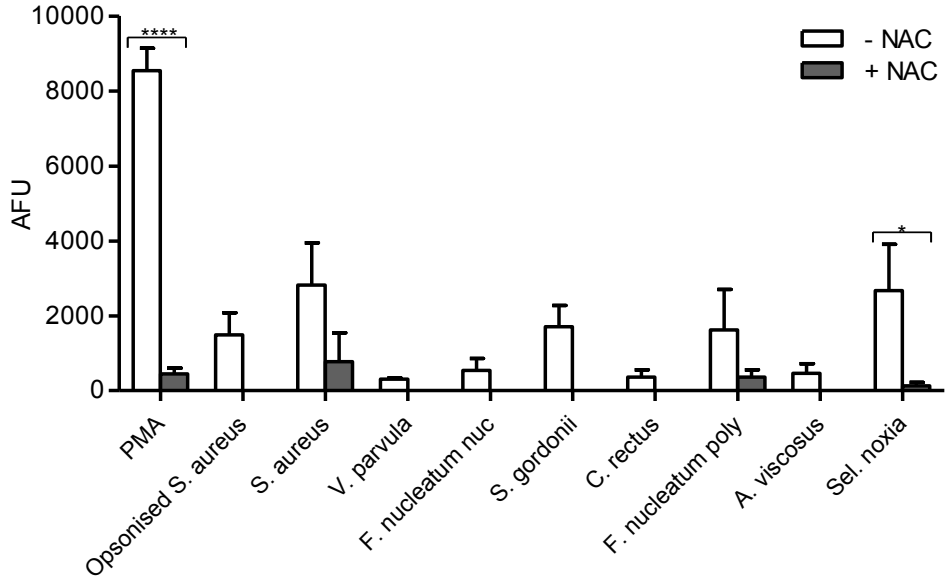

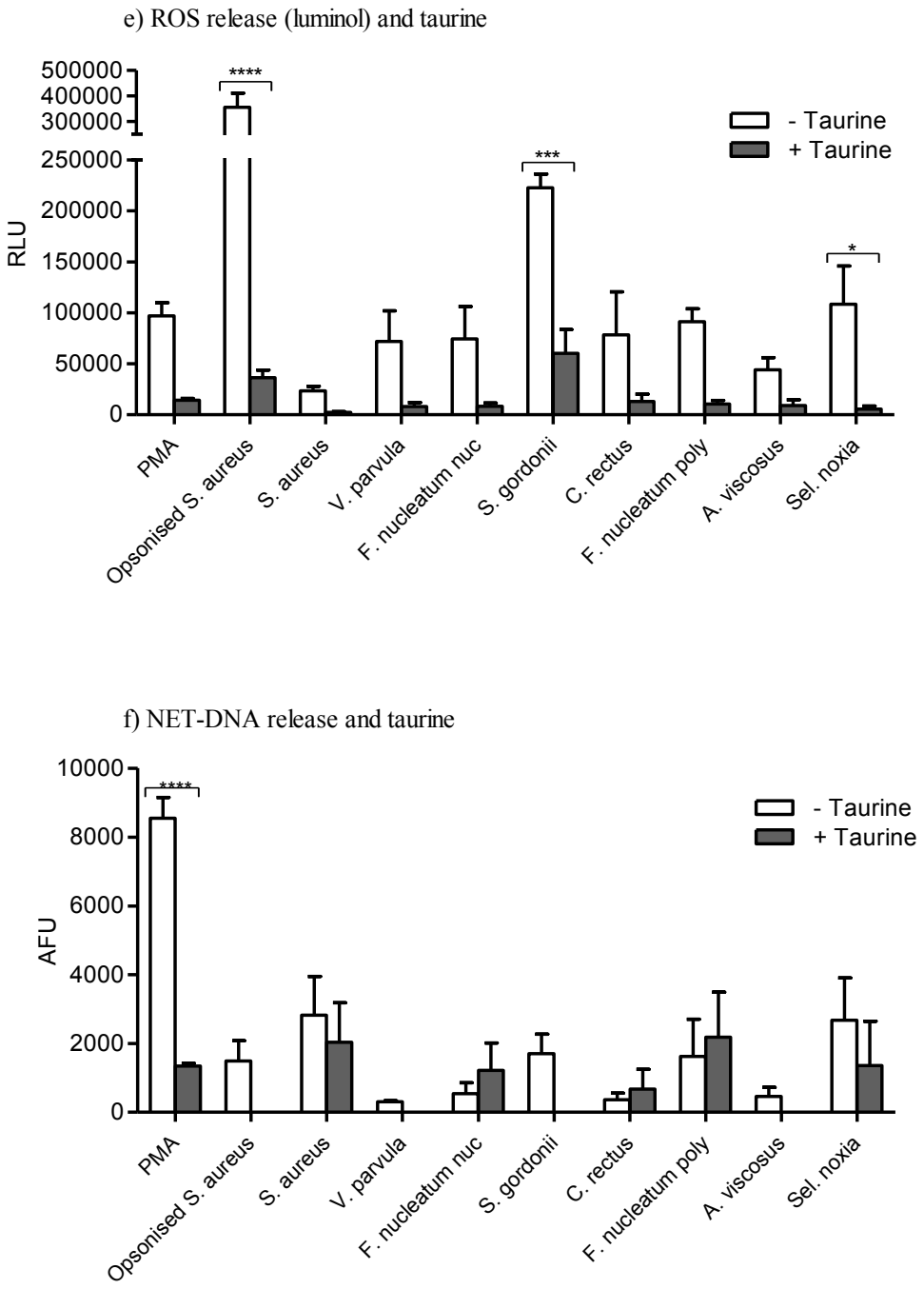

Figure 4.8: Effect of NADPH-oxidase pathway modulating agents on ROS and NET production

Total ROS production and NET production were quantified in response to a panel of periodontal bacteria ($1x10^8$ and MOI of 1000), as well as PMA (50nM) and opsonised *S. aureus* ($5x10^7$ and MOI of 500) following pre-incubation (30 mins) with (a, b) DPI (25μM), (c, d) NAC (10mM) or (e, f) taurine (100mM). Statistical significance was calculated using 2way ANOVA and Bonferroni post-tests (*$p<0.05$, **$p<0.01$, ****$p<0.0001$, ns=not significant). Data presented as (a, c, e) RLU (relative light units) and (b, d, f) AFU (arbitrary fluorescence units). Data expressed as mean ± SEM (n=3 in duplicate).

4.8 Effect of TLR inhibition on ROS and NET production

To attempt to dissect the signalling involved in ROS NET activation, the effect of TLR inhibitors was investigated (section 2.2.2.3). Isolated neutrophils were incubated with chloroquine (100μM), which inhibits TLRs 3, 7 and 9, or OxPAPC (30μg/ml), which inhibits TLRs 2 and 4, or both TLR inhibitors. Neutrophil total ROS and NET production were measured following pre-incubation with the inhibitor for 30 mins prior to stimulation with PMA (50nM), opsonised *S. aureus* ($5x10^7$ and MOI of 500) and a panel of 9 selected heat-killed periodontal bacteria ($1x10^8$ and MOI of 1000).

Chloroquine pre-treatment had a differential effect on neutrophil total ROS production. Whilst chloroquine significantly reduced ROS production following stimulation with opsonised *S. aureus* (***p<0.01), V. parvula* (**p<0.*05) and S. *gordonii* (*****p<0.0001),* chloroquine pre-treatment caused a significant increase in total ROS in PMA-stimulated neutrophils (**p<0.*05) (2way ANOVA and Bonferroni post-tests, n=3) (Figure 4.9a). Chloroquine pre-treatment resulted in a moderate reduction in NET production in response to bacterial stimuli, but treatment prior to stimulation with PMA and opsonised *S. aureus* caused a non-significant increase in NET release (2way ANOVA *p>0.05*) (Figure 4.9b).

OxPAPC pre-treatment was not found to have an inhibitory effect on ROS production, but was found to increase total ROS release relative to cells that did not receive OxPAPC treatment. This was statistically significant for stimulation with opsonised *S. aureus*, which produced significantly higher levels of total ROS following OxPAPC pre-incubation (2way ANOVA and Bonferroni post-test ****p<0.001*, n=3) (Figure 4.9c). OxPAPC pre-treatment resulted in a non-significant reduction in NET release in response to opsonised *S. aureus and* bacterial stimulation; however OxPAPC treatment prior to PMA stimulation caused a non-significant increase in NET release (2way ANOVA *p>0.05*) (Figure 4.9d).

Chloroquine and OxPAPC pre-treatment produced a differential effect on neutrophil total ROS production relative to cells that did not receive pre-treatment. Chloroquine and OxPAPC pre-treatment caused a significant increase in ROS by PMA-stimulated neutrophils (2way ANOVA and Bonferroni post-test $^{**}p=0.01$, n=3) and a significant decrease in ROS by opsonised *S. aureus*-stimulated neutrophils (2way ANOVA and Bonferroni post-test $^{*}p=0.05$, n=3) (Figure 4.9e). Chloroquine and OxPAPC pre-treatment resulted in a non-significant reduction in NET production in response to bacterial stimuli. However, treatment prior to stimulation with PMA and opsonised *S. aureus* caused a non-significant increase in NET release (2way ANOVA $p>0.05$) (Figure 4.9f).

a) ROS release (luminol) and chloroquine

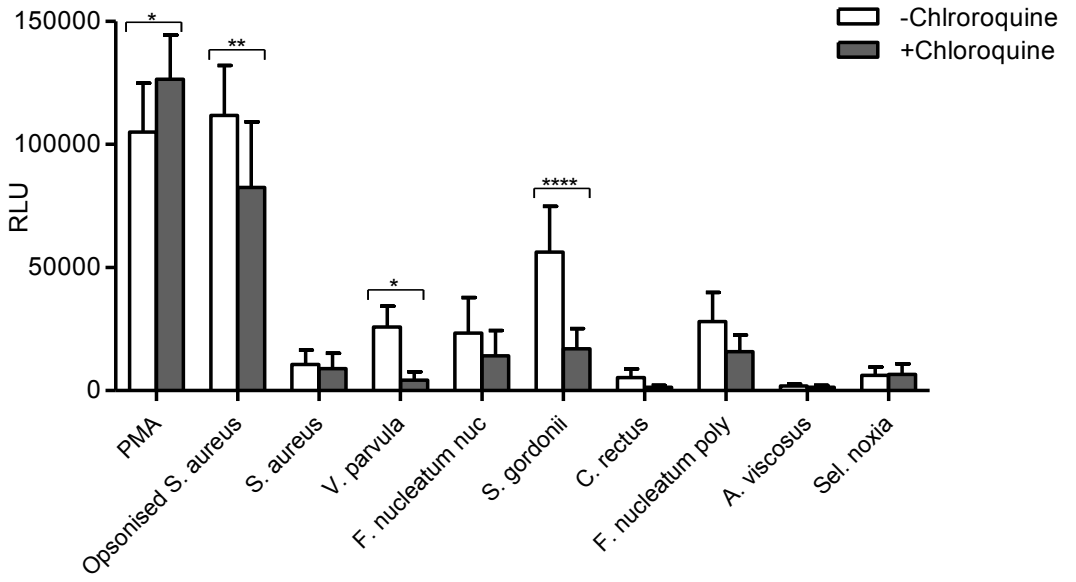

b) NET-DNA release and chloroquine

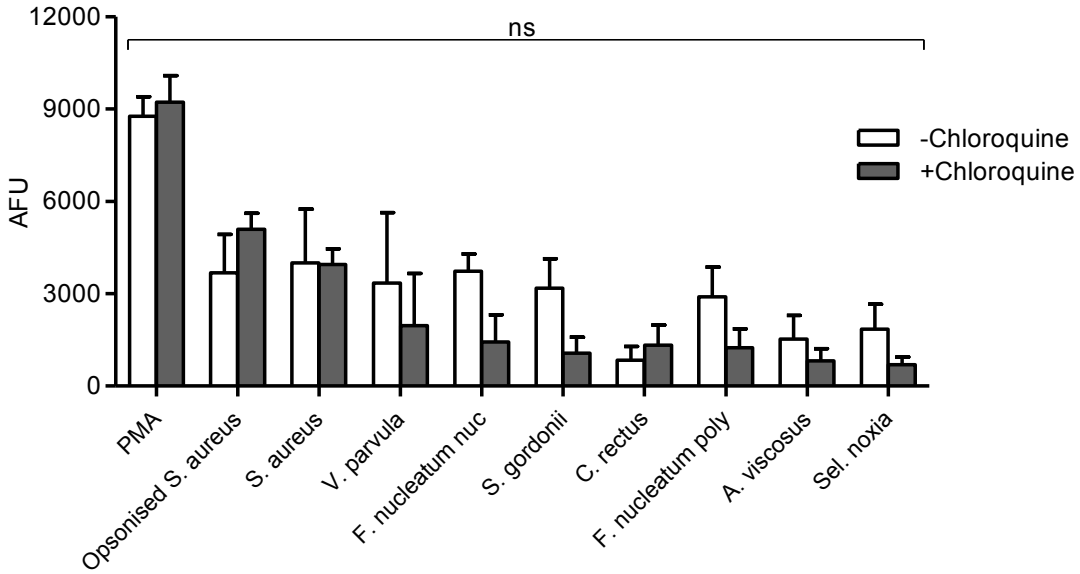

c) ROS release (luminol) and OxPAPC

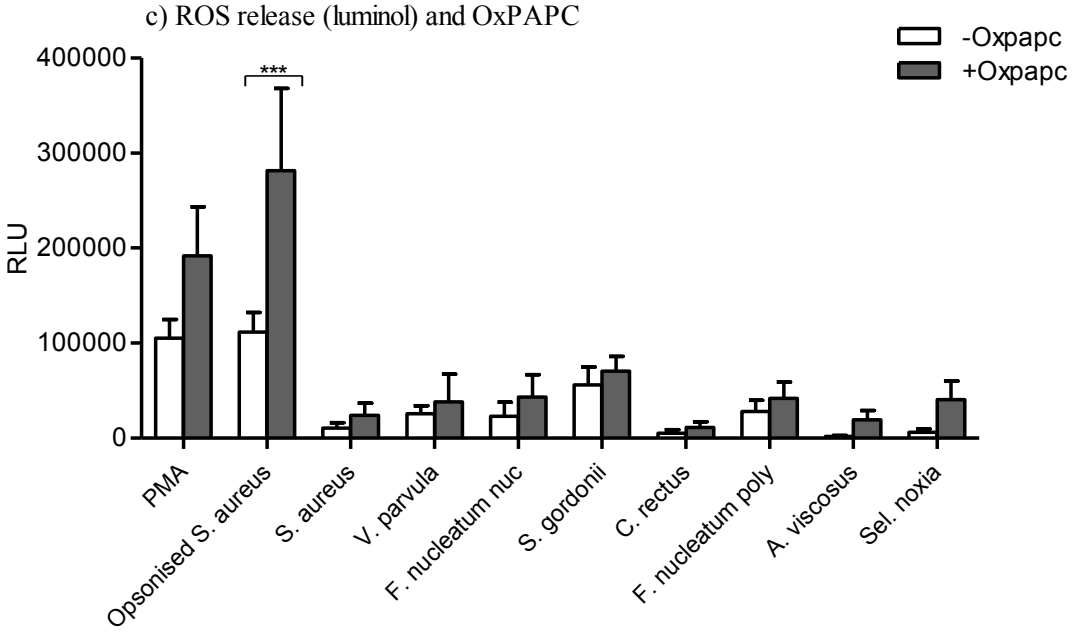

d) NET-DNA release and OxPAPC

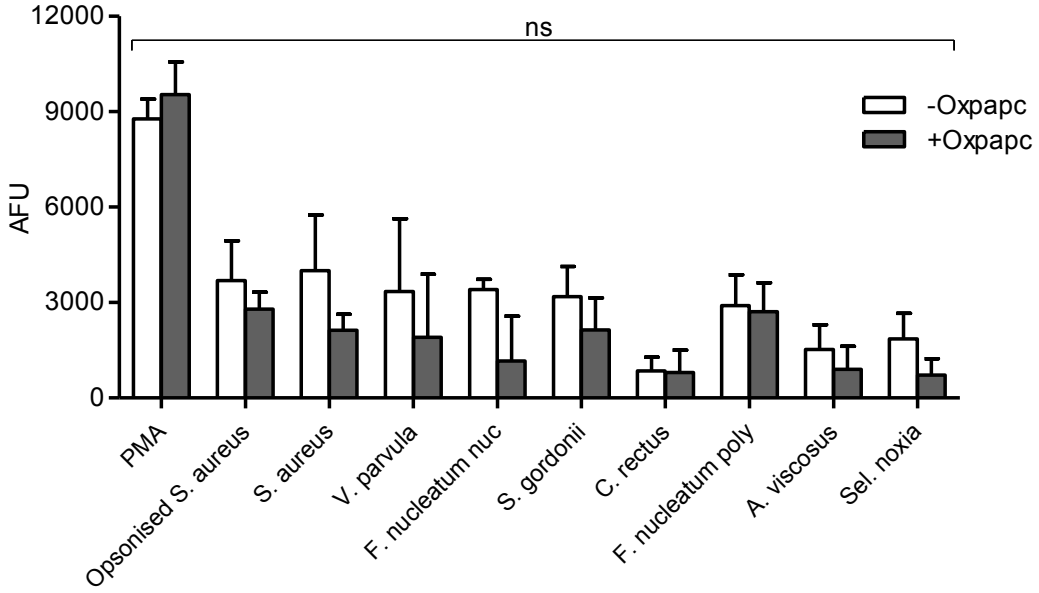

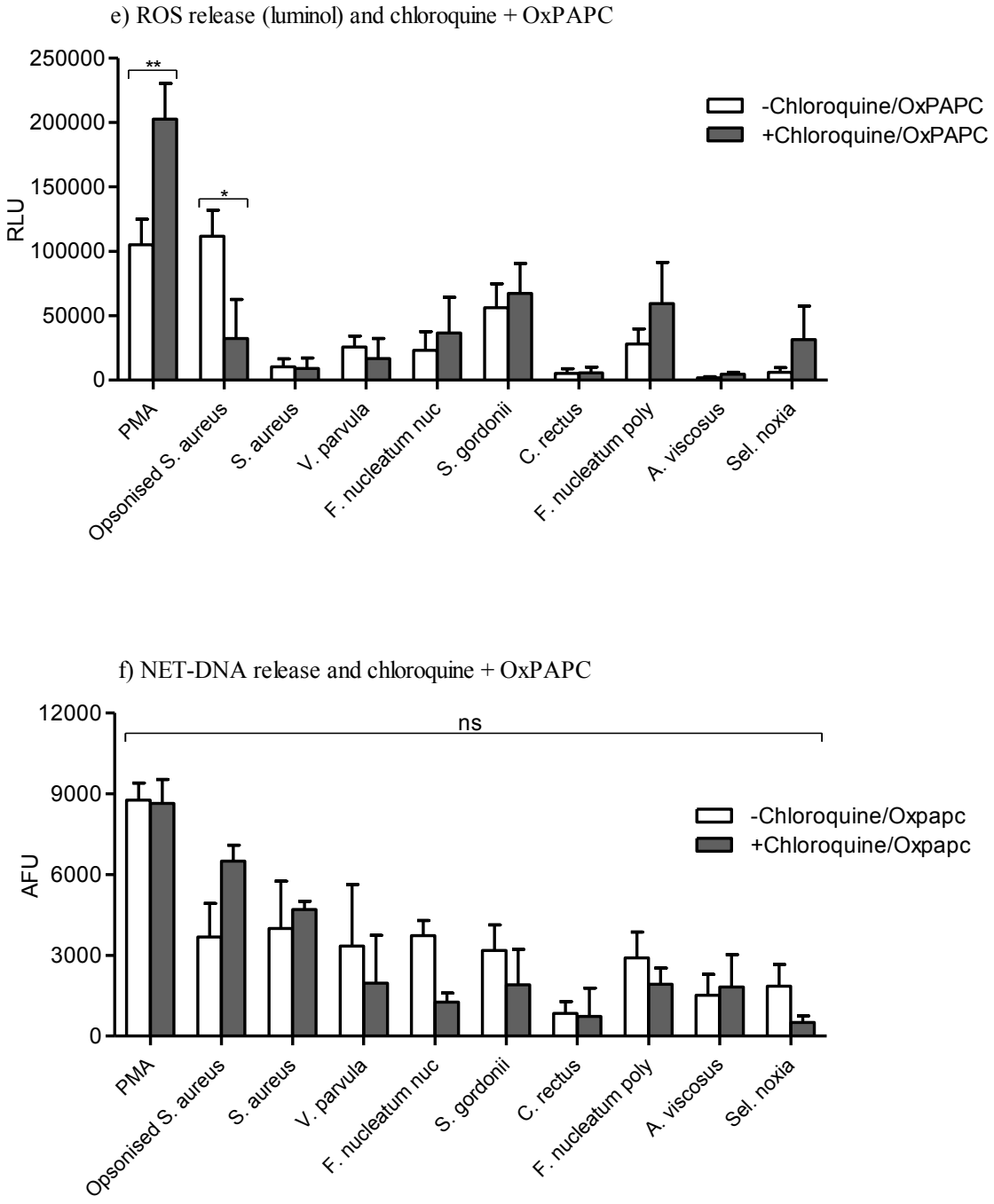

Figure 4.9: Effect of TLR inhibition on ROS and NET production

Total ROS production and NET production were quantified in response to a panel of periodontal bacteria ($1x10^8$ and MOI of 1000), as well as PMA (50nM) and opsonised *S. aureus* ($5x10^7$ and MOI of 500) following pre-incubation (30 mins) with (a, b) Chloroquine (100µM), (c, d) OxPAPC (30µg/ml) or (e, f) Chloroquine and OxPAPC. Statistical significance was calculated using 2way ANOVA and Bonferroni post-tests (**p<0.05,* ***p<0.01,* *****p<0.0001,* ns=not significant). Data presented as (a, c, e) RLU (relative light units) and (b, d, f) AFU (arbitrary fluorescence units). Data expressed as mean ± SEM (n=3 in duplicate).

4.9 Discussion

Neutrophil ROS production is a vital component of the innate immune response which enables the killing and clearance of pathogens. Pathogenic bacteria are known to stimulate ROS production via NADPH-oxidase, whereby molecular oxygen is reduced by electrons to form $O_2^{\cdot-}$. The $O_2^{\cdot-}$ is initially converted to H_2O_2, and finally, H_2O_2 is converted to HOCl in a reaction catalysed by MPO (Chapple 1996, Robinson 2008). Neutrophils are the predominant immune cell in periodontitis, and the results presented here support findings that stimulation of peripheral blood neutrophils with periodontal bacteria promotes extracellular, intracellular and superoxide ROS release; however data indicates that this may be species specific (section 4.2). Indeed, certain *Streptococcal* and *F. nucleatum* species consistently elicited higher neutrophil ROS production while, under these experimental conditions, other bacteria such as *P. gingivalis,* were not found to significantly promote ROS release. Interestingly, *P. gingivalis* is reportedly resistant to neutrophil-derived ROS production, which is attributed to a non-heme iron protein, rubrerythrin, which shields the bacteria from oxidative stress (Mydel *et al.,* 2006). It is possible that the low levels of *P. gingivalis*-induced ROS may function to afford protection to other biofilm organisms that are not resistant to ROS.

Whilst it is recognised that ROS facilitate microbial killing, the progression of periodontitis appears host-mediated via an exaggerated inflammatory response to microbial plaque (Hajishengallis 2014). ROS release does not discriminate between pathogens and host tissues, and therefore tissue injury can arise from plaque-induced extracellular ROS production. ROS is reported to contribute to periodontitis progression by direct mechanisms, such as tissue degradation (Sharma & Sharma 2011), lipid peroxidation (Dix & Aikens 1993) and DNA strand breaks (Dix *et al.* 1996). In addition, ROS are believed to promote disease progression indirectly , by for example increasing osteoclast differentiation (Waddington *et*

al., 2000) and initiating a self-perpetuating cycle that activates immune cells to generate further ROS (Dahiya *et al.,* 2013). Notably, Matthews *et al.,* (2007a, 2007b) demonstrated increased ROS production in chronic periodontitis, and in light of reports indicating that patients also have elevated levels of circulating neutrophils (Al-Rasheed *et al.,* 2012); it is possible that periodontitis patients are more susceptible to ROS-induced tissue damage. A mechanism by which patients may be more susceptible to the deleterious effects of ROS is due to the discordance between oxidant/antioxidant levels may exist. This is supported by Chapple *et al.,* (2007), who reported that total antioxidant activity is lower in the saliva of periodontitis patients. Neutrophil chemotaxis is also reported to be compromised in chronic periodontitis, which is likely to increase neutrophil tissue transit times and thereby potentially exacerbating ROS-mediated collateral tissue damage (Roberts *et al.,* 2015).

Quantification of NET-DNA and NET-bound components demonstrated differential NET production in response to a panel of periodontal bacteria (section 4.3). DNA is released in other forms of neutrophil cell death processes and the quantification of NET-bound components (NE, MPO and CG) provides a DNA-independent measure of NETs. Other published methods to quantify NET production include microscopy (Brinkmann *et al.,* 2004), automated microscopy (Hakkim *et al.,* 2011) and immunostaining (Brinkman *et al.,* 2004, 2010). It is noteworthy that inter-individual differences between volunteers, such as neutrophil responsiveness to stimuli, can also affect NET quantification results regardless of the analytical method employed (Barrientos *et al.,* 2013, Halverson *et al.,* 2015). In the current work, assays were not conducted to determine whether bacteria-induced NETs contained nuclear or mitochondria DNA (Yousefi *et al.,* 2009). However, reportedly mitochondrial DNA is 100,000 times less abundant in granulocyte NET structures (Pilsczek *et al.,* 2010); thus it is likely that nuclear NET-DNA represents a larger proportion of the NET structures quantified. NET production in response to individual periodontal bacteria

suggests these events may occur *in vivo,* and thus differences in NET induction between species may be compensated for when these species co-exist within a biofilm structure. NETs have previously been shown to exist in purulent exudate from periodontal pockets, where they are postulated to entrap invading microbes and prevent their dissemination (Vitkov *et al.,* 2009, 2010). This is corroborated by recent findings by Hirchfeld *et al.,* (2015), who demonstrated that following the recruitment of neutrophils to the oral biofilm, they can infiltrate the dental plaque and subsequently release NET structures. Further support for the presence of NET production in periodontitis is that periodontal pockets reportedly provide an appropriate environment for ROS production, by the provision of sufficient oxygen tension and pH (Mettraux *et al.,* 1984, Eggert *et al.,* 1991). This may suggest that the periodontal pocket environment is likely to enable ROS-dependent NET release. Recent findings have also suggested that some periodontal bacteria reduce complement-induced NET production, which may also afford protection to other biofilm bacteria by evading NET entrapment (Palmer *et al.,* 2015). Collectively, these findings highlight that whilst periodontal bacteria can stimulate for NET release, prospective studies are needed to fully elucidate the role of NETs in periodontitis, in particular within the local diseased tissue environment.

HOCl-induced NETs were found to entrap all periodontal bacteria to some extent (section 4.4), which is consistent with previous findings suggesting NETs can ensnare a significant majority of microorganisms, including Gram-positive and Gram-negative bacteria (Brinkmann *et al.,* 2004). It is noteworthy that reports by Brinkmann *et al.,* (2012) observed that *in vivo*, and space permitting, NETs may occupy and therefore immobilise bacteria in areas 10-15 times larger than the cell they originated from. Interactions between bacteria and NETs are believed to be the result of charge differences between the negatively charged chromatin NET backbone and the pathogens' cell surface (Urban *et al* 2009). Furthermore,

many periodontal bacteria are reported to release DNases, which in addition to regulating biofilm formation (Whitchurch *et al.,* 2002), may have the ability to disassemble NET structures and contribute to biofilm pathogenicity and NET evasion (Palmer *et al.,* 2012). In support of this hypothesis, *S. aureus* nuclease production reportedly confers resistance to NET-mediated entrapment and killing. Indeed bacterial DNase expression may explain why some periodontal species showed less entrapment, such as *S. constellatus,* which reportedly releases large quantities of DNase (Palmer *et al.,* 2012). However, further work is required to elucidate whether DNase release by specific pathogens allows only these species to disseminate, or if DNase release provides a mutually beneficial environment in which non-DNase producing bacteria present in the biofilm are also afforded protection from NET entrapment.

Following bacterial entrapment, the high local concentration of AMPs associated with NETs is postulated to kill pathogens (Brinkmann *et al.,* 2012). In support of this, NET-bound NE is believed to cleave bacterial virulence factors (Brinkmann *et al.,* 2004), and in addition MPO and CG are reported to be vital for the clearance of invading bacteria (Parker *et al.,* 2012, Lappann *et al.,* 2013). The nuclear DNA backbone is also believed to exhibit direct bactericidal properties by disrupting bacterial membrane integrity and lysing bacterial cells (Halverson *et al.,* 2015). The authors postulate that given the low abundance of AMPs on NETs (<1-6%), and that a key virulence factor is the release of DNases, it is possible that nuclear DNA is the predominant antibacterial component of NETs (Halverson *et al.,* 2015). Under the experimental conditions applied here, the incubation of NETs with periodontal bacteria did not appear to impede bacterial growth or survival (section 4.6). However, it is difficult to ascertain whether the ongoing growth was a result of NETs not being capable of killing these bacteria, or a result of these specific experimental conditions. Interestingly, Menegazzi *et al.,* (2012) also questioned the robustness of NET killing assays and suggested

that previous studies where bacteria were not released from NET structures post-incubation did not prove that the microbes trapped within NETs were in fact dead. Indeed, subsequent experiments by Menegazzi *et al.,* (2012) addressing this revealed that NETs do not have the capacity to kill *S. aureus* or *C. albicans,* which is consistent with the protocol applied and the results presented here. Alternatively, an apparent inability of NETs to kill bacteria could be due to various stages of the assay that may compromise NET antibacterial capacity, or not correctly identifying numbers of viable bacteria; examples of this include MNase digestion of NETs prior to co-incubation, incubation conditions, measuring bacterial killing by the enumeration of colonies or the bacteria and NET concentrations (MOI). Future experiments to quantify NET-mediated killing may benefit from application of multiple assays performed in parallel, such as enumeration of colonies, turbidity measurements (Harris 2012), flow cytometry and microscopy of SYTO9/propidium iodide stained bacteria (Halverson *et al.,* 2015). Whilst the importance of NETs is evident in individuals with reduced NET release, such as neonates (Yost *et al.,* 2009), CGD patients (Bianchi *et al.,* 2009) and PLS patients (Sorensen *et al.,* 2014), this could be due to increased bacterial dissemination rather than the direct antimicrobial properties of NET structures (Menegazzi *et al.,* 2012). Conversely, if NETs are interacting with, but not killing, periodontal pathogens, it is possible that NET-bacteria complexes may provide a source of autoantigens and trigger further inflammatory responses, as observed in cystic fibrosis (Marcos *et al.,* 2010). This also raises questions regarding NET production within the microbial biofilm (Hirschfeld *et al.,* 2015), as it is not known whether NETs prevent bacteria dissemination, or in fact promote biofilm stability and growth.

Treatment of neutrophils with DPI (NADPH-oxidase inhibitor) abrogated total ROS release in response to PMA and bacterial stimulation, as expected (section 4.7). ROS inhibition also translated to decreased NET release following stimulation with PMA (as previously reported

by Fuchs *et al.,* 2007 & Palmer *et al.,* 2012), as well as following bacterial stimulation. These findings confirm that NAPDH-oxidase, at least in part, necessitates NET release; this is also evidenced in CGD patients who harbour an NADPH-oxidase mutation and consequently do not produce NETs in response to infection (Bianchi *et al.,* 2009). Notably, DPI had a relatively mild effect on NET production in response to *S. aureus,* which is consistent with findings by Pilsczek *et al.,* (2010), who hypothesised that *S. aureus* may trigger the release of NADPH-oxidase independent NET release 1-2 hours after stimulation, followed by oxidase dependent NET release at 3-4 hours. In the current studies, NET quantification at 4 hours does not discriminate between oxidase-dependent and -independent NET release, which suggests that oxidase-independent NETs are also present, and hence, DPI does not significantly reduce the quantification of NETs. Noteworthy is a report that explored the role of autophagy, a homeostatic process facilitating intracellular degradation, which has also been suggested to play a role in cell death. The authors demonstrated that both NADPH activity and autophagy are required for NET release, and without autophagy, NADPH is insufficient to cause the decondensation of chromatin and mediate NET release (Remijsen *et al.,* 2011).

To establish the contribution of H_2O_2 to NET release, the effect of increased removal of H_2O_2 was determined by the addition of a glutathione peroxidase precursor substrate (NAC), which promotes the removal of H_2O_2 (section 4.7). NAC pre-treatment of neutrophils demonstrated reduced total ROS and NET release, notably the smallest decrease in NET release following NAC pre-treatment was again quantified in response to *S. aureus.* Reduced NET production following NAC treatment is consistent with findings by Palmer *et al.,* (2012) and confirms the role of H_2O_2 in bacterial-induced NET release.

Subsequently, further work to ascertain whether other H_2O_2 metabolites are required for NET release was undertaken (section 4.7). One potential pathway involved utilises the conversion

of H_2O_2 to HOCl in a reaction catalysed by MPO, which produces further reactive oxidants to facilitate the removal of invading pathogens. The importance of HOCl in NET production was determined by treating cells with taurine, which scavenges HOCl. The addition of taurine resulted in a reduction in total ROS release, however a differential effect on NET production was observed. Whilst PMA-induced NET release decreased, which is consistent with findings by Palmer *et al.,* (2012), taurine caused increased NET release in response to certain bacterial stimuli. These findings emphasise the differences between stimuli, as PMA may induce NETs dissimilar to those evoked by physiologically relevant bacteria. Furthermore, given that taurine has been suggested to reduce NET release by rescuing cells from cell death (Palmer *et al.,* 2012); the current results further highlight the need for a greater understanding of NETosis and whether bacteria-induced NET release is indeed a form of programmed cell death.

Further experiments aimed to establish the role of TLR activation in NET production (section 4.8). Whilst pre-treatment of neutrophils with Chloroquine (intracellular TLR3, 7 and 9 inhibitor) associated with a moderate decrease in total ROS release in response to opsonised *S. aureus* and bacterial stimuli, PMA-induced ROS production increased. In addition, Chloroquine treatment resulted in moderately reduced bacteria-induced NET production; however NET release in response to PMA and opsonised *S. aureus* increased. Notably, neutrophils are reportedly not responsive to TLR 3 and 7 ligands (Janke *et al.,* 2009), which suggests that these observations are attributed to decreased TLR9 signalling. TLR9 is central to the activation of neutrophils by bacterial DNA, which promotes phagocytosis, pro-inflammatory cytokine release and ROS production (El Kebir *et al.,* 2009). The importance of TLR9 signalling is particularly interesting in light of recent reports suggesting that NET-DNA can further activate TLR9 on neutrophils and dendritic cells, which may aid the

activation of the immune response (e.g. further NET release), or conversely initiate autoimmune responses (Itagaki *et al.,* 2015, Lande *et al.,* 2011).

Treatment of cells with OxPAPC (cell surface TLR2 and 4 inhibitor) exhibited increased ROS production and a mild decrease in bacteria-induced NET release (section 4.8). Similarly, very little differences were observed in NET production in cells pre-treated with Chloroquine and OxPAPC. Previous findings have suggested that ROS release is TLR2 and 4 dependent (Sabroe *et al.,* 2005); however Gould *et al.,* (2014) demonstrated that TLR2 and 4 blocking antibodies did not abolish NET release. Further experiments are required to determine whether these discrepancies are a result of differences in experimental procedures (such as the stimuli employed), or whether alternative activation pathways are being utilised (such as TLR co-receptors or ROS independent NET release) to compensate for the TLR inhibition (Perera *et al.,* 2001).

In summary, these data demonstrated variability between periodontal bacteria in their ability to stimulate neutrophil ROS production and NET responses. This variability may contribute to the pathogenesis of periodontitis by mechanisms such as bacterial avoidance of NET stimulation and thus persistence of infection, or excess NET release with associated autoimmunity. The ability of NETs to entrap bacteria may facilitate pathogen containment and prevent their dissemination within tissues and disease progression; however further work is needed to elucidate how NETs interact with a bacterial biofilm and whether bacterial DNases allow colonising bacteria to subvert NET defences. Under the experimental conditions applied here NETs appeared unable to kill bacteria; if NETs are interacting with, but not killing, periodontal pathogens, it is possible that NET-bacteria complexes may provide a source of autoantigens. Furthermore, treatment of neutrophils with activation

modulating agents demonstrated that NADPH-oxidase, H_2O_2, HOCl and intracellular TLRs modulate bacteria-induced NET production.

CHAPTER 5: NET PRODUCTION BY PERIPHERAL BLOOD NEUTROPHILS IN CHRONIC PERIODONTITIS: A LONGITUDINAL INTERVENTION STUDY

5.1 Introduction

The results presented in this chapter are based on clinical work in a study coordinated by Dr Martin Ling in 2013 and preliminary data from this study concerning NET production have previously been reported in Ling (2015); all NET assays and analyses were however performed as part of this thesis. Chronic periodontitis patients, with age and gender-matched periodontally healthy controls, were recruited to the study (2.2.6.3). Neutrophils were isolated from the peripheral blood of all volunteers to determine the effect of the periodontal inflammatory process on peripheral blood neutrophil NET responses (West Midlands Research Ethics Committee 10/H1208/48). The patients received tailored oral hygiene instruction and non-surgical periodontal treatment that involved scaling and root surface debridement of periodontal pockets >4mm. Patients were reviewed 3 months post-therapy, at which point blood was also collected to determine the impact of reducing local periodontal inflammation via treatment upon peripheral NET production. At both time points periodontitis patients were assayed in parallel with their matched healthy controls. The periodontal status of patients was recorded at both time points, and healthy controls were assessed upon recruitment to the study (2.2.6.3.2). NET-DNA was quantified by quantifying NET-DNA with Sytox green (2.2.3.3) and the effect of volunteer age and disease severity upon NET production was also analysed.

5.2 Volunteer information

Patient and control details are illustrated in Table 5.1. For inclusion and exclusion criteria please see section 2.2.6.3.1. There was no significant difference in age between patients and controls (unpaired t-test $p=0.501$). One volunteer patient (#13) decided they no longer wished to receive periodontal treatment and withdrew from the study; resulting in n=20 pairs pre-treatment and n=19 pairs post-treatment.

Table 5.1: Age and gender of volunteers in the study
Age and gender of patients and healthy age- and gender-matched controls (n=20 pairs). There was no significant difference in age between patients and controls (12 males and 8 females, unpaired t-test *p=0.501*).

Volunteer number	Patient		Gender-matched control
	Gender	Age	Age
1	Male	42	44
2	Male	45	42
3	Male	40	45
4	Female	56	63
5	Male	42	41
6	Male	46	47
7	Female	47	51
8	Male	39	33
9	Male	38	38
10	Female	38	43
11	Male	59	55
12	Male	37	45
13	Female	48	43
14	Female	61	59
15	Male	51	58
16	Female	42	39
17	Female	37	35
18	Female	52	52
19	Male	57	48
20	Male	48	48
Mean		**46**	**46**
SD		**8**	**8**

5.2.1 Clinical measures of periodontitis

To determine the severity of periodontitis and the response to treatment, several parameters were measured (section 2.2.6.3.2). Clinical attachment loss (CAL), periodontal probing pocket depths (PPD), bleeding on probing (BOP) from the pocket base, gingival index (GI) and plaque index (PI) were recorded pre- and post-treatment in periodontitis patients. Chronic periodontitis was defined by a minimum of 2 non-adjacent sites per quadrant with probing pocket depth >4mm, which bled upon probing and displayed radiographic bone loss >30% of the root length, as defined by the European Federation of Periodontology (Tonetti & Claffey 2005). All clinical parameters were measured immediately prior to blood collection for neutrophil assays by a single experienced examiner, who also confirmed periodontal health in the healthy controls.

5.2.2 Clinical attachment loss

Clinical attachment loss (CAL) was calculated pre-treatment by summation of periodontal pocket depth and gingival recession measurements in accordance with Haffajee & Socransky (1986). Mean CAL and percentage sites with 1-2, 3-4 and >4mm CAL are shown in Table 5.2 and corresponds to mild, moderate and severe disease, respectively. From the 20 patients recruited to the study, n=12 (60%) presented with generalised moderate and localised severe chronic periodontitis, n=3 (15%) presented with generalised mild and localised severe chronic periodontitis, and n=5 (25%) presented with generalised severe chronic periodontitis.

5.2.3 Periodontal Pocket depth

The number of sites measuring over 4mm was significantly higher in patients, compared with healthy controls (unpaired t-test ****$p<0.0001$, n=20 pairs). This difference between patients and controls was reduced although still evident following treatment (unpaired t-test ***$p=0.0017$, n=19 pairs). However, there was a significant difference in the number of sites

over 4mm present in periodontitis patients pre- and post-treatment, demonstrating that non-surgical therapy significantly reduced pocket depths (unpaired t-test ***$p=0.0023$, n=19 pairs) in patients, but not to control levels (Table 5.3).

5.2.4 Bleeding on probing

The percentage of sites that displayed bleeding on probing (BOP) pre-treatment was significantly higher in patients compared with healthy controls (unpaired t-test ****$p<0.0001$, n=20 pairs). This difference between patients and controls reduced but remained significant post-treatment (unpaired t-test *$p=0.0478$, n=19 pairs). However, there was a significant difference in the percentage of sites that bled upon probing in periodontitis patients pre- and post-treatment (unpaired t-test ****$p<0.0001$, n=19 pairs) (Table 5.4).

5.2.5 Cumulative gingival index

Cumulative gingival index (GI) was significantly higher in patients compared with healthy controls pre-treatment (unpaired t-test ****$p<0.0001$, n=20 pairs). This difference between patients and controls was no longer significant as a result of treatment (unpaired t-test $p=0.101$, n=19 pairs) and GI was significantly different in periodontitis patients pre- and post-treatment (unpaired t-test ****$p<0.0001$, n=19 pairs) (Table 5.5).

5.2.6 Plaque index

Cumulative plaque index (PI) was significantly higher in patients, compared with the healthy controls pre-treatment (unpaired t-test ****$p<0.0001$, n=20 pairs). The difference between patients and controls was corrected as a result of treatment (unpaired t-test $p=0.679$, n=19 pairs) and PI was significantly different in periodontitis patients pre- and post-treatment (unpaired t-test ****$p<0.0001$, n=19 pairs) (Table 5.6).

Table 5.2: Clinical attachment loss in periodontitis patients

Measurements from patients pre-treatment (n=20 pairs). Data is presented as percentage sites with 1-2, 3-4 and >4mm clinical attachment loss (mean ± SD and range).

Clinical attachment loss (% sites)				
Volunteer Number	**Mean ± SD (mm)**	**% sites 1-2mm**	**% sites 3-4mm**	**% sites >4mm**
1	4.4±3.2	39.1	21.8	39.1
2	2.4±1.9	66.7	26.3	7.0
3	3.7±2.1	36.5	35.3	28.2
4	3.5±1.8	35.9	41.0	23.1
5	2.8±1.6	59.0	24.4	16.6
6	3.7±2.1	37.0	31.2	31.8
7	3.4±2.4	55.6	21.6	22.8
8	2.4±0.9	67.9	28.6	3.5
9	3.4±1.6	36.9	45.8	16.3
10	2.8±1.3	44.4	48.3	7.2
11	2.2±1.8	85.7	5.4	8.9
12	2.9±2.6	66.1	13.3	20.6
13	6.0±2.7	5.8	33.3	60.8
14	3.3±2.0	46.4	34.5	19.0
15	3.9±1.6	20.1	50.3	29.6
16	3.2±2.2	55.7	25.9	18.4
17	5.9±3.3	25.6	11.9	62.5
18	2.2±1.5	78.0	16.7	5.3
19	4.1±2.5	33.3	33.3	33.3
20	1.9±1.4	79.0	15.6	5.4
Mean	**3.4**	**48.7**	**28.2**	**23.0**
SD	**1.1**	**21.1**	**12.4**	**16.8**

Table 5.3: Comparison of probing pocket depth in periodontitis patients and healthy controls

Measurements from patients pre-treatment (n=20 pairs) and post-treatment (n=19 pairs), compared with healthy matched controls. Data is presented as probing pocket depths (mean ± SD and range) and the number of sites >4mm.

Probing pocket depth									
Volunteer Number	**Patient**						**Healthy Control**		
	Pre-treatment			**Post-treatment**					
	Mean ± SD (mm)	**Range (mm)**	**No. sites >4mm**	**Mean ± SD (mm)**	**Range (mm)**	**No. sites >4mm**	**Mean ± SD (mm)**	**Range (mm)**	**No. sites >4mm**
1	3.5±2.8	1-12	45	2.7±1.4	1-9	24	2.1±0.9	1-5	1
2	2.2±1.5	1-12	7	2.2±0.9	1-7	8	2.1±0.9	1-5	1
3	3.4±2.0	1-9	36	2.7±1.3	1-7	15	1.8±0.7	1-4	0
4	3.4±1.7	1-9	33	1.6±0.7	0-4	0	2.0±0.8	1-5	3
5	2.6±1.5	1-7	22	2.0±0.8	0-5	2	1.2±0.4	1-2	0
6	3.4±2.1	1-8	45	2.5±1.0	1-7	7	1.5±0.6	1-3	0
7	2.9±1.9	1-12	28	2.2±1.4	1-10	9	1.7±0.6	1-4	0
8	2.3±0.9	1-7	5	1.4±0.8	0-5	1	2.2±0.9	1-5	4
9	3.4±1.6	1-8	29	2.4±1.1	1-6	7	1.3±0.5	1-3	0
10	2.6±1.2	1-7	10	1.8±0.9	1-4	0	1.4±0.6	1-3	0
11	2.1±1.8	1-9	14	1.5±1.1	0-9	2	1.1±0.4	1-3	0
12	2.8±2.4	0-12	35	2.5±2.1	1-10	23	1.1±0.4	1-3	0
13	5.0±2.6	1-13	54	Withdrew			1.1±0.3	1-2	0
14	2.9±1.7	0-8	25	1.8±1.2	0-6	5	1.8±0.9	1-5	1
15	2.8±1.4	1-7	23	2.4±1.5	1-8	16	1.3±0.5	1-3	0
16	3.2±2.2	1-9	32	2.0±1.3	0-9	9	1.1±0.3	1-3	0
17	4.8±2.7	1-12	91	3.5±2.2	1-10	52	1.4±0.5	1-3	0
18	2.1±1.5	0-11	8	1.5±0.9	0-7	1	1.7±0.7	1-4	0
19	2.8±1.6	1-9	13	2.2±1.3	1-9	8	1.6±0.6	1-3	0
20	1.5±1.0	1-7	5	1.5±0.8	1-7	1	1.3±0.6	1-4	0
Mean	**3.0**			**2.1**			**1.5**		
SD	**0.8**			**0.5**			**0.4**		

Table 5.4: The number of sites that bled from the pocket base upon periodontal probing in periodontitis patients and healthy controls
Measurements from patients pre-treatment (n=20 pairs) and post-treatment (n=19 pairs), compared with healthy matched controls. Data is presented as percentage sites with bleeding on periodontal probing.

Bleeding on probing (% sites)			
Volunteer Number	**Patient**		**Healthy Control**
	Pre-treatment	**Post-treatment**	
1	37	23	39
2	16	14	17
3	87	33	0
4	51	8	0
5	26	5	0
6	47	12	0
7	44	11	16
8	42	18	20
9	72	15	0
10	63	13	1
11	21	10	0
12	53	22	0
13	41	Withdrew	0
14	70	14	20
15	23	20	2
16	21	5	0
17	63	35	9
18	33	5	16
19	43	14	17
20	17	3	8
Mean	**43.5**	**14.7**	**8.3**
SD	**20.1**	**8.9**	**10.8**

Table 5.5: Gingival indices in periodontitis patients and healthy controls
Measurements from patients pre-treatment (n=20 pairs) and post-treatment (n=19 pairs), compared with healthy matched controls. Data is presented as individual median gingival index (and interquartile range) and full-mouth cumulative values.

Gingival Index						
Volunteer Number	**Patient**				**Healthy Control**	
	Pre-treatment		**Post-treatment**			
	Individual	**Cumulative**	**Individual**	**Cumulative**	**Individual**	**Cumulative**
1	1 (1-2)	195	1 (0-1)	111	1 (0-1)	136
2	1 (1-2)	187	1 (0-1)	137	1 (0-1)	141
3	3 (2-3)	426	1 (1-2)	216	1 (0-1)	103
4	3 (2-3)	405	1 (1-1)	169	1 (1-2)	190
5	2 (2-2)	322	1 (0-1)	94	0 (0-1)	77
6	2 (2-2)	350	1 (0-1)	149	1 (0-1)	136
7	2 (1-2)	310	1 (1-2)	216	1 (1-1)	185
8	2 (1-2)	316	1 (1-2)	235	0 (0-1)	87
9	2 (1-2)	296	1 (1-1)	126	0 (0-1)	43
10	1 (1-2)	292	1 (0-1)	112	0 (0-0)	26
11	1 (1-1)	203	1 (0-1)	122	0 (0-1)	36
12	2 (1-3)	338	1 (0-1)	125	0 (0-0)	23
13	2 (2-3)	274	Withdrew		0 (0-1)	43
14	2 (1-4)	338	1 (0-1)	106	1 (0-1)	140
15	2 (2-2)	358	0 (0-1)	105	1 (0-1)	108
16	1 (1-2)	274	0 (0-1)	83	0 (0-1)	49
17	2 (2-2)	390	1 (0-1)	147	0 (0-1)	81
18	2 (1-2)	266	0 (0-1)	37	1 (0-1)	108
19	2 (2-2)	269	1 (1-1)	145	1 (1-1)	178
20	1 (1-2)	250	0 (0-1)	72	1 (1-1)	177
Mean		**303.0**		**131.9**		**103.4**
SD		**66.4**		**50.39**		**55.62**

Table 5.6: Plaque indices in periodontitis patients and healthy controls
Measurements from patients pre-treatment (n=20 pairs) and post-treatment (n=19 pairs), compared with healthy matched controls. Data is presented as median plaque index (and interquartile range) and full-mouth cumulative values.

Plaque Index						
Volunteer Number	**Patient**				**Healthy Control**	
	Pre-treatment		**Post-treatment**			
	Individual	**Cumulative**	**Individual**	**Cumulative**	**Individual**	**Cumulative**
1	1 (1-2)	210	1 (1-2)	185	1 (1-1)	168
2	1 (1-1)	137	1 (1-2)	197	1 (0-1)	125
3	3 (2-3)	429	2 (1-2)	244	1 (1-1)	182
4	2 (2-3)	382	1 (1-1)	150	2 (1-2)	249
5	2 (2-3)	367	1 (0-1)	141	1 (1-2)	186
6	2 (2-2)	311	1 (1-2)	212	1 (1-2)	253
7	2 (1-3)	351	1 (1-2)	218	1 (1-2)	212
8	2 (1-2)	314	2 (1-2)	265	1 (0-1)	145
9	2 (1-2)	256	1 (1-1)	150	0 (0-1)	60
10	1 (1-2)	228	1 (0-1)	100	1 (1-1)	157
11	1 (1-2)	250	0 (0-1)	73	1 (1-1)	119
12	2 (1-2)	267	1 (0-1)	117	0 (0-1)	61
13	3 (3-4)	345	Withdrew		1 (0-1)	124
14	2 (2-3)	339	1 (1-2)	135	1 (1-2)	156
15	2 (2-3)	353	1 (1-1)	116	1 (0-1)	128
16	2 (1-2)	272	0 (0-1)	51	1 (0-1)	125
17	2 (1-3)	324	1 (0-1)	106	1 (0-1)	143
18	2 (1-3)	279	0 (0-1)	57	1 (1-1)	150
19	2 (2-3)	271	1 (1-2)	147	1 (1-1)	175
20	2 (2-3)	366	1 (0-1)	122	1 (1-2)	162
Mean		**302.6**		**146.6**		**154.0**
SD		**68.6**		**60.5**		**49.7**

5.3 Comparison of NET production by periodontitis patients and healthy matched controls

Neutrophils isolated from the peripheral blood of periodontitis patients and healthy matched controls were stimulated for NET production with PMA (50nM) and HOCl (0.75mM) (section 2.2.3.3). Baseline NET production in response to PBS (negative unstimulated control) was also quantified. Patient and healthy matched paired samples were assayed in parallel and analysed using fluorometric quantification. There were no significant differences between patient and control NET production assessed fluorometrically when neutrophils were treated with PBS (unstimulated negative control), PMA or HOCl (Wilcoxon matched pairs *p=0.78*, *p=0.30, p=0.69,* respectively, n=20 pairs) (Figure 5.1).

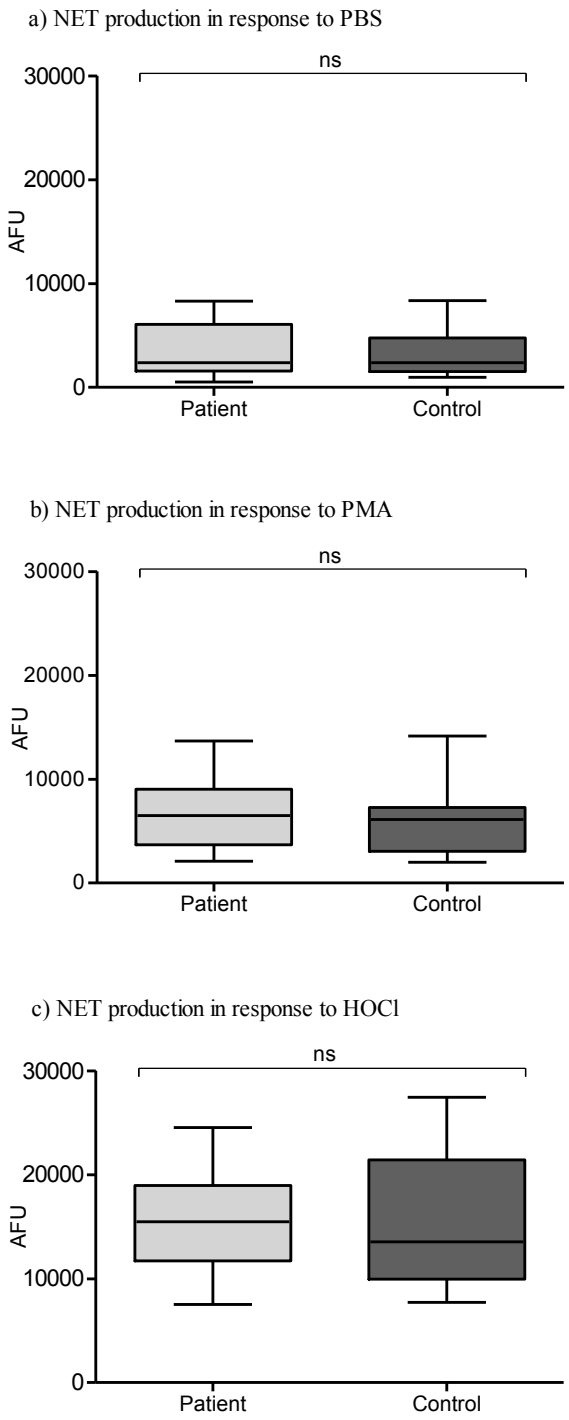

Figure 5.1: NET production in periodontitis patients (pre-treatment) and healthy controls

Pre-treatment NET production was quantified fluometrically following a 3 hour incubation period after neutrophil stimulation. (a) PBS (unstimulated negative control), (b) PMA (50nM) or (c) HOCl (0.75mM). Statistical significance calculated using Wilcoxon matched pairs tests (ns=not significant). Data are presented as AFU (arbitrary fluorescence units) and expressed as mean ± SEM (n=20 pairs in quadruplicate).

5.3.1 NET production by periodontitis patients and healthy matched controls following successful treatment

Three months post-treatment, patients were reviewed and neutrophils from the peripheral blood of periodontitis patients and healthy matched controls were isolated and stimulated for NET production with PMA (50nM) and HOCl (0.75mM) (section 2.2.3.3). Baseline NET production in response to PBS (negative unstimulated control) was also quantified. 19 matched pairs were assayed in parallel and analysed by fluorometric quantification. There were significant differences detected between patients and controls in response to PBS exposure (unstimulated negative control) (Figure 5.2a) and PMA (Figure 5.2b) (Wilcoxon matched pairs $*p=0.041$, $*p=0.021$, respectively, n=19 pairs). However, there were no significant differences detected between comparators when neutrophils were stimulated with HOCl (Figure 5.2c) (Wilcoxon matched pairs $p=0.62$, n=19 pairs). To control for day-to-day variations in neutrophil responsiveness, differences in NET production between pre-treatment and post-treatment were expressed as a ratio of patient matched healthy controls. NET production by patient neutrophils significantly decreased following treatment in response to PBS (unstimulated), PMA (50nM) and HOCl (0.75mM) (Wilcoxon matched pairs $**p=0.007$, $**p=0.004$, $*p=0.012$, respectively, n=19 pairs) (Figure 5.3).

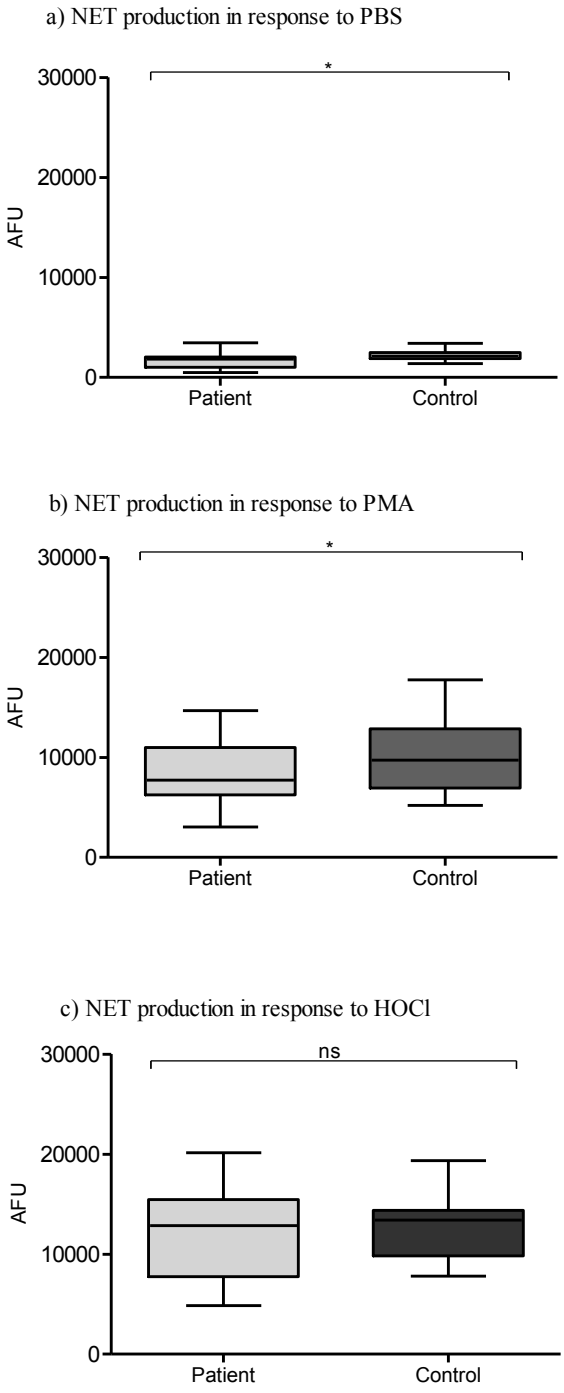

Figure 5.2: NET production in post-treatment periodontitis patients and healthy controls

Post-treatment NET production was fluorometrically quantified following successful treatment (MNase digestion and Sytox green staining). (a) PBS (unstimulated negative control), (b) PMA (50nM), (c) HOCl (0.75mM). Statistical significance calculated using Wilcoxon matched pairs tests (*$p<0.05$, ns=not significant). Data are presented as AFU (arbitrary fluorescence units) and expressed as mean ± SEM (n=19 pairs in quadruplicate).

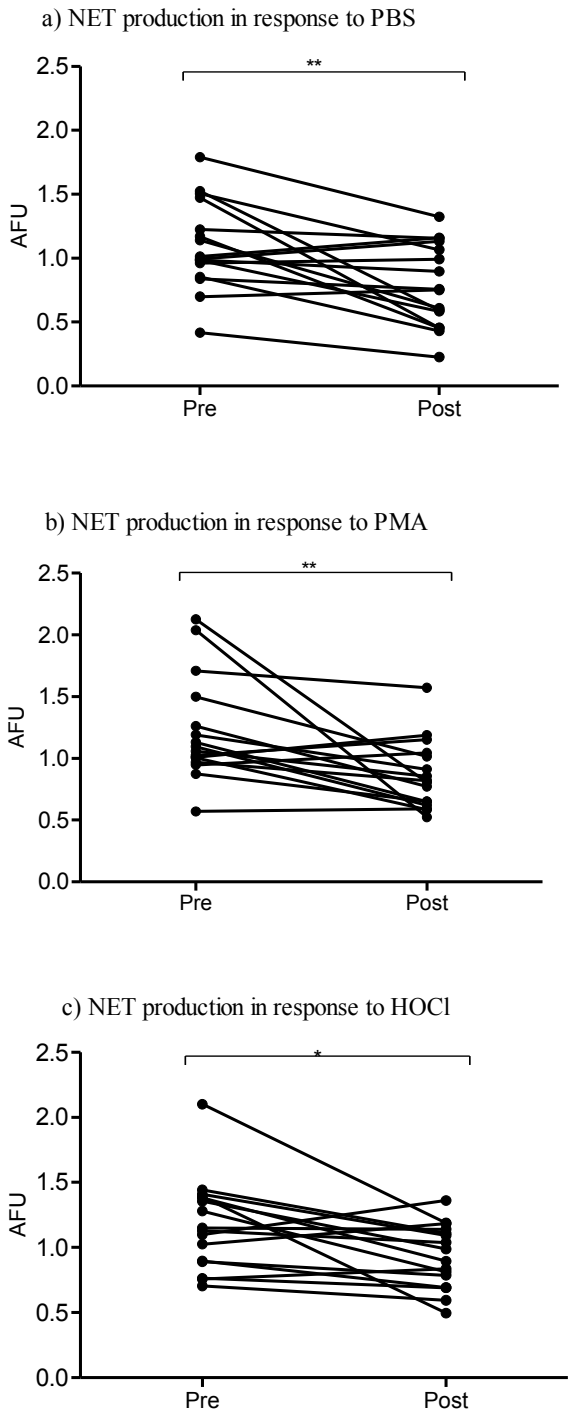

Figure 5.3: Pre- and post-treatment NET production by periodontitis patients
NET production pre- and post-treatment expressed as a ratio of patients to matched controls. (a) PBS (unstimulated negative control), (b) PMA (50nM) and (c) HOCl (0.75mM) Statistical significance calculated using Wilcoxon matched pairs tests (*$p<0.05$, **$p<0.01$). Data are presented as AFU (arbitrary fluorescence units) (n=19 pairs in quadruplicate).

5.3.2 Fluorescence microscopy of NETs from patient and controls pre-treatment

There was no apparent qualitative difference observed between patient and control NET production visualised following fluorometric staining with Sytox green (section 2.2.3.7). Both PMA (50nM) and HOCl (0.75mM) stimulated NETs, as shown by the extracellular web-like structures that stained positive with the DNA-stain, Sytox green (Figure 5.4). PBS-treated neutrophils (negative unstimulated control) also stained positive for DNA, which is likely to be due to cell death during the incubation period that allowed for Sytox green to permeate the compromised cell membrane.

5.3.3 Fluorescence microscopy of NETs from patient and controls post-treatment

There were no qualitative differences observed between patient and control NETs visualised by fluorescence microscopy (Figure 5.5). Consistent with pre-treatment observations, both PMA (50nM) and HOCl (0.75mM) produced extracellular web-like structures.

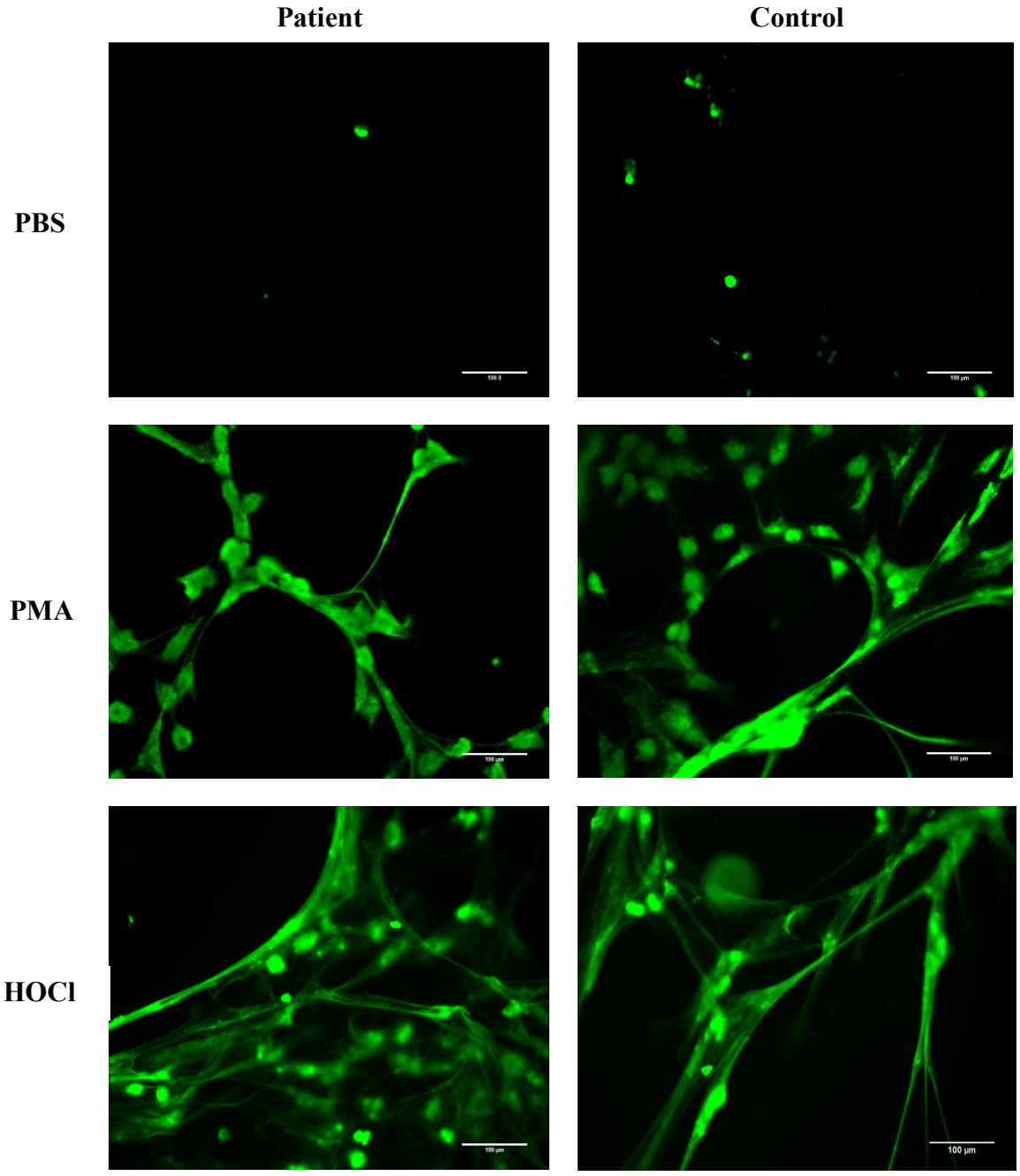

Figure 5.4: Fluorescence microscopy of NETs from patient and controls pre-treatment
NETs were visualised by fluorescence microscopy (x20 magnification) with Sytox green staining in response to PBS (unstimulated negative control), PMA (50nM) and HOCl (0.75mM) exposure for 3 hours. Images are representative of 2 experiments performed in triplicate. Scale bars are 100µm.

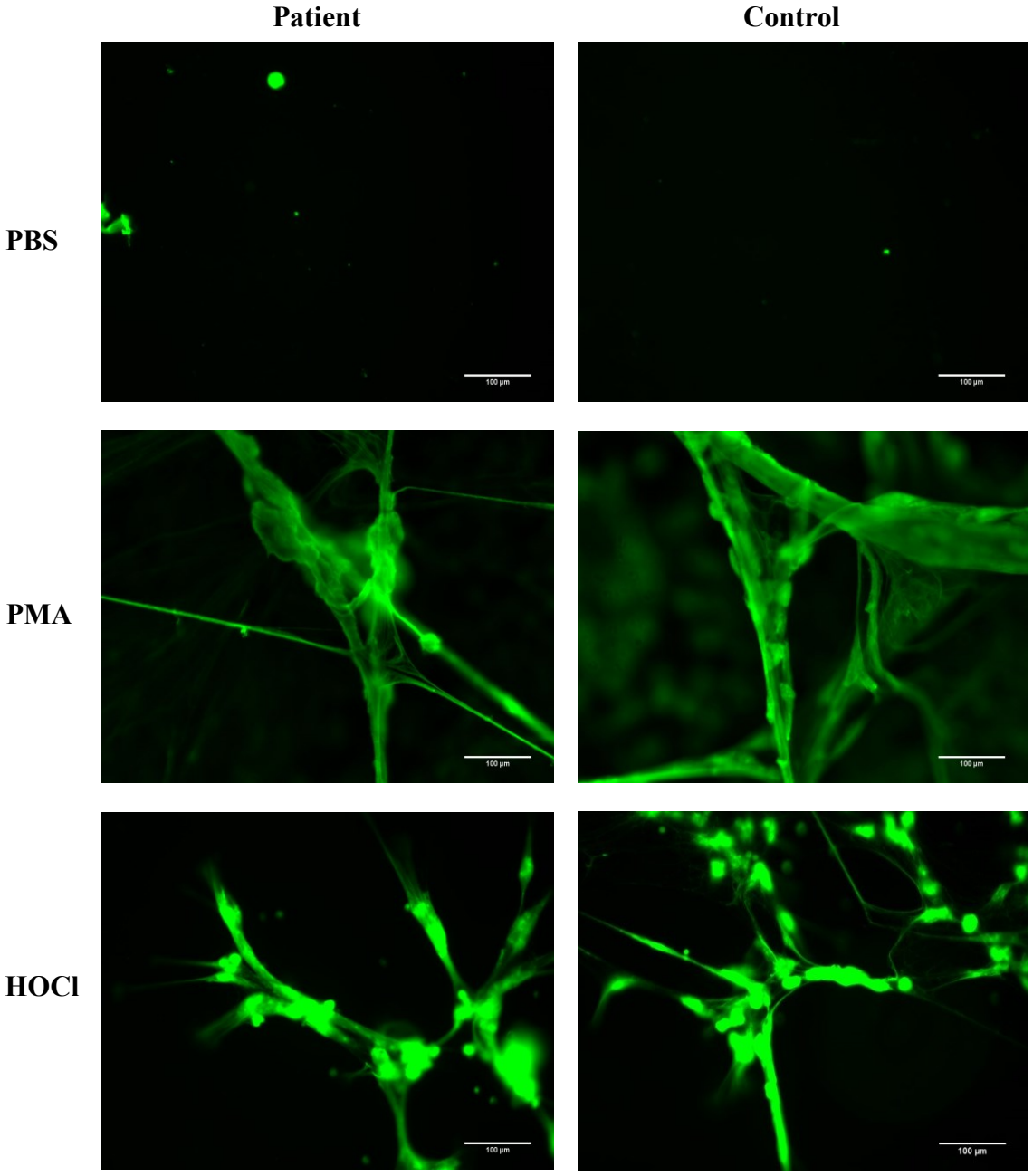

Figure 5.5: Fluorescence microscopy of NETs from patient and controls post-treatment NETs were visualised following successful treatment by fluorescence microscopy (x20 magnification) with Sytox green staining in response to PBS (unstimulated negative control), PMA (50nM) and HOCl (0.75mM) stimulation for 3 hours. Images are representative of 2 experiments in triplicate. Scale bar is 100µm.

5.4 Effect of age on NET production

NET production levels were analysed following stratification for age (<50 years vs >50 years old) in pre-treatment patients and controls (published in Hazeldine *et al.,* 2014). Data was available for 13 patients and 13 matched controls who were under 50 years (mean age 42 ± 4.9 years), and 6 patients and controls who were over 50 years of age (mean 57 ± 3.4 years). NET production by older periodontally healthy volunteers was significantly reduced compared with healthy volunteers under 50 years old (Mann-Whitney PBS **p=0.045*; PMA; **p=0.045*; HOCl **p=0.026,* respectively, n=20 pairs). NET production was also reduced in periodontitis patients over 50 years of age in response to HOCl (0.75mM) (Mann-Whitney **p=0.026).* There was a similar non-significant reduction in NET production in periodontitis patients in response to PBS and PMA (Figure 5.6a).

NET production was also analysed by age (<50 years vs >50 years old) in post-treatment patients and controls. Following the discontinuation of the study by volunteer 13, there were data from 12 patients and age matched controls under 50 years and 6 patients and controls over 50 years of age which could be used for analysis. No statistically significant differences in NET production between volunteers under 50 years and those over 50 years were observed in response to PBS (unstimulated), PMA (50nM) or HOCl (0.75mM) in patients or controls (Mann-Whitney *p=0.089*) (Figure 5.6b).

a) Pre-treatment

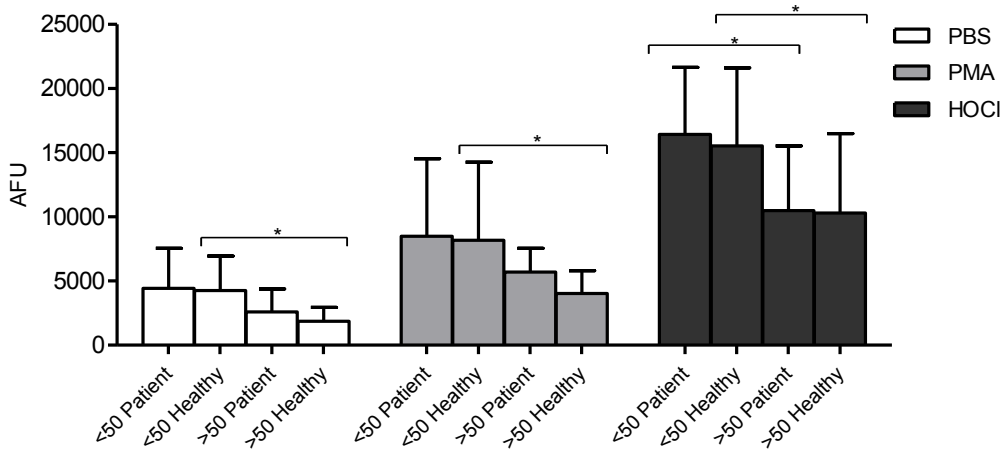

b) Post-treatment

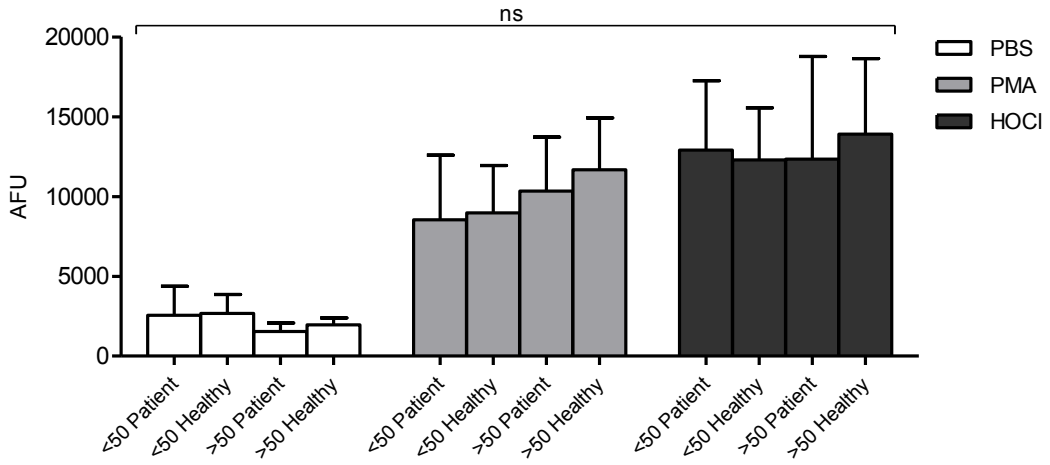

Figure 5.6: The effect of age on pre- and post-treatment NET production in patients and healthy controls

NET production in volunteers <50 (n=13 patients and controls) and >50 (n=6 patients and controls) following no stimulation (PBS) and in response to PMA (50nM) and HOCl (0.75mM) (a) pre-treatment and (b) post-treatment. Statistical significance calculated using Mann-Whitney tests (*$p<0.05$, ns=not significant). Data are presented as AFU (arbitrary fluorescence units) and expressed as mean ± SEM.

5.5 Analysis of the association between severity of periodontitis and NET production pre- and post-treatment

No significant correlation was observed between pocket depth and NET production pre-treatment (linear regression *p=0.92, p=0.94* and *p=0.92* for PBS, PMA and HOCl, respectively, n=20 pairs) or post-treatment (linear regression *p=0.28, p=0.74* and *p=0.84* for PBS, PMA and HOCl, respectively, n=19 pairs) (Figure 5.7a&b). No significant correlation was observed between bleeding on probing and NET production pre-treatment (linear regression *p=0.19, p=0.52* and *p=062* for PBS, PMA and HOCl, respectively, n=20 pairs) or post-treatment (linear regression *p=0.72, p=0.53* and *p=0.61* for PBS, PMA and HOCl, respectively, n=19 pairs) (Figure 5.7c&d). Furthermore, no significant correlation was observed between cumulative gingival index and NET production pre-treatment (linear regression *p=0.55, p=0.91* and *p=0.77* for PBS, PMA and HOCl, respectively, n=20 pairs) or post-treatment (linear regression *p=0.93, p=0.11* and *p=0.41* for PBS, PMA and HOCl, respectively, n=19 pairs) (Figure 5.8a&b). There was also no significant correlation between cumulative plaque index and NET production pre-treatment (linear regression *p=0.44, p=0.17* and *p=067* for PBS, PMA and HOCl, respectively, n=20 pairs). However post-treatment results revealed a significant negative correlation between plaque index and NET production in response to PMA (linear regression **p=0.022,* n=19 pairs) (Figure 5.8c&d).

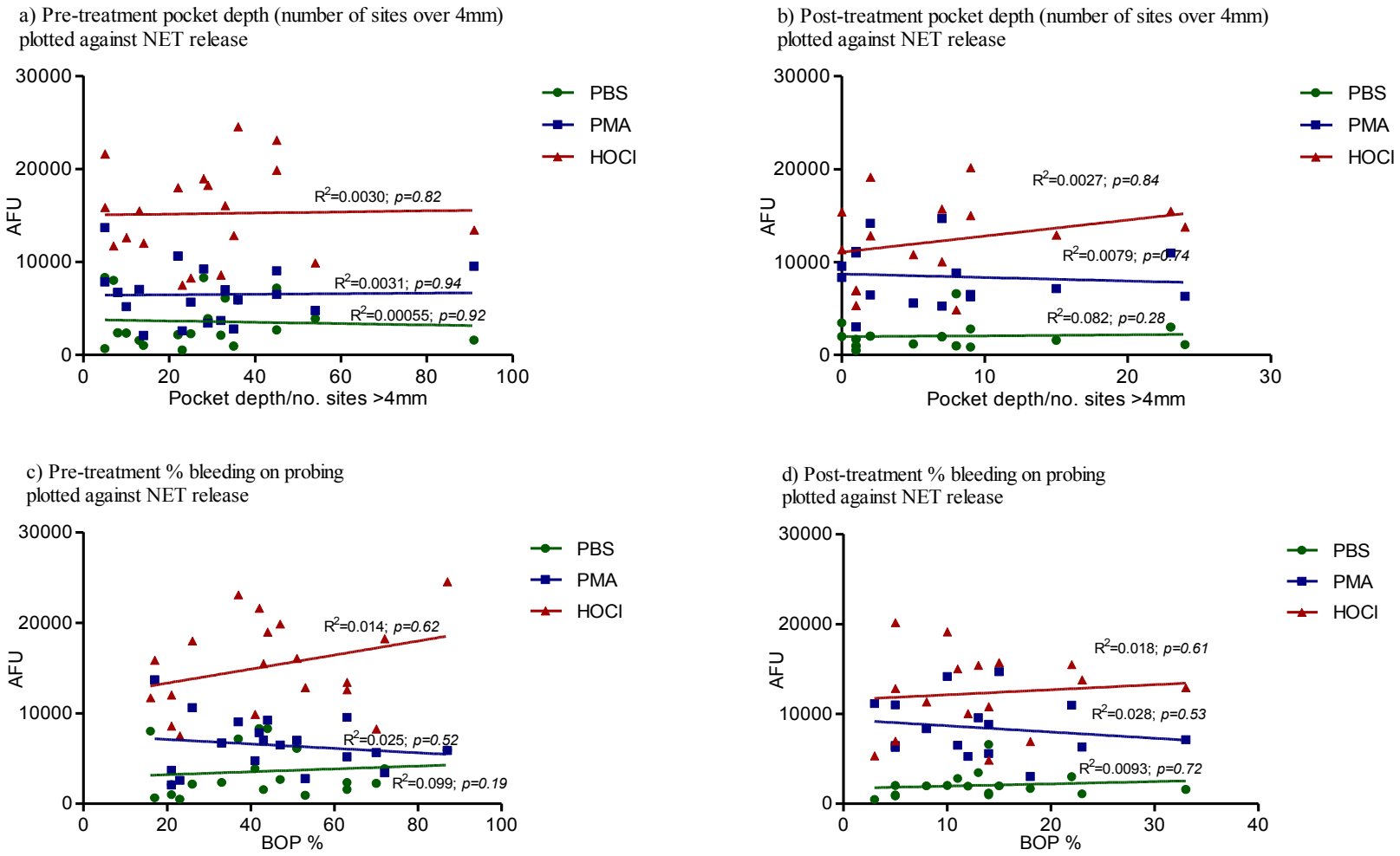

Figure 5.7: Analysis of the association between severity of periodontitis and NET production pre- and post-treatment

Disease severity was plotted against NET production in response to PBS (unstimulated negative control), PMA (50nM) and HOCl (0.75mM). Clinical measures included pocket depth and percentage bleeding on probing (BOP %). There was no significant correlation between pocket depth (number of sites over 4mm) or bleeding on probing and NET production either pre- or post-treatment (linear regression *p>0.05).* Data are presented as AFU (arbitrary fluorescence units) (n=19 in quadruplicate).

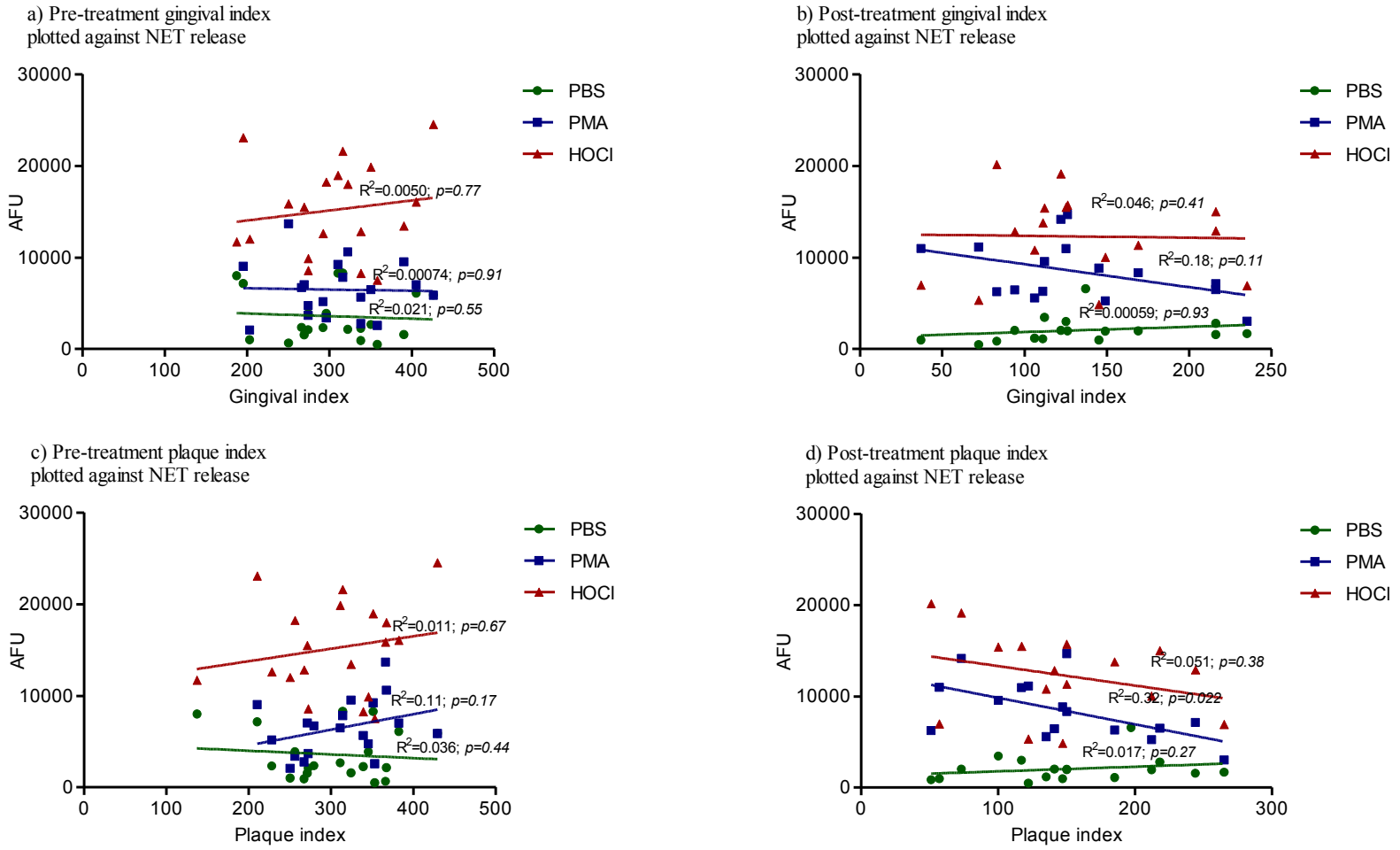

Figure 5.8: Analysis of the association between periodontitis disease severity and NET production pre- and post-treatment

Disease severity was plotted against NET production in response to PBS (unstimulated negative control), PMA (50nM) and HOCl (0.75mM). There was no significant correlation between gingival index and NET production pre- or post-treatment (linear regression *p>0.05).* No significant correlation was observed for plaque index pre-treatment, however a negative correlation was observed between post-treatment PMA-induced NET production and plaque index (linear regression **p=0.022).* Data are presented as AFU (arbitrary fluorescence units) (n=19 in quadruplicate).

5.6 Discussion

Neutrophils play a critical role within the periodontal lesion in response to colonisation by subgingival bacteria in chronic periodontitis patients (Miyasaki 1991, Schenkein 2000). Chronic activation of accumulating neutrophils in the periodontal tissues is thought to induce further tissue damage by releasing their cytotoxic arsenal into the extracellular space (Kantarci *et al.,* 2003). There is also evidence to suggest that peripheral neutrophils in periodontitis patients exhibit hyperactivity (in the absence of an exogenous stimulus) and hyper-reactivity (in response to periodontal bacteria) with regard to ROS production (Matthews *et al.,* 2007a, 2007b). This has been partly attributed to elevated levels of plasma-derived pro-inflammatory cytokines measured in periodontitis patients, such as IL-8 and GM-CSF, which may prime circulating neutrophils (Dias *et al.,* 2011). There is also evidence for constitutively defective redox signalling pathways, which may also contribute to neutrophil hyper-responsiveness in periodontitis (Dias *et al.,* 2013). There is however currently no data exploring whether these abnormalities extend to aberrant NET production in chronic periodontitis patients. In the present study, to account for interpersonal and intrapersonal variability in neutrophilic responses previously described (Harris 2012), neutrophils were isolated from chronic periodontitis patients in parallel with age and gender matched healthy controls. To circumvent the potential observer bias that can arise with NET quantification by microscopy, NET production was quantified by fluorometric detection of a DNA label. Notably qualitative visual characterisation of NET images has also been reported to be susceptible to experimental artefacts and misinterpretation. Indeed Krautgartner *et al.,* (2010) observed that SEM images of NETs were not able to distinguish NET structures from fibrin.

This is the first time NET release has been investigated in peripheral blood neutrophils from periodontitis patients. No differences were found between patients and controls (5.3), a finding consistent with a parallel study performed by collaborators in a Greek cohort (Dimitra

Sakellari, Aristotle University of Thessaloniki - personal communication, unpublished data). The data presented here indicate that the elevated ROS release previously reported in periodontitis patients (Matthews *et al.,* 2007) may not translate to increased NET production, suggesting that NET release may not be solely ROS-dependent and mechanisms that lead to ROS-independent NETosis may exist. This is consistent with reports by Pilsczek *et al.,* (2010), who found that NETs were rapidly produced in response to *S. aureus* in an NADPH-oxidase independent manner. In this study the authors postulated that NADPH-oxidase independent NET production may also arise from vesicular exocytosis, resulting in nuclear envelope destruction and the release of nuclear DNA into the cytoplasm prior to release into the extracellular space. However this has, to date, only been demonstrated for *S. aureus* stimulation and other Gram-positive and -negative bacteria previously studied, as well as stimulation with PMA, did not elicit such responses.

Increases in intracellular calcium are also required for NET release. Parker *et al.,* (2012) reported that whilst NADPH-oxidase assembly was essential for PMA-activated NET release, it was not necessary for the production of NETs by the calcium ionophore, ionomycin. Ionomycin stimulation activates NADPH-oxidase; however inhibition of the oxidative burst with DPI did not attenuate NET release. Furthermore, a recently reported self-protective mechanism within glutathione deficient periodontitis neutrophils involves re-siting of the NADPH-oxidase to membrane-associated lipid rafts. Neutrophils are believed to be endowed with the molecular equipment to direct excess ROS extracellularly, and thus ROS cannot act intracellularly to facilitate elevated NET production (Dias *et al.,* 2013). This could also explain the discordance in ROS and NET production in periodontitis patients reported here. Supporting this premise is that the ROS hyperactivity observed in chronic periodontitis patients' neutrophils is specific to extracellular release, rather than the intracellular ROS that would necessitate NET production (Matthews *et al.,* 2007).

A further explanation for elevated ROS production with no significant increase in NET release may be that if ROS are a prerequisite for NET production, the elevated ROS production associated with neutrophil hyperactivity in chronic periodontitis patients may not be sufficient to trigger the same increases in NET release, or may be antagonised by the intracellular antioxidant repertoire. Findings by Palmer *et al.,* (2012) lend support to this thesis, who reported that concentrations of over 0.5mM of HOCl were needed to trigger NET production. Indeed, Al-Rasheed *et al.,* (2012) reported that levels of peripheral white blood cells (including neutrophils) are significantly higher in periodontitis patients (7.22 ± 1.42 x 10^9 cells/L) compared with healthy controls ($5.64 \pm 1.56 \times 10^9$ cells/L). The current *in vitro* assays utilised neutrophils derived from patients and controls re-suspended at the same concentration; however *in vivo* it is possible that whilst patients may not exhibit hyperactivity or reactivity in terms of NET production, NET responses may be greater due to a leukocytosis.

Data presented here indicate that NET production following successful non-surgical treatment deceased in periodontitis patients (5.3.1). This was more pronounced when the results were expressed as a ratio of patients to control pre- and post-treatment, an analysis designed to control for the day-to-day variability of neutrophil assays. While there are currently no published longitudinal studies looking at the effect of periodontal treatment on peripheral NET production there have, however, been studies quantifying neutrophil ROS production following successful periodontal therapy (Matthews *et al.,* 2007). These studies reported the normalisation of hyper-reactive total ROS production in response to FcγR stimulation post-treatment, however the hyperactive extracellular ROS release measured pre-treatment persisted following treatment. Ling (2015) also demonstrated that hyperactivity and –reactivity with regard to O_2^- production following bacterial stimulation normalised to control levels as a result of successful treatment. Notably, these findings were reported in the

same patients and matched controls employed for the current NET assays, and all assays were conducted on the same day. Whilst there is evidence to suggest NADPH-oxidase independent NETosis can occur, significant decreases in O_2^- production following periodontal treatment may associate with reduced NET release. Interestingly, Remijsen *et al.,* (2011) have demonstrated that superoxide production and autophagy are both required for PMA-induced NET production, but function independently of each other. Superoxide is believed to be the primary ROS capable of stimulating autophagy and it has been suggested that autophagy may provide one of the links to ROS dependence in the decondensation of chromatin during NET formation.

Keshari *et al.,* (2012) has previously demonstrated that cytokines, such as IL-1β and TNFα, can induce NETs. Work by Ling (2015) demonstrated that chronic periodontitis neutrophils are hyper-reactive to stimulation by *F. nucleatum* with regard to the release of IL-1β and TNFα, as well as IL-6 and IL-8. No significant difference in TNFα release was measured between patients and controls following successful treatment. This is consistent with the premise that periodontitis associates with a perturbed neutrophil phenotype, which successful periodontal therapy can partially normalise. Considering that cytokines can impact upon other neutrophilic responses, such as NET release, it is possible that reduced TNFα concomitantly attenuates NET release in chronic periodontitis patients. Notably the other cytokines assayed by Ling (2015), IL-1β IL-6 and IL-8, were not restored to the same level as the controls, but remained hyper-reactive post-treatment. This may be explained by systemic inflammation in periodontitis patients remaining higher than in unaffected controls, or may also relate to a constitutive component to neutrophil hyper-reactivity in periodontitis neutrophils.

In terms of age, pre-treatment results demonstrated NET production was lower in those over 50 years of age (published in Hazeldine *et al.,* 2014) (5.4). This was most pronounced in healthy individuals, with NET production being significantly lower in response to stimulation by PBS, PMA and HOCl. By contrast, patients over 50 years of age only produced significantly fewer NETs in response to HOCl. It has previously been reported that ROS production by TNFα primed neutrophils in response to IL-8 and LPS stimulation significantly decreases with age, which may cause a decline in NADPH-oxidase dependent NET release and provide a mechanistic explanation for the results observed (Hazeldine *et al.,* 2014, Fulop *et al.,* 2004). It is possible that these results occur in those over 50 years due to an aberrant response to TNFα priming or IL-8 and LPS stimulation. However, the activation and phosphorylation of a signalling molecule downstream of TNFα, p38 mitogen-activated protein kinases (MAPK), did not exhibit age-related changes (Hazeldine *et al.,* 2014, Tortorella *et al.,* 2004). The expression of the IL-8 receptors (CXCR1 and CXCR2) and LPS receptors (TLR4) has also been reported to be comparable between old and young individuals (Fulop *et al.,* 2004). Thus it is postulated that age-related reductions in NET production may be associated with receptor signalling, rather than receptor expression.

Differences in age-associated NET production were not observed in patients or controls post-treatment (5.4). It is possible that the declines in NET production in periodontitis patients post-treatment affected the data when analysed in terms of age, however this would not explain the loss of age-related differences in NET production by healthy controls. Whilst the study aimed to control for as many variables as possible, such as blood being collected immediately prior to isolation to minimise the inadvertent activation of neutrophils, it is likely that day-to-day variation in neutrophilic responses arise as a result of other variables. For example, food consumed prior to donating blood may affect NADPH-oxidase dependent NET release as dietary glucose has been suggested to cause exaggerated NADPH oxidase

activity (Chapple 2009). A further limitation of this analysis is that stratification for age reduced volunteer numbers and may have resulted in an under powering of the study for sub analysis.

NET production by patients was not strongly correlated with the clinical parameters of periodontitis, namely pocket depth, bleeding on probing, gingival index and plaque index (5.5). This is not entirely unexpected given that chronic periodontitis was not found to associate with aberrant NET release. However, following successful treatment, a decreased plaque index was significantly correlated with reduced NET release in response to PMA; however no correlations were observed between the other more physiologically relevant stimuli and clinical measures. Plaque index decreased in patients as a result of treatment and it is therefore possible that plaque dysbiosis plays a key role in altering peripheral neutrophil function, as colonising bacteria and their virulence factors can disseminate into the systemic circulation (Li *et al.,* 2000). Wahaidi *et al.,* (2009) demonstrated that plaque accumulation is associated with neutrophil total ROS hyper-reactivity in response to fMLP. Significant reductions in plaque following treatment may therefore represent a possible mechanism that contributes to abrogated NADPH-oxidase dependent NET production in patients; however a study with a larger patient cohort and multiple time points would be required to establish this.

In conclusion, this is the first study to quantify peripheral NET release in periodontitis, and no differences were observed in NET production between chronic periodontitis patients and healthy controls; a finding consistent with a parallel study in a Greek cohort. However, as a result of successful treatment, NET production significantly decreased in patients, which may be a result of decreases in O_2^- production following periodontal treatment. Age was found to associate with decreased NET release; however this was independent of periodontal health status suggesting that decreased peripheral NET production does not predispose individuals

to periodontitis. Furthermore, whilst post-treatment plaque deposits were negatively correlated with peripheral NET release; no other clinical measures of periodontitis were associated with alterations in NET production. Overall, the data presented here indicates that the neutrophil hyperactivity and hyper-reactivity previously reported in periodontitis patients may not translate to peripheral NET production; however it would be interesting to quantify peripheral and localised NET release in response to periodontally relevant bacteria in chronic periodontitis patients.

CHAPTER 6: NET DEGRADATION AND ITS POTENTIAL EFFECTS ON NEUTROPHIL RESPONSES AND THE ORAL EPITHELIUM

6.1 Introduction

This chapter outlines preliminary experiments aimed at investigating the production and degradation of NET structures *in vitro*, followed by the quantification of NET degradation in chronic periodontitis patients and healthy matched controls (2.2.5.1). Plasma levels of cystatin C, IgG (1-4 subclasses) and FLCs were also determined in patients and orally healthy controls as possible contributing factors for altered NET degradation in chronic periodontitis (undertaken by The Binding Site Group Ltd, Birmingham, UK, section 2.2.5.2, Appendix V). The potential effects of delayed or ineffective NET degradation was investigated by evaluating the impact of NET supernatants (2.2.5.3) on neutrophil responses, including ROS production (2.2.3.2), further NET production (2.2.3.3) and the ability of NETs to function as chemoattractants (2.2.4.2.3). The effect of NETs on H400 oral epithelial cell growth was also determined by incubating NET supernatants with H400 oral epithelial cells and quantifying apoptotic activity, metabolic activity and cell membrane integrity.

6.2 NET degradation over 24 hours

To determine the duration of NET stability *in vitro,* NETs were quantified over a 24-hour period with and without MNase degradation. At each time point there was a significant difference between the number of NETs quantified following MNase digestion and the addition of PBS (negative control) (2way ANOVA and Bonferroni post-tests ****$p<0.0001$ at 1, 2 and 3 hours, n=3). However this difference between MNase digestion and the negative PBS control was reduced at 12 and 24 hours (2way ANOVA and Bonferroni post-tests ***$p<0.001$, n=3), due to a noticeable increase in the number of NETs quantified following PBS treatment (negative control), suggesting NETs are less stable after 12 hours of incubation (Figure 6.1).

6.2.1 NET degradation with plasma

NETs were incubated with different concentrations of plasma (from a periodontally and sytemically healthy individual) for 3 hours. Percentage NET degradation was calculated based on a 1U/ml Mnase digestion for 15 mins which represented 100% degradation (Hakkim *et al.,* 2010). Minimal difference in NET degradation was observed following the addition of between 50% and 5% plasma, however below 5% plasma supplementation there was a noticeable concentration dependent decrease in NET degradation (Figure 6.2).

6.2.2 NET degradation with plasma over 24 hours

To assess the incubation period necessary for plasma (from a healthy individual) to degrade NETs, NETs were incubated with 10% plasma (Hakkim *et al.,* 2010) or PBS (negative control) and quantified at selected time points over 24 hours. NET degradation increased up to 12 hours, and subsequently levels plateaued. Similarly to MNase experiments (section 6.2), there was a significant difference between the number of NETs quantified following plasma digestion and the addition of PBS (negative control). This was statistically significant

at 2, 3, 12 and 24 hours (2way ANOVA and Bonferroni post-tests (*$p<0.05$, ***$p<0.001$, ****$p<0.0001$, n=3). However once again the number of NETs quantified following a PBS incubation increased at the 12 and 24-hours time-points (Figure 6.3).

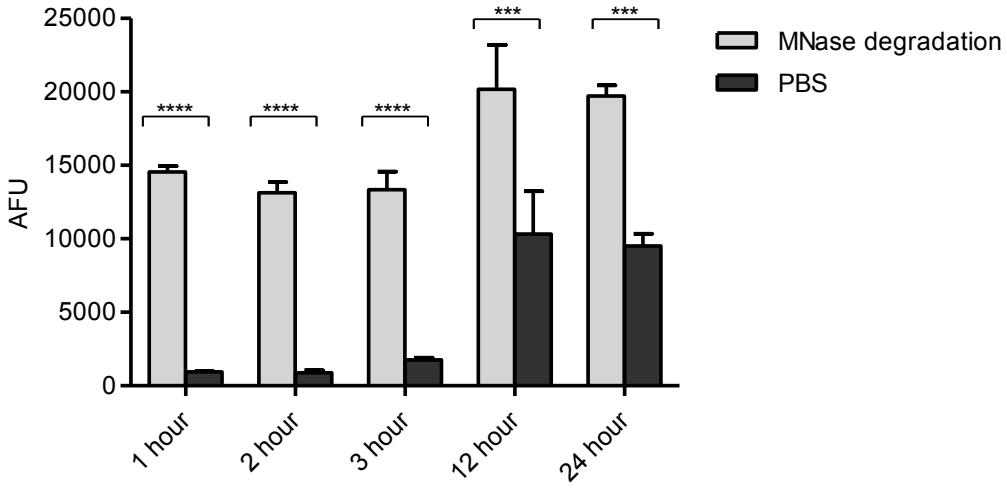

Figure 6.1: NET degradation over 24 hours
Neutrophils were stimulated to produce NETs (0.75mM HOCl) and NET-DNA quantified at different time points (Sytox green) following an MNase digestion (1U/ml) or following a no digestion control (PBS). A significantly higher number of NETs were quantified following MNase digestion relative to PBS (2way ANOVA ***$p<0.001$, ****$p<0.0001$). Data is presented as AFU (arbitrary fluorescence units) and expressed as mean ± SEM (n=3 in triplicate).

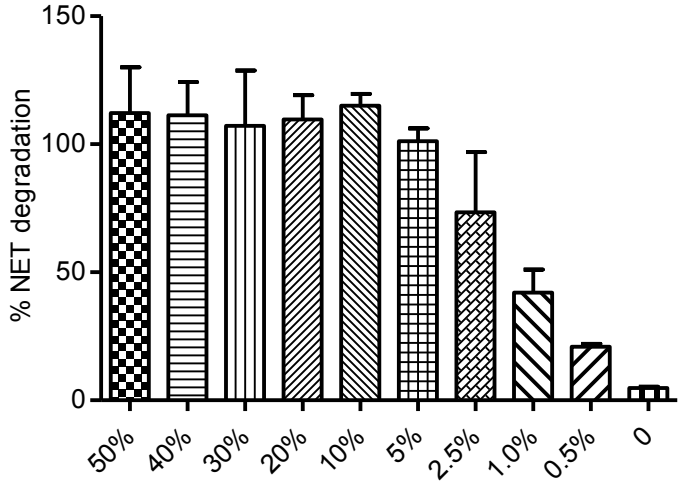

Figure 6.2: NET degradation with plasma
Neutrophils were stimulated to produce NETs (0.75mM HOCl) and NETs were subsequently incubated with different percentage concentrations of plasma for 3 hours and quantified (Sytox green). % NET degradation was calculated based on a 1U/ml MNase digest representing 100%. Plasma samples were derived from periodontally healthy individuals. Data expressed as mean ± SEM (n=3 in triplicate).

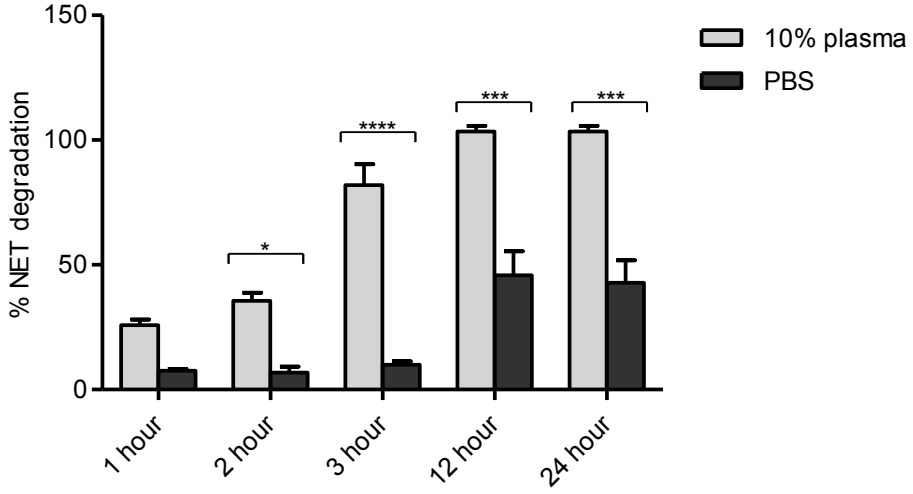

Figure 6.3: NET degradation by plasma over 24 hours
Neutrophils were stimulated to produce NETs (0.75mM HOCl) and subsequently incubated with 10% plasma or PBS (negative control) over 24 hours prior to fluorometric analysis with Sytox green. Statistical significance calculated using 2way ANOVA and Bonferroni post-tests (*$p<0.05$, ***$p<0.001$, ****$p<0.0001$). Data expressed as mean ± SEM (n=3 in triplicate).

6.3 NET degradation by plasma from periodontitis patient's pre- and post-periodontal treatment

Neutrophils were stimulated for NET production using HOCl (0.75mM) and NETs produced were then subjected to a 3 hour 10% plasma incubation. NETs were incubated with plasma derived from periodontitis patients or healthy age/gender matched controls. Following incubation, the numbers of degraded NETs were quantified fluorometrically using Sytox green. The percentage of NETs degraded was calculated in relation to a 15 min MNase digestion, which was used to represent the 100% digestion standard (Hakkim *et al.,* 2010, section 2.2.5.1). In the 19 matched pairs analysed there was a significant difference in NET degradation by patient and control plasma prior to periodontal treatment (unpaired t-test ****$p=0.0001$, n=19), with periodontitis patients degrading significantly fewer NET structures. Patient results also exhibited a larger variance with a range of 77.1 % NET degradation, compared with the control range of 52.5 % NET degradation (Figure 6.4a). Following successful periodontal treatment NET degradation by patients and healthy matched controls was repeated. NET degradation by post-treatment periodontitis patients' plasma was comparable to that of the controls (unpaired t-test $p=0.322$, n=19). However a larger % NET degradation variance was still observed in patients, with a range of 72.0, compared with the control range which was 47.02 (Figure 6.4b).

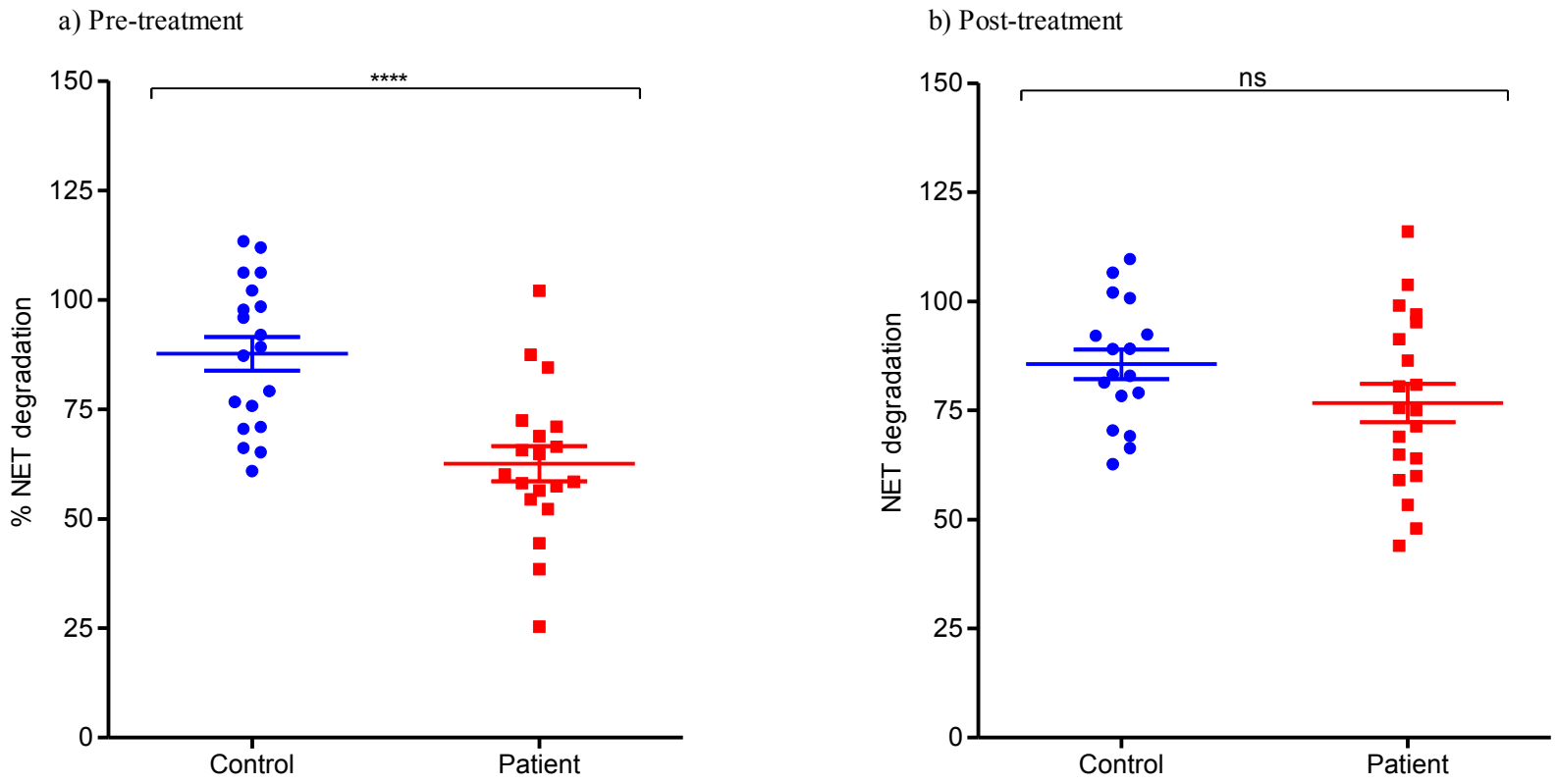

Figure 6.4: NET degradation by plasma from periodontitis patients pre- and post- periodontal treatment

HOCl-stimulated (0.75mM) neutrophils were incubated with 10% plasma from periodontitis patients and healthy age/gender matched controls for 3 hours. NETs were quantified fluorometrically using the Sytox green assay. % NET degradation was calculated based on a 1U/ml MNase 15 minute digestion which was used to represent the 100% standard. (a) A significant difference between patient and control NET degradation was observed pre-treatment (unpaired t-test ****$p=0.0001$), however this difference was absent when the assay was repeated post-treatment (b) (unpaired t-test ns=not significant). Data expressed as mean ± SEM (n=19 matched pairs).

6.3.1 Variability in NET degradation with patient age

Plasma NET degradation from periodontitis patients was analysed to determine whether an age-associated link exists. Percentage NET degradation was calculated based on a 1U/ml MNase degradation representing 100% (Hakkim *et al.,* 2010). NET degradation results for 19 patients were plotted against their corresponding age. No significant correlation was found between NET degradation and age (linear regression $p=0.52$, n=19) (Figure 6.5).

6.3.2 MNase-treated patient plasma

To determine whether the addition of MNase to plasma samples could restore NET degradation in periodontitis patients, 1U/ml MNase-spiked 10% plasma was incubated with NETs for 3 hours. % NET degradation was calculated based on a 1U/ml MNase digest representing 100% degradation. A significant difference was observed between periodontitis plasma and MNase-spiked plasma (unpaired t-test ****$p=0.0001$, n=10). Of the 10 plasma samples treated with 1U/ml MNase, the significant increase in NET degradation was observed in 9 patients. One sample however did not show any considerable increase in NET degradation in the presence of MNase supplementation (Figure 6.6).

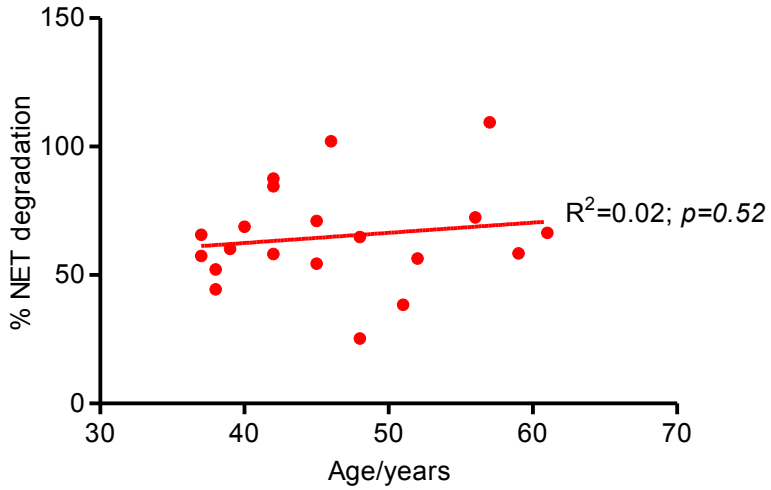

Figure 6.5: NET degradation plotted against patient age
Percentage NET degradation by periodontitis patient plasma was plotted against patient age. % NET degradation was calculated based on a 1U/ml MNase digest which was used to represent the 100% standard. No significant difference was observed between the amount of NET degradation and age. Data expressed ± SEM (n=19 in triplicate).

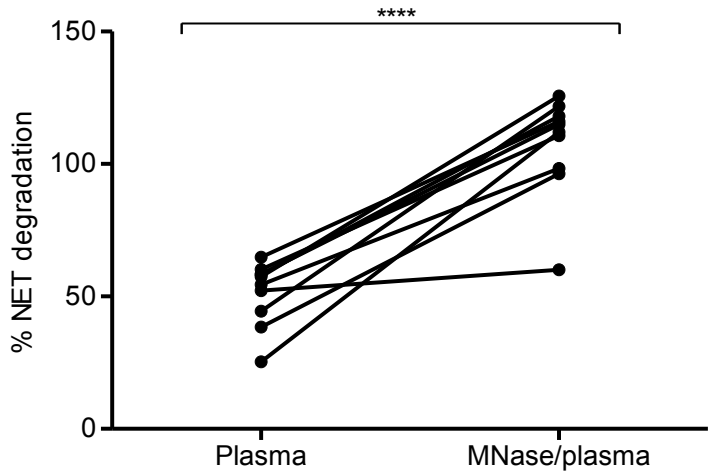

Figure 6.6: MNase-treated patient plasma
NETs incubated with 1U/ml MNase-spiked periodontitis plasma for 3 hours were quantified fluorometrically (Sytox green). % NET degradation was calculated based on a 1U/ml MNase digest, which was used to represent the 100% digestion standard. A significant difference was observed between periodontitis plasma and MNase-spiked plasma (unpaired t-test ****$p=0.0001$) (n=10 plasma samples in triplicate).

Reduced NET degradation in periodontitis patients may be due to elevated circulating antibodies or immunoglobulin free light chains (FLCs), which may provide a physical barrier and prevent NET digestion by DNase (Hakkim *et al.,* 2010). To evaluate this hypothesis, plasma IgG subclasses 1-4 and FLC concentrations were measured in periodontitis patients and age- and gender-matched controls.

6.3.3 Plasma IgG concentrations in periodontitis and controls

IgG subclass 1-4 concentrations were measured in plasma samples from periodontitis patients and healthy matched controls pre- and post- periodontal treatment. Protein turbidimetric analysis demonstrated that patient IgG1 detection was marginally higher than that of the controls pre- and post-treatment, however this was not statistically significant (unpaired t-test *p=0.50, p=0.43* pre- and post-treatment, respectively) (Figure 6.7a). Plasma IgG subclass 2 concentrations in patients were significantly higher than controls (unpaired t-test **p=0.038*). However no significant difference was observed between patient and control plasma IgG2 levels post-treatment (*p=0.11*) (Figure 6.7b). IgG3 plasma levels were significantly higher in patients pre- and post-treatment compared with their matched controls (unpaired t-test ****p=0.0007, **p=0.0042* pre and post-treatment, respectively) (Figure 6.7c). The detection of plasma IgG4 levels in patients and controls demonstrated higher levels in patients, however this was only significant post-treatment (unpaired t-test **p=0.042*) (Figure 6.7d). A small number of sample readings fell outside of the IgG reference ranges (IgG1: 3.824-9.286g/litre, IgG2: 2.418-7.003g/litre, IgG3: 0.218-1.761g/litre, IgG4 0.039-0.864) (Schauer *et al.,* 2003). This appeared to be dependent upon disease status, as whilst 8 control readings were below the reference ranges (3 pre-treatment and 5 post-treatment), this only occurred in 3 periodontitis patient samples (1 pre-treatment and 2 post-treatment). Conversely, no

control readings were above the reference ranges, compared with 9 periodontitis patient samples (5 pre-treatment and 4 post-treatment).

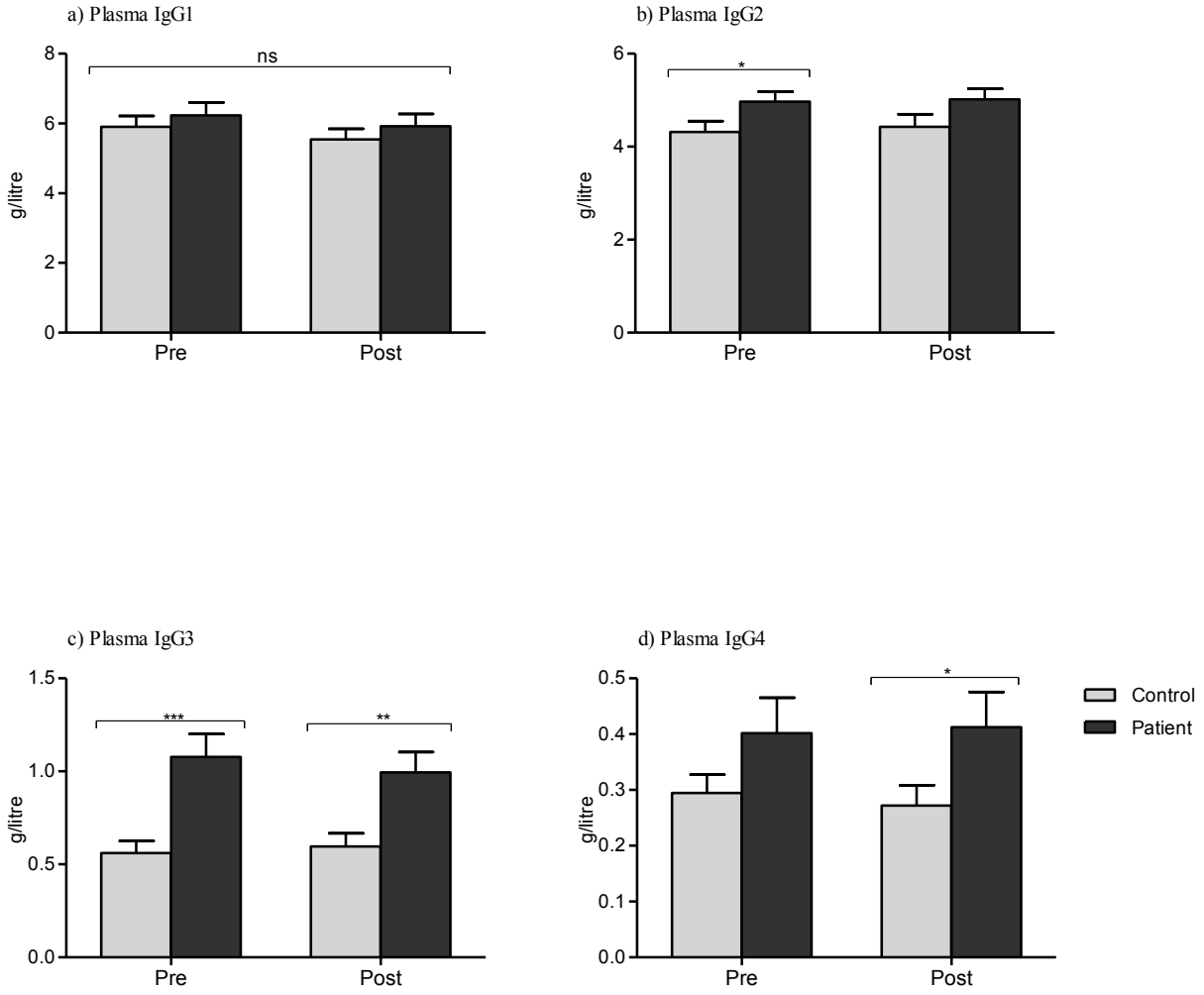

Figure 6.7: Plasma IgG concentrations in periodontitis and controls
IgG subclasses 1-4 concentrations were measured by protein turbidimetric analysis in plasma samples from periodontitis patients and healthy matched controls pre- and post-treatment. Statistical significance was calculated using unpaired t-tests (*$p<0.05$, **$p<0.01$, ***$p<0.001$, ns=not significant). Data expressed as means ± SEM (n=19 matched pairs).

6.3.3.1 Plasma IgG subclasses concentration plotted against NET degradation

Plasma-derived IgG subclass 1-4 measurements (g/litre) were plotted against pre-treatment % NET degradation results for each patient and control (n=19 pairs). No significant correlation by linear regression was observed between IgG subclasses 1-3 and NET degradation (*p=0.52, p=0.60, p=0.37* for IgG1, IgG2 and IgG3, respectively). Notably, a significant negative correlation was observed between IgG4 and NET degradation (**p=0.023*) (Figure 6.8).

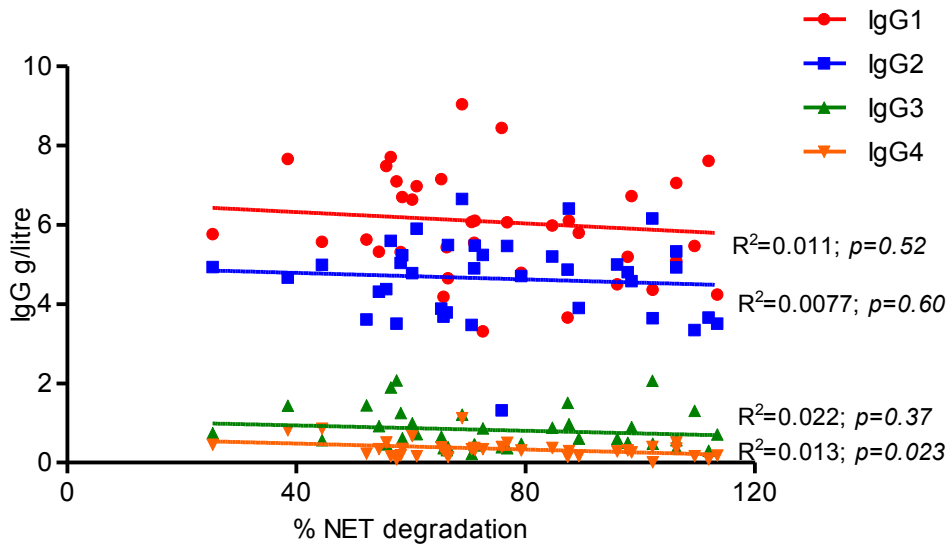

Figure 6.8: Plasma IgG subclasses concentration plotted against NET degradation
Plasma IgG subclasses 1-4 measurements (g/litre) were plotted against pre-treatment % NET degradation results for each patient and matched control. A significant negative correlation was observed between IgG4 concentration and NET degradation (linear regression **p=0.023*) (n=19 matched pairs).

6.3.4 Plasma FLC concentrations in periodontitis and controls

Free kappa and lambda light chains were assayed in plasma samples from periodontitis patients and healthy matched controls pre- and post-treatment. Protein turbidimetric analysis demonstrated that free kappa light chain concentrations were significantly higher in patients than controls, both pre- and post-treatment (unpaired t-test $*p=0.049$, $*p=0.048$ pre- and post-treatment, respectively) (Figure 6.9a). Free lambda light chain concentrations in patient plasma were higher than controls pre- and post-treatment, however this did not reach statistical significance (unpaired t-test $p=0.22$, $p=0.23$ pre- and post-treatment, respectively) (Figure 6.9b). The kappa/lambda ratio demonstrated higher levels in patients pre-treatment (unpaired t-test $*p=0.047$), but not post-treatment ($p=0.66$) (Figure 6.9c). Similar results were observed for summated FLC values, in which patients exhibited significantly higher levels pre-treatment (unpaired t-test $*p=0.032$), however this was not statistically significant post-treatment ($p=0.085$) (Figure 6.9d). A small number of sample readings fell outside of the reference ranges (free kappa light chains: 3.3-19.4mg/litre, free lambda light chains: 5.71-26.3mg/litre, kappa/lambda ratio: 0.26-1.65, summated FLC: 9.01-45.7) (Katzmann *et al.,* 2002). Deviation from the reference range appeared to be dependent on disease state, as whilst 4 control readings were below the reference ranges (1 pre-treatment and 3 post-treatment), this did not occur in any patients. Conversely, 5 control IgG readings were above the reference ranges (2 pre-treatment and 3 post-treatment), compared with 13 patients (6 pre-treatment and 7 post-treatment).

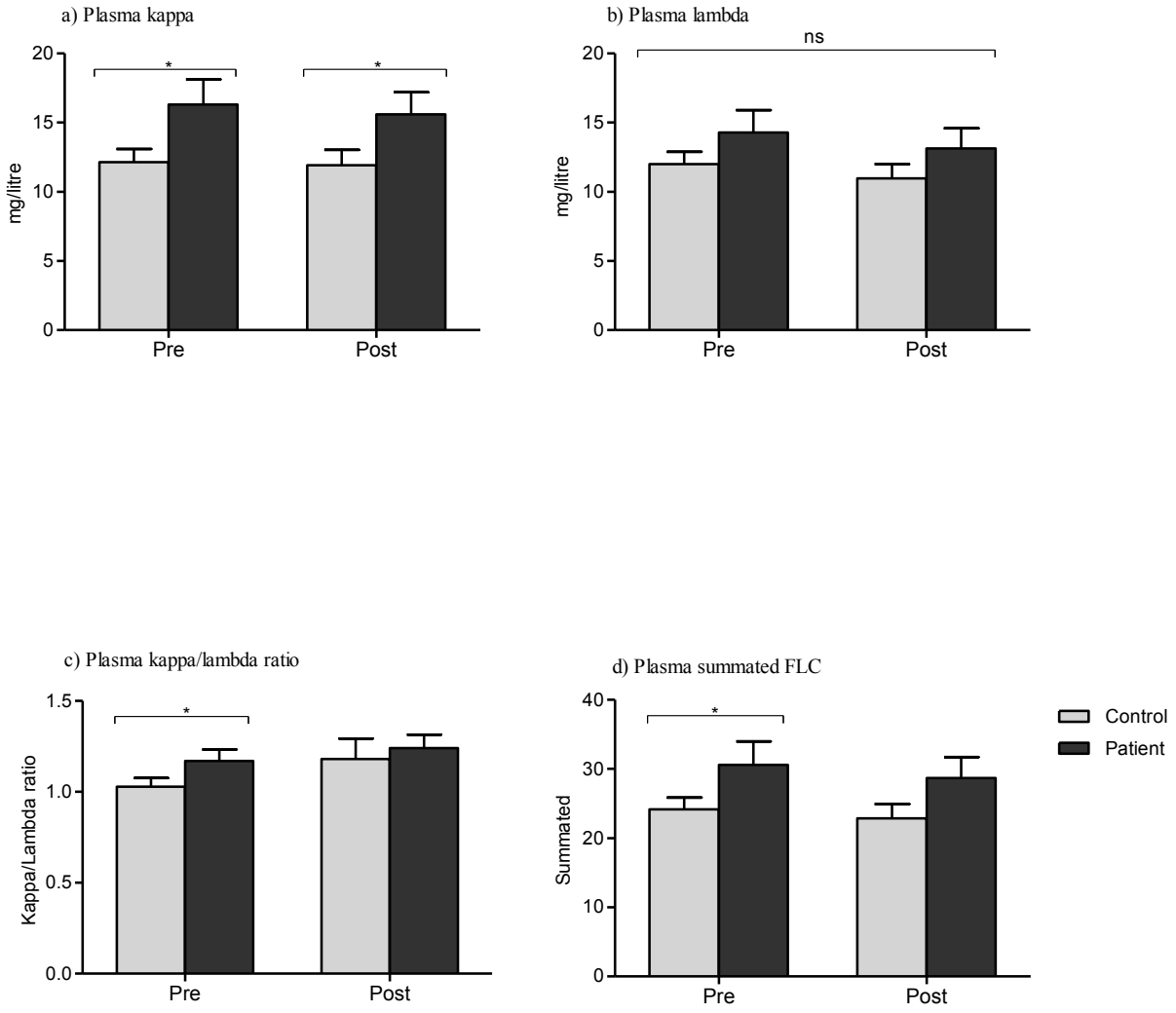

Figure 6.9: Plasma FLC concentrations in periodontitis and controls

Free kappa light chains, free lambda light chains, the kappa/lambda ratio and summated FLCs were measured by protein turbidimetric analysis in plasma samples from periodontitis patients and healthy matched controls pre- and post-treatment. Statistical significance was calculated using unpaired t-tests (*$p<0.05$, ns=not significant). Data expressed as means ± SEM (n=19 matched pairs).

6.3.4.1 Plasma FLC concentration plotted against NET degradation

Plasma-derived free kappa light chains (mg/litre), free lambda light chains (mg/litre), kappa/lambda ratio and summated FLC measurements were plotted against pre-treatment NET degradation data (n=19 pairs). No significant correlation was observed between FLC detection and NET degradation (linear regression *p=0.96, p=0.078, p=087, p=0.57* for free kappa light chains, free lambda light chains, kappa/lambda ratio and summated FLC, respectively) (Figure 6.10).

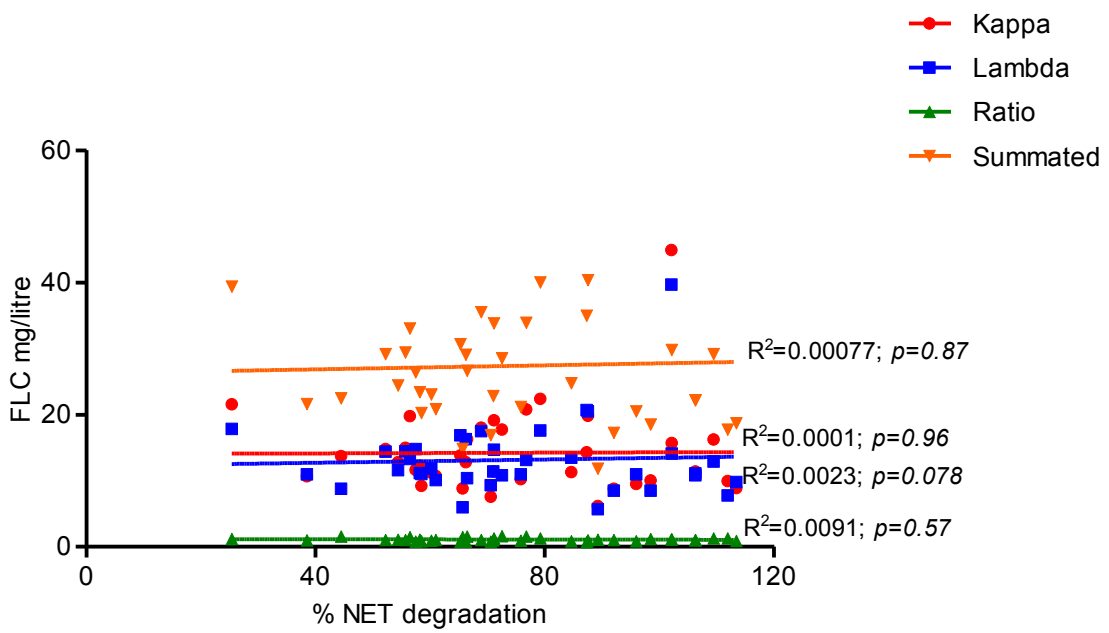

Figure 6.10: Plasma FLC concentration plotted against NET degradation
Plasma-derived free kappa light chains (mg/litre), free lambda light chains (mg/litre), the kappa/lambda ratio and summated FLC measurements were plotted against pre-treatment % NET degradation data for each patient and matched control. No significant correlation was observed between FLCs and NET degradation (linear regression $p>0.05$) (n=19 matched pairs).

Elevated levels of FLC may be the result of excess production by plasma cells, or reduced clearance of FLCs by the kidneys (Randers *et al.,* 2000). To determine whether the increased FLC concentrations measured in periodontitis patients were due to impeded FLC clearance, cystatin C concentrations were measured in plasma samples from periodontitis patients and healthy matched controls as an independent measure of kidney function. Cystatin C is an inhibitor of cysteine proteinases and considered a marker of renal function, where elevated levels of cystatin C are positively correlated with decreased renal function (Randers *et al.,* 2000).

6.3.5 Plasma-derived cystatin C detection in periodontitis

Protein turbidimetric analysis demonstrated there was no significant difference in cystatin C levels (mg/litre) between control and patient plasma samples pre- and post-treatment (unpaired t-test $p=0.74$, $p=0.82$ pre- and post-treatment, respectively, n=19 matched pairs). A small minority of samples were higher than the cystatin C reference range (0.56-0.99mg/litre); however as this encompassed both patients and controls, this did not appear related to periodontal disease status (Figure 6.11).

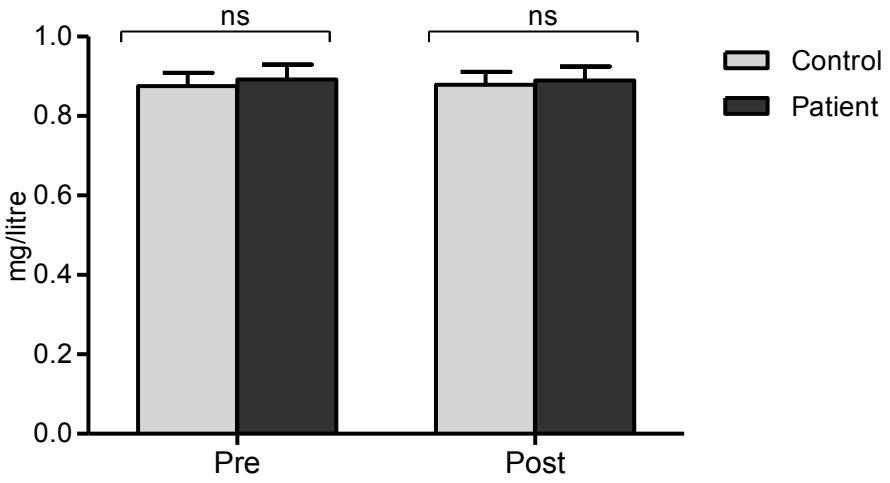

Figure 6.11: Plasma-derived cystatin C detection in periodontitis
Cystatin C detection by protein turbidimetric analysis revealed no significant difference between control and patient plasma samples pre- and post-treatment (unpaired t-test ns=not significant). Data expressed as means ± SEM (n=19 matched pairs).

To evaluate the effect of reduced NET degradation on neutrophil responses and the epithelium, neutrophils from healthy individuals were stimulated to produce NETs (0.75mM HOCl) and the washed NET supernatants collected by MNase digestion (section 2.2.5.3) and stored at -80°C by snap freezing (Appendix VI) until required. NET supernatants were subsequently pooled to determine the effect of NET exposure on the neutrophil responses of ROS and NET production, chemotaxis and their effect on H400 oral epithelial cells.

6.4 Determination of the DNA-content in NET supernatants

NET supernatants were used at concentrations of 25%, 50% and 100% (section 2.2.5.4). To ensure outcomes were as a result of exposure to NET structures and not the HOCl stimulus initially employed to generate the NETs, a HOCl cell-free supernatant was also collected for future assay controls. To determine the concentration of NET supernatants, NET-DNA was quantified in pooled samples (n=10) with Sytox green and compared with a standard curve generated using calf thymus DNA (n=5) to provide interpolated values (Palmer 2010). NET supernatants were applied in a volume of 50µl to investigate whether NETs could stimulate neutrophils to release ROS, release NETs and the effect of NET supernatants on H400 epithelial cells growth. For chemotaxis assays, NET supernatants were used at a volume of 80µl. The concentration of DNA present in the HOCl cell-free control and 25%, 50% and 100% NET supernatant test sample (50µl and 80µl) is presented in table 6.1.

Table 6.1: Determination of the DNA-content in NET supernatants
Pooled NET supernatants DNA content was determined using the Sytox green assay (n=10) and compared with a standard curve generated with calf thymus DNA (n=5) to provide interpolated values. Volumes of 50µl of NET supernatants were employed for ROS, NET and H400 assays, whilst 80µl were required for chemotaxis assays. Data presented as AFU (arbitrary fluorescence units).

NET concentration	AFU reading	DNA (µg/50µl)	DNA (µg/80µl)
HOCl cell free	126	0.0013	0.0021
25%	2734	0.14	0.23
50%	5434	0.30	0.47
100%	10199	0.57	0.96

6.4.1 NET supernatants as a stimulus for ROS production

To determine whether NET supernatants can stimulate peripheral blood neutrophils from a different subject to produce ROS, ROS release in response to treatment with HOCl-induced NET supernatants was quantified with luminol (2.2.3.2). ROS release following PBS (unstimulated negative control) and PMA (25nM) treatment were employed as negative and positive controls, respectively. PMA induced significantly higher ROS production compared with PBS treatment alone (1way ANOVA and Bonferroni post-tests ****$p<0.0001$, n=5). However, NET supernatants at 25%, 50% and 100% did not stimulate neutrophils to release ROS when compared with the PBS control (1way ANOVA $p>0.05$). HOCl cell free supernatants (additional control) did not stimulate neutrophils to release ROS (Figure 6.12a). The time-course of ROS production was also analysed following stimulation with NET supernatants. Neutrophils were stimulated at 30 mins and ROS production quantified for 170 mins after stimulation. Consistent with the peak ROS signal data, time-course ROS production data revealed that PMA induced total ROS production relative to the PBS control. ROS production in response to PMA peaked at ~20 mins post-stimulation, followed by a

steep decline in ROS release. NET supernatants (25%, 50% and 100%) and the HOCl-cell free supernatant control did not stimulate ROS release (Figure 6.12b).

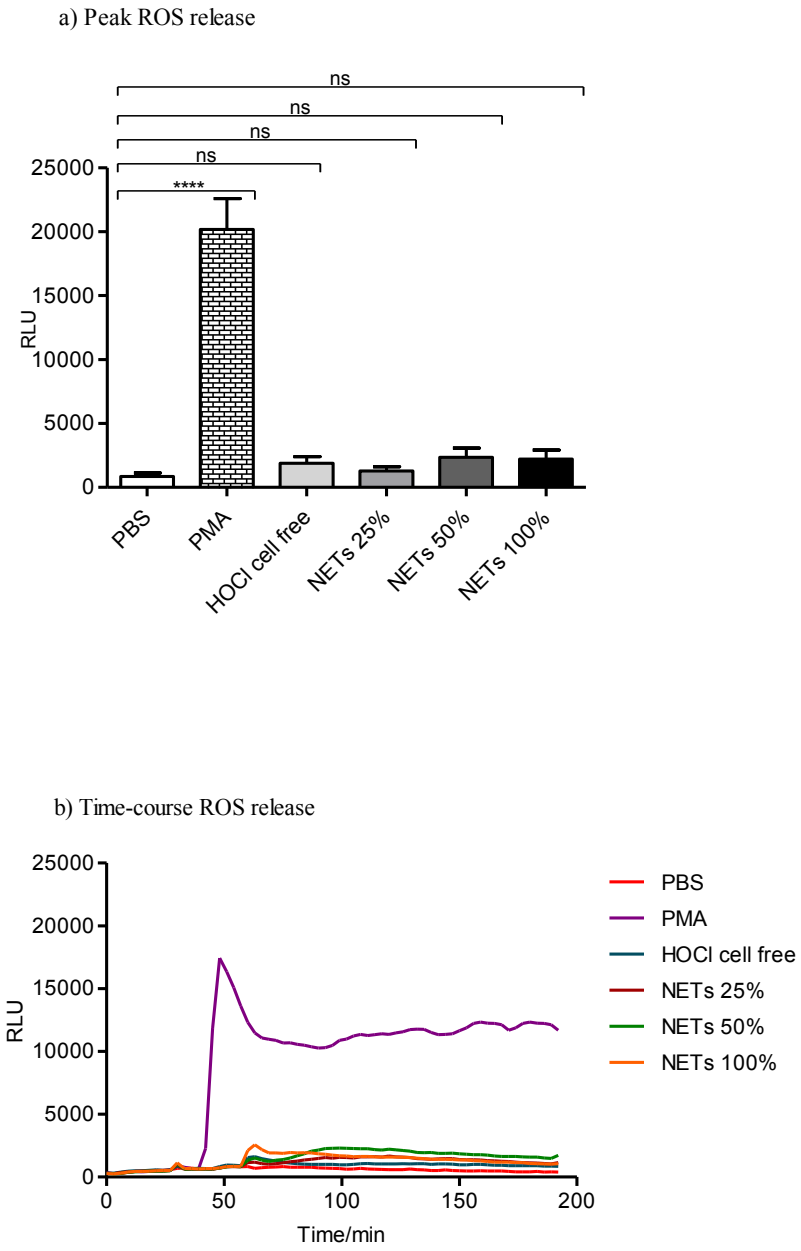

Figure 6.12: NET supernatants as a stimulus for ROS production

(a) Total ROS production was quantified with luminol in response to PBS (unstimulated), PMA (25nM), HOCl cell free supernatant or NET supernatants (25%, 50% and 100%). Statistical significance calculated using 1way ANOVA and Bonferroni post-tests (****$p<0.0001$, ns=not significant). Data is expressed as mean ± SEM. (b) Time course total ROS production over 200 mins by cells stimulated with PBS (unstimulated), PMA (50nM), HOCl cell free supernatant or NET supernatants (25%, 50% and 100%). Data is presented as RLU (relative light units) (n=5 in triplicate).

6.4.2 NET supernatants as a stimulus for NET production

To determine whether NET supernatants can stimulate neutrophils to produce NETs, NET production in response to treatment (4 hours) with HOCl-induced NET supernatants was quantified using the Sytox green assay (2.2.3.3). NET release following PBS (unstimulated) and PMA (50nM) treatment were employed as negative and positive controls, respectively. PMA induced significantly higher NET release compared with PBS treatment (1way ANOVA and Bonferroni post-tests ****$p<0.0001$, n=5). However NET supernatants at 25%, 50% and 100% did not stimulate neutrophils to release NETs, evidenced by no significant increase in NETs relative to the PBS control treatment (1way ANOVA $p>0.05$). HOCl cell free supernatants (additional control) did not stimulate neutrophils to release NETs (Figure 6.13).

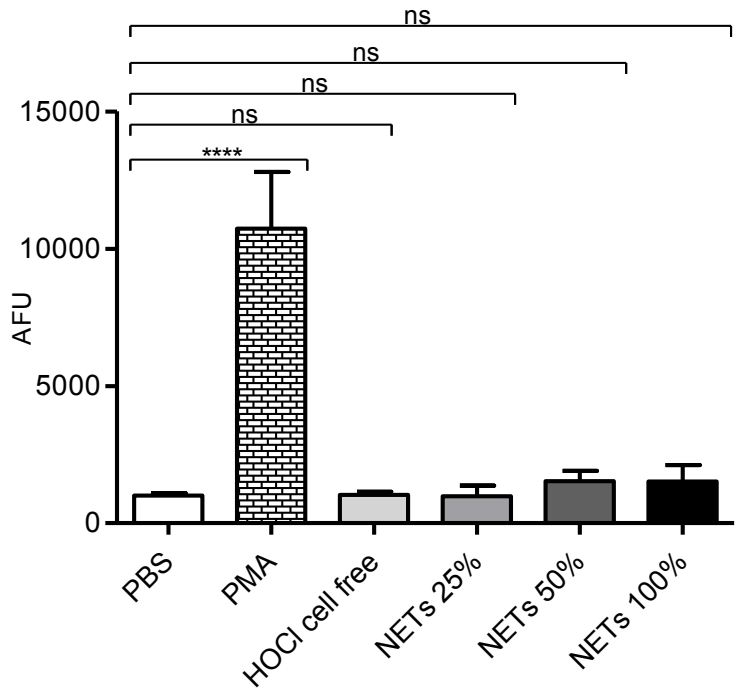

Figure 6.13: NET supernatants as a stimulus for NET production
NET-DNA production was quantified with Sytox green in response to PBS (unstimulated), PMA (50nM), HOCl cell free supernatant or NET supernatants (25%, 50% and 100%). Statistical significance calculated using 1way ANOVA and Bonferroni post-tests (****$p<0.0001$, ns=not significant). Data presented as AFU (arbitrary fluorescence units) and expressed as mean ± SEM (n=5 in triplicate).

6.4.3 The ability of NETs to induce neutrophil chemotaxis

To determine whether NETs serve as chemoattractants and induce the directional migration of neutrophils towards them, NET supernatants were employed as chemoattractants and neutrophil chemotaxis was analysed using the Insall Chamber (2.2.4.2.3). The movement of 15 randomly chosen cells was tracked by video microscopy and the quantitative data generated used to produce spider plots and to calculate neutrophil speed, velocity and resultant vector length (Roberts *et al.,* 2015).

Spider plots enable visualisation of individual cell movement (μm) from a central point, where the top of the Y-axis represents the source of the chemoattractant. Cells displayed directional movement towards the known chemoattractant, fMLP. Neutrophil migration was observed in response to 25% NET supernatants, and to greater extent with 50% and 100% NET supernatants; however this movement did not appear to be towards the chemoattractant source, and lacked directionality (Figure 6.14).

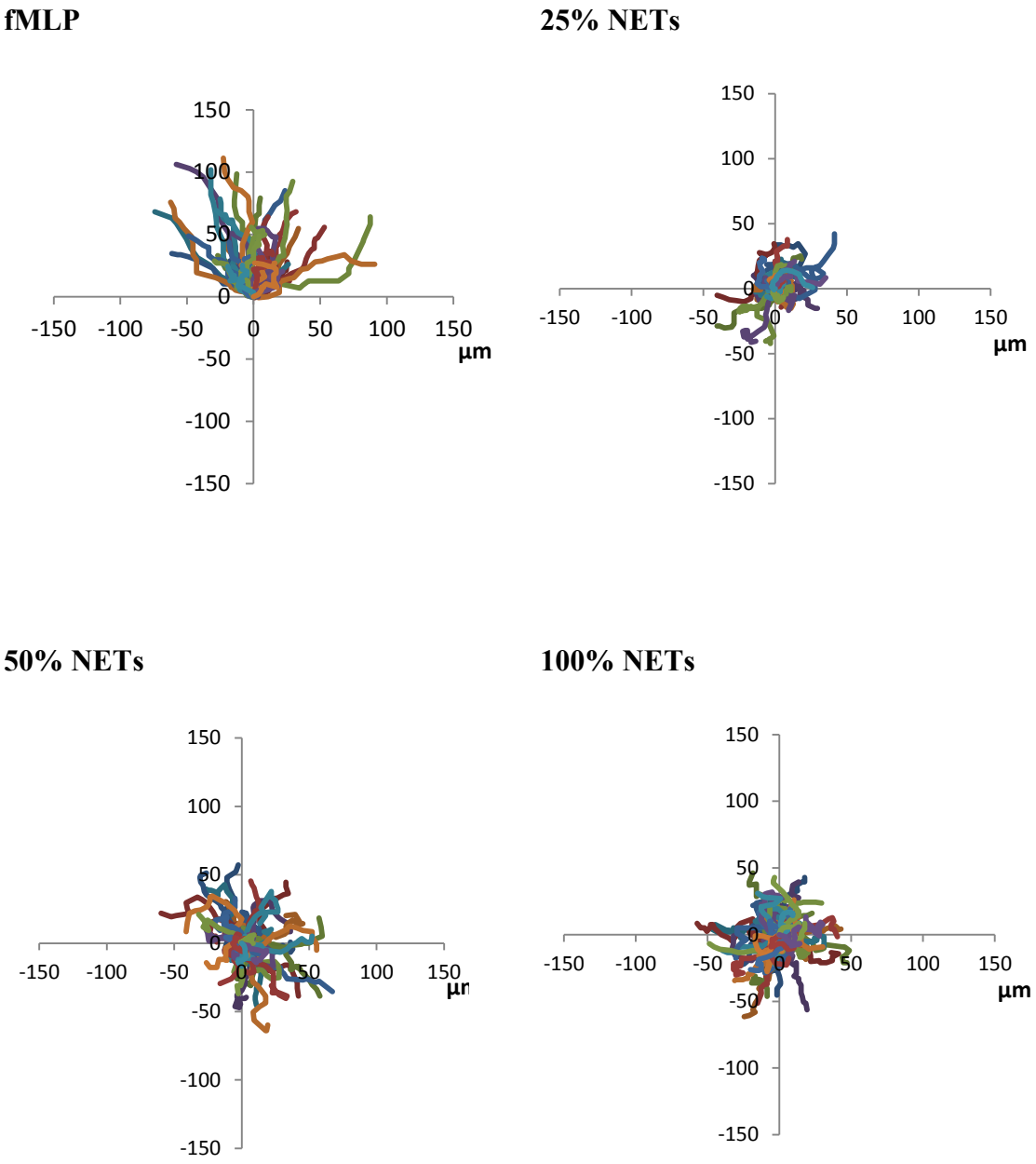

Figure 6.14: Spider plots representing neutrophil migration in response to NET supernatants

Spider plots show the tracking (µm) of individual neutrophils (n=15 cells from n=5 experiments) from a central reference point (0, 0) towards the chemoattractant. The top of the Y-axis represents the source of the chemoattractant. Neutrophil chemotaxis in response to a known chemoattractant, fMLP (100nM), was employed as a positive control. Cell migration was tracked in response to 25%, 50% and 100% NET supernatants.

Whilst spider diagrams represent a relatively novel way to visualise cell migration in response to a chemoattractant, they cannot be used objectively or quantitatively to measure neutrophil movement. Thus, the data generated from tracking 15 individual cells was used to quantify the speed, velocity and directional accuracy of neutrophil migration.

6.4.3.1 Neutrophil speed in response to NET supernatants

Neutrophil speed (μm/min) in response to fMLP (100nM, positive control) was significantly greater than for RPMI (negative control) (1way ANOVA and Bonferroni post-test ****$p<0.0001$, n=5). The speed of neutrophil migration in response to NET supernatants (25%, 50% and 100%) was also significantly higher than RPMI (1way ANOVA and Bonferroni post-test ****$p<0.0001$ for 25%, 50% and 100%, n=5). However, increased neutrophil speed in response to NET supernatants was significantly lower than for fMLP-induced migration (positive control) (1way ANOVA and Bonferroni post-test ****$p<0.0001$ for 25%, 50% and 100%, n=5, statistics not shown on graph). Notably, HOCl cell free supernatants (additional control) did not induce an increase in neutrophil speed (1way ANOVA $p>0.05$) (Figure 6.15).

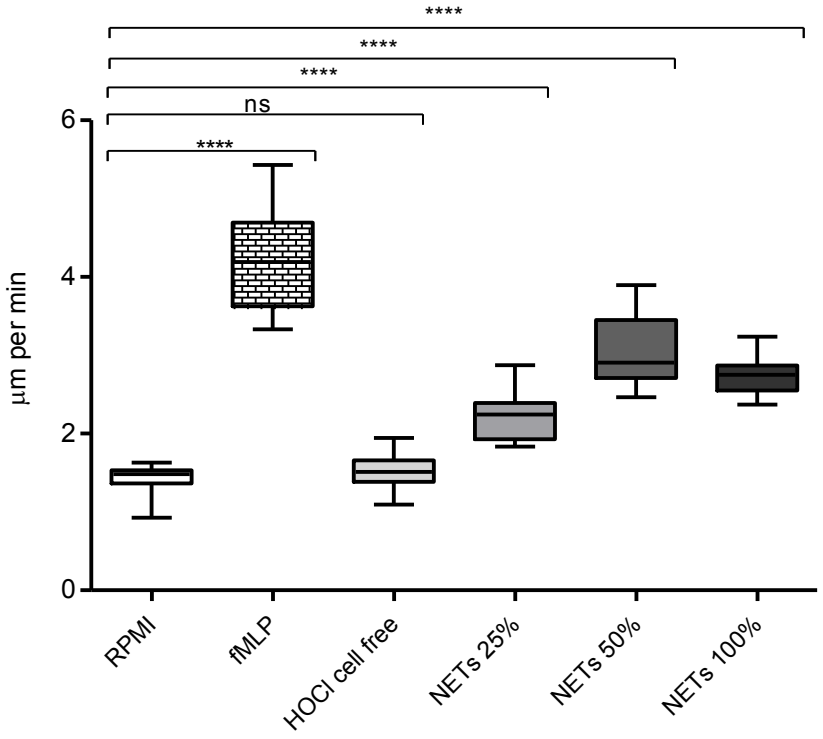

Figure 6.15: Neutrophil speed in response to NET supernatants
Neutrophil chemotactic speed (µm/min) in response to fMLP (100nM, positive control), RPMI (negative control) and different concentrations of NET supernatants was measured. Statistical significance calculated using 1way ANOVA and Bonferroni post-test (****$p<0.0001$, ns=not significant). Data calculated from the tracking of 15 cells and is expressed as mean ± SEM (n=5).

6.4.3.2 Neutrophil velocity in response to NET supernatants

Velocity is the speed of movement in a specific direction towards a chemoattractant. Neutrophil velocity in response to fMLP (100nM, positive control) was significantly higher than for RPMI (negative control) (1way ANOVA and Bonferroni post-test ****$p<0.0001$, n=5). However NET supernatant-induced velocity was not significantly different to (1way ANOVA $p>0.05$) (Figure 6.16).

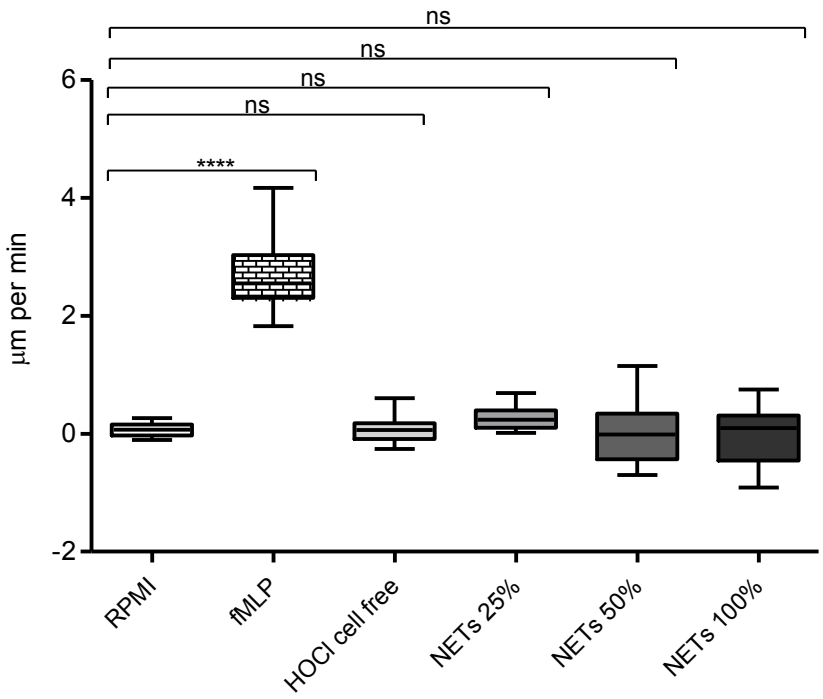

Figure 6.16: Neutrophil velocity in response to NET supernatants
Neutrophil velocity (µm/min) in response to fMLP (100nM, positive control), RPMI (negative control) and different concentrations of NET supernatants was measured. Statistical significance calculated using 1way ANOVA and Bonferroni post-test (****$p<0.0001$, ns=not significant). Data calculated from the tracking of 15 cells and is expressed as mean ± SEM (n=5).

6.4.3.3 Directional accuracy of neutrophil movement (resultant vector length)

Representative angular histograms and resultant vector plots of neutrophil directional chemotaxis in response to fMLP (100nM) or 100% NET supernatants were plotted. The angular histograms measure cell directionality and strength of this movement, which is determined by the histogram bar angle and width, respectively. Angular histograms and resultant vector plots of neutrophil migration in response to fMLP (100nM, positive control) show strong directional accuracy of movement towards the chemoattractant. However neutrophil chemotaxis in response to 100% NET supernatants exhibited movement that was not directionally targeted towards the source of the chemoattractant (90°), evidenced by the cell movement endpoint (blue circles on circle circumference) being in every direction and the shortness of the red line (Figure 6.17).

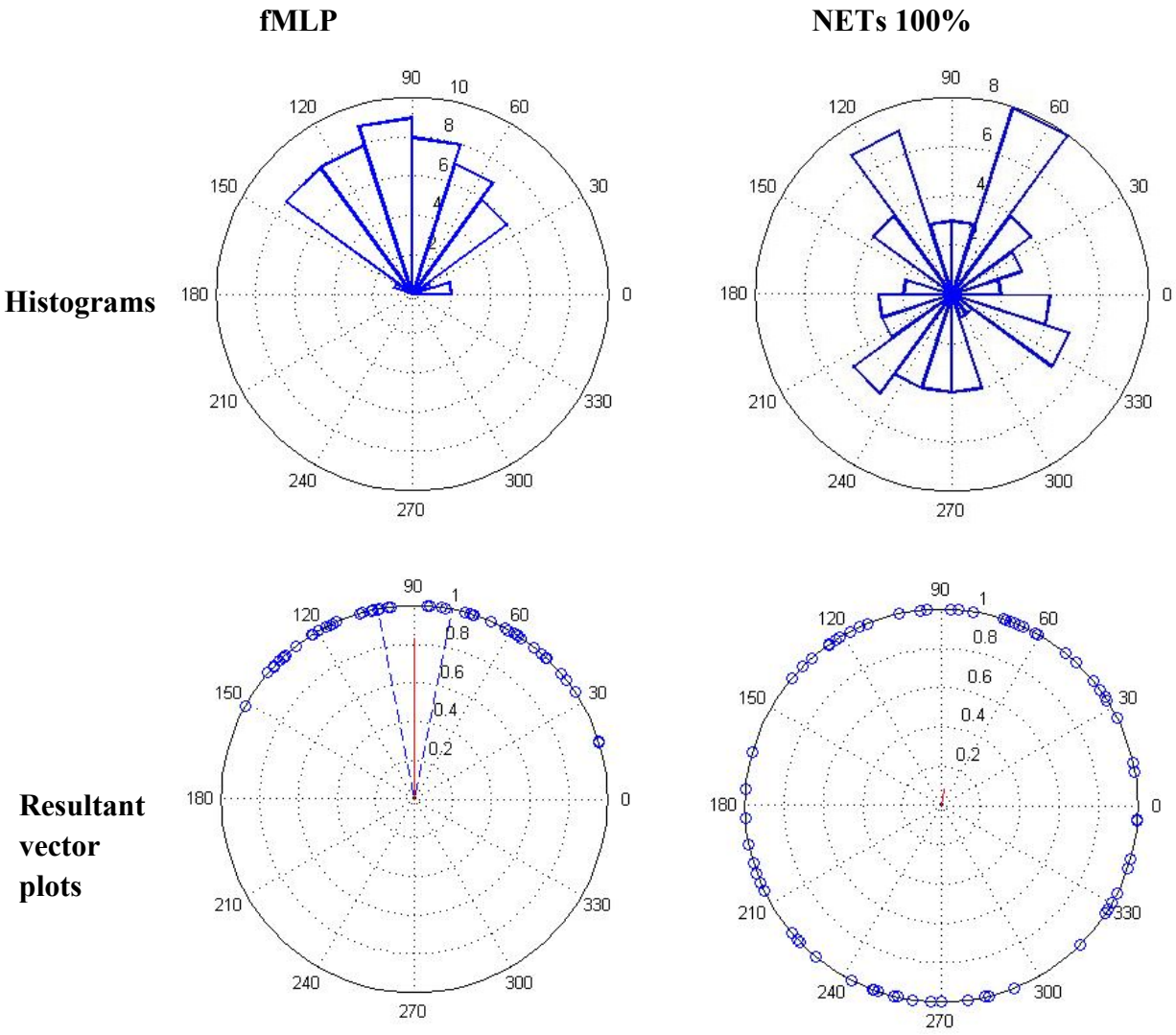

Figure 6.17: Directional accuracy of neutrophil movement (resultant vector length)
Representative angular histograms and resultant vector plots of neutrophils treated with fMLP (100nM) or 100% NET supernatants. The angle and width of the histogram bars indicates the direction and the proportion of cells migrating in that direction, respectively. The resultant vector plots indicate the strength and directionality of the cells in response to the chemoattractant. The red line denotes the mean resultant vector and the dashed line shows the variation (95% confidence intervals) within the entire cohort of cells. The length of the red line is indicative of the strength of cell directionality. The blue circles along the circumference of the plot represent individual neutrophil migration end-points. For both plots, 90° at the top of both plots represents the source of the chemoattractant.

6.4.3.4 Neutrophil resultant vector length

The resultant vector length measures the directional accuracy of neutrophil chemotaxis towards the chemoattractant. Resultant vector length was calculated from the resultant vector plots, in which the red line denotes the mean resultant vector and the dashed line shows the variation (95% confidence intervals) within the entire cohort of cells. The length of the red line is indicative of the strength of cell directionality. Resultant vector length in response to fMLP (100nM, positive control) was found to be significantly higher than neutrophil migration when RPMI (negative control) was employed as a chemoattractant (1way ANOVA and Bonferroni post-test ***$p<0.001$, n=5). However NET supernatant-induced chemotaxis did not cause a significant increase in neutrophil directional movement, compared with the RPMI control (1way ANOVA $p>0.05$) (Figure 6.18).

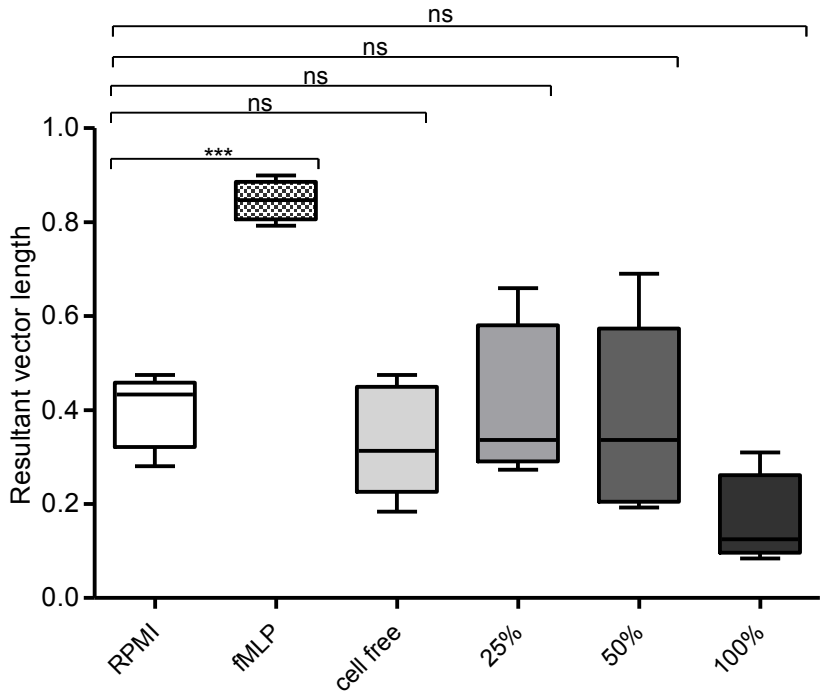

Figure 6.18: Neutrophil resultant vector length

Resultant vector length of neutrophil chemotaxis in response to fMLP (100nM, positive control), RPMI (negative control) and different concentrations of NET supernatants was measured. Statistical significance calculated using 1way ANOVA and Bonferroni post-test (****p<0.001*, ns=not significant). Data calculated from the tracking of 15 cells and is expressed as mean ± SEM (n=5).

6.5 The effect of NETs on H400 oral epithelial cell responses

To evaluate the effect of reduced NET degradation on the activity and viability of oral epithelial cells, H400s were cultured in a 96-well plate (until 90% confluent) and incubated with NET supernatants (25%, 50% and 100%). At 4 and 24 hours, the impact of NET supernatants on H400 oral epithelial cell growth was determined by quantifying caspase activity (apoptosis), ATP activity (metabolic activity) and LDH release (cytotoxicity). HOCl cell free supernatants were employed as a control, RPMI and 0.1% triton were used as negative and positive treatment controls, respectively.

6.5.1 The effect of NETs on H400 oral epithelial cell apoptosis

To investigate whether NET supernatants induce apoptosis in H400 oral epithelial cells, caspase-3 and 7 production by H400s (90% confluent) was measured at 4 and 24 hours (2.2.1.2.4). Treatment with triton (0.1%, positive control) caused a decrease in caspase activity at 4 and 24 hours, relative to the RPMI negative control, however this was not statistically significant (1way ANOVA $p>0.05$, n=5). Caspase activity in response to RPMI (negative control), HOCl cell free supernatants and NET supernatants (25%, 50% and 100%) was higher at 24 hours than 4 hours. A concentration dependent decrease in caspase-3 and 7 production was observed at 24 hours following treatment with 25%, 50% and 100% NET supernatants, however this was not statistically significant (1way ANOVA $p>0.05$, n=5) (Figure 6.19).

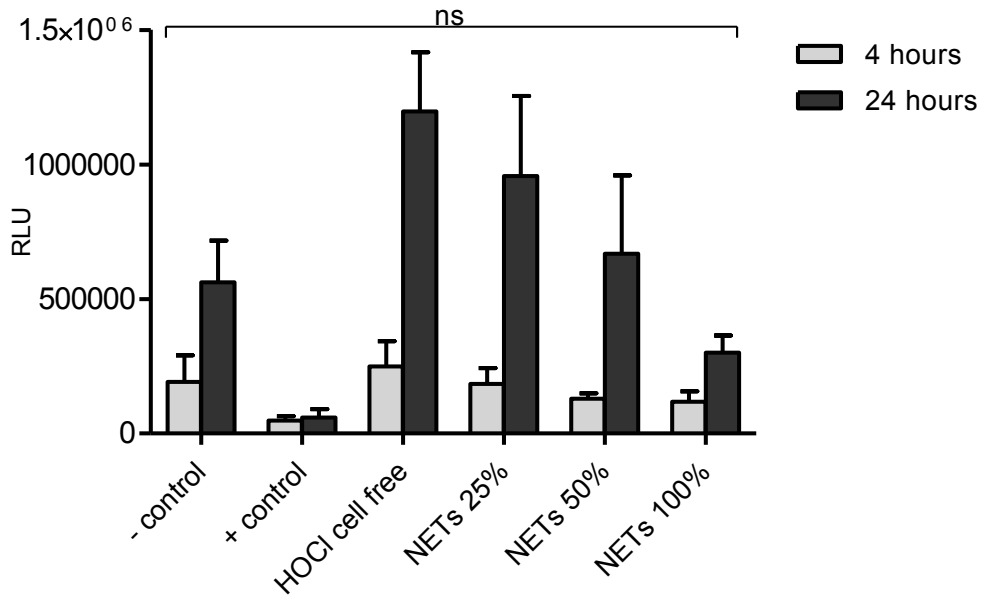

Figure 6.19: The effect of NETs on H400 oral epithelial cell caspase activity
Apoptotic activity in H400 oral epithelial cells was determined by measuring caspase-3 and -7 activity at 4 and 24 hours in response to RPMI (negative control), 0.1% triton (positive control), HOCl cell free supernatants (additional control) and NET supernatants (25%, 50% and 100%). Statistical significance calculated using 1way ANOVA (ns=not significant). Data expressed as RLU (relative light units) and mean ± SEM (n=5 in triplicate).

6.5.2 The effect of NETs on H400 oral epithelial cell metabolic activity

To investigate the metabolic activity of H400 oral epithelial cells in response to NET supernatants, ATP production by H400s (90% confluent) was measured at 4 and 24 hours (2.2.1.2.5). Treatment with triton (0.1%, positive control) caused a significant decrease in metabolic activity at 4 and 24 hours, relative to the RPMI negative control (1way ANOVA and Bonferroni post-tests $^{**}p<0.01$, $^{***}p<0.001$ at 4 and 24 hours, respectively, n=5). Metabolic activity in response to RPMI (negative control), HOCl cell free supernatants and NET supernatants (25%, 50% and 100%) was higher at 24 hours, relative to 4 hours. A concentration dependent decrease in ATP production was observed at 24 hours following treatment with 25%, 50% and 100% NET supernatants, however this was not statistically significant (1way ANOVA $p>0.05$, n=5) (Figure 6.20).

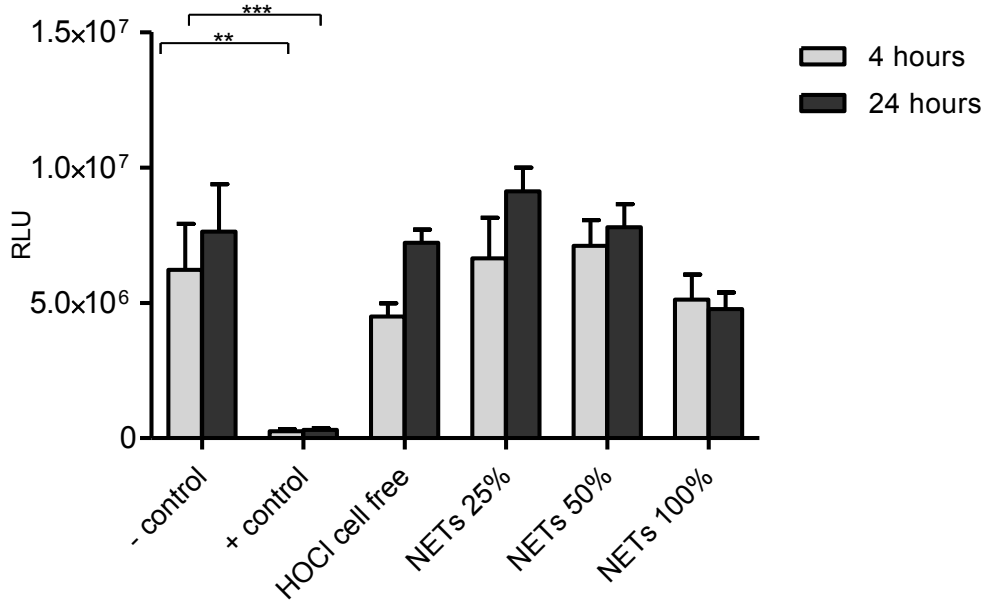

Figure 6.20: The effect of NETs on H400 oral epithelial cell metabolic activity
Metabolic activity of H400 oral epithelial cells was determined by measuring ATP release at 4 and 24 hours in response to RPMI (negative control), 0.1% triton (positive control), HOCl cell free supernatants (additional control) and NET supernatants (25%, 50% and 100%). Statistical significance calculated using 1way ANOVA and Bonferroni post-test (***p<0.01*, ****p<0.001*). Data expressed as RLU (relative light units) and mean ± SEM (n=5 in triplicate).

6.5.3 The effect of NETs on H400 oral epithelial cell lactate dehydrogenase release

To investigate whether NETs induce cytotoxicity in H400 oral epithelial cells, lactate dehydrogenase (LDH) was measured at 4 and 24 hours (2.2.5.7). LDH is released by damaged membranes, therefore an increase in LDH, and thus an increase in AFU, is associated with reduced membrane integrity. Treatment with triton (0.1%, positive control) caused a significant increase in LDH release at 4 and 24 hours, relative to the RPMI negative control (1way ANOVA and Bonferroni post-tests ****$p<0.0001$ at 4 and 24 hours, n=5). LDH release in response to RPMI (negative control), HOCl cell free supernatants and NET supernatants (25%, 50% and 100%) was higher at 24 hours, relative to 4 hours. Despite a noticeable increase in LDH release at 24 hours following treatment with 100% NET supernatants, this was not statistically significant. There was no significant increase in LDH release as a result of treatment with HOCl free supernatants or NET supernatants (25% and 50%) (1way ANOVA $p>0.05$, n=5) (Figure 6.21).

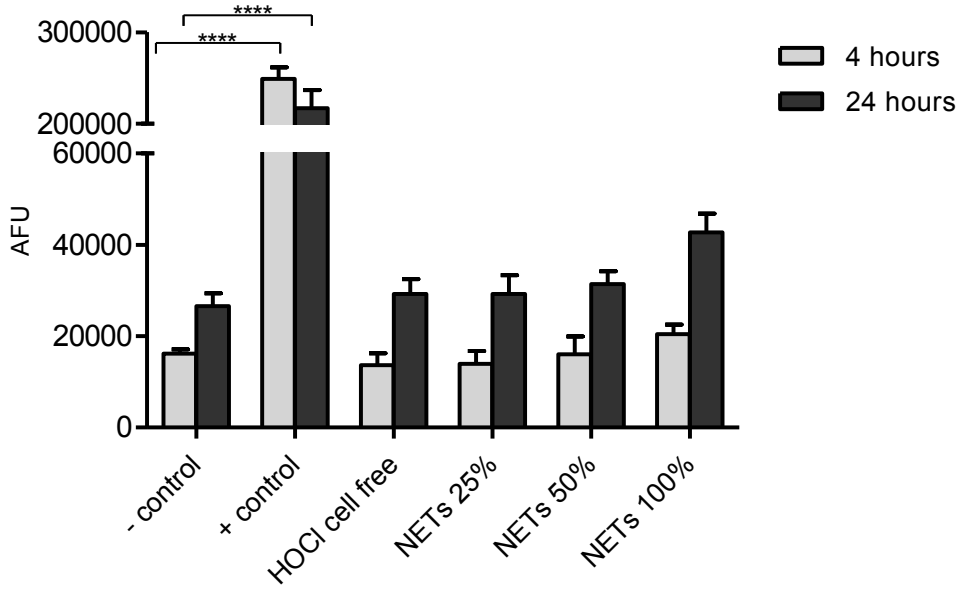

Figure 6.21: The effect of NETs on H400 oral epithelial cell lactate dehydrogenase release

LDH released into the media was quantified at 4 and 24 hours in response to RPMI (negative control), 0.1% triton (positive control), HOCl cell free supernatants (additional control) and NET supernatants (25%, 50% and 100%). Statistical significance calculated using 1way ANOVA and Bonferroni post-test (****$p<0.0001$). Data expressed as AFU (arbitrary fluorescence units) and mean ± SEM (n=5 in triplicate).

6.6 Discussion

Plasma-derived NET degradation was significantly lower in chronic periodontitis patients pre-treatment relative to periodontally healthy matched controls (section 6.3). This is the first report evaluating NET degradation in periodontitis, however the removal of NETs has been well characterised in other diseases such as systemic lupus erythematosus (SLE) patients, in which NET clearance by sera was reportedly impeded in a subset of patients (Hakkim *et al.,* 2010, Leffler *et al.,* 2012). The mechanisms involved in the removal of NETs remain to be thoroughly elucidated; however reports indicate that degradation of the DNA backbone by DNase 1 initiates their removal, followed by the engulfment of degraded structures by macrophages and further degradation in the lysosome. Key to this process is NET clearance resembles a mechanism similar to that of apoptosis, whereby macrophages behave non-phlogistic, do not release pro-inflammatory cytokines and thus NET disassembly is regarded as an "immunologically silent" process (Farrera & Fadeel 2013). Possible reported explanations for attenuated NET degradation in SLE patients include the presence of DNase1 inhibitors preventing the enzymatic removal of the NETs (Yeh *et al.,* 2003), or alternatively higher antibody titers in patients' plasma, which may provide a physical barrier to NET removal by binding to NETs and blocking the DNase cleavage sites (Hakkim *et al.,* 2010, Leffler *et al.,* 2012). Notably contradictory findings are reported regarding the effect of supplementing patient sera with DNase to restore NET degradation in all "low-degrading" patients (Hakkim *et al.,* 2010, Leffler *et al.,* 2012). In the periodontitis cohort studied here, 9 out of 10 patients displayed restored NET degradation following the addition of MNase (section 6.3.2), suggesting that if enzymatic inhibitors are present, they may be DNase specific. Following non-surgical treatment, NET degradation in periodontitis patients was restored and no significant difference was detected between patients and controls. This is consistent with reports by Leffler *et al.,* (2012), who demonstrated that NET degradation was

improved when SLE patients were in remission, relative to during a disease flare. Notably, as with the SLE cohort, reduced NET degradation was a variable phenomenon and only observed in a subset of periodontitis patients; this could be linked to disease susceptibility, disease severity, disease activity status or bacterial load and virulence factors (such as bacteria-derived DNases).

To establish whether a physical barrier, such as circulating antibodies or immunoglobulin free light chains (FLC), may be preventing the enzymatic removal of NETs, IgG subclasses were quantified in patient and matched control plasma samples. In addition to analysing immunoglobulins, levels of FLCs were measured. Immunoglobulins comprise 2 identical heavy and 2 identical light chains (either kappa or lambda), however during their normal synthesis by B cells, there is an excess of light chain production which is released into circulation and known as FLCs (Solomon 1985). However, FLC overproduction has been reported in several chronic diseases, such as SLE (Aggarwal *et al.,* 2011) and rheumatoid arthritis (RA) (Gottenberg *et al.,* 2007), which may be the result of chronic immune stimulation (Brebner & Stockley 2013). Periodontitis has been linked to these pathologies (Fabbri *et al.,* 2014, Smit *et al.,* 2012), and furthermore, periodontitis is a disease exacerbated by a chronic inflammatory-immune host response and notably overactive B cells are deemed partly responsible (Reinhardt *et al.,* 1988). Accordingly, the results reported here demonstrate increased plasma-derived FLCs and IgG 1-4 subclasses in periodontitis patients (sections 6.3.3, 6.3.4). Increased IgG levels are consistent with the findings of Graswinckel *et al.,* (2004), who reported higher levels of IgG1 and IgG2 in periodontitis patients relative to controls. In the present study, cystatin C levels were also measured to establish whether excessive plasma FLCs in periodontitis patients resulted from insufficient renal FLC clearance; notably no differences in renal clearance were observed between patients and controls. There is a paucity of data pertaining to FLCs and periodontitis; however the results

here suggest that in this patient cohort, periodontitis is associated with elevated FLC production. Further experiments are therefore warranted to determine whether increasing circulating levels of antibodies and FLCs prevents the enzymatic degradation of NETs in periodontitis.

Attenuated NET removal may constitute an antimicrobial host response during periods of infection, as NETs can prevent microbial dissemination by entrapping various periodontal bacteria (section 4.4). In support of the contribution of NETs to the host response in SLE, impeded NET production in NADPH-oxidase KO mice exhibited exacerbated lupus-like symptoms, which led the authors to conclude that NET release does not contribute to SLE *in vivo* (Campbell *et al.,* 2012). The host's ability to adjust the extracellular "life-span" of NETs in response to the microbial biofilm may also explain why no differences in peripheral NET release were observed between periodontitis patients and controls (see Chapter 4). Notably, it has been reported that mice immunised with NETs produced *in vitro* with H_2O_2 did not demonstrate a break in immune tolerance as a result of NET-derived immunogens. In support of the premise that NETs are non-immunogenic, the work in this chapter demonstrated that under the reported experimental conditions, treatment of peripheral neutrophils with HOCl-stimulated NET supernatants did not prompt ROS or NET production. In addition, no NET-mediated cytotoxicity was identified in H400 cells following their incubation with NET supernatants. This is contradictory to findings by Saffarazadeh *et al.,* (2012), who demonstrated that NETs induced cell death in epithelial cells. These differences may be a result of different cell lines (Saffarazadeh employed alveolar epithelial cells), or due to differences in the NET supernatants, for example Saffarazadeh employed PMA-induced NETs whereas HOCl was the NET stimulus of choice in the work outlined here.

NET supernatants employed as chemoattractants did however increase neutrophil chemotaxis; albeit non-directional movement, suggesting that whilst increased motility was observed, neutrophils were not being recruited to NET structures (section 6.4.3). Increased neutrophil speed in the absence of directionality may be detrimental to the host, as the random movement of cells may cause ROS-mediated collateral tissue damage during neutrophil tissue transit (Roberts *et al.,* 2015). It is difficult to ascertain whether these observations reflect *in vivo* chemotaxis, where bacteria and host derived chemoattractants will also be present and may provide a chemical hierarchy (Kim & Haynes 2012) that overrides the chemotactic signals produced by NETs. Interestingly, NETs have been suggested to provide danger signals that activate DNA receptors (such as TLR9), which subsequently alert the immune system (Brinkmann *et al.,* 2012). Activation of DNA receptors was not investigated here; however the work outlined in this chapter suggests that under the experimental conditions reported, NETs do not activate neutrophil effector functions.

Evaluating pro-inflammatory responses to NETs produced *in vitro* is subject to various limitations and may not be representative of the localised NET production in periodontitis. For example, *in vivo* NETs are produced in response to a diverse microbial biofilm, the host response is chronic, and inflammatory mediators may prime neutrophils prior to NET production (Matthews *et al.,* 2007a, 2007b). Notably, NET-evoked pro-inflammatory responses have been suggested to act synergistically with the presence of microbes, whereby immune response proteins in the extracellular milieu are required in addition to NET structures (Farrera & Fadeel 2013). In accordance with this, several studies have suggested that NETs complexed with bacteria and anti-NET antibodies may be resistant to degradation and may exacerbate diseases such as cystic fibrosis (Dwyer *et al.,* 2014) and small vessel vasculitis (SVV) (Kessenbrock *et al.,* 2009). Several of the peptides associated with the

NET-DNA backbone are reportedly autoantigens, such as MPO and PR3, which in SVV, trigger the release of anti-neutrophil cytoplasmic antibodies (ANCAs), and notably the production of ANCAs subsequently induce the production of NETs (Kessenbrock *et al.,* 2009). Findings by Gomes *et al.,* (2009) suggest this may also be of relevance in periodontitis, as the induction of experimental periodontitis in rats resulted in significantly elevated levels of MPO in the gingival tissues, however whether this was NET-bound MPO was not determined. Furthermore, in the light of our findings that circulating IgG levels are higher in periodontitis patients (6.3.3), it's noteworthy that IgG reportedly interacts with chromatin, and these IgG-chromatin complexes potentiate autoantibody production (Leadbetter *et al.,* 2002). Thus in chronic periodontitis, increased IgG levels, a bacterial biofilm and delayed NET removal may break immune tolerance, resulting in autoantibody production and further impeded NET removal which generates a self-perpetuating disease cycle.

Histones represent 70% of NET-associated proteins (Urban *et al.,* 2009) and are proposed to be key autoantigens in autoimmune diseases (Van Bavel *et al.,* 2011). Histones undergo post-translational modifications during the formation of NETs, whereby arginine residues are converted to citrulline by the enzymatic activity of PAD4. Notably, autoantibodies produced in Felty's syndrome, a form of rheumatoid arthritis, preferentially react with citrullinated histones; this suggests that NET release and the protein modifications required for this mechanism to occur are implicated in autoimmunity (Dwivedi *et al.,* 2012, 2014). Notably recent findings investigating the association between RA and periodontitis demonstrated higher levels of anti-citrullinated protein antibody (ACPAs) against citrullinated and uncitrullinated peptides in periodontitis patients. It is possible that NET production in periodontal tissues may serve as a plausible mechanism for ACPA production following a break in immune tolerance to NET-derived citrullinated peptides released by neutrophils (de

Pablo *et al.,* 2009), and this process may be exacerbated if NETs are not removed in a timely manner.

The recent discovery that *P. gingivalis* possesses a unique PAD enzyme (PPAD) capable of citrullinating bacterial and host proteins might also contribute to the generation of ACPAs (Wegner *et al.,* 2010). It has been suggested that PPADs can likely disseminate from the bacterial biofilm, thus it is possible that NETs and PPADs interact during colonisation by *P. gingivalis*. This raises questions as to whether PPADs have the ability to citrullinate proteins associated with NETs that would ordinarily be citrullinated by host PADs. For example, the NET-bound peptide, LL-37, is citrullinated by host-derived PAD2 and PAD4, and certain citrullinated LL-37 peptides are reportedly pro-inflammatory relative to the uncitrullinated peptide (Kilsgard *et al.,* 2012). It is interesting to speculate that if *P. gingivalis* is also able to citrullinate NET-derived peptides that promote pro-inflammatory responses, it may utilise this mechanism to bring about non-resolving inflammation that is characteristic of periodontitis. Furthermore, in SLE, LL-37 reportedly promotes the production of autoantibodies and the production of immune complexes that are capable of stimulating plasmacytoid dendritic cells to release type 1 IFN (Lande *et al.,* 2011). This may be of relevance in periodontitis, where the reduced NET degradation reported here may provide a possible explanation for the increased levels of type 1 IFN observed in chronic periodontitis patients (Wright *et al.,* 2008).

In summary, a subset of periodontitis patients displayed impeded NET degradation; however NET degradation was restored following successful non-surgical treatment. This may be the result of increased circulating IgGs and FLCs in patients, which may provide a physical barrier preventing enzymatic removal of NETs; further experiments are however warranted to confirm this. Subsequent assays to determine the effect of delayed NET removal demonstrated that NETs did not stimulate for neutrophil ROS production, further NET

release, or induce NET-mediated cytotoxicity in H400 cells. Notably, NETs employed as neutrophil chemoattractants caused increased neutrophil migration speed, however this movement did not exhibit directionality. Whilst no NET-induced pro-inflammatory responses were observed here, NETs are implicated in disease progression in several pathologies (Cooper *et al.,* 2013), thus it is possible that *in vitro* assays do not fully mimic the *in vivo* environment in periodontitis, comprising a microbial biofilm, complex pro-inflammatory mediators and chronic immune activation.

CHAPTER 7: EFFECT OF CIGARETTE SMOKE EXTRACT ON NEUTROPHIL RESPONSES

7.1 Introduction

Smoking is a significant risk factor for periodontitis, and cigarette smoke extract (CSE) has previously been shown to impact upon neutrophil ROS production (section 1.7.3, Matthews *et al.,* 2011, 2012). However, there is no published data on the effects of CSE upon NET formation; therefore to further understand the impact of smoking on neutrophilic responses, healthy neutrophils were treated with CSE previously prepared (section 2.2.4.1, Matthews *et al.,* 2011). In addition to CSE, the effect of specific cigarette constituents on neutrophil responses was also assayed, including pre-incubation with nicotine, cotinine and thiocyanate (SCN-) (University of Birmingham Ethics Reference ERN_13-0325) (section 2.2.4.2.1). Neutrophil directional chemotaxis in response to the known chemoattractants, fMLP and IL-8, was also measured in cells primed with increasing concentrations of CSE. The speed, velocity and directional chemotactic accuracy were measured using the Insall chamber and real-time video microscopy (sections 2.2.4.2.3 & 2.2.4.2.4, Roberts *et al.,* 2015). Finally, the impact of CSE and SCN- treatment on neutrophil inflammatory and redox related gene expression was determined by real time PCR (2.2.4.3).

7.2 Effect of cigarette smoke extract on NET release

NET production was determined as previously described by quantifying NET-DNA in the Sytox green assay (2.2.4.2.1, Appendix VIII) Matthews *et al.,* 2011, 2012). The effect of CSE (at concentrations of 1%, 5% or 10%) on NET release did not differ significantly from PBS-treated cells (unstimulated negative control) (1way ANOVA $p=0.99$, n=10) (Figure 7.1a). By contrast, CSE priming and subsequent stimulation with PMA (50nM) was associated with significantly decreased NET production at concentrations of 5% and 10% CSE (1way ANOVA and Dunnett's post-tests $*p<0.05$, $****p<0.0001$ for 5% and 10% CSE, respectively, n=10) (Figure 7.1b). However, when cells were primed with CSE and stimulated with HOCl (0.75mM), no differences in NET production due to CSE priming were observed (1way ANOVA $p=0.90$, n=10) (Figure 7.1c).

7.2.1 Fluorescence visualisation of NETs following treatment with CSE

NET production in response to PMA (50nM) stimulation (Figure 7.2a) was qualitatively compared visually between neutrophils primed for 30 mins with increasing concentrations of CSE prior to stimulation (2.2.4.2.2). NETs were visualised by fluorescence microscopy after staining with Sytox green, which targets DNA. NET-like structures appeared aggregated when primed with 1% CSE prior to PMA stimulation (Figure 7.2b). In contrast, cells that were primed with 5% or 10% CSE and subsequently stimulated with PMA did not form visible web-like structures, however aggregates of DNA were observed (Figures 7.2c&d).

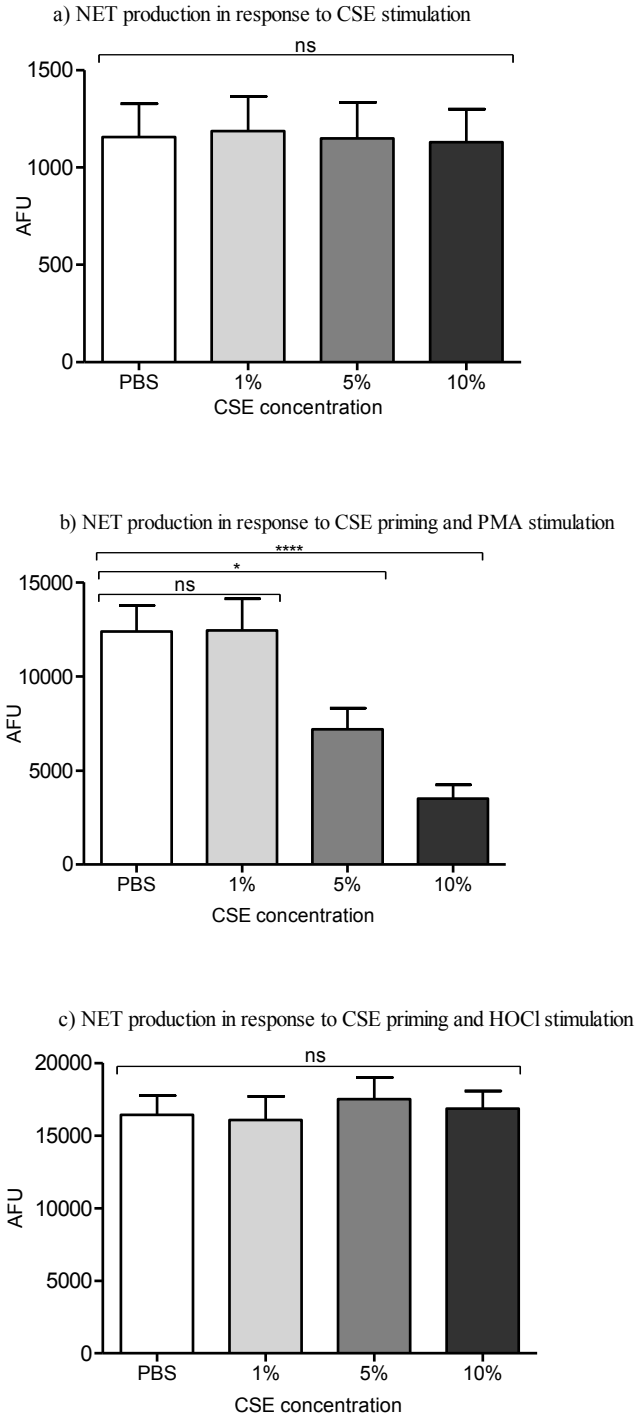

Figure 7.1: Effect of cigarette smoke extract on NET production

NET-DNA was quantified fluorometrically in response to stimulation with 1, 5 or 10% CSE and compared with PBS-treated cells (unstimulated negative control). (a) 4 hour stimulation of neutrophils with CSE, (b) 30 min CSE priming prior to stimulation with PMA (50nM), (c) 30 min CSE priming prior to stimulation with HOCl (0.75mM). Statistical significance was calculated using 1way ANOVA and Dunnett's post-tests (*$p<0.05$, ****$p<0.0001$, ns=not significant). Data are presented as AFU (arbitrary fluorescence units) and are expressed as mean ± SEM (n=10 in triplicate).

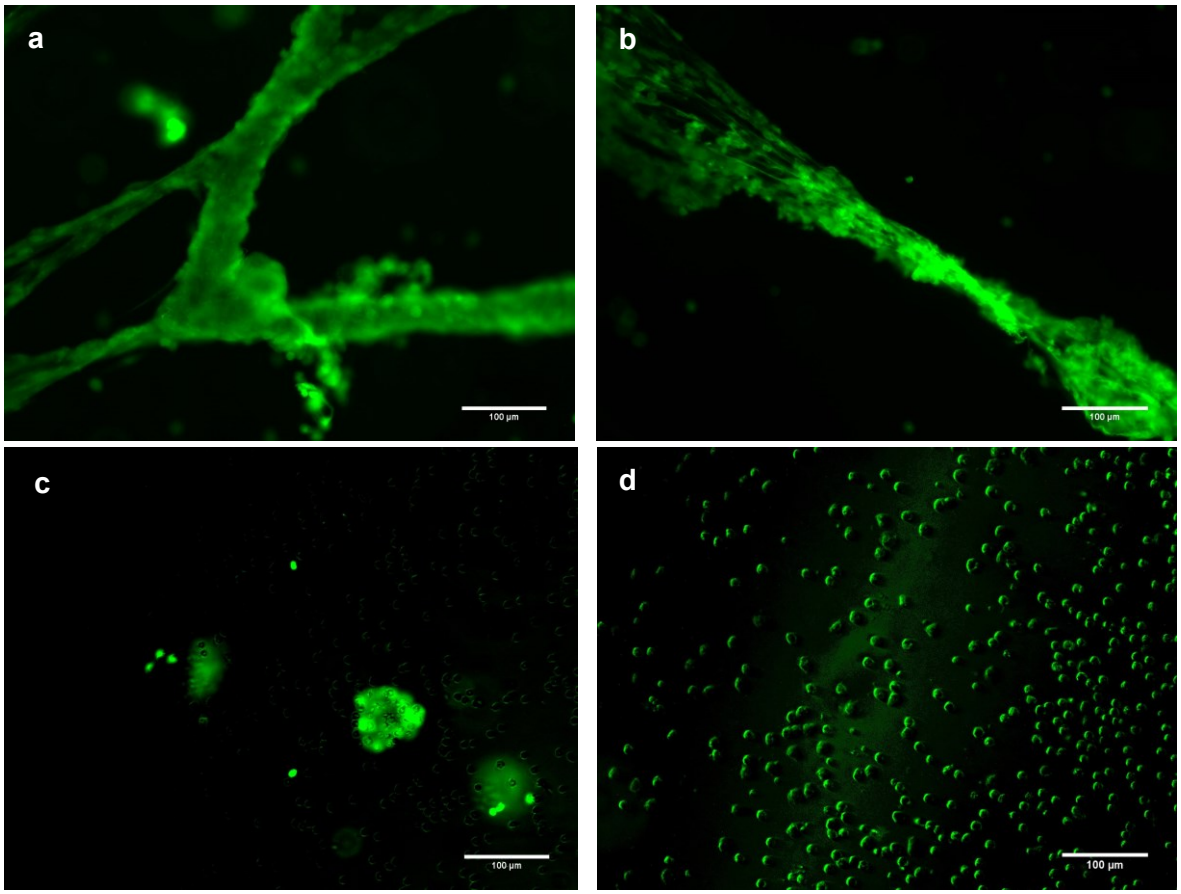

Figure 7.2: Fluorescence visualisation of NETs in response to cigarette smoke extract
NETs were visualised with Sytox green using fluorescence microscopy (x20 magnification), following stimulation with (a) PMA (50nM), or primed for 30 mins with (b) 1% CSE, (c) 5% CSE or (d) 10% CSE, prior to PMA stimulation. Images are representative of 2 experiments in duplicate. Scale bar represents 100µm.

7.3 Effect of CSE components on NET release

To attempt to determine whether specific CSE components of CSE were contributing to the attenuated NET release observed, the effect of specific cigarette constituents on NET release were investigated, including nicotine, cotinine and SCN-.

Effect of nicotine on NET production

Nicotine stimulation (applied at concentrations of 1µg/ml, 5µg/ml or 10µg/ml) (2.1.4.1, 2.2.4.2.1) did not alter NET production compared with unstimulated control cells (1way ANOVA *p=0.23,* n=10). Nicotine priming for 30 mins and subsequent stimulation with PMA (50nM) and HOCl (0.75mM) was also found to have no apparent effect on NET release, compared with cells primed with PBS (1way ANOVA *p=0.98*, *p=0.75* for PMA and HOCl respectively, n=10) (Figure 7.3a).

Effect of cotinine on NET production

Cotinine stimulation (applied at concentrations of 1µg/ml, 5µg/ml or 10µg/ml) (2.1.4.2, 2.2.4.2.1) did not alter NET production compared with PBS (negative control cells) (1way ANOVA *p=0.85*, n=10). Cotinine priming for 30 mins and subsequent stimulation with PMA (50nM) and HOCl (0.75mM) was also found to have no effect on NET release (1way ANOVA *p=0.96, p=0.99* for PMA and HOCl respectively, n=10) (Figure 7.3b).

Effect of thiocyanate on NET production

SCN- stimulation at lower concentrations (applied at concentrations of 50µM, 100µM) (2.1.4.3, 2.2.4.2.1) did not alter NET production relative to unstimulated control cells. However stimulation with 150µM SCN^- resulted in a significant increase in NET release (1way ANOVA and Dunnett's post-tests *$p<0.05$). SCN- priming for 30 mins prior to PMA (50nM) stimulation inhibited NET release compared with un-primed neutrophils; this was

observed at all concentrations of SCN^- (1way ANOVA and Dunnett's post-tests ***$p<0.001$ for each concentration). SCN- priming for 30 mins prior to HOCl (0.75mM) stimulation also inhibited NET release compared with un-primed neutrophils; this was observed in all concentrations of SCN^- (1way ANOVA and Dunnett's post-tests ***$p<0.001$ for each concentration) (Figure 7.3c).

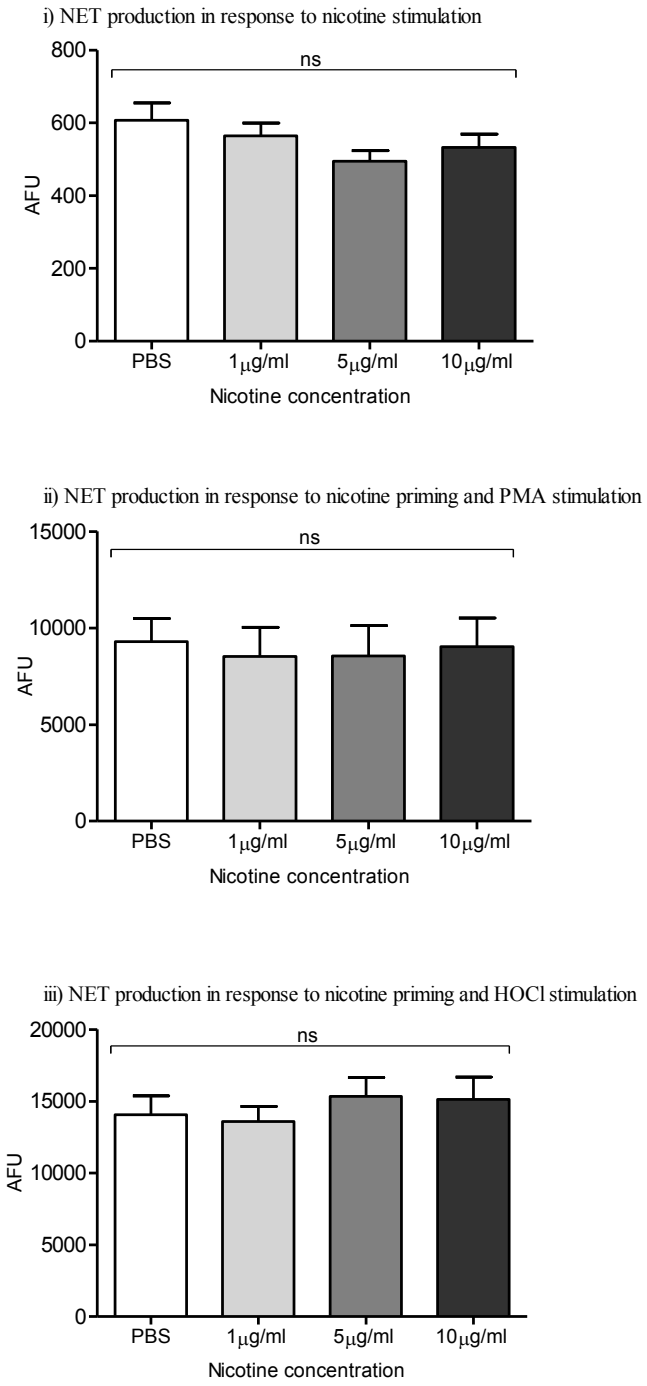

Figure 7.3a: Effect of nicotine on NET production

NET-DNA production was quantified fluorometrically in response to stimulation with 1µg/ml, 5µg/ml or 10µg/ml nicotine and PBS-treated cells (unstimulated negative control). (i) 4 hour stimulation of neutrophils with nicotine, (ii) 30 min nicotine priming prior to stimulation with PMA (50nM), (iii) 30 min nicotine priming prior to stimulation with HOCl (0.75mM). Statistical significance was calculated using 1way ANOVA and Dunnett's post-tests (ns=not significant). Data are presented as AFU (arbitrary fluorescence units) and are expressed as mean ± SEM (n=5 in triplicate).

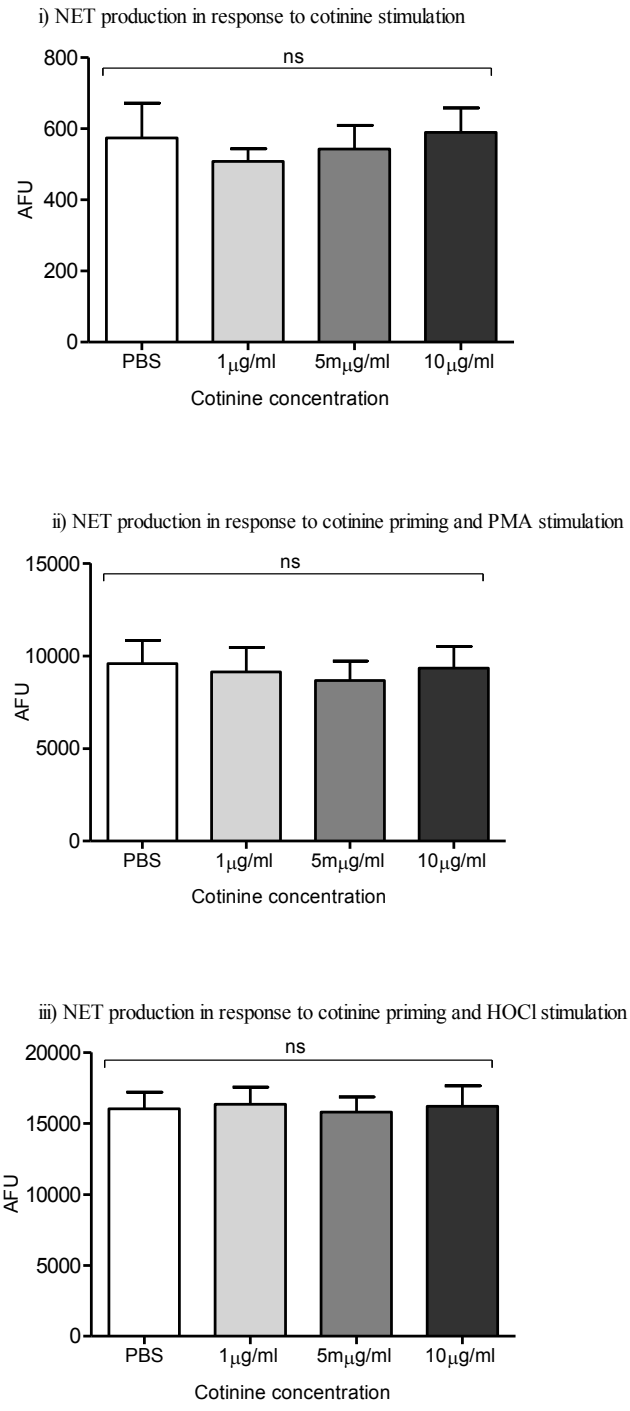

Figure 7.3b: Effect of cotinine on NET production

NET-DNA production was quantified fluorometrically in response to stimulation with 1µg/ml, 5µg/ml or 10µg/ml cotinine with PBS-treated cells (unstimulated negative control). (i) 4 hour stimulation of neutrophils with cotinine, (ii) 30 min cotinine priming prior to stimulation with PMA (50nM), (iii) 30 min cotinine priming prior to stimulation with HOCl (0.75mM). Statistical significance was calculated using 1way ANOVA and Dunnett's post-tests (ns=not significant). Data are presented as AFU (arbitrary fluorescence units) and are expressed as mean ± SEM (n=5 in triplicate).

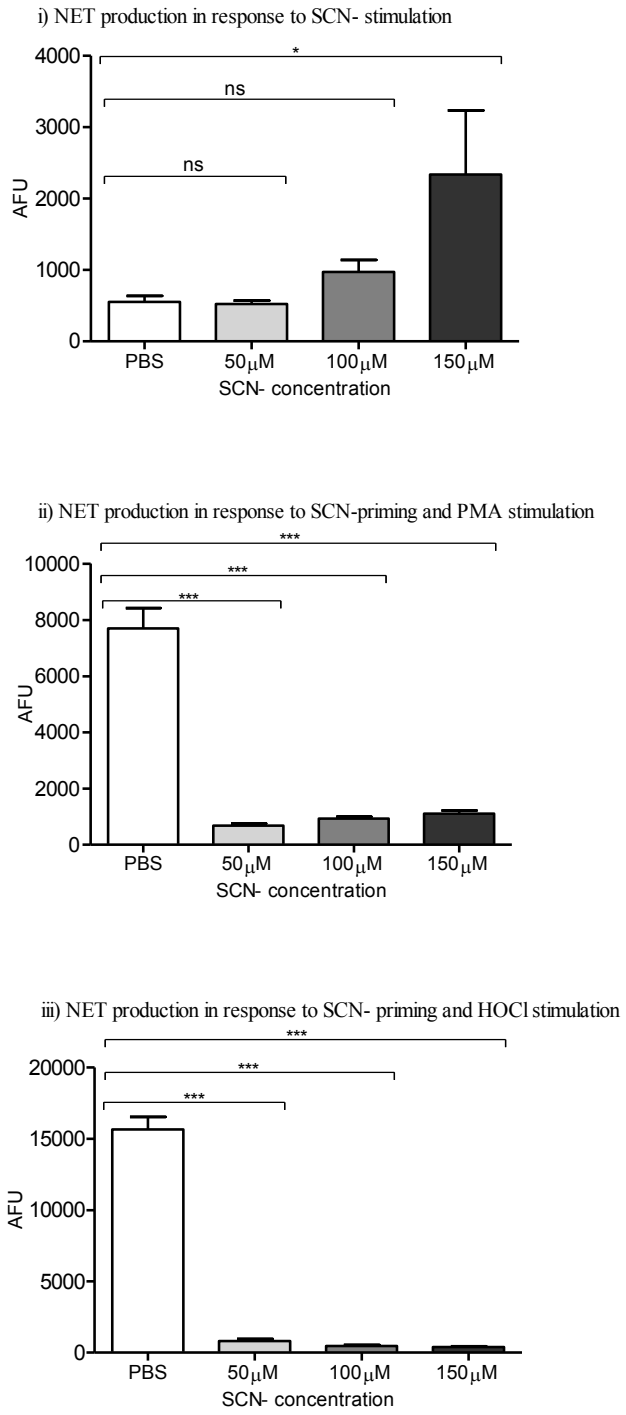

Figure 7.3c: Effect of thiocyanate (SCN-) on NET production

NET-DNA production was quantified fluorometrically in response to stimulation with 50μM, 100μM or 150μM SCN- and PBS-treated cells (unstimulated negative control). (i) 4 hour stimulation of neutrophils with SCN-, (ii) 30 min SCN- priming prior to stimulation with PMA (50nM), (iii) 30 min SCN- priming prior to stimulation with HOCl (0.75mM). Statistical significance was calculated using 1way ANOVA and Dunnett's post-tests (*$p=0.05$, ***$p<0.001$, ns=not significant). Data are presented as AFU (arbitrary fluorescence units) and are expressed as mean ± SEM (n=5 in triplicate).

7.3.1 Fluorescence visualisation of NETs following nicotine, cotinine and thiocyanate treatment

NET production was visualised following 30 mins priming with increasing concentrations of nicotine, cotinine and SCN, and followed by stimulation with PMA (50nM) (2.2.4.2.2). Fluorescence microscopy of Sytox green stained DNA was employed. Nicotine (1µg/ml, 5µg/ml or 10µg/ml) and cotinine (1µg/ml, 5µg/ml or 10µg/ml) priming prior to PMA stimulation resulted in NET production, as shown by the extracellular web-like structures that stained positive with Sytox green. In contrast, cells that were primed with SCN- (50µM, 100µM or 150µM) prior to PMA stimulation formed no apparent NET-like structures, however aggregates of DNA were observed (Figure 7.4). Sytox green can also stain non-viable cells, as it is able to permeate the compromised cell membrane; however Sytox green staining does not differentiate between DNA derived from NETs and DNA released by other cell processes, such as necrosis. It is therefore possible that SCN- treatment led to cell necrosis rather than NETosis (investigated in section 7.3.2).

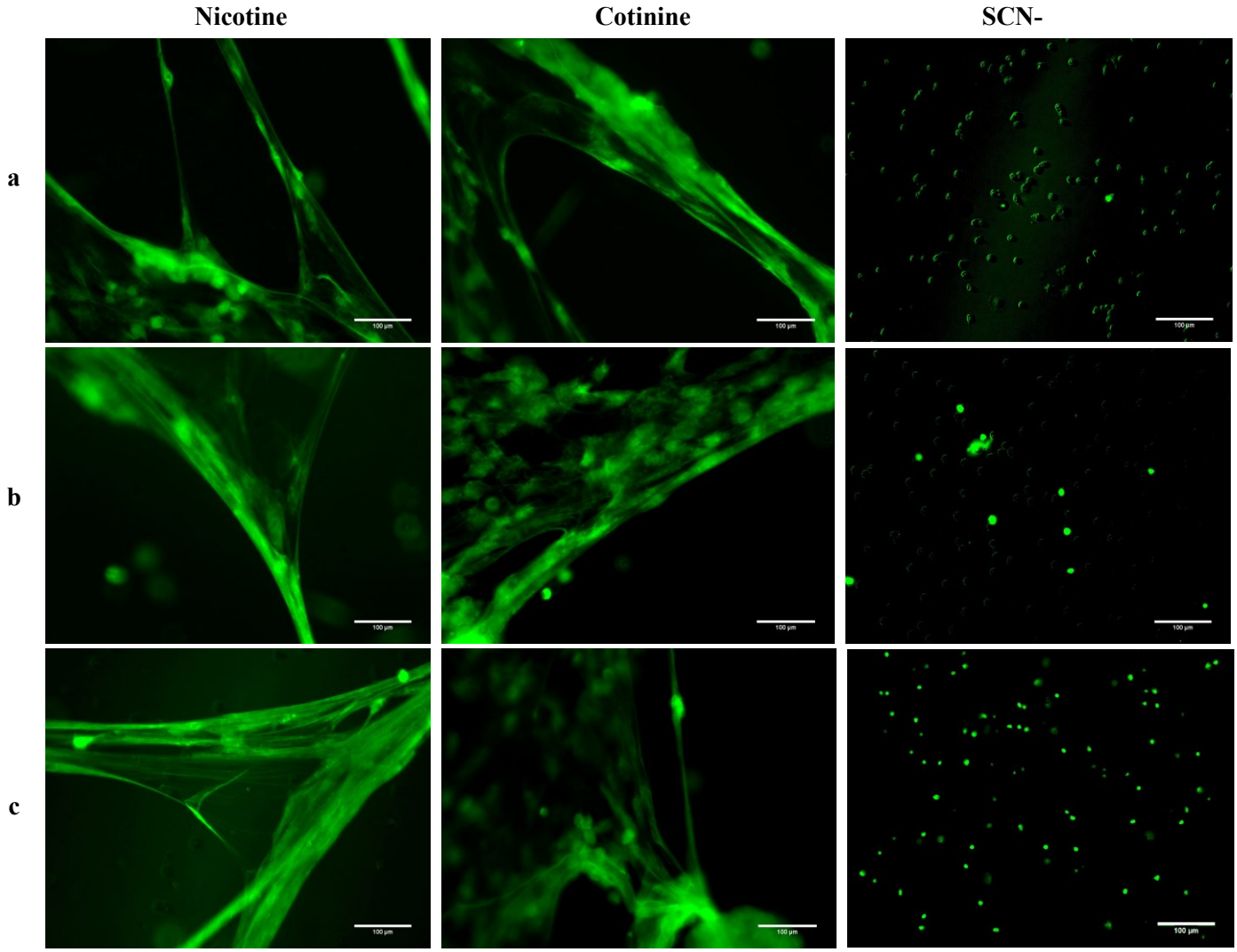

Figure 7.4: Fluorescence visualisation of NETs in response to CSE and its key components

NETs were visualised following Sytox green staining using fluorescence microscopy (x20 magnification). NETs visualised in response to nicotine (a) 1µg/ml, (b) 5µg/ml or (c) 10µg/ml; cotinine (a) 1µg/ml, (b) 5µg/ml or (c) 10µg/ml; or SCN- (a) 50µM, (b) 100µM or (c) 150µM. Images are representative of 2 experiments in duplicate. Scale bar represents 100µm.

7.3.2 Cell viability following treatment with CSE and CSE components

To determine whether reduced NET production may be due to CSE- or CSE components-induced neutrophil cell death, the effect of CSE and CSE components (nicotine, cotinine and SCN^-) on neutrophil viability was compared with unstimulated cells (PBS). Following 4 hours of incubation, trypan blue exclusion revealed that CSE and CSE components did not significantly affect neutrophil viability (1way ANOVA *p=0.23*). Data are presented as the percentage number of viable cells (Figure 7.5).

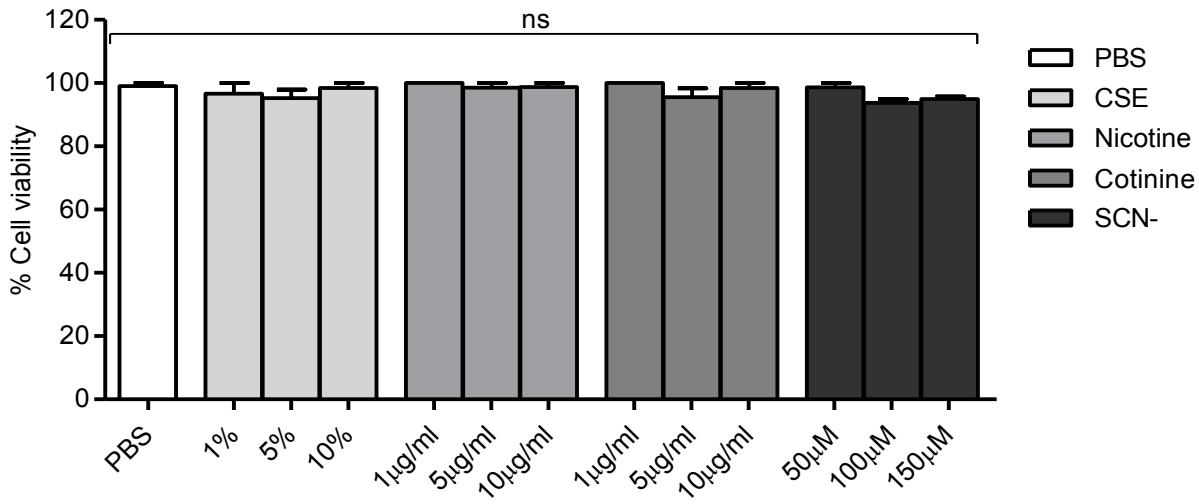

Figure 7.5: Cell viability following treatment with CSE and CSE components
Percentage cell viability was determined by differential counts of cells stained with trypan blue (1:1 dilution). Viability of neutrophils treated with CSE, nicotine, cotinine and SCN- was not significantly different from PBS-treated cells (unstimulated negative control). Statistical significance calculated using a 1way ANOVA (ns=not significant). Data are presented as the percentage of viable cells and are expressed as mean ± SEM (n=3 in duplicate).

7.4 Neutrophil chemotactic accuracy

Neutrophil directional chemotaxis following 30 mins incubation with PBS (negative control) or CSE (1%, 5% or 10%) was determined by real-time video microscopy. Neutrophil migration was measured in response to known chemoattractants, fMLP (100nM) and IL-8 (10nM), as well as RPMI (negative control). The movement of 15 randomly chosen cells (validated by H. Roberts) was tracked and the quantitative data generated used to generate spider plots and calculate neutrophil speed, velocity and resultant vector length.

7.4.1 Analysis of migration of CSE-treated neutrophils in response to fMLP using spider plots

Spider plots enable visualisation of individual cell movement (μm) from a central point, where the top of the Y-axis represents the source of the chemoattractant (100nM fMLP). Cells incubated with PBS displayed directional movement towards the source of the chemotactic signals. However this directionality appeared reduced in cells incubated with increasing concentrations of CSE, demonstrated by the non-directional cell movement following 1% and, to a greater extent, 5% CSE treatment. Cells incubated with 10% CSE showed minimal migrational movement in any direction (Figure 7.6).

The movement of individual cells from a central point in response to IL-8 (10nM) was also visualised using spider plots. Movement of cells incubated with PBS displayed directionality of movement towards the source of the chemotactic signals; however it was noted that IL-8 did not behave as strongly as fMLP as a chemoattractant, evidenced by the reduced directionality in cell movement. There was greater variation in cell movement following treatment with 1% and 5% CSE, with less directional movement towards the chemoattractant. Consistent with the observations for fMLP, neutrophils treated with 10% CSE exhibited very little movement in any direction (Figure 7.7).

fMLP: PBS control

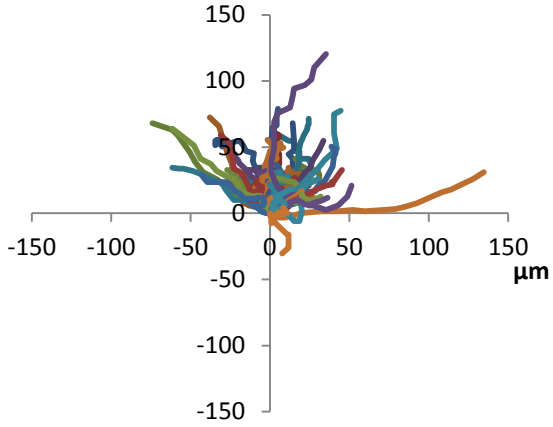

fMLP: 1% CSE

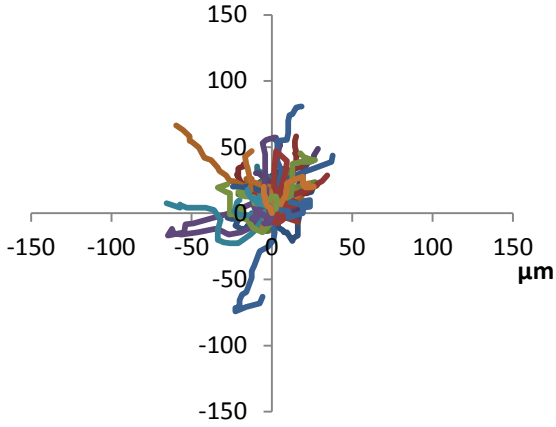

fMLP: 5% CSE

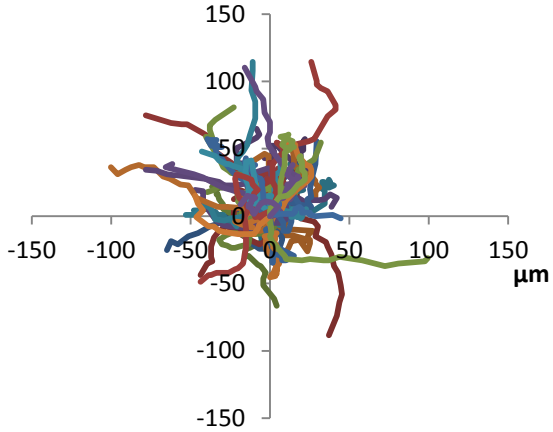

fMLP: 10% CSE

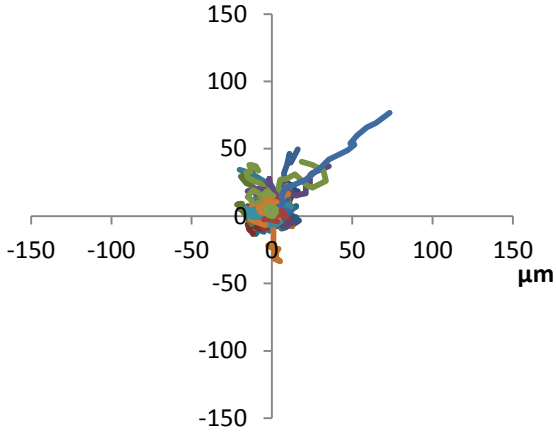

Figure 7.6: Analysis of migration of CSE-treated neutrophils in response to fMLP using spider plots

Spider plots of individual neutrophils (n=15 cells from n=5 experiments) from a central reference point (0, 0) in response to fMLP (100nM). Cells were incubated with PBS (control) or CSE (1%, 5% or 10%) prior to the addition of fMLP. The top of the Y-axis represents the source of the chemoattractant (fMLP). Whilst PBS-treated neutrophils generally moved towards the source of the chemoattractant signal, CSE-treated neutrophils exhibited less directional movement.

IL-8: PBS control

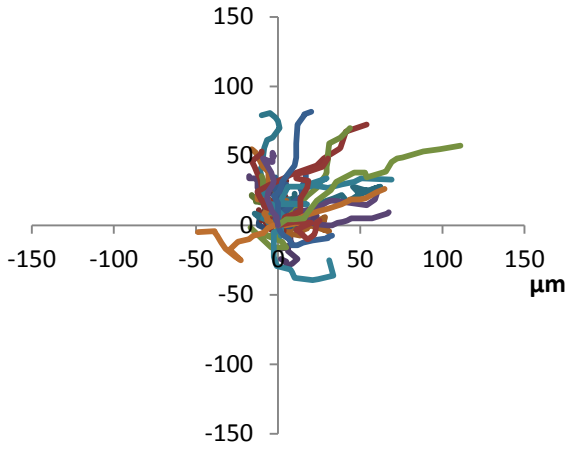

IL-8: 1% CSE

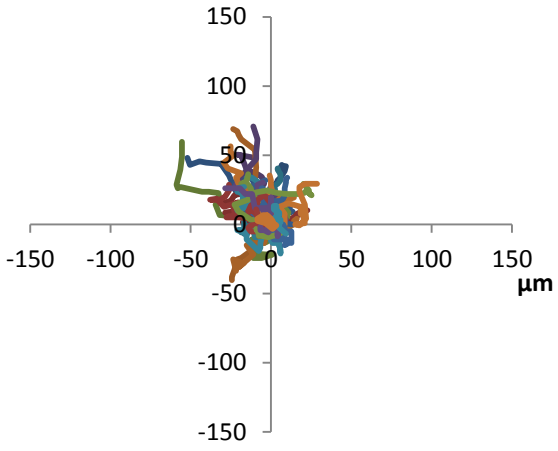

IL-8: 5% CSE

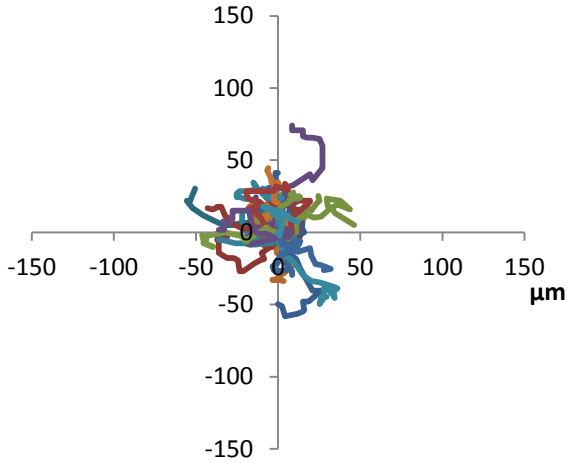

IL-8: 10% CSE

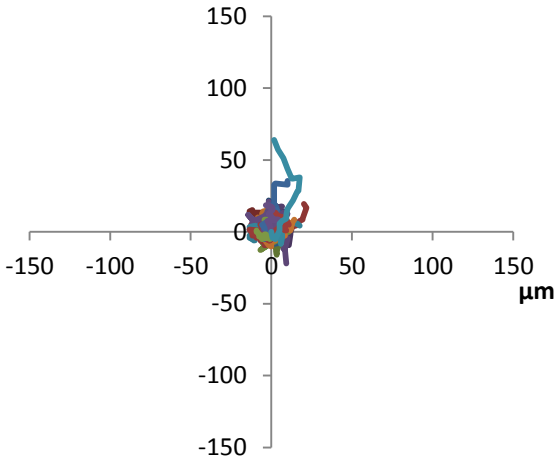

Figure 7.7: Analysis of migration of CSE-treated neutrophils in response to IL-8 using spider plots

Spider plots show the tracking (µm) of individual neutrophils (n=15 cells from n=5 experiments) from a centre reference point (0, 0) in response to IL-8 (10nM). Cells were incubated with PBS (control) or CSE (1%, 5% or 10%) prior to the addition of IL-8. The top of the Y-axis represents the source of the chemoattractant (fMLP).

Whilst PBS-treated neutrophils generally moved towards the source of the chemoattractant signal, CSE-treated neutrophils exhibited less directional movement.

Whilst spider diagrams represent a novel way to visualise cell migration in response to a chemoattractant, they cannot be used to quantify neutrophil movement. Thus, the data generated from tracking 15 individual cells was used to quantify the speed, velocity and directional accuracy of neutrophil migration.

7.4.1.1 Speed of CSE treated neutrophils

The speed (μm/minute) of neutrophil chemotaxis in response to fMLP (100nM) significantly increased following incubation with 5% CSE, compared with cells incubated with PBS (1way ANOVA and Bonferroni post-test ***$p<0.001$, n=5). However, treatment with 10% CSE resulted in significantly decreased speed of neutrophil migration in response to fMLP (1way ANOVA and Bonferroni post-test ***$p<0.001$, n=5). Notably the speed of 10% CSE-treated neutrophils in response to fMLP was not significantly different from cells moving in response to the negative control chemoattractant, RPMI. Neutrophil speed in response to IL-8 (10nM) following 10% CSE treatment was significantly lower than that for PBS controls (1way ANOVA and Bonferroni post-test ***$p<0.001$, n=5) (Figure 7.8).

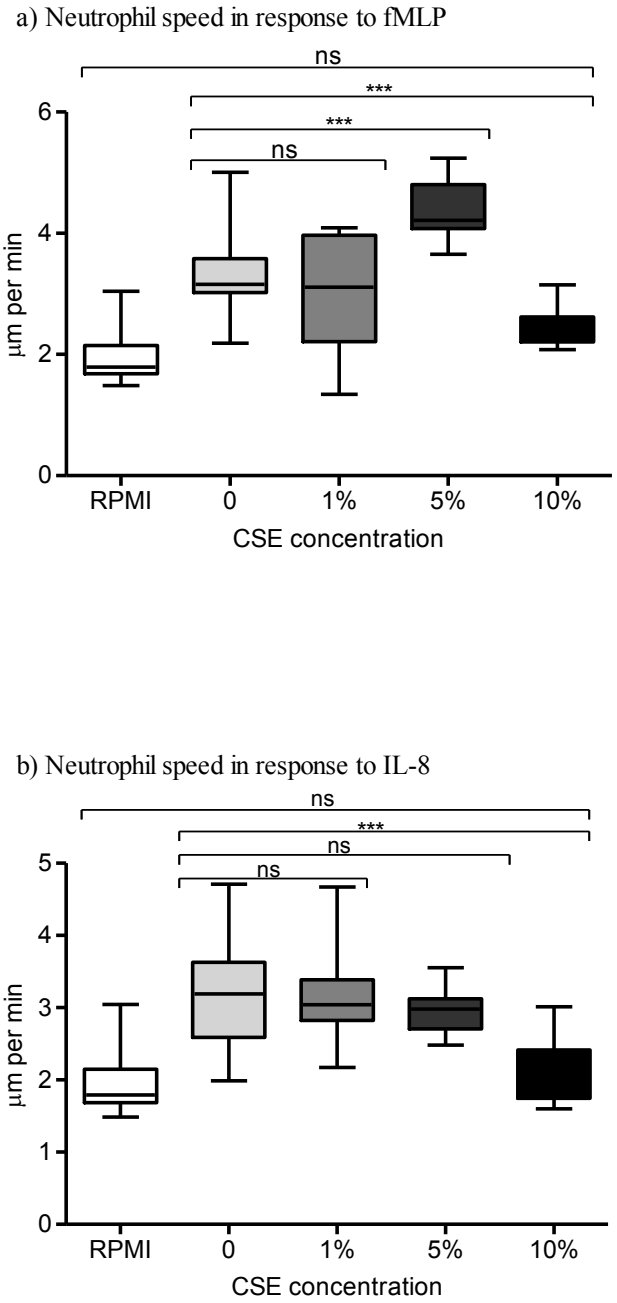

Figure 7.8: Speed of CSE treated neutrophils
Neutrophil speed (µm/min) following incubation with CSE (0 [PBS], 1%, 5% or 10%) in response to (a) fMLP (100nM), (b) IL-8 (10nM) and RPMI (negative control, shown on each graph). Statistical significance was calculated using 1way ANOVA and Bonferroni post-tests (*$p<0.05$, ***$p<0.001$, ns=not significant). Data calculated from the tracking of 15 cells and data is expressed as mean ± SEM (n=5).

7.4.1.2 Velocity of CSE treated neutrophils

Velocity is the speed of movement in a specific direction towards a chemoattractant. Neutrophil velocity was significantly decreased in response to fMLP (100nM) following treatment with 1%, 5% and 10% CSE, compared with those treated with PBS (1way ANOVA and Bonferroni post-test *$p<0.05$, **$p<0.01$ and ****$p<0.0001$ for 1%, 5% and 10% for CSE treatment, respectively, n=5). The velocity of 10% CSE-treated neutrophils in response to fMLP was not significantly different from cells moving in response to the negative control chemoattractant, RPMI ($p>0.05$). Neutrophil velocity in response to IL-8 (10nM) was also significantly lower in CSE treated cells compared to cells incubated with PBS (1way ANOVA Bonferroni post-test ****$p<0.0001$ for 1%, 5% and 10% CSE treatment, n=5). The velocity of 5% and 10% CSE-treated neutrophils in response to IL-8 was not significantly different from cells moving in response to the negative control chemoattractant, RPMI ($p>0.05$, n=5) (Figure 7.9).

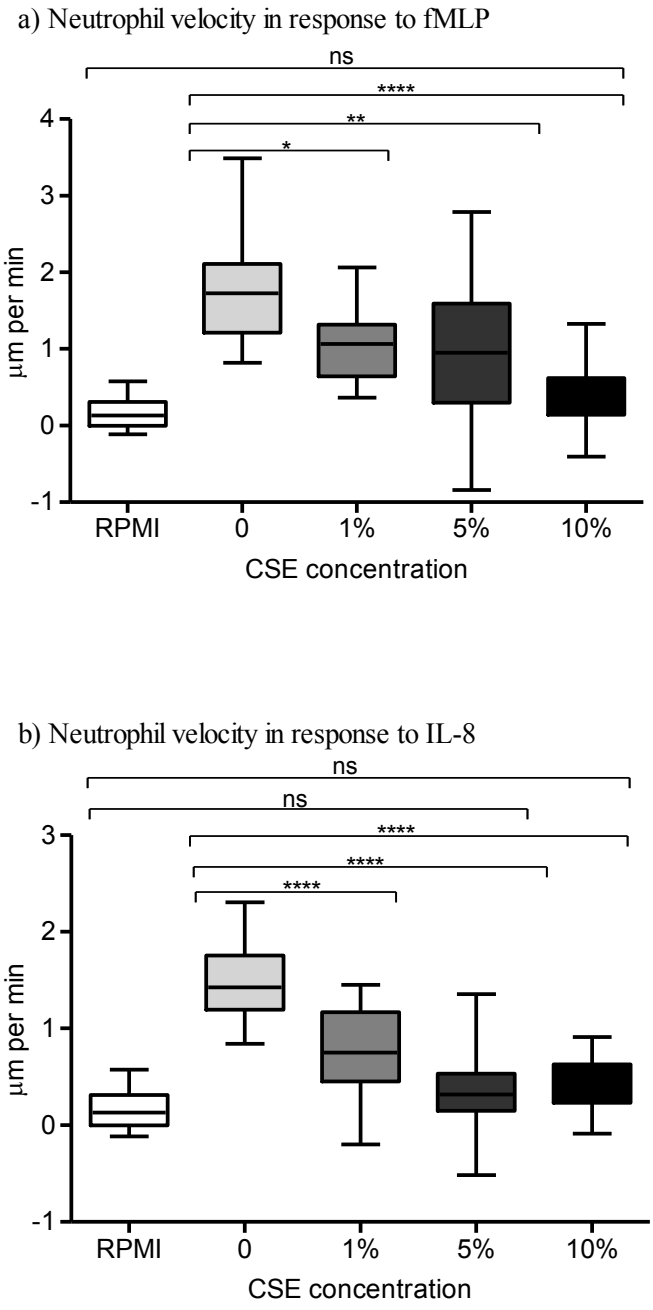

Figure 7.9: Velocity of CSE treated neutrophils

Neutrophil velocity (µm/minute) following incubation with CSE (0 [PBS], 1%, 5% or 10%) in response to (a) fMLP (100nM), (b) IL-8 (10nM) and RPMI (negative control, shown on each graph). Statistical significance was calculated using 1way ANOVA and Bonferroni post-tests (*$p<0.05$, **$p<0.01$, ****$p<0.0001$, ns=not significant). Data calculated from the tracking of 15 cells and data is expressed as mean ± SEM (n=5).

7.4.1.3 Directional accuracy of neutrophil movement (resultant vector length)

Representative angular histograms and resultant vector plots of neutrophils treated with PBS (control) or 10% CSE in response to fMLP (100nM) were produced. The angular histograms measure cell directionality and strength of this directional movement, which is determined by the histogram bar angle and width, respectively.

Angular histograms and resultant vector plots in response to fMLP

Whilst there was a relatively strong movement towards the chemoattractant in cells treated with PBS (negative control), 10% CSE-treated neutrophils demonstrated very little directionality towards fMLP (100nM). These plots are consistent with the histograms, where 10% CSE-treated cells exhibited a lack of directional movement (Figure 7.10).

Angular histograms and resultant vector plots in response to IL-8

Representative angular histograms and resultant vector plots of neutrophils treated with PBS (control) in response to IL-8 (10nM) also demonstrated migration towards the source of the chemotactic signals. However, whilst 10% CSE-treated cells were found to have reduced directional movement to IL-8, this was to a lesser extent than for fMLP (Figure 7.11).

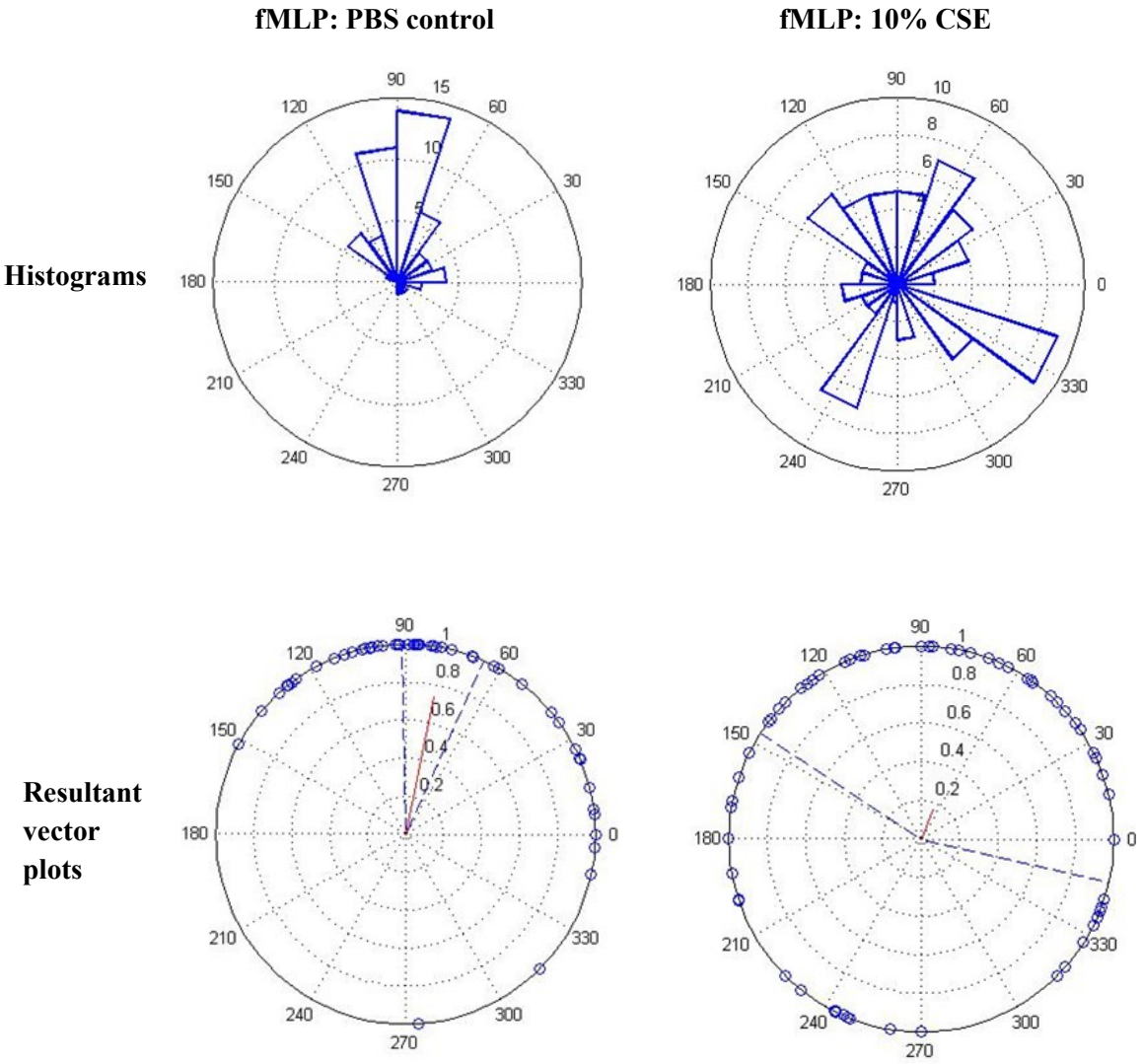

Figure 7.10: Directional accuracy of neutrophil movement (resultant vector length)
Representative angular histograms and resultant vector plots of neutrophils treated with PBS (control) or 10% CSE in response to fMLP (100nM). The angle and width of the histogram bars indicates the direction and the proportion of cells migrating in that direction, respectively. The resultant vector plots indicate the strength and directionality of the cells in response to the chemoattractant. The red line denotes the mean resultant vector and the dashed line shows the variation (95% confidence intervals) within the entire cohort of cells. The length of the red line is indicative of the strength of cell directionality. The blue circles along the circumference of the plot represent individual neutrophil migration end-points. For both plots, 90° at the top of both plots represents the source of the chemoattractant (fMLP). The above plots show neutrophil directional chemotaxis is reduced in 10% CSE-treated neutrophils compared with PBS-treated control cells, evidenced by the distribution and strength of cell directionality.

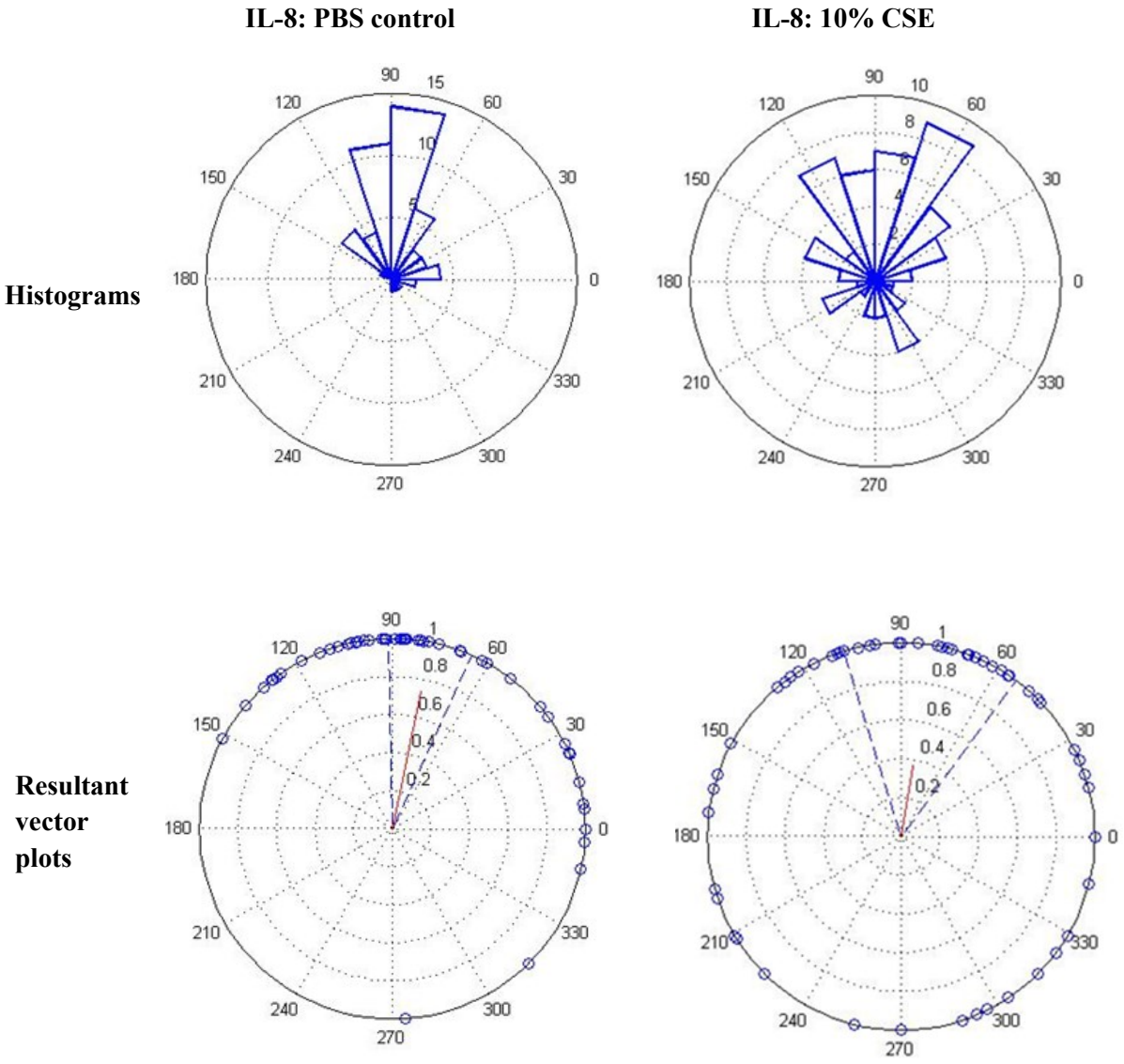

Figure 7.11: Directional accuracy of neutrophil movement (resultant vector length)
Representative angular histograms and resultant vector plots of neutrophils treated with PBS (control) or 10% CSE in response to IL-8 (10nM). The angle and width of the histogram bars indicates the migrational direction and the proportion of cells migrating in that direction, respectively. The resultant vector plots indicate the strength and directionality of the cells in response to the chemoattractant. The red line denotes the mean resultant vector and the dashed line shows the variation (95% confidence intervals) within the entire cohort of cells. The length of the red line is indicative of the strength of cell directionality. The blue circles along the circumference of the plot represent individual neutrophil migration end-points. For both plots, 90° at the top of both plots represents the source of the chemoattractant (IL-8). The above plots show neutrophil directional chemotaxis is reduced in 10% CSE-treated neutrophils compared with PBS-treated control cells, evidenced by the distribution and strength of cell directionality.

7.4.1.4 Resultant vector length of CSE-treated neutrophil migration

The resultant vector length measures the directional accuracy of neutrophil chemotaxis towards the chemoattractant. The resultant vector lengths were calculated from the resultant vector plots, in which the red line denotes the mean resultant vector and the dashed line shows the variation (95% confidence intervals) within the entire cohort of cells. The length of the red line is indicative of the strength of cell directionality. Incubation of neutrophils with 5% and 10% CSE caused significant decreases in resultant vector length in response to fMLP (100nM), compared with cells incubated with PBS (negative control) (1way ANOVA and Bonferroni post-test $*p<0.05$, $**p<0.001$ for 5% and 10% CSE, respectively, n=5). The resultant vector lengths of 5% and 10% CSE-treated neutrophils in response to fMLP was not significantly different from cells moving in response to the negative control chemoattractant, RPMI ($p>0.05$) (Figure 7.12a). Neutrophil resultant vector lengths in response to IL-8 (10nM) were also significantly lower in 5% and 10% CSE-treated cells compared with cells incubated with PBS (1way ANOVA and Bonferroni post-test $**p<0.01$, $*p<0.05$ for 5% and 10% CSE treatment, respectively, n=5). The resultant vector length of 5% and 10% CSE-treated neutrophils in response to IL-8 was not significantly different from cells moving in response to the negative control chemoattractant, RPMI ($p>0.05$) (Figure 7.12b).

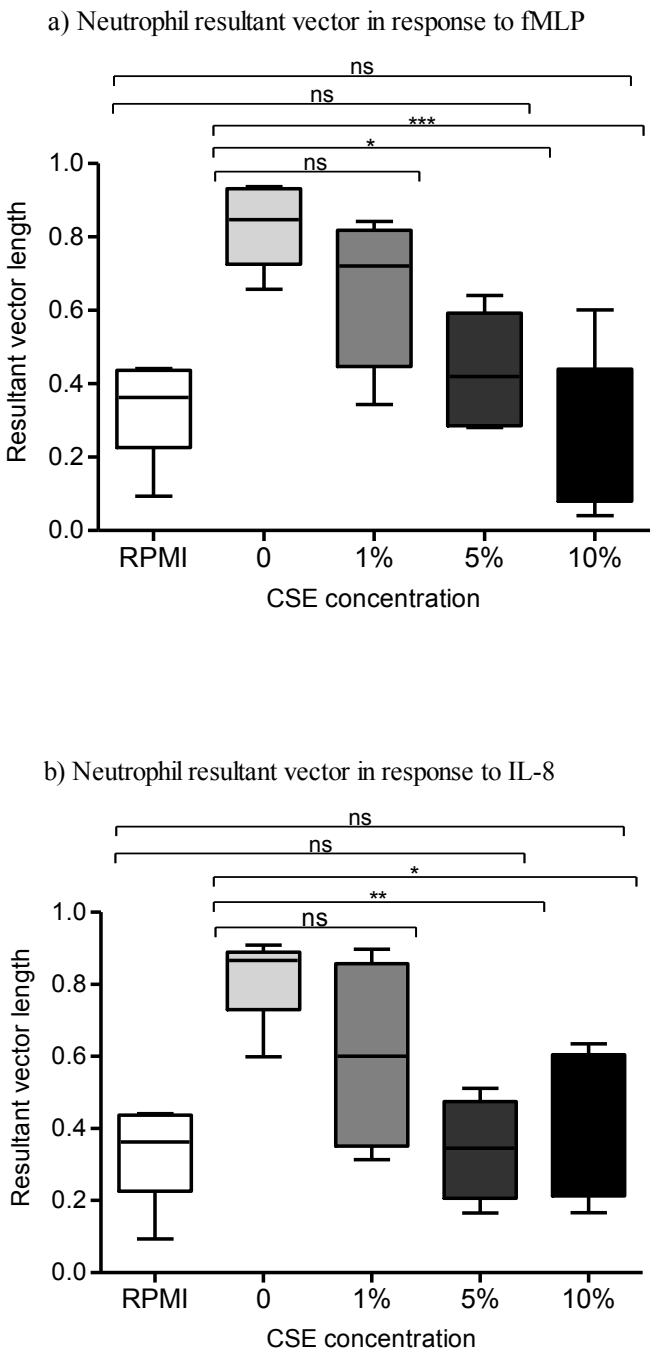

Figure 7.12: Resultant vector length of CSE-treated neutrophil migration
Resultant vector length following incubation with CSE (0 [PBS], 1%, 5% or 10%) was determined in response to (a) fMLP (100nM), (b) IL-8 (10nM) and RPMI (negative control shown on each graph). Statistical significance was calculated using 1way ANOVA and Bonferroni post-tests (*$p<0.05$, **$p<0.01$, ***$p<0.001$, ns=not significant). Data calculated from the tracking of 15 cells and data is expressed as mean ± SEM (n=5).

7.5 Gene expression following CSE and SCN- treatment

Quantitative real-time PCR analysis was employed to compare neutrophil inflammatory and redox related gene expression profiles in response to CSE and SCN- treatment (Please also see Appendices IX, X, XI, XII).

7.5.1 Impact of CSE on neutrophil gene expression

Neutrophil gene expression of NF-κB, HSP40, IL-8, P-47^{phox}, P-67^{phox} and GP-91^{phox} was quantified by real-time PCR following CSE treatment (1%, 5% or 10%). Data are expressed as a ratio of the reference gene, YWHAZ, and RNA expression of cells treated with PBS (negative control) was normalised to 1. In response to CSE treatment, HSP40 expression increased, and was statistically significant at concentrations of 5% and 10% CSE (2way ANOVA and Bonferroni post-tests ****$p=0.0001$ for 5% and 10%, n=3 technical repeats). Other trends included a CSE-concentration dependent decrease in NF-κB and GP-91^{phox} expression. Reduced expression of P-47^{phox} and P-67^{phox} was also observed, however these differences were not statistically significant (Figure 7.13a).

7.5.2 Impact of thiocyanate on neutrophil gene expression

Neutrophil gene expression of NF-κB, HSP40, IL-8, P-47^{phox}, P-67^{phox}, GP-91^{phox} were quantified by real-time PCR following SCN- treatment (50μM, 100μM or 150μM). Data are expressed as a ratio of the reference gene, YWHAZ, and RNA expression of cells treated with PBS (negative control) was normalised to 1. In response to all concentrations of SCN- treatment, HSP40 expression significantly increased (2way ANOVA and Bonferroni multiple comparisons tests ****$p=0.0001$ for 50μM, 100μM or 150μM, n=3 technical repeats). The expression of P-47^{phox} increased, and was statistically significant following 150μM SCN- treatment (2way ANOVA and Bonferroni multiple comparisons tests ****$p=0.0001$, n=3 technical repeats). P-67^{phox} expression was also elevated following treatment with 100μM

and 150μM SCN- (2way ANOVA and Bonferroni multiple comparisons tests ****$p<0.0001$ for both concentrations, n=3 technical repeats). SCN- treatment at all concentrations was found to have an inhibitory effect on the expression of GP-91$^{phox;}$ however this was not statistically significant (Figure 7.13b).

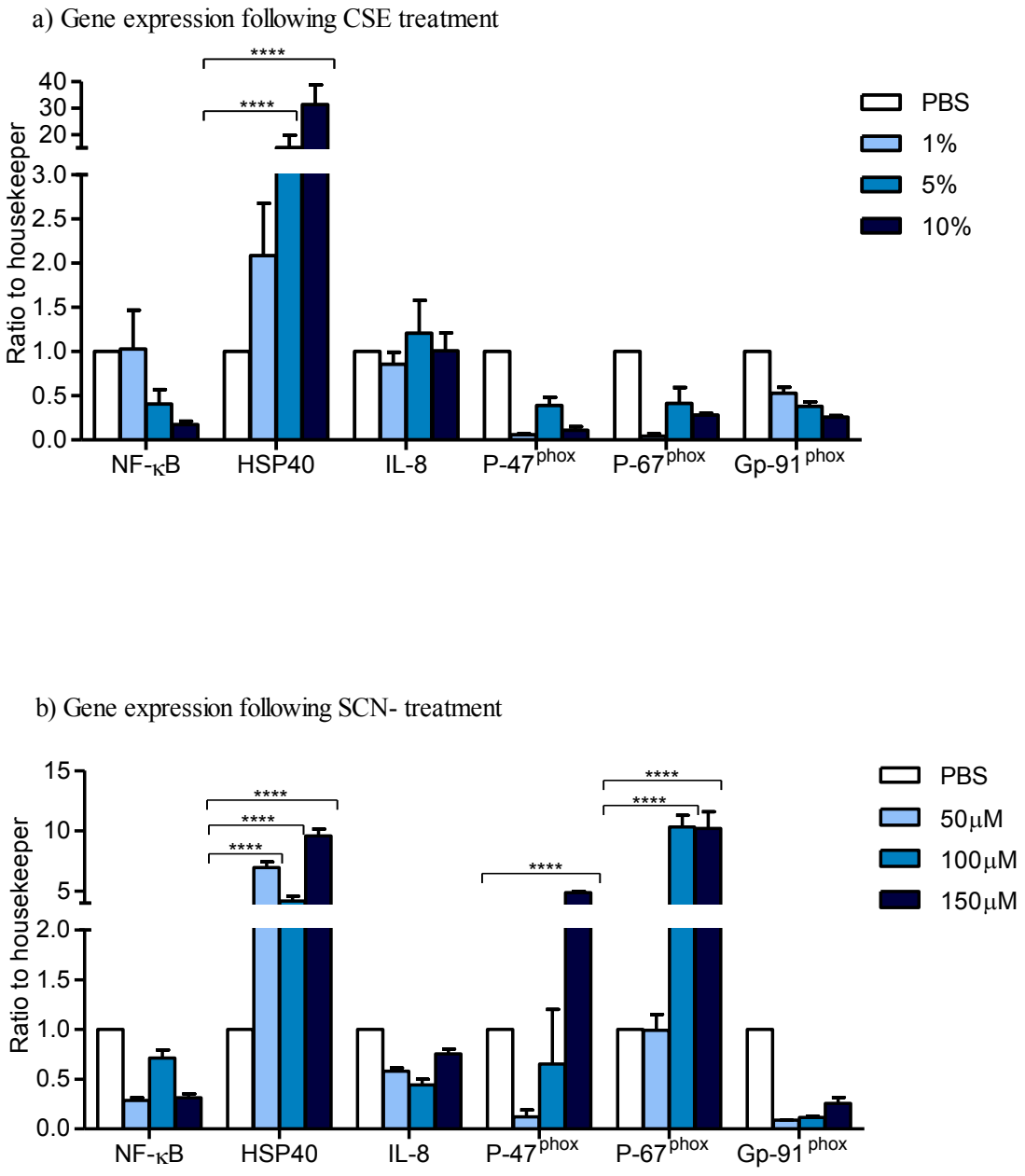

Figure 7.13: Gene expression following cigarette smoke extract or thiocyanate treatment

Neutrophil gene expression following treatment with (a) CSE or (b) SCN- is expressed as a ratio to the reference gene, YWHAZ, and RNA expression in cells treated with PBS (unstimulated negative control) is normalised to 1. Statistical significance was calculated using 1way ANOVA and Bonferroni post-tests (*****p<0.0001*). Data is expressed as mean ± SEM (n=10 pooled biological repeats and n=3 technical repeats in triplicate).

7.6 Discussion

The data reported in this chapter demonstrated that CSE has a differential effect upon *ex vivo* NET release, with CSE priming having an inhibitory effect upon PMA-induced NET production, but no effect on HOCl-induced NET formation. However, direct stimulation of neutrophils with CSE did not trigger NET release (section 7.2). This is in line with findings by Buls *et al.,* (2015), who also demonstrated attenuated PMA-induced NET release following CSE treatment. Notably the authors highlight commonalities between the effects of the anti-inflammatory drug Mesalazine and CSE, suggesting that smoking has a beneficial role in ulcerative colitis (UC) due to its ability to reduce NET release, and therefore reduce the aberrant inflammatory response. Whilst this may be true in UC, an inflammatory condition characterised by an exaggerated neutrophil response in the absence of a microbial infection, disease severity in pathologies such as periodontitis is positively correlated with smoking (Grossi *et al.,* 1994, 1995). This may be due to the presence of a pathogenic biofilm in periodontitis, whereby reduced NET production as a result of smoking may indirectly associate with reduced bacterial clearance and thus disease chronicity.

There is a paucity of literature investigating smoking and NET release, however there are several reports demonstrating the inhibitory effect of CSE on PMA-induced neutrophil ROS production (Ryder *et al.,* 1998, Nguyen *et al.,* 2001). PMA is a potent agonist for PKC, which triggers neutrophil NADPH-oxidase activation, and subsequent ROS production and ROS-dependent NET release. Whilst it is recognised that smoke exposure can alter PKC signalling and therefore influence cell inflammatory responses (Wyatt *et al.,* 1999, Whang *et al.,* 2013), the exact mechanisms involved in the cigarette-associated inhibition of neutrophil responses are not fully understood. Reduced neutrophil total and extracellular ROS and superoxide following CSE pre-treatment (Matthews *et al.,* 2011, 2012) have been observed in response to the periodontal pathogen, *F. nucleatum.* This suggests that smoking may subvert

the elimination of periodontal bacteria, as neutrophils are unable to effectively kill the colonising pathogens. No observable differences in HOCl-induced NET production following CSE priming supports a mechanism involving perturbed PKC signalling, as unlike PMA, HOCl activates neutrophils downstream of PKC (Palmer *et al.,* 2012). Notably the current data demonstrates that the inhibitory effects of CSE on NET release are not due to cytotoxic effects, as neutrophil viability was shown by trypan blue dye exclusion.

No differences were observed in NET release following pre-treatment with nicotine or cotinine, which is consistent with previous reports showing no differences in ROS production as a result of nicotine or cotinine exposure (Matthews *et al.,* 2011, 2012). On the other hand, SCN- stimulation caused a concentration dependent increase in NET release, whilst SCN- priming reduced PMA- and HOCl-induced NET production (section 7.3). SCN- is a product of hydrogen cyanide and the preferred substrate of MPO, which results in an increase in the production of hypothiocyanous acid (HOSCN) and a decrease in HOCl. HOSCN levels are therefore of particular interest in smokers, as SCN- is markedly increased in the plasma of these individuals (Morgan *et al.,* 2011). HOSCN selectively reacts with thiols (such as glutathione) (Nagy *et al.,* 2009), and due to elevations in HOSCN in smokers, causes increased depletion of thiols in these individuals. Interestingly increases in HOSCN, following a switch from HOCl production as a result of increased SCN-, is believed to afford protection against non-thiol targets and HOCl-mediated tissue damage (Talib *et al.,* 2012), yet HOSCN is still toxic towards pathogenic bacteria (Chandler *et al.,* 2013). Notably in order to benefit from increased levels of HOSCN, it is believed that adequate thiol repair systems are required, which if compromised, for example in smokers who reportedly have decreased antioxidant capacity (Reilly *et al.,* 1996), increased levels of HOSCN may actually exacerbate tissue damage. Thus Talib *et al.,* (2012) concluded that equilibrium between

HOSCN and HOCl production is required, and whether this is deleterious or beneficial may depend upon each individual's antioxidant defences.

With that in mind, salivary SCN- is reportedly implicated in the delayed wound healing observed in smokers (Mosely *et al.,* 1977). Conversely, a study investigating the effects of SCN- on gingival health demonstrated that toothpaste containing SCN- and H_2O_2 can inhibit plaque accumulation and gingivitis in periodontally healthy non-smokers (Rosin *et al.,* 2001). The authors hypothesise that this is the result of a synergistic process comprising the antimicrobial effects of SCN- and the ability of SCN- to enhance tissue regeneration (Kramer & Böhland 1996). A further consideration, which may be of particular relevance in periodontitis, where neutrophils are the predominant immune cell, is that HOSCN has been shown to up-regulate adhesion molecules such as E-selectin and intracellular adhesion molecule-1 (ICAM-1) in *in-vitro* experiments with human umbilical vein endothelial cells (HUVEC). Notably HOSCN-treated HUVEC monolayers bound 8-fold more neutrophils compared with untreated monolayers, which suggests HOSCN may promote neutrophil extravasation (Jian-Guo *et al.,* 2006). These findings may extend to periodontitis, whereby increased neutrophil accumulation in the gingival tissues of smokers, as a result of increased SCN-, may contribute to the self-perpetuating inflammation characteristic of the disease.

Chemotaxis is the movement of cells along a chemical signal gradient towards an infectious stimulus, which is orchestrated by various chemoattactants. During this process, neutrophils form pseudopods in the direction of the gradient following the ligation of GPCRs in response to chemoattactants (Andrew & Insall 2007). Neutrophils pre-treated with CSE exhibited reduced speed, velocity and directionality (resultant vector length) relative to untreated neutrophils, in response to fMLP and IL-8 (7.4). Notably, neutrophils were washed following pre-treatment with CSE, suggesting that the continued presence of CSE is not

required to exert its inhibitory effects on chemotaxis and thus transient cigarette exposure may have long-standing effects. Neutrophil chemotaxis is believed to be modulated by ROS, as chemotaxis in CGD patients and healthy DPI-treated (DPI is an NADPH-oxidase inhibitor) neutrophils exhibit reduced directionality (Hattori *et al.,* 2010). The authors postulate that neutrophils produce multiple pseudopods and NADPH-derived ROS are involved in modulating neutrophil directionality by destroying pseudopods that are not in the direction of the chemoattractant. This may be of interest in CSE-treated neutrophils, as CSE treatment has been found to have a significant inhibitory effect on neutrophil ROS release (Matthews *et al.,* 2011, 2012); therefore reduced ROS as a result of CSE treatment may contribute to the reduced chemotactic directionality observed in these studies. As previously discussed (1.7.3) smoking is a major risk factor for the development of periodontitis (Grossi *et al.,* 1994, 1995), and indeed recent findings by Roberts *et al.,* (2015) have demonstrated that neutrophil chemotaxis is dysfunctional in chronic periodontitis patients.

Conversely, whilst smoking may associate with reduced chemotaxis, the severity of periodontitis (determined by pocket depth) is positively correlated with neutrophil counts in dental plaque, saliva and GCF (Bhadbhade *et al.,* 2012). This suggests that whilst chemotactic accuracy may be compromised in periodontitis, neutrophils still reach the infected tissues, albeit with longer tissue transit times that may associate with increased neutrophil-mediated tissue damage. Worthy of note is the role of the matrikine, proline-glycine-proline (PGP), an extracellular matrix-derived peptide implicated in many cellular processes, including neutrophil chemotaxis, which is regulated by various MMPs, and increased levels have been reported to cause dose dependent neutrophil chemotaxis (van Houweligen *et al.,* 2008). Cigarette smoking is reported to increase MMP and PGP production, as well as inactivating leukotriene A4 hydrolase, which normally functions to reduce PGP-mediated neutrophil chemotaxis (Wells *et al.,* 2014). Collectively, these results

suggest that smoking promotes elevations in PGP-mediated neutrophil chemotaxis and recruitment; however whilst the contribution of smoking and PGP-mediated chemotaxis is described in inflammatory diseases such as COPD (Snelgrove *et al.,* 2010), their role in periodontitis remains to be elucidated.

Relative to the reference gene, YWHAZ, CSE and SCN- treatment caused a concentration dependent increase in neutrophil HSP40 expression (section 7.5.1). HSPs are highly conserved molecular chaperones that are involved in the protection of other proteins by orchestrating processes such as protein translation and folding (Benjamin & McMillan 1998). HSP expression is elevated in response to cell stressors, such as heat shock (Edwards & Hansen 1996) and wound healing (Laplante *et al.,* 1998), which affords protection and facilitates cell recovery. HSP40 is also believed to interact with and regulate many processes performed by HSP70 (Fan *et al.,* 2003). Guzik *et al.,* (2011) demonstrated that HSP70 significantly increases immediately following 100% CSE treatment, and notably HSP70 reportedly confers cell protection by inhibiting caspase dependent and independent apoptosis. This is consistent with findings by Matthews *et al.,* (2011), who also reported reduced neutrophil caspase-3 and -7 activity following CSE treatment. Elevations in HSP40 in response to CSE and SCN- treatment shown in the current work may therefore suppress apoptosis by interactions with HSP70. In the periodontal tissues of smokers, this may associate with neutrophil longevity and necrosis, which may contribute to exacerbated inflammation tissue damage and adverse treatment responses (Delima *et al.,* 2010).

Following treatment with SCN-, P-47^{phox} and P-67^{phox} gene expression levels were significantly increased. Both P-47^{phox} and P-67^{phox} are cytosolic subunits that play a critical role in the activation of NADPH-oxidase (section 7.5.2). The current findings investigating the ability of SCN- to stimulate neutrophils suggests that SCN- results in a concentration

dependent increase in NET release, which was supported by the gene expression data whereby SCN- activates NADPH-oxidase. It would be interesting to characterise this mechanism further by analysing gene expression in response to priming with SCN- prior to stimulation with periodontal bacteria, however due to time constraints this was not investigated in the present work. Differences in P-47^{phox} and P-67^{phox} expression were not observed following CSE treatment, highlighting that despite SCN- being a major component of cigarette smoke, these substances alter neutrophil function by distinct mechanisms. Notably the expression of P-47^{phox} and P-67^{phox} does not differ between non-smoker chronic periodontitis patients and healthy controls (Matthews *et al.,* 2007), suggesting that other mechanisms are involved in the exaggerated neutrophil responses observed in periodontitis. Furthermore, despite not reaching statistical significance, GP-91^{phox} expression was considerably lower in response to all concentrations of CSE and SCN- treatment. Findings by Matthews *et al.,* (2007) demonstrated that GP-91^{phox} expression was down-regulated in both healthy and periodontitis patient-derived neutrophils following stimulation with periodontal bacteria. In SCN- treated cells, this may well be a protective mechanism to compensate for the increased expression of P-47^{phox} and P-67^{phox} observed following SCN- treatment. Notably, abolished GP-91^{phox} expression is characteristic of X-linked CGD, which is associated with reduced ROS production and consequently recurrent bacterial infections (Williams *et al.,* 1995). As previously discussed, decreased ROS production is reported in CSE-treated neutrophils (Matthews *et al.,* 2011, 2012), thus it is possible that reduced GP-91^{phox} gene expression also contributes to attenuated ROS release and the subsequent reductions in NADPH-oxidase dependent NET production observed in CSE and SCN- primed neutrophils.

In conclusion, the presented data demonstrates that CSE and SCN- priming have an inhibitory effect on NET release, albeit these responses appear stimulus specific, and CSE

treated neutrophils exhibit reduced chemotaxis in response to known chemoattractants. CSE and SCN- both promoted HSP40 expression; however differential Phox gene expression was observed in response to CSE and SCN- treatment. Collectively these data suggest that cigarette smoking alters neutrophil activation and SCN- is one component of cigarettes that may contribute to the perturbed innate immune responses observed *in vivo*.

CHAPTER 8: NET PRODUCTION IN OTHER INFLAMMATORY PERIODONTAL DISORDERS: GINGIVITIS & PAPILLON LEFÈVRE SYNDROME

8.1 Introduction

To enhance our understanding of the temporality of NET production following plaque accumulation and their contribution to periodontal tissue damage, studies of neutrophil function during the transition from health to gingivitis were performed (section 8.2). In addition, NET production in patients with Papillon Lefèvre syndrome (PLS) was systematically evaluated in order to shed light upon key stages in the process, which may be dependent upon the cathepsin C and neutrophil serine proteases (NSPs) reported to be deficient in PLS patients (section 8.3).

8.2 Experimental gingivitis

To quantify peripheral neutrophil responses in experimental gingivitis, a split mouth 21-day experimental gingivitis model was investigated in 10 healthy volunteers (Loe *et al.,* 1965). (2.2.6.2). Volunteers wore a mouth guard that covered the maxillary left 4-6 teeth (test) during brushing for 21 days (3 weeks) (South Birmingham Research Ethics Committee 2004/074). At day 21 of plaque accumulation all plaque was removed by prophylaxis and volunteers recommenced normal brushing prior to final assessment at day 35 (designated as return to health). The maxillary right 4-6 teeth (control) were used as a control, as these teeth were subjected to normal oral hygiene procedures throughout the 21-day period of non-brushing at test sites. Neutrophils were isolated from the peripheral blood of volunteers to study NET production in response to known stimuli during transition from gingival health to gingivitis (2.2.3.3, 2.2.3.4). Plasma-derived NET degradation and plasma levels of IgG (1-4 subclasses) and FLCs were also determined (undertaken by The Binding Site Group Ltd, Birmingham, UK, sections 2.2.5.1, 2.2.5.2). In addition, the effect of plaque on neutrophil ROS and NET responses were also investigated.

8.2.1 Clinical measures of gingivitis

To confirm the development of gingival inflammation and subsequent resolution of gingivitis at 35 days, several clinical parameters were measured (section 2.2.6.3.2). Plaque index (PI) and gingival index (GI) were recorded at days 0, 7, 14, 21 and 35 from test and control sites. The volume of gingival crevicular fluid (GCF) was also measured using a calibrated Periotron 8000^{TM} (Chapple *et al.,* 1999). GCF was collected over a 30 sec period by inserting Periopaper strips (OraFlow) into the mesio-buccal gingival crevices of test and control sites. All clinical parameters were measured immediately prior to blood collection for neutrophil assays by a single experienced examiner.

8.2.1.1 Plaque index

Mean plaque indices measured across 3 sites from volunteers at days 0, 7, 14, 21 and 35 were significantly higher at the test site compared with the control site at days 7, 14 and 21 (2way ANOVA and Bonferonni post-test $^{**}p<0.01$, $^{****}p<0.0001$, $^{****}p<0.0001$ for days 7, 14 and 21, respectively, n=10) (Table 8.1).

8.2.1.2 Gingival index

Mean gingival indices measured across 3 sites from volunteers at days 0, 7, 14, 21 and 35 were significantly higher at the test site compared with the control site at days 14 and 21 (2way ANOVA and Bonferonni post-test $^{**}p<0.01$, $^{*}p<0.05$ for days 14 and 21, respectively, n=10) (Table 8.2).

8.2.1.3 Gingival crevicular fluid

Mean gingival crevicular fluid (GCF) calibrated volumes recorded from 3 test and control sites at days 0, 7, 14, 21 and 35 were higher at test sites at days 7, 14 and 21; however this did not reach statistical significance (n=10) (Table 8.3).

Table 8.1: 21-day gingivitis model: plaque index

Plaque indices were recorded from volunteers' test and control sites at days 0, 7, 14, 21 and 35. Data are presented as mean plaque index across 3 sites (mean ± SD and range) (n=10).

Plaque Index										
Volunteer Number	**Control**					**Test**				
	Day: 0	**Day: 7**	**Day: 14**	**Day: 21**	**Day: 35**	**Day: 0**	**Day: 7**	**Day: 14**	**Day: 21**	**Day: 35**
1	1.33	0.67	0.33	0.33	0.33	1.00	1.67	1.33	4.67	0.00
2	1.00	1.00	1.33	1.00	1.00	0.67	1.33	3.67	2.33	1.00
3	1.67	1.33	1.33	1.33	0.67	1.00	1.00	1.67	3.67	0.33
4	2.00	0.33	1.00	2.00	1.33	1.67	2.33	3.33	4.33	1.33
5	1.33	0.67	0.00	0.33	0.33	1.67	3.67	5.00	5.00	1.00
6	0.33	0.00	0.33	0.00	0.33	0.67	1.00	3.33	5.00	0.33
7	2.00	1.00	1.00	1.00	2.33	1.67	3.67	5.00	5.00	2.00
8	0.67	0.00	0.00	0.00	0.00	0.67	1.33	3.67	3.00	0.33
9	0.33	0.00	0.33	0.00	0.33	0.33	1.67	3.00	2.00	0.33
10	1.33	0.33	0.33	0.00	1.00	1.67	4.00	5.00	5.00	0.67
Mean	**1.2**	**0.5**	**0.6**	**0.6**	**0.8**	**1.1**	**2.2**	**3.5**	**4.0**	**0.7**
SD	**0.6**	**0.5**	**0.5**	**0.7**	**0.7**	**0.5**	**1.2**	**1.3**	**1.2**	**0.6**

Table 8.2: 21-day gingivitis model: gingival index

Gingival index measurements were recorded from volunteers' test and control sites at days 0, 7, 14, 21 and 35. Data presented as mean gingival index across 3 sites (mean ± SD and range) (n=10).

Gingival Index										
Volunteer Number	**Control**					**Test**				
	Day: 0	**Day: 7**	**Day: 14**	**Day: 21**	**Day: 35**	**Day: 0**	**Day: 7**	**Day: 14**	**Day: 21**	**Day: 35**
1	0.00	0.00	0.33	0.33	0.33	1.67	0.33	1.00	0.33	0.33
2	0.00	0.33	0.33	0.00	0.67	2.00	1.67	1.33	1.33	0.00
3	0.00	0.00	0.00	0.67	0.00	0.67	0.33	0.33	0.33	0.00
4	0.00	0.00	0.33	0.00	0.00	0.67	1.00	1.33	1.33	0.67
5	0.33	0.67	1.33	0.67	0.00	0.33	1.00	1.67	1.67	0.00
6	0.67	0.00	0.00	1.00	0.33	0.67	2.33	2.00	1.67	0.33
7	0.67	0.00	0.33	0.00	0.00	1.00	1.00	2.33	2.00	1.33
8	0.33	0.33	0.00	0.67	0.33	1.00	0.67	1.00	1.00	0.00
9	0.33	0.00	0.00	0.00	0.00	0.00	0.67	0.33	0.33	0.00
10	0.33	0.00	0.00	0.00	0.00	0.67	1.00	1.00	1.33	0.67
Mean	**0.3**	**0.1**	**0.3**	**0.3**	**0.2**	**0.9**	**1.0**	**1.2**	**1.1**	**0.3**
SD	**0.3**	**0.2**	**0.4**	**0.4**	**0.2**	**0.6**	**0.6**	**0.6**	**0.6**	**0.4**

Table 8.3: 21-day gingivitis model: gingival crevicular fluid volume

Gingival crevicular fluid (GCF) volumes were recorded from volunteers' test and control sites at days 0, 7, 14, 21 and 35. Data presented as mean volumes (µl) across 3 sites (mean ± SD and range) (n=10).

Gingival crevicular fluid calibrated volumes (µl)										
Volunteer Number	**Control**					**Test**				
	Day: 0	**Day: 7**	**Day: 14**	**Day: 21**	**Day: 35**	**Day: 0**	**Day: 7**	**Day: 14**	**Day: 21**	**Day: 35**
1	0.06	0.17	0.11	0.08	0.08	0.12	0.21	0.18	0.36	0.14
2	0.28	0.11	0.14	0.22	0.11	0.51	0.63	0.34	0.53	0.59
3	0.05	0.03	0.06	0.39	0.06	0.06	0.23	0.23	0.79	0.52
4	0.13	0.40	0.50	0.11	0.20	0.08	0.59	1.11	2.50	1.16
5	0.07	0.32	0.25	0.49	1.38	0.15	1.08	0.56	0.39	2.64
6	0.04	0.17	0.08	0.05	0.14	0.09	0.13	0.27	0.14	0.20
7	0.54	1.12	0.33	1.29	0.24	0.68	3.75	5.12	4.92	0.33
8	0.15	0.05	0.05	0.05	0.12	0.16	0.25	0.17	0.32	0.30
9	0.06	0.15	0.07	0.07	0.10	0.07	0.14	0.08	0.09	0.06
10	0.09	0.06	0.08	0.05	0.09	0.17	0.47	0.79	0.44	0.18
Mean	**0.1**	**0.3**	**0.2**	**0.3**	**0.3**	**0.2**	**0.7**	**0.9**	**1.0**	**0.6**
SD	**0.2**	**0.3**	**0.1**	**0.4**	**0.4**	**0.2**	**1.1**	**1.5**	**1.5**	**0.8**

8.2.2 NET production during the 21-day experimental gingivitis model

Blood was collected from study volunteers at days 0, 21 and 35 to assay NET-DNA production in response to PMA (50nM) and HOCl (0.75mM) (2.2.3.3). Baseline NET production in response to PBS (negative unstimulated control) was also quantified. There was no significant difference in NET production between each time-point in any treatment condition (1way ANOVA *p=0.1621, p=0.1092, p=0.0546* in response to PBS (unstimulated), PMA or HOCl, respectively, n=10) (Figure 8.1).

8.2.3 Visualisation of NET production during the 21-day experimental gingivitis model

There was no qualitative difference observed in NET production at days 0, 21 and 35 (2.2.3.7). Both PMA (50nM) and HOCl (0.75mM) produced NETs, and some PBS-treated neutrophils also stained positive for DNA, which is likely due to necrosis during the incubation period, which enables Sytox green to permeate the compromised cell membrane (Figure 8.2).

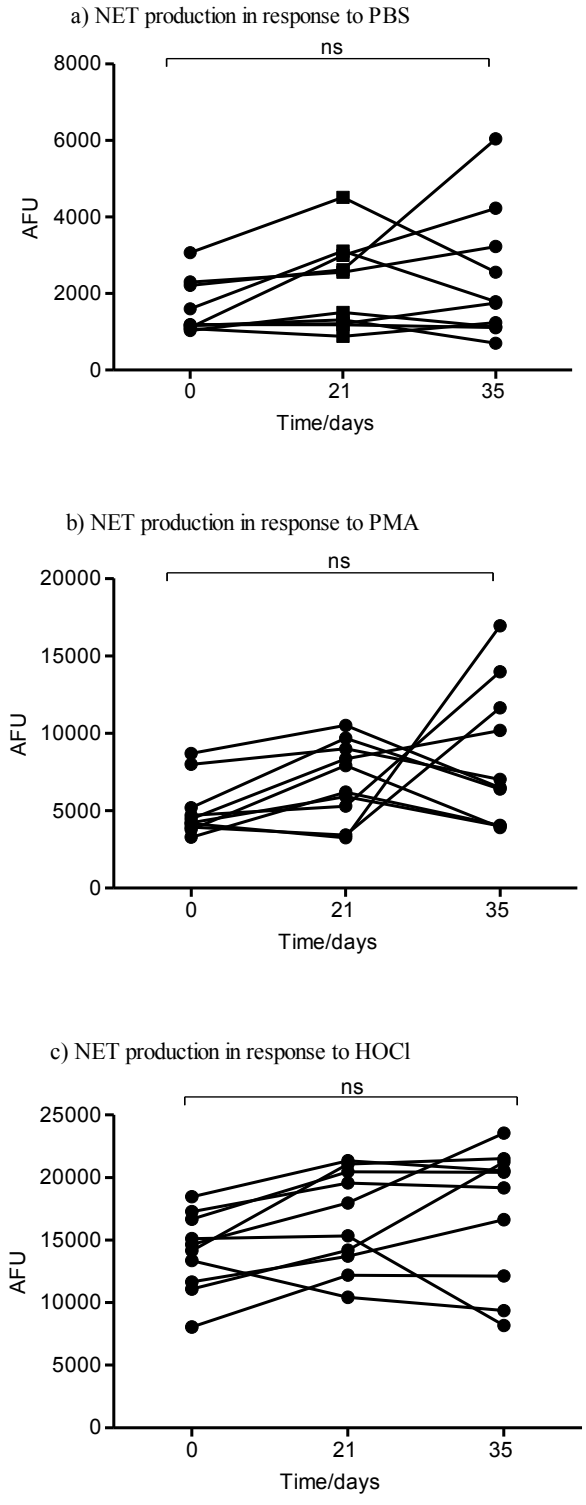

Figure 8.1: NET production during the 21-day experimental gingivitis model
NETs were quantified fluorometrically following a 3 hour incubation period at days 0, 21 and 35. (a) PBS (unstimulated negative control), (b) PMA-stimulated neutrophils (50nM) and (c) HOCl-stimulated neutrophils (0.75mM). Statistical significance calculated using 1way ANOVA (ns=not significant). Data presented as arbitrary fluorescence units (AFU) and expressed as mean ± SEM (n=10 in triplicate).

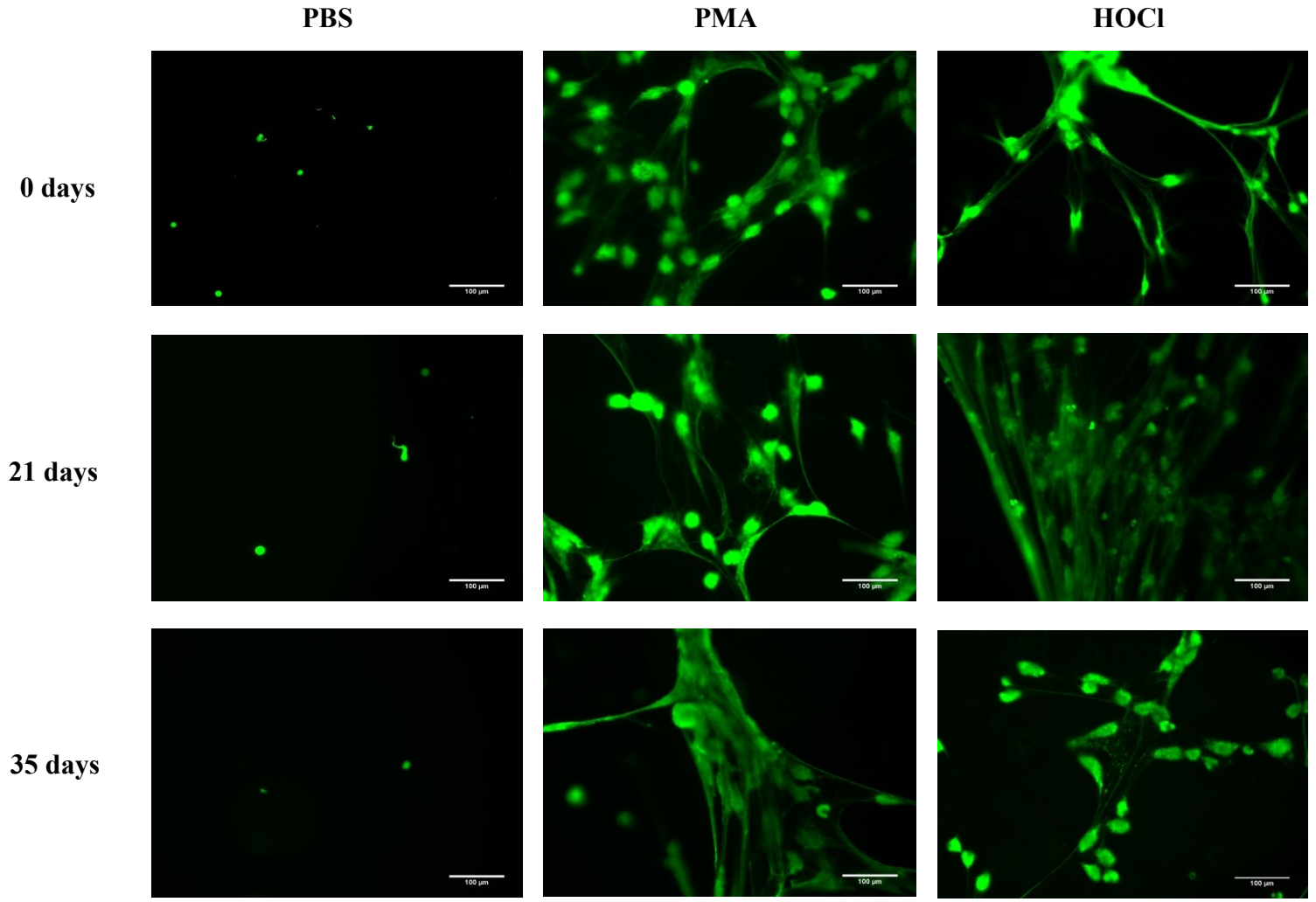

Figure 8.2: Visualisation of NET production during the 21-day experimental gingivitis model
NETs were visualised by fluorescence microscopy (x20 magnification) with Sytox green staining in response to PBS (negative unstimulated control), PMA (50nM) and HOCl (0.75mM) at days 0, 21 and 35. Images are representative of 10 volunteers in duplicate. Scale bar is 100µm.

8.2.4 NET degradation by volunteer plasma during the 21-day experimental gingivitis model

To investigate the effect of gingivitis upon NET degradation by plasma, neutrophils were stimulated for NET production with HOCl (0.75mM) and NETs were subsequently subjected to 3 hours incubation with 10% plasma (2.2.5.1). NETs from periodontally and systemically healthy volunteers were incubated with plasma derived from experimental gingivitis volunteers at 0, 21 and 35 days. Following incubation, the number of degraded NETs was quantified fluorometrically using the Sytox green assay. The percentage of NETs degraded was calculated in relation to a 15 min MNase digestion, which was used to represent the 100% digestion standard (Hakkim *et al.,* 2010). In the 10 volunteers analysed there was no significant difference in NET degradation between the different time-points (1way ANOVA *p=0.3828,* n=10). It was also noted that the lowest NET-degrading plasma (27%, 47% and 26% at time-points 0, 21 and 35 days respectively) were from the same individual (Figure 8.3).

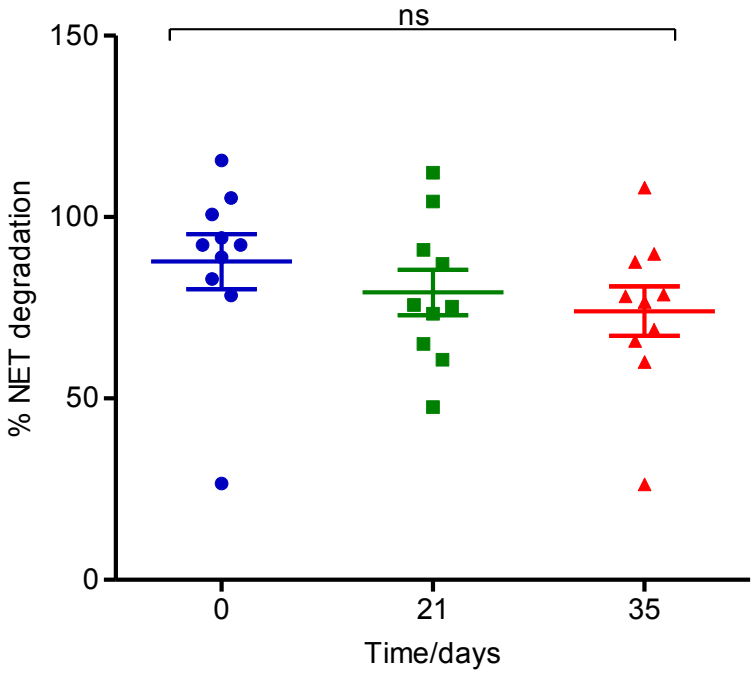

Figure 8.3: NET degradation by volunteer plasma during the 21-day experimental gingivitis model

HOCl-stimulated (0.75mM) neutrophils were incubated with 10% plasma from volunteers at days 0, 21 and 35. NETs were quantified fluorometrically using the Sytox green assay. % NET degradation was calculated based on a 1Unit/ml MNase digest, which was used to represent the 100% standard. Statistical significance calculated using 1way ANOVA (ns=not significant). Data presented as % NET degradation and expressed as mean ± SEM (n=10 in triplicate).

Whilst NET degradation appeared unimpeded in experimental gingivitis relative to health, chronic periodontitis patients exhibited reduced NET degradation by plasma, which may be the result of increased levels of IgGs and free light chains (FLCs) (Chapter 6). To determine whether volunteers with experimental gingivitis also had elevated levels of circulating IgGs and FLCs, IgG subclass 1-4 and FLC concentrations were measured in plasma collected at days 0, 21 and 35 (2.2.5.2, Appendix V).

8.2.4.1 Plasma IgG concentrations during the 21-day experimental gingivitis model

IgG subclasses 1-4 concentrations were measured in plasma samples from study volunteers at days 0, 21 and 35. Protein turbidimetric analysis demonstrated no significant differences between the detection of IgG1, IgG2, IgG3 or IgG4 at the different time-points analysed (1 way ANOVA *p=0.903, p=0.996, p=0.924, p=0.952* for IgG1, IgG2, IgG3 and IgG4, respectively, n=10). A small number of samples were outside of the IgG reference ranges (IgG1: 3.824-9.286g/L, IgG2: 2.418-7.003g/L, IgG3: 0.218-1.761g/L, IgG4 0.039-0.864) (Schauer *et al.,* 2003), however, this was not associated with specific time-points in the gingivitis model (Figure 8.4).

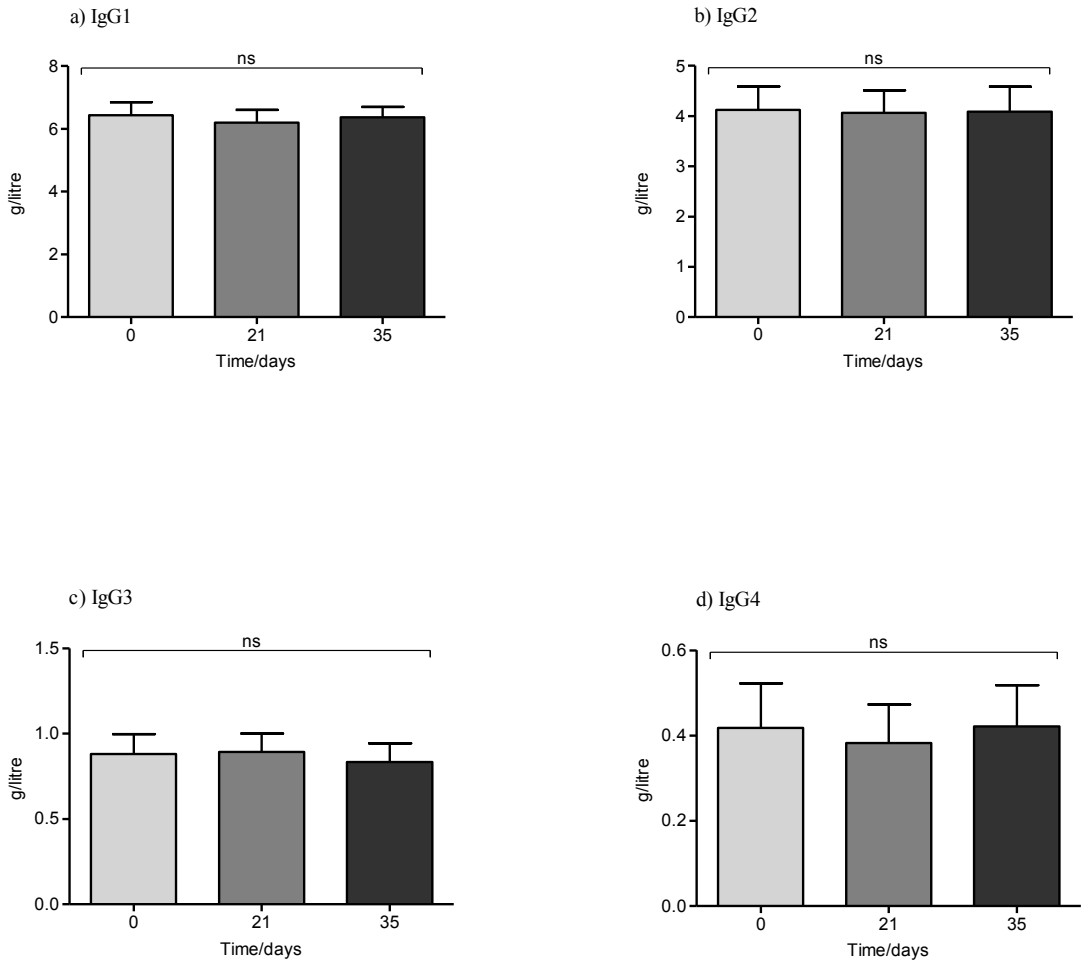

Figure 8.4: Plasma IgG concentrations during the 21-day experimental gingivitis model
IgG subclasses 1-4 concentrations were measured in plasma samples from study volunteers at days 0, 21 and 35. Protein turbidimetric analysis demonstrated no significant difference between the detection of IgG1, IgG2, IgG3 or IgG4 at the different time points (1 way ANOVA, ns=not significant). Data expressed as means ± SEM (n=10).

8.2.4.2 Plasma FLC concentration during the 21-day experimental gingivitis model

Free kappa and lambda light chains were measured in plasma samples from study volunteers at days 0, 21 and 35. Protein turbidimetric analysis demonstrated no significant differences between the detection of free kappa light chain, free lambda light chains, the kappa/lambda ratio or summated FLC values (1 way ANOVA *p=0.972, p=0.741, p=0.969, p=0.833* for free kappa light chain, free lambda light chains, kappa/lambda ratio or summated FLC values, respectively, n=10). A small number of samples were outside of the reference ranges (free kappa light chains: 3.3-19.4mg/litre, free lambda light chains: 5.71-26.3mg/litre, kappa/lambda ratio: 0.26-1.65, summated FLC: 9.01-45.7) (Katzmann *et al.,* 2002), however, this was not associated with specific time-points in the gingivitis model (Figure 8.5).

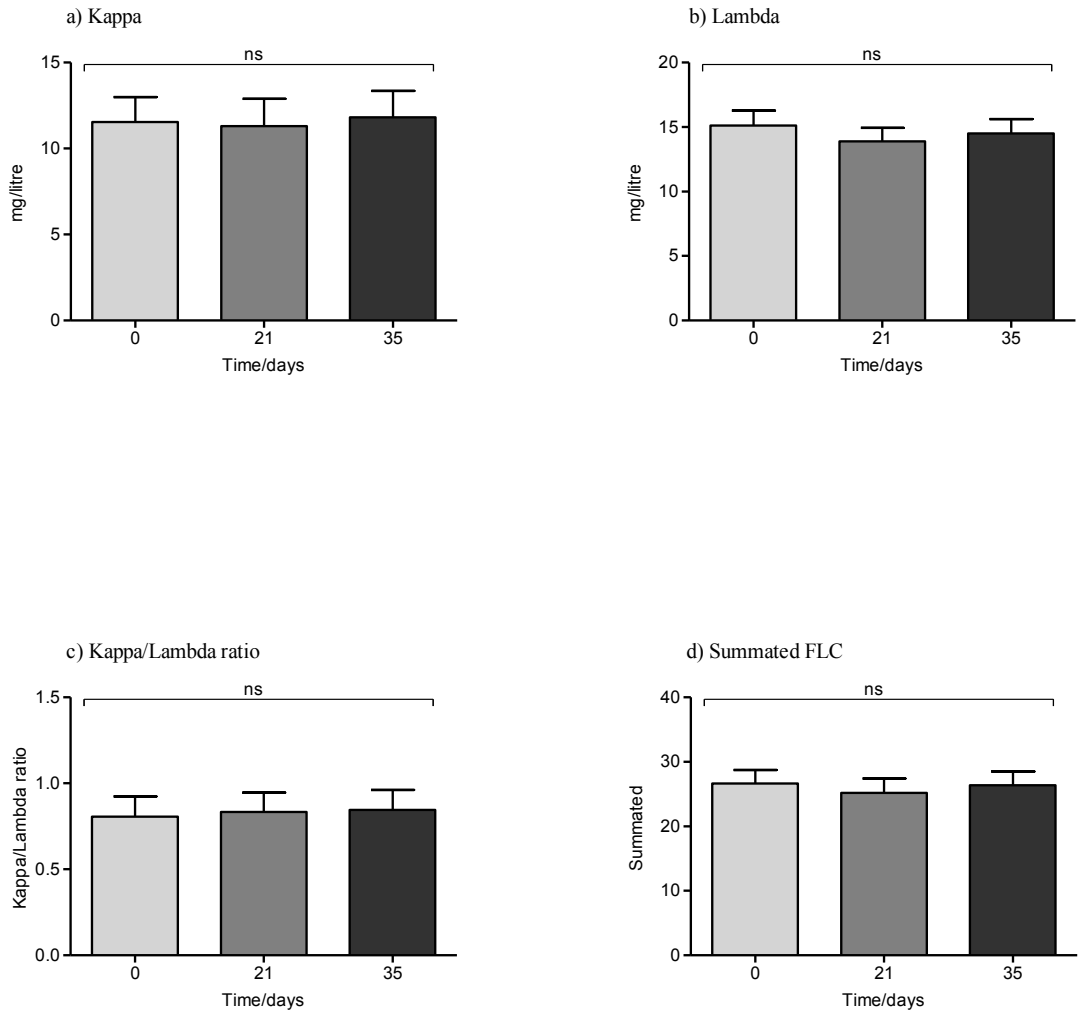

Figure 8.5: Plasma FLC concentration during the 21-day experimental gingivitis model Free kappa and free lambda light chains, the kappa/lambda ratio and summated FLCs were measured in plasma samples from study volunteers at days 0, 21 and 35. Protein turbidimetric analysis demonstrated no significant difference between the detection of free kappa light chain, free lambda light chains, the kappa/lambda ratio or summated FLC values (1 way ANOVA, ns=not significant). Data expressed as means ± SEM (n-10).

The ability of a plaque biofilm to stimulate neutrophil responses

Increasing concentrations of plaque were employed as a stimulus for ROS and NETs in neutrophils derived from a healthy volunteer to investigate whether plaque activates neutrophil effector functions (2.2.6.2.4). Neutrophil NET and ROS production were quantified in response to stimulation with plaque at increasing percentage concentrations (0, 12.5, 25, 50 75 and 100%), compared with PMA (50nM) stimulation (Figure 8.6). There was a gradual increase in NET and ROS production in response to neutrophil stimulation by plaque (n=2). Based on these results, subsequent experiments assaying NET and ROS production in response to plaque derived from the experimental gingivitis model were diluted in PBS and used at 25%.

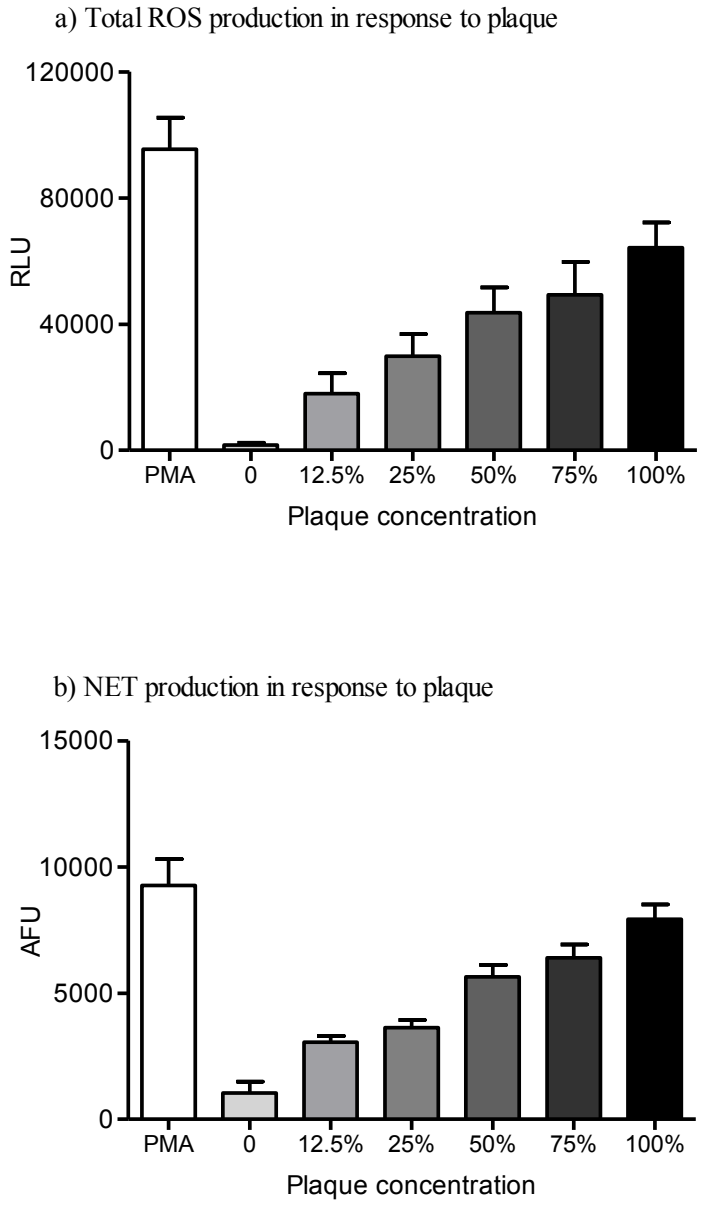

Figure 8.6: The ability of a plaque biofilm to stimulate neutrophil responses
The effect of increasing concentrations of plaque (0, 12.5, 25, 50, 75 and 100%) and PMA (50nM) on neutrophils (a) ROS and (b) NET production. Data expressed as mean ± SEM. Data is presented as (a) RLU (relative light units) and (b) AFU (arbitrary fluorescence units) (n=2 in triplicate).

8.2.5 Neutrophil ROS and NET production in response to plaque stimulation

Plaque was collected from test and control sites from 10 volunteers at days 0, 7, 14, 21 and 35. Plaque samples (n=10) were homogenised, pooled and diluted (to 25% of the original concentration) for subsequent assays in which plaque was employed as a stimulus for NET and ROS production in healthy volunteers (n=5) (2.2.6.2.4). To characterise the plaque samples collected, the amount of protein (2.2.6.2.5.3), LPS (2.2.6.2.5.1) and DNA (2.2.6.2.5.2) in the pooled plaque samples were measured to enable the ROS and NET quantification results to be normalised for the plaque content.

ROS production normalised for protein content

Plaque collected from test sites at 7, 14 and 21 days induced significantly higher ROS production after normalising for plaque protein content (2way ANOVA and Bonferroni post-tests $**p<0.01$, $****p<0.0001$ and $**p=0.01$ at days 7, 14 and 21, respectively, n=10 samples and n=5 technical repeats) (Figure 8.7a)

ROS production normalised for LPS content

Plaque collected from test sites at 7, 14 and 21 days induced significantly higher ROS production after normalising for plaque LPS content (2way ANOVA and Bonferroni post-tests $*p<0.05$, $****p<0.0001$, $**p<0.01$ at days 7, 14 and 21, respectively, n=10 samples and n=5 technical repeats) (Figure 8.7b)

ROS production normalised for DNA content

Plaque collected from test sites at 7, 14 and 21 days induced significantly higher ROS production after normalising for plaque DNA content (2way ANOVA and Bonferroni post-tests $****p<0.0001$, $****p<0.0001$, $*p<0.05$ at days 7, 14 and 21, respectively, n=10 samples and n=5 technical repeats) (Figure 8.7c).

a) ROS results normalised for plaque proetin content

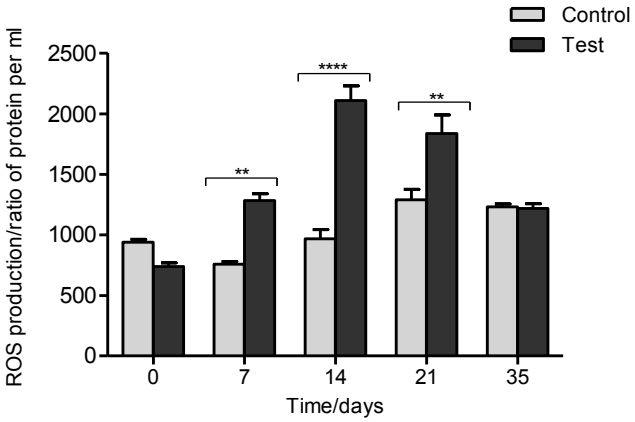

b) ROS results normalised for plaque LPS content

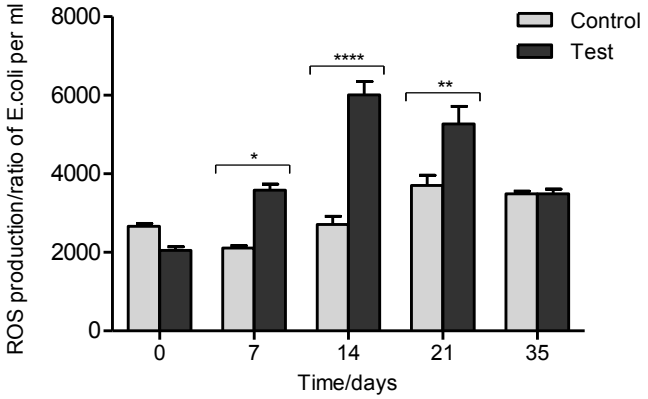

c) ROS results normalised for plaque DNA content

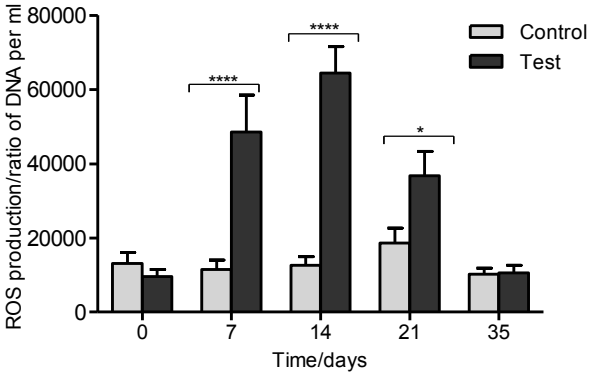

Figure 8.7: ROS production in response to plaque stimulation

ROS production was quantified in response to plaque stimulation (25%) collected at 0, 7, 14, 21 and 35 days from test and control sites and employed as a stimulus on healthy volunteer neutrophils. ROS production was normalised for (a) plaque protein content, (b) plaque LPS content, (c) plaque DNA content. Statistical significance was calculated using 2way ANOVA and Bonferroni post-tests (*$p<0.05$, ****$p<0.0001$). Data presented as RLU (relative light units) and expressed as mean ± SEM (n=10 samples and n=5 technical repeats).

NET production normalised for protein content

Plaque collected from test sites at 7, 14 and 21 days induced significantly higher NET production after normalising for plaque protein content (2way ANOVA and Bonferroni post-tests $p<0.01$, $p<0.0001$, $p=0.01$ for days 7, 14 and 21, respectively, n=10 samples and n=5 technical repeats) (Figure 8.8a).

NET production normalised for LPS content

Plaque collected from test sites at 7, 14 and 21 days induced significantly higher NET production after normalising for plaque LPS content (2way ANOVA and Bonferroni post-tests $p<0.01$, $p<0.0001$, $p<0.01$ at days 7, 14 and 21, respectively, n=10 samples and n=5 technical repeats) (Figure 8.8b).

NET production normalised for DNA content

Plaque collected from test sites at 7 and 14 days induced significantly higher NET production after normalising for plaque DNA content (2way ANOVA and Bonferroni post-tests $p<0.0001$for days 7 and 14, n=10 samples and n=5 technical repeats) (Figure 8.8c).

a) NET production normalised for plaque protein content

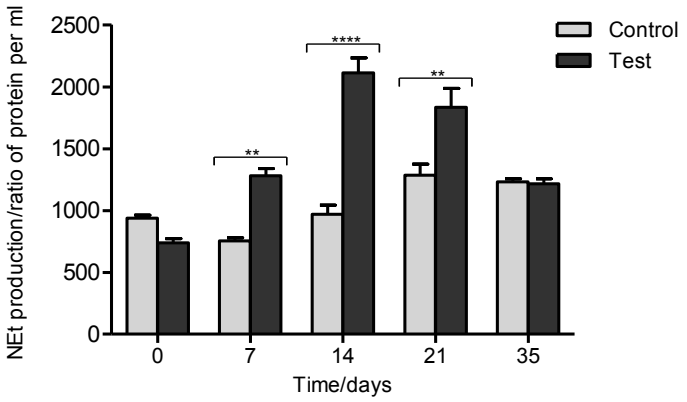

b) NET production normalised for plaque LPS content

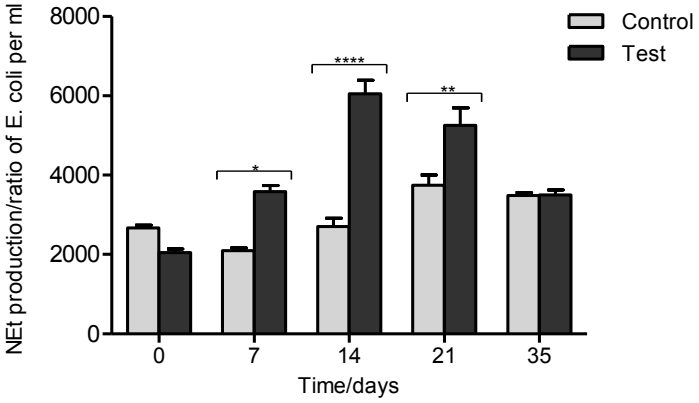

c) NETs production normalised for plaque DNA content

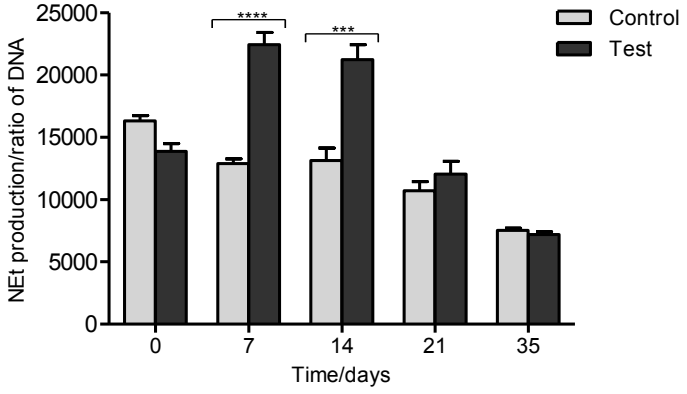

Figure 8.8: NET production in response to plaque stimulation

NETs were quantified in response to plaque stimulation (25%) collected at 0, 7, 14, 21 and 35 days from test and control sites and employed as a stimulus on healthy volunteer neutrophils. NET production was normalised for (a) plaque protein content, (b) plaque LPS content, (c) plaque DNA content. Statistical significance was calculated using 2way ANOVA and Bonferroni post-tests (*$p<0.05$, **$p<0.01$, ****$p<0.0001$). Data presented as AFU (arbitrary fluorescence units) and expressed as mean ± SEM (n=10 samples and n=5 technical repeats).

8.3 Papillon Lefèvre syndrome

The release of NETs represents a multi-stage process that is reliant on the neutrophil serine protease (NSP), neutrophil elastase (NE) (Papayannopoulos *et al.,* 2010). NE is activated by cathepsin C, which is the deficient cysteine protease in PLS patients. Therefore, PLS patients provide an interesting clinical model for the study of NET biology in relation to periodontitis. NET responses in PLS patients with severe pre-pubertal periodontitis were investigated alongside healthy gender-matched controls (2.2.6.4). All PLS patients were genotyped, assessed for co-morbidities and their dermatological and periodontal health determined (2.2.6.4.1). Neutrophils were isolated from patients and controls to investigate what effect cathepsin C deficiency in PLS had upon peripheral NET production. NETs were quantified by the release of NET-DNA (Sytox green) and also NET-bound proteases (neutrophil elastase [NE], myeloperoxidase [MPO] and cathepsin G [CG]) (2.2.3.3, 2.2.3.4). Plasma samples were also collected from patients and controls and subsequent experiments analysed plasma samples for the expression of NE and LL-37 (2.2.6.4.2). Whilst the production of NET-DNA was quantified in all patients, due to low patient blood neutrophil counts, subsequent NET assays did not include patient 1 or 2.

Table 8.4: Clinical measures of PLS

PLS patient volunteer information, including age, sex, ethnicity, PLS type, mutation, oral health, dermatological health, co-morbidities and current medication. Abbreviations: BMI, (body mass index), PPK (palmar plantar hyperkeratosis)

Volunteer no.	Age	Sex	Ethnicity	BMI	PLS type	Mutation	Oral health	Dermatological health	Co-morbidities	Medication
1	12	Male	Caucasian	18.93	Heterozygous	1/2 G139R; 1/2 N427T	No significant pocketing	No skin problems	None recorded	None recorded
2	14	Female	Indian	19.90	Heterozygous	Unidentified	Tooth pain & discomfort, teeth very mobile, bleeding on brushing.	Moderate PPK	β-thalassemia carrier (from mother)	None recorded
3	14	Female	Pakistani	20.04	Homozygous	2/2 R272P	Dentures	PPK - quite bad on feet, deep fissures; hands ok	None recorded	Acitretin once daily. Vitamin D replacement therapy
4	9	Male	Pakistani	22.83	Not done	2/2 R272P	Teeth OK and good oral hygiene.	Lips prone to cracking	Vitamin D deficiency. Previous cerebral intracranial abscesses.	Acitretin once daily
5	14	Male	Pakistani	18.15	Homozygous	2/2 R272P	Dentures with pain on replacing and denture stomatitis.	Mild PPK - hands very good	History of recurrent infections since birth.	Acitretin once daily

8.3.1 Comparison of NET production by PLS patients and healthy controls

Venous blood was collected from PLS patients and controls to quantify their NET-DNA production in response to a 4 hour stimulation with PMA (50nM), HOCl (0.75mM), opsonised *S. aureus* ($5x10^7$ and MOI of 500)*, S. gordonii* ($1x10^8$ and MOI of 1000) or *F. nucleatum poly* ($1x10^8$ and MOI of 1000) (2.2.3.3). Baseline NET production in response to PBS (unstimulated negative control) was also quantified. There was no significant difference in NET-DNA production between patients and controls in response to PBS (2way ANOVA and Bonferroni post-tests $p>0.05$). Systemically and periodontally healthy controls exhibited higher NET release in response to stimulation, which was statistically significant for PMA, HOCl and *F. nucleatum poly* (2way ANOVA and Bonferroni post-tests $p<0.0001$, $p<0.0001$, $p<0.001$, respectively) (Figure 8.9a).

8.3.1.1 Quantification of NET-bound components in PLS patients and healthy controls

In addition to quantifying NET-DNA, NET release from PLS patients and controls was determined by quantifying NET-bound proteins (2.2.3.4). NE, MPO and CG were colorimetrically quantified in response to 4 hours stimulation with PMA (50nM), HOCl (0.75mM), *A. actinomycetemcomitans* (serotype b) or *V. parvula* (all bacteria at $1x10^8$ and MOI of 1000) and PBS (unstimulated negative control).

Quantification of NET-bound neutrophil elastase

Healthy controls produced significantly more NETs, as determined by NET-bound neutrophil elastase (NE), compared with PLS patients in response to PMA (50nM), HOCl (0.75mM), *A. actinomycetemcomitans* (serotype b) and *V. parvula* (all bacteria at $1x10^8$ and MOI of 1000) (2way ANOVA and Bonferroni post-tests $****p<0.0001$, $****p<0.0001$, $***p<0.001$, $****p<0.0001$, respectively). There was no difference between control and patient NET

production in response to PBS (unstimulated negative control) (2way ANOVA and Bonferroni post-tests *p>0.05*) (Figure 8.9b).

Quantification of NET-bound myeloperoxidase

Healthy controls produced significantly more NETs, as determined by NET-bound myeloperoxidase (MPO), compared with PLS patients in response to PMA (50nM), HOCl (0.75mM), *A. actinomycetemcomitans* (serotype b) and *V. parvula* (all bacteria at $1x10^8$ and MOI of 1000) (2way ANOVA and Bonferroni post-tests *$p<0.05$, ***$p<0.001$, *$p<0.05$, *$p<0.05$,* respectively). There was no difference between control and patient NET production in response to PBS (unstimulated negative control) (2way ANOVA and Bonferroni post-tests *p>0.05*) (Figure 8.9c).

Quantification of NET-bound cathepsin G

Healthy controls produced significantly more NETs, as determined by NET-bound cathepsin G (CG), compared with PLS patients following stimulation with HOCl, *A. actinomycetemcomitans* (serotype b) or *V. parvula* (2way ANOVA and Bonferroni post-tests ****$p<0.0001$, ***$p<0.001$, ****$p<0.0001$, respectively). There was no difference between control and patients NET production in response to PMA or PBS (unstimulated negative control) (Figure 8.9d).

a) NET-DNA

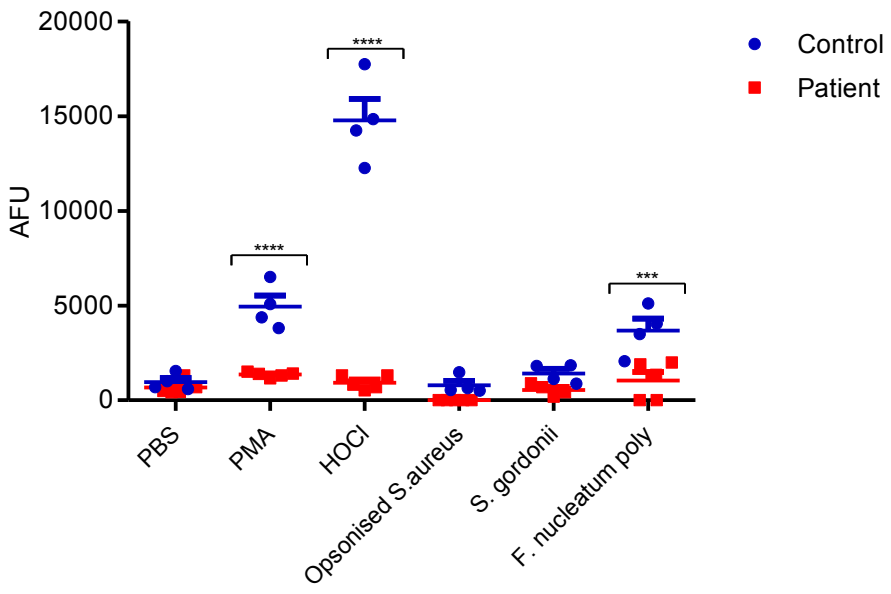

b) NET-bound neutrophil elastase

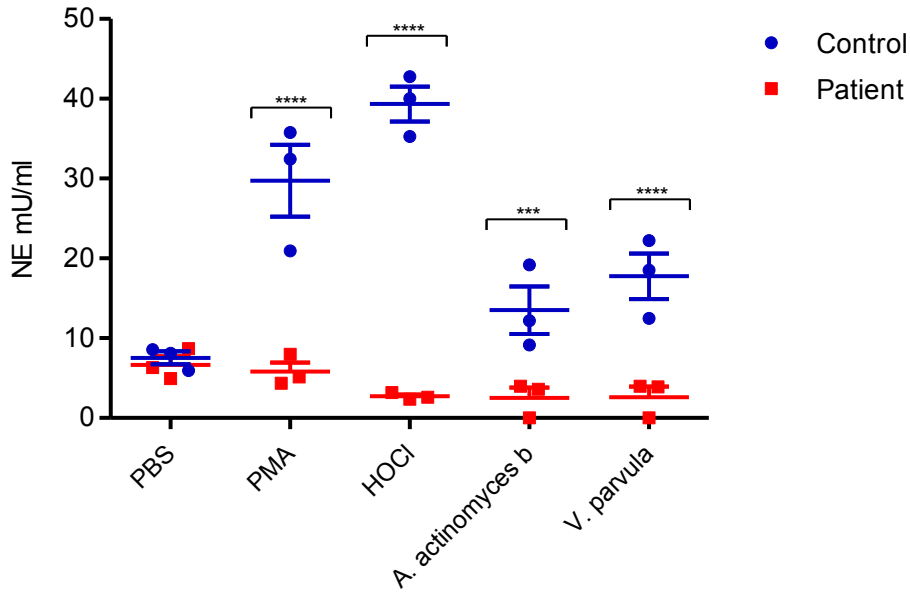

c) NET-bound myeloperoxidase

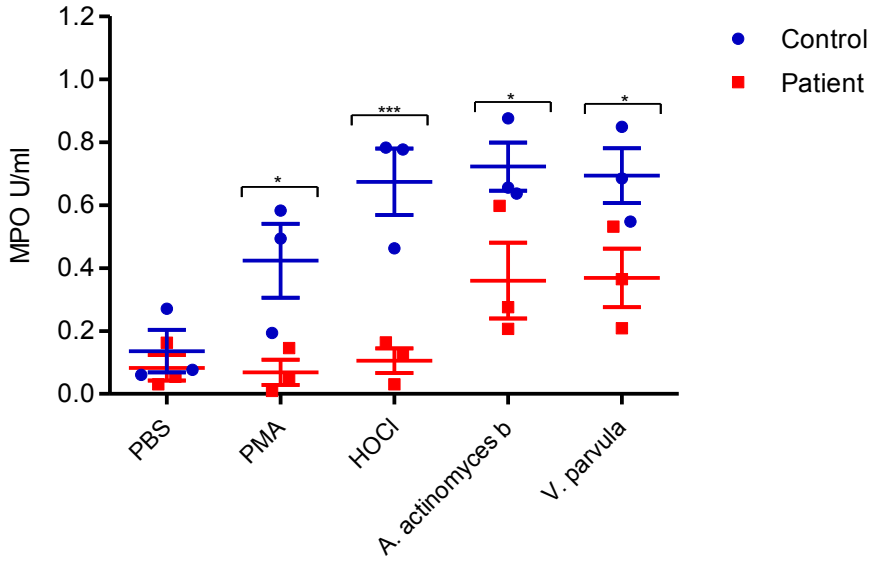

d) NET-bound cathepsin G

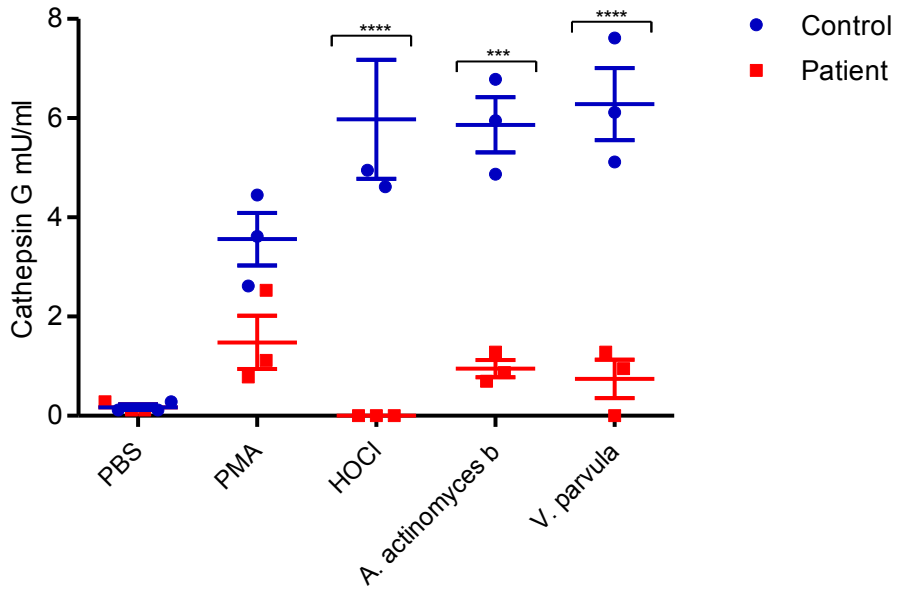

Figure 8.9: Comparison of NET production by PLS patients and healthy controls
NET bound (a) NET-DNA (n=5 patients, n=4 controls) (b) NET-bound NE, (c) NET-bound MPO and (d) NET-bound CG were quantified in PLS patients and healthy controls fluorometrically in response to 4 hours of stimulation with PMA (50nM), HOCl (0.75mM), opsonised *S. aureus* ($5x10^7$ and MOI of 500), or heat-killed bacteria ($1x10^8$ and MOI of 1000). Statistical significance was calculated using 2way ANOVA and Bonferroni post-tests (*$p<0.05$, ***$p<0.001$, ****$p<0.0001$). Data is presented as (a) AFU (arbitrary fluorescence units), (c) U/ml or (d, e) mU/ml and expressed as mean ± SEM (quantification of NET-bound components n=3 pairs).

8.3.2 Fluorescence visualisation of NET production in PLS patients

A qualitative difference was observed in NET production between PLS patients and healthy controls, with patients producing fewer PMA-induced (50nM) extracellular web-like structures that stained positive with the DNA-stain, Sytox green (2.2.3.7). No difference in NET production was observed between patients and controls in PBS-treated neutrophils, however some cells stained positive for DNA, which is likely to be cells that have necrosed during the incubation period and enabled Sytox green to permeate the compromised cell membrane (Figure 8.10).

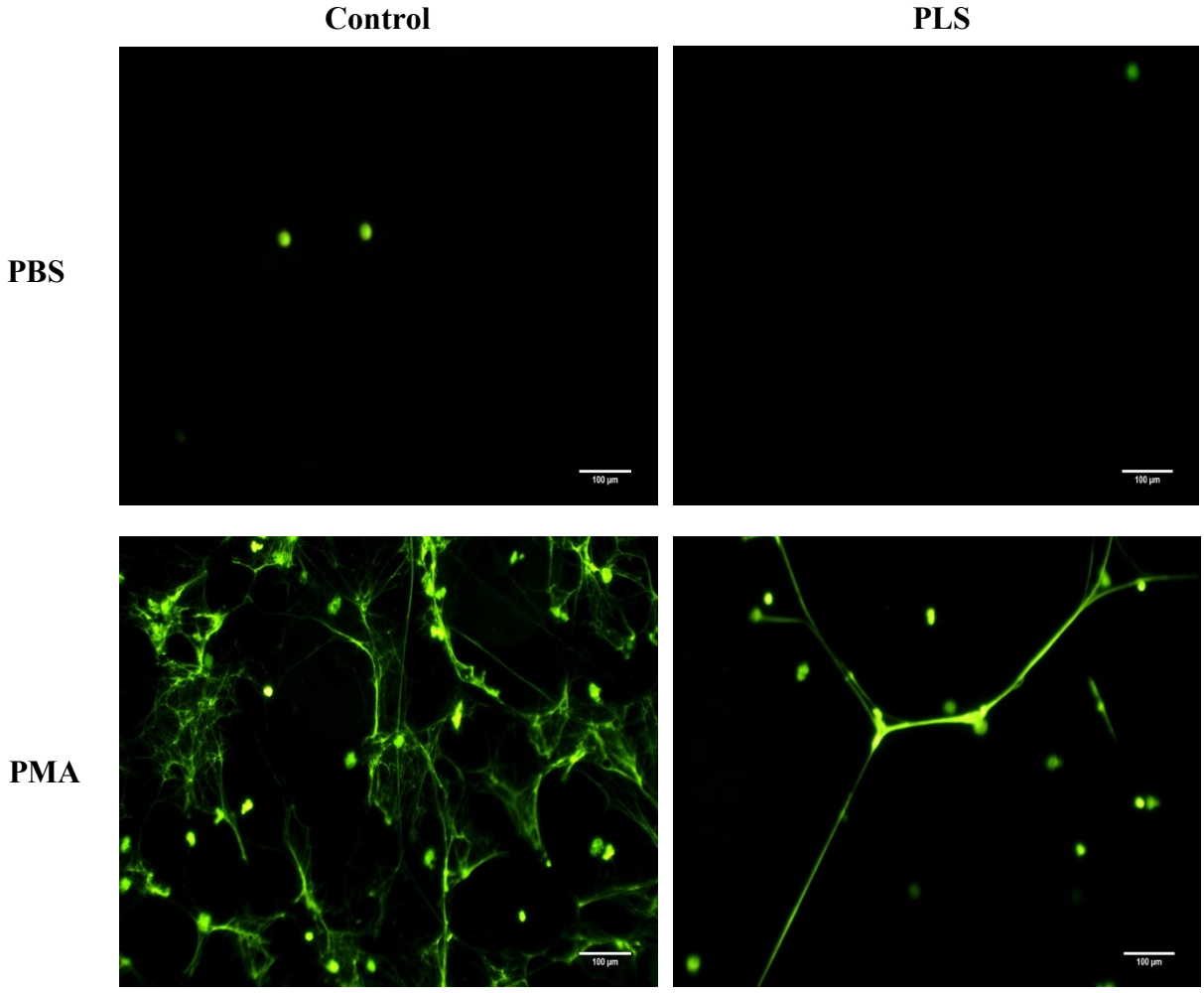

Figure 8.10: Fluorescence visualisation of NET production in PLS patients
NETs were visualised (x10 magnification) with Sytox green in response to treatment with PBS (negative control) or PMA (50nM) for 3 hours. Images are representative of 5 experiments performed in duplicate. Scale bar represents 100µm.

8.3.3 Quantification of plasma NE in PLS

Plasma was isolated from the peripheral blood of PLS patients and controls (2.2.6.2.3). Plasma-derived NE was quantified by ELISA and demonstrated significantly less NE in PLS patients (Mann-Whitney *$p=0.0294$) (2.2.6.4.2.1). A NE standard curve enabled absorbance readings to be converted into ng/ml of NE (Figure 8.11a).

8.3.4 Quantification of plasma LL-37 in PLS

Plasma was isolated from the peripheral blood of PLS patients and controls (2.2.6.2.3). Plasma-derived LL-37 was quantified by ELISA and demonstrated significantly less LL-37 in PLS patients (Mann-Whitney *$p=0.0297$) (2.2.6.4.2.2). An LL-37 standard curve enabled absorbance readings to be converted into ng/ml of LL-37 (Figure 8.11b).

a) Neutrophil elastase

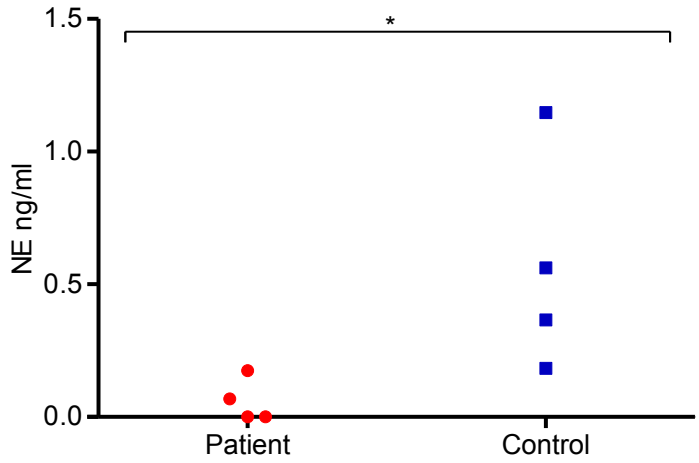

b) LL-37

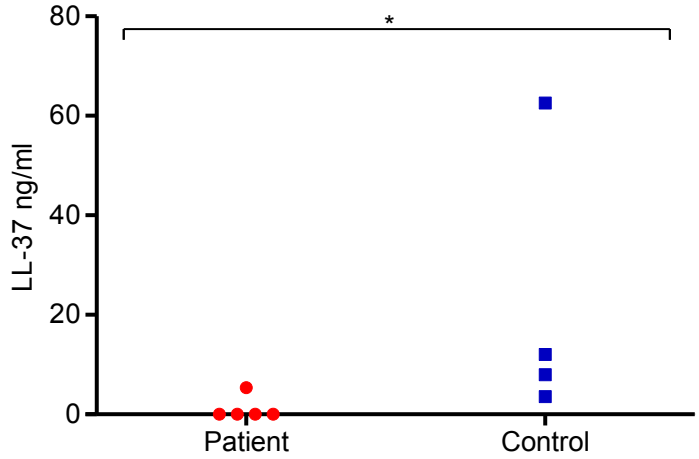

Figure 8.11: Quantification of plasma derived neutrophil elastase and LL-37 in PLS
Plasma derived (a) NE and (b) LL-37 were quantified in plasma from PLS patients and healthy controls by ELISA. Statistical significance was calculated using Mann-Whitney tests *$p=0.0294$, *$p=0.0297$ for NE and LL-37, respectively). Data presented as ng/ml and expressed as mean ± SEM (n=4 pairs).

8.4 Discussion

Gingivitis is an inflammatory response to bacterial plaque that precedes periodontitis in susceptible individuals (Hajishengallis 2014). Gingivitis, whilst normally chronic in nature, can be rapidly induced and reversed, and therefore the 21-day gingivitis model developed by Loe *et al.,* (1965) constitutes a useful model to investigate the role of a supragingival plaque biofilm in the pathogenesis of periodontal disease and systemic diseases with periodontal manifestations. In the current study, no significant differences were observed in peripheral blood NET production during the 21-day gingivitis model (section 8.2.2). This is not unexpected, as peripheral NET release by chronic periodontitis patients was no different to healthy controls (Chapter 5). Furthermore, there was no significant difference in plasma-derived NET degradation or plasma levels of IgG and FLCs throughout the gingivitis study period. Clinical measures of inflammation increased up to 21 days (plaque accumulation) on the test side, followed by a decrease at 35 days (return to health), which confirms volunteer compliance and the validity of the study for both the induction and resolution of inflammation (section 8.2.1). Consistent with our findings, Wahaidi *et al.,* (2009) demonstrated no systemic oxidative response to the accumulation of plaque in a 21-day gingivitis model. Conversely, it has been reported that plaque accumulation during the 21-day experimental gingivitis model results in significant increases in peripheral blood neutrophil counts (Kowolik *et al.,* 2001).

Plaque was collected from test and control sites at 0, 7, 14, 21 and 35 days and pooled. Plaque was used as a stimulus for neutrophil ROS and NET production, and results normalised to plaque DNA, LPS and protein content. Neutrophil ROS and NET production increased in response to homogenised plaque collected from test sites at 7, 14 and 21 days (plaque accumulation), and there was no difference at 0 (baseline) or 35 days (return to health) (section 8.2.5). Given that all results were normalised to the plaque content (DNA,

LPS, protein content), this data suggests that increased neutrophil responses may be due to changes in plaque composition, rather than the quantify. However, microbial characterisation of the biofilm was not performed as part of this study, however this would be interesting to explore. Indeed, a study by Eberhard *et al.,* (2013) which identified bacterial species in plaque produced from a 21-day experimental gingivitis model included species such as *P. gingivalis, F. nucleatum* and *V. parvula,* and notably, experiments in Chapter 4 revealed that these bacterial species were capable of stimulating healthy neutrophils to produce ROS and NETs. Consistent with this, Hirschfeld *et al.,* (2015) demonstrated that the 21-day plaque biofilm comprises neutrophils and NET structures. The authors hypothesised that neutrophils are recruited to supragingival plaque, where they exert bactericidal activity, such as phagocytosis, degranulation and NET release. However, as discussed previously (Chapter 4), further work is needed to elucidate whether NETs prevent bacterial dissemination, or whether the infiltration of neutrophils and the release of NETs in supragingival plaque actually promotes biofilm stability and growth (Hirschfeld *et al.,* 2015).

The study population may be a limitation of the current study, as whilst there were both male and female volunteers, all volunteers were aged between 19 and 21. Furthermore it has been suggested that the 21-day model of experimental gingivitis may not fully reflect persistent chronic gingivitis, as a study by Loesche & Grossman (2001) comparing experimental and chronic gingivitis revealed that volunteers enrolled in the 21-day model demonstrated higher levels of plaque accumulation. This discordance is believed to be a limitation of the experimental model, for example, individuals with persistent gingivitis do not neglect all forms of oral hygiene (as is the case with the vinyl mouth guard), and gingivitis is a chronic state that persists for longer than 21 days.

PLS is an autosomal recessive disease causes by a mutation in the *CTSC* gene that encodes the lysosomal cysteine protease, cathepsin C. Cathepsin C plays a vital role in the post-translational processing of neutrophil serine proteases (NSPs), where it removes N-terminal amino acids that block the active site of NSPs. Thus, a lack of cathepsin C results in the production of NSPs that do not exhibit enzymatic activity. NSPs, such as NE, CG and PR3, are synthesised as inactive pro-enzymes in the bone marrow and prior to storage in neutrophil azurophilic granules as zymogens, they undergo cathepsin-C mediated processing. In response to neutrophil activation, these lysosomal proteins are released into the phagolysosome or undergo limited exocytosis to facilitate bacterial clearance. The loss of cathepsin C activity in PLS patients results in the cessation of NSP function and stability, which is associated with severe periodontal destruction (Sorensen *et al.,* 2014).

This study demonstrated impeded NET release in PLS patients (NET-DNA and NET-bound components) (sections 8.3.1, 8.3.1.1), which is consistent with recent findings by Sorensen *et al.,* (2014), who demonstrated abrogated NET release in a single adult female PLS patient. It is postulated that the reduced NET production is a result of dysfunctional NE in PLS patients (Sorensen *et al.,* 2014), as Papayannopoulos *et al.,* (2010) demonstrated that NE is necessary for NET release. Following neutrophil activation, NE is reportedly released from azurophilic granules and translocates to the nucleus where it promotes chromatin decondensation prior to NET expulsion (Papayannopoulos *et al.,* 2010). The importance of NE in NET production is also exemplified in *ELA2*-neutropenia, in which deficient NE associates with diminished NET production; however this is not observed when NE is fully functional in *HAX1*-neutropenia (Happle *et al.,* 2011). In the absence of post-translational processing in PLS patients, NSP proforms have been suggested to either be constitutively released following their synthesis in the bone marrow (Garwicz *et al.,* 2005), or degraded (Pham & Lay 1999). Indeed Sorensen *et al.,* (2014) demonstrated that NSP production and

allocation to granules appeared normal in PLS immature neutrophils, however the proteins were absent from mature neutrophils; suggesting NSPs are degraded prior to their release from the bone marrow. Accordingly, in the current study NE levels were significantly lower in patient-derived plasma samples, relative to the controls (section 8.3.3).

In healthy individuals PR3 cleaves cathelicidin (hCAP-18) extracellularly to produce the bactericidal peptide LL-37. In PLS patients, deficient LL-37 results from a failure to encode fully functioning cathepsin C, and consequently compromised PR3 activity. Confirming this, LL-37 was significantly lower in PLS plasma samples relative to healthy controls (section 8.3.4). This is consistent with the findings of de Haar *et al.,* (2006), who reported that in addition to LL-37 deficiency, neutrophils derived from PLS patients demonstrate a reduced capacity to kill *A. actinomycetemcomitans* compared with healthy controls. This may, however, be a direct result of inhibited LL-37 antimicrobial activity, as LL-37 is reportedly involved in the clearance of *A. actinomycetemcomitans* (Ji *et al.,* 2007). Notably patients with Morbus Kostmann syndrome, a severe congenital neutropenia that is associated with LL-37 deficiency, are also susceptible to a high prevalence of *A. actinomycetemcomitans* infection and severe periodontitis in adulthood (Putsep *et al.,* 2002, Gonzales & Frydman 2014); supporting the hypothesis that LL-37 plays a vital role in bacterial clearance. It has also been suggested that the overgrowth of *A. actinomycetemcomitans* in PLS patients may provide favourable conditions for the proliferation of other periodontal bacteria, such as *P. gingivalis* (Eick *et al.,* 2014).

It is noteworthy that despite the loss of function of NSPs, the associated immunodeficiency is modest, with 15-20% of patients reporting recurrent infections, such as tonsillitis and liver abscesses (Sorensen *et al.,* 2014, Almuneef *et al.,* 2002). Accordingly, the physical examination of one patient revealed that IgGs, complement, as well as T- and B-cell

responses were within the normal reference ranges (Sorensen *et al.,* 2014). The fact that patients do not succumb to major illnesses, and also reports from *in vitro* studies demonstrating that PLS neutrophils elicit normal bactericidal activity against infection (Pham *et al.,* 2004), suggests that NSPs do not constitute the only antimicrobial defence mechanism. This also indicates that NE-dependent NETs may not play a critical role in host defence, or that alternative compensatory defence mechanisms have evolved in PLS. It is also unlikely that deficient NET release accounts for the severe periodontitis observed in PLS, as CGD patients, who also lack the ability to produce NETs, do not present with severe periodontal destruction (Bianchi *et al.,* 2009). Thus, severe periodontitis may be the result of other neutrophil abnormalities, such as perturbed chemotaxis, which is reportedly defective in PLS patients. However, normal neutrophil levels are reported in the GCF of PLS patients, suggesting that whilst the neutrophils are recruited normally, they may exhibit longer tissue transit times and contribute to collateral periodontal tissue destruction (Firatli *et al.,* 1996). A possible explanation for the mild systemic immunodeficiency observed in PLS are recent findings by Glenthoj *et al.,* (2015), who demonstrated that NSPs are not required for the processing and activity of neutrophil α-defensins, which are a family of peptides that possess antimicrobial activity. Notably, PLS patients are able to synthesise α-defensins, which constitute 50% of azurophil granules (Rice *et al.,* 1987), and it has been proposed that the presence of these microbicidal peptides may afford protection and compensate for absent NSPs.

In conclusion, peripheral NET production did not change throughout the 21-day gingivitis model study; however neutrophil ROS and NET production significantly increased in response to stimulation with homogenised plaque samples collected from test sites. These findings suggest that whilst the plaque biofilm evokes ROS and NET release *in situ*, biofilm accumulation and the subsequent localised inflammation in gingivitis do not impact upon

systemic neutrophil responses. NET production was impeded in PLS patients, which is hypothesised to be the result of absent NE. Furthermore, LL-37, which reportedly plays an important role in the clearance of *A. actinomycetemcomitans*, was lower in PLS patient plasma samples compared with controls. However, despite the severe periodontal destruction, the majority of PLS patients are not susceptible to recurrent infections, which suggests that NSPs and NET release is not the only process involved in host defence. Further work is thus required to elucidate the mechanisms that result in dysfunctional NSPs associated with severe periodontitis in PLS.

CHAPTER 9: CONCLUDING REMARKS

9.1 Summary of main findings

The aim of this thesis was to further explore the role of NETs in periodontal diseases, including experimental gingivitis, chronic periodontitis and Papillon Lefèvre syndrome (PLS) patients. Specific aims were to investigate:

1. The interactions between NETs and a range of periodontal bacteria.
2. NET production by peripheral blood neutrophils from healthy volunteers developing experimental gingivitis, chronic periodontitis patients and PLS patients.
3. NET degradation by periodontitis patients' plasma and the potential effects of NETs on neutrophil responses.
4. The impact of CSE upon NET production, neutrophil chemotaxis and the expression of key genes involved in neutrophil activation.

In order to study NET release, neutrophils were isolated from the peripheral blood of volunteers using discontinuous Percoll gradients. Preliminary experiments (Chapter 3) investigated neutrophil preparation techniques and Percoll appeared to be the most appropriate isolation method, evidenced by the metabolic activation and higher NET release by Percoll-isolated cells. Percoll was subsequently selected as the isolation technique for all *ex vivo* neutrophil assays in this thesis.

Neutrophil stimulation with a panel of periodontal bacteria demonstrated differential ROS and NET release between organisms (Chapter 4). This variability may contribute to the pathogenesis of periodontal diseases by mechanisms such as bacterial avoidance of host responses, which may promote bacteria colonisation and persistence of infection. Whilst neutrophil responses may limit dysbiosis and the emergence of pathogenic bacteria, excessive NET and ROS release may conversely cause periodontal tissue damage and indirectly support the proliferation of pathogenic bacteria by providing a source of nutrients.

NETs were found to entrap all periodontal bacteria tested to some extent, consistent with previous findings suggesting NETs can entrap a significant majority of microorganisms (Brinkmann *et al.,* 2004). Notably, many periodontal bacteria are reported to release DNases, which may have the ability to disassemble NET structures and contribute to biofilm pathogenicity (Palmer *et al.,* 2011). However, further work is required to elucidate whether DNase release by certain bacterial pathogens specifically allows these species to disseminate, or whether DNase release provides a mutually beneficial environment in which all biofilm bacteria are also afforded protection. Recent findings by Hirschfeld *et al.,* (2015) demonstrated that following the recruitment of neutrophils to the oral biofilm, they can infiltrate the dental plaque and subsequently release NET structures. Whilst the *ex vivo* NET assays presented in this thesis further our understanding of the interactions that occur between NETs and specific periodontal bacteria, these data are not representative of an *in vivo* bacterial biofilm. It is interesting to speculate that differences in NET induction between periodontal species may be compensated for when these species co-exist within a biofilm structure. Under the experimental conditions employed, the incubation of NETs with periodontal bacteria did not appear to impede bacterial growth or survival. It is difficult to ascertain whether this uninhibited growth was the result of NETs being unable to kill these bacteria, or a result of the experimental conditions, as the robustness of NET killing assays previously published has been questioned (Menegazzi *et al.,* 2011).

To investigate NET release by peripheral blood neutrophils in chronic periodontitis, a longitudinal intervention study was undertaken (Chapter 5). This is the first study to quantify peripheral NET release in periodontitis, and no differences were observed in NET production between chronic periodontitis patients and healthy controls; a finding consistent with a collaborative parallel study in a Greek cohort. Given that NET production is ROS-dependent, and it is well established that chronic periodontitis patient neutrophils are

hyperactive and hyper-reactive with respect to ROS release (Matthews *et al.,* 2007a, 2007b), no differences in NET release between patients and controls suggests that the hyper-responsive phenotype does not extend to NET release. Notably, NET production following successful non-surgical periodontal treatment decreased in periodontitis patients. In terms of age, pre-treatment results demonstrated NET production was lower in healthy controls, and to lesser extent, patients, over 50 years of age (published in Hazeldine *et al.,* 2014). It is postulated that age-related reductions in NET production may be associated with reduced receptor signalling in response to stimulation (Hazeldine *et al.,* 2014); however, further work is required to understand the age-associated changes in NET production, which appear to be independent of periodontal inflammatory status.

NET degradation by chronic periodontitis patients' plasma was measured, for the first time, and demonstrated that NET degradation was significantly lower in a subset of chronic periodontitis patients pre-treatment, relative to periodontally healthy matched controls (Chapter 6). Following non-surgical treatment, NET degradation in periodontitis patients was comparable to controls. Attenuated NET degradation has been reported in SLE, and has been suggested to be the result of DNase 1 inhibitors or the presence of a physical barrier that prevents DNase 1 access to cleavage sites on the NET backbone (Hakkim *et al.,* 2010, Leffler *et al.,* 2012). Consistent with findings in SLE, plasma IgG subclass concentrations were significantly higher in periodontitis patients, relative to controls. In addition, plasma immunoglobulin FLC concentrations were higher in patients, and notably plasma cystatin C levels (an independent measure of renal clearance) demonstrated that elevated FLC in patients is not a result of insufficient renal FLC clearance, and thus likely to be due to FLC overproduction by B cells. Increased circulating IgG and FLCs in periodontitis patients may provide a physical barrier and prevent the enzymatic degradation of NETs by DNase 1, however further experiments are required to confirm this hypothesis in periodontitis.

Attenuated NET removal may constitute an antimicrobial host response during periods of infection, as NETs can prevent microbial dissemination by entrapping various periodontal bacteria (Chapter 4). Indeed, under the reported experimental conditions, treatment of peripheral neutrophils with NET supernatants did not prompt ROS or further NET production, or induce NET-mediated cytotoxicity in H400 cells; suggesting NETs are non-immunogenic (Chapter 6). Conversely, it is possible that NET production in periodontal tissues may serve as a plausible mechanism for anti-citrullinated protein antibodies (ACPAs) production following a break in immune tolerance, and this process may be exacerbated if NETs are not removed efficiently (dePablo *et al.,* 2009). Whilst no NET-induced pro-inflammatory responses were observed in this thesis, it is possible that *ex vivo* assays do not fully mimic the *in vivo* environment in periodontitis, comprising a microbial biofilm, other pro-inflammatory mediators and chronic activation of immune defence systems.

Pre-treatment of peripheral neutrophils with cigarette smoke extract (CSE) had an inhibitory effect on NET release, which may be due to alterations in PKC signalling and subsequently attenuated neutrophil ROS production (Matthews *et al.,* 2011, 2012) (Chapter 7). Cigarette smoking may therefore subvert the elimination of periodontal bacteria *in vivo*, as neutrophils are unable to effectively kill the colonising pathogens, which may be one mechanism to explain why smoking is a major risk factor for the development of periodontitis (Grossi *et al.,* 1994, 1995). Notably, no differences were observed in NET release following pre-treatment with nicotine or cotinine. However, neutrophil priming with thiocyanate (SCN-), the preferred substrate for MPO causing the production of hypothiocyanous acid (HOSCN), caused a reduction in NET release. Increased HOSCN production concomitantly decreases HOCl production, a process that may afford protection of non-thiol targets against HOCl-mediated tissue damage (Talib *et al.,* 2012).

Neutrophils pre-treated with CSE exhibited reduced chemotactic speed, velocity and directionality (resultant vector length), which may be the result of attenuated ROS production (Hattori *et al.,* 2010) (Chapter 7). However, given that the severity of periodontitis is positively correlated with neutrophil counts in dental plaque, saliva and GCF (Bhadbhade *et al.,* 2012), whilst chemotactic accuracy may be compromised in smokers, neutrophils still reach the infected tissues, albeit with longer tissue transit times, which may be associated with increased neutrophil-mediated tissue damage (Roberts *et al.,* 2015). Furthermore, relative to the reference gene YWHAZ, CSE and SCN- treatment caused a concentration dependent increase in neutrophil HSP40 expression. SCN- treatment was also associated with a significant increase in P-47^{phox} and P-67^{phox} expression; however this was not observed following CSE treatment of neutrophils, highlighting that despite SCN- being a major component of cigarette smoke, these substances alter neutrophil activation and function by distinct mechanisms.

NET production by peripheral blood neutrophils did not alter during the 21-day experimental gingivitis study period (Chapter 8), consistent with chronic periodontitis patients (Chapter 5). Neutrophil ROS and NET production significantly increased in response to stimulation with homogenised plaque samples collected from volunteer test sites. These findings suggest that whilst the local periodontal inflammation does not impact upon systemic neutrophil responses, the plaque biofilm evokes ROS and NET release *in situ*. Indeed, findings by Hirschfeld *et al.,* (2015) demonstrated that the plaque biofilm that results from the 21-day gingivitis model comprises neutrophils and NET structures. However, whether *ex vivo* assays (Chapter 4) are reflective of the *in vivo* interactions between the biofilm bacteria and NETs remains to be determined.

Peripheral NET release was impeded in PLS patients (Chapter 8) relative to healthy controls, which is consistent with recent findings by Sorensen *et al.,* (2014), who hypothesised that decreased NET production results from absent NSPs from mature neutrophils, and subsequently absent NE. Accordingly, in the current study NE concentrations were significantly lower in patient-derived plasma samples, relative to the non-PLS controls. Additionally, LL-37, which is reportedly involved in the clearance of *A. actinomycetemcomitans* (Tanaka *et al.,* 2000), was significantly lower in PLS plasma samples compared with control samples. However, despite the severe prepubertal periodontal destruction seen in PLS patients, the majority of PLS patients are not susceptible to recurrent infections, which suggests that NSPs and NET release do not play a predominant role in host periodontal defence or that compensatory mechanisms exist which are less effective in the periodontium. It is therefore likely that the periodontal destruction seen in PLS arises due to a constant stimulation of neutrophil recruitment and activation by the plaque biofilm and absent NSPs impacts upon multiple pathways that result in periodontal tissue destruction.

9.2 Overall conclusion and recommendations for future research

This thesis contributes to our understanding of NET release and function in the pathogenesis of periodontal diseases. The data presented in this thesis indicate that NETs contribute to innate immunity, as they are released in response to a homogenised plaque biofilm and to specific bacteria that are associated with periodontitis. However, given that periodontitis pathogenesis is characterised by exaggerated neutrophil responses, NETs may also facilitate the progression of the disease, as if NET degradation and removal is inefficient they may provide a source of autoantigens. It is hoped that a greater understanding of NET responses in periodontal diseases in the future may contribute to improvements in prevention, diagnostic and treatment strategies.

Additional questions and further areas of research identified from the results presented in this thesis remain. Therefore recommendations for future research include:

- Quantification of peripheral NET production in response to a bacterial biofilm. Whilst NETs were quantified in response to individual bacterial species associated with periodontitis (Chapter 4), it is possible that peripheral NET responses by neutrophils exposed to biofilm of varying complexity. In addition to studying peripheral NET hyperactivity/hyper-reactivity, it would be interesting to quantify *in situ* NET release in the gingival tissues of chronic periodontitis patients.

- NET degradation was significantly impeded in periodontitis patients relative to healthy controls. It is hypothesised that this is the result of increased circulating antibodies and FLCs that provide a physical barrier and prevent enzymatic degradation of NET structures (Chapter 6). Indeed antibody and FLC concentrations were higher in the plasma of periodontitis patients, however subsequent experiments are required to confirm that this is resulting in attenuated NET removal. Experiments involving the removal of IgGs and FLCs from "low-degrading" plasma samples prior to quantifying NET degradation would address the current hypothesis.

- The effect of CSE and SCN pre-treatment on NET production in response to stimulation with periodontally-relevant bacteria. CSE and SCN- were found to have an inhibitory effect on PMA-induced NET production (Chapter 7). Whilst PMA is a known NET stimulus, it is possible that cigarette components will have a different effect on bacteria-induced NET production, which would be of relevance in chronic periodontitis patients.

REFERENCES

Abramson SB, Given WP, Edelson HS, Weissmann G (1983). Neutrophil aggregation induced by sera from patients with active systemic lupus erythematosus. *Arthritis & Rheumatism* 26(5)*:*630-636.

Aggarwal R, Sequeira W, Kokebie R, Mikolaitis RA, Fogg L, Finnegan A *et al.* (2011). Serum free light chains as biomarkers for systemic lupus erythematosus disease activity. *Arthritis care & research* 63(6)*:*891-898.

Alghamdi AS, Foster DN (2005). Seminal DNase frees spermatozoa entangled in neutrophil extracellular traps. *Biology of reproduction* 73(6)*:*1174-1181.

Almuneef M, Al Khenaizan S, Al Ajaji S, Al-Anazi A (2003). Pyogenic liver abscess and Papillon-Lefevre syndrome: not a rare association. *Pediatrics* 111(1)*:*e85-e88.

Ambrose JA, Barua RS (2004). The pathophysiology of cigarette smoking and cardiovascular disease: an update. *Journal of the American College of Cardiology* 43(10)*:*1731-1737.

Amulic B, Cazalet C, Hayes GL, Metzler KD, Zychlinsky A (2012). Neutrophil function: from mechanisms to disease. *Annual review of immunology* 30(459-489.

Andonegui G, Kerfoot SM, McNagny K, Ebbert KV, Patel KD, Kubes P (2005). Platelets express functional Toll-like receptor-4. *Blood* 106(7)*:*2417-2423.

Andrew N, Insall RH (2007). Chemotaxis in shallow gradients is mediated independently of PtdIns 3-kinase by biased choices between random protrusions. *Nature cell biology* 9(2)*:*193-200.

Arai Y, Nishinaka Y, Arai T, Morita M, Mizugishi K, Adachi S *et al.* (2014). Uric acid induces NADPH oxidase-independent neutrophil extracellular trap formation. *Biochemical and biophysical research communications* 443(2)*:*556-561.

Ariane N, Evelien T, Andreas N, Richard LG, Timo M, Victor N *et al.* (2014). The antimicrobial peptide LL-37 facilitates the formation of neutrophil extracellular traps. *Biochemical Journal* 464(1)*:*3-11.

Armitage GC (1996). Periodontal diseases: diagnosis. *Annals of periodontology/the American Academy of Periodontology* 1(1)*:*37.

Aulik NA, Hellenbrand KM, Klos H, Czuprynski CJ (2010). Mannheimia haemolytica and its leukotoxin cause neutrophil extracellular trap formation by bovine neutrophils. *Infection and immunity* 78(11)*:*4454-4466.

Bach JN, Levan NE (1968). Papillon-Lefevre syndrome. *Archives of dermatology* 97(2)*:*154-158.

Baker VS, Imade GE, Molta NB, Tawde P, Pam SD, Obadofin MO *et al.* (2008). Cytokine-associated neutrophil extracellular traps and antinuclear antibodies in Plasmodium falciparum infected children under six years of age. *Malar J* 7(41).

Barrientos L, Marin-Esteban V, de Chaisemartin L, Le-Moal VL, Sandré C, Bianchini E *et al.* (2013). An improved strategy to recover large fragments of functional human neutrophil extracellular traps. *Frontiers in immunology* 4.

Bascones-Martínez A, Muñoz-Corcuera M, Noronha S, Mota P, Bascones-Ilundain C, Campo-Trapero J (2009). Host defence mechanisms against bacterial aggression in periodontal disease: Basic mechanisms. *Med Oral Patol Oral Cir Bucal* 14(12)*:*e680-685.

Behrendt JH, Ruiz A, Zahner H, Taubert A, Hermosilla C (2010). Neutrophil extracellular trap formation as innate immune reactions against the apicomplexan parasite Eimeria bovis. *Veterinary immunology and immunopathology* 133(1)*:*1-8.

Beiter K, Wartha F, Albiger B, Normark S, Zychlinsky A, Henriques-Normark B (2006). An endonuclease allows Streptococcus pneumoniae to escape from neutrophil extracellular traps. *Current Biology* 16(4)*:*401-407.

Benjamin IJ, McMillan DR (1998). Stress (heat shock) proteins molecular chaperones in cardiovascular biology and disease. *Circulation research* 83(2)*:*117-132.

Berends ET, Horswill AR, Haste NM, Monestier M, Nizet V, von Köckritz-Blickwede M (2010). Nuclease expression by Staphylococcus aureus facilitates escape from neutrophil extracellular traps. *Journal of innate immunity* 2(6)*:*576.

Bergmann S, Rohde M, Chhatwal GS, Hammerschmidt S (2001). α-Enolase of Streptococcus pneumoniae is a plasmin (ogen)-binding protein displayed on the bacterial cell surface. *Molecular microbiology* 40(6)*:*1273-1287.

Bergström J, Eliasson S, Dock J (2000). A 10-year prospective study of tobacco smoking and periodontal health. *Journal of periodontology* 71(8)*:*1338-1347.

Bhadbhade SJ, Acharya AB, Thakur S (2012). Correlation between probing pocket depth and neutrophil counts in dental plaque, saliva, and gingival crevicular fluid. *Quintessence international (Berlin, Germany: 1985)* 43(2)*:*111-117.

Bianchi M, Hakkim A, Brinkmann V, Siler U, Seger RA, Zychlinsky A *et al.* (2009). Restoration of NET formation by gene therapy in CGD controls aspergillosis. *Blood* 114(13)*:*2619-2622.

Bianchi M, Niemiec MJ, Siler U, Urban CF, Reichenbach J (2011). Restoration of anti-Aspergillus defense by neutrophil extracellular traps in human chronic granulomatous disease after gene therapy is calprotectin-dependent. *Journal of Allergy and Clinical Immunology* 127(5)*:*1243-1252. e1247.

Borregaard N, Cowland JB (1997). Granules of the human neutrophilic polymorphonuclear leukocyte. *Blood* 89(10)*:*3503-3521.

Branzk N, Lubojemska A, Hardison SE, Wang Q, Gutierrez MG, Brown GD *et al.* (2014). Neutrophils sense microbe size and selectively release neutrophil extracellular traps in response to large pathogens. *Nature immunology*.

Brebner JA, Stockley RA (2013). Polyclonal free light chains: a biomarker of inflammatory disease or treatment target? *F1000 medicine reports* 5(

Brill A, Fuchs T, Savchenko A, Thomas G, Martinod K, De Meyer S *et al.* (2012). Neutrophil extracellular traps promote deep vein thrombosis in mice. *Journal of Thrombosis and Haemostasis* 10(1)*:*136-144.

Brinkmann V, Reichard U, Goosmann C, Fauler B, Uhlemann Y, Weiss DS *et al.* (2004). Neutrophil extracellular traps kill bacteria. *science* 303(5663)*:*1532-1535.

Brinkmann V, Zychlinsky A (2007). Beneficial suicide: why neutrophils die to make NETs. *Nature Reviews Microbiology* 5(8)*:*577-582.

Brinkmann V, Laube B, Abed UA, Goosmann C, Zychlinsky A (2010). Neutrophil extracellular traps: how to generate and visualize them. *Journal of visualized experiments: JoVE* 36).

Brinkmann V, Goosmann C, Kühn LI, Zychlinsky A (2012). Automatic quantification of in vitro NET formation. *Frontiers in immunology* 3.

Buis M, Sinnema N, Blokzijl T, Faber K-N, Westra J, Dijkstra G Mesalazine and cigarette smoke inhibit neutrophil extracellular trap formation in vitro. Journal of crohns & colitis 2015: Oxford Univ Press Great Clarendon St, Oxford, England.

Burns D (1991). Cigarettes and cigarette smoking. *Clinics in chest medicine* 12(4)*:*631.

Byrd AS, O'Brien XM, Johnson CM, Lavigne LM, Reichner JS (2013). An extracellular matrix–based mechanism of rapid neutrophil extracellular trap formation in response to Candida albicans. *The Journal of Immunology* 190(8)*:*4136-4148.

Campbell AM, Kashgarian M, Shlomchik MJ (2012). NADPH oxidase inhibits the pathogenesis of systemic lupus erythematosus. *Science translational medicine* 4(157)*:*157ra141-157ra141.

Carlin AF, Uchiyama S, Chang Y-C, Lewis AL, Nizet V, Varki A (2009). Molecular mimicry of host sialylated glycans allows a bacterial pathogen to engage neutrophil Siglec-9 and dampen the innate immune response. *Blood* 113(14)*:*3333-3336.

Carlos TM, Harlan JM (1994). Leukocyte-endothelial adhesion molecules. *Blood* 84(7)*:*2068-2101.

Chandler JD, Nichols DP, Nick JA, Hondal RJ, Day BJ (2013). Selective metabolism of hypothiocyanous acid by mammalian thioredoxin reductase promotes lung innate immunity and antioxidant defense. *Journal of Biological Chemistry* 288(25)*:*18421-18428.

Chapple I, Landini G, Griffiths G, Patel N, Ward R (1999). Calibration of the Periotron 8000® and 6000® by polynomial regression. *Journal of periodontal research* 34(2)*:*79-86.

Chapple I, Brock G, Milward M, Ling N, Matthews J (2007). Compromised GCF total antioxidant capacity in periodontitis: cause or effect? *Journal of clinical periodontology* 34(2)*:*103-110.

Chapple IL (1996). Role of free radicals and antioxidants in the pathogenesis of the inflammatory periodontal diseases. *Clinical Molecular Pathology* 49(5)*:*M247.

Chapple IL (2009). Potential mechanisms underpinning the nutritional modulation of periodontal inflammation. *The Journal of the American Dental Association* 140(2)*:*178-184.

Chen K, Nishi H, Travers R, Tsuboi N, Martinod K, Wagner DD *et al.* (2012). Endocytosis of soluble immune complexes leads to their clearance by FcγRIIIB but induces neutrophil extracellular traps via FcγRIIA in vivo. *Blood* 120(22)*:*4421-4431.

Chow OA, von Köckritz-Blickwede M, Bright AT, Hensler ME, Zinkernagel AS, Cogen AL *et al.* (2010). Statins enhance formation of phagocyte extracellular traps. *Cell host & microbe* 8(5)*:*445-454.

Christofidou-Solomidou M, Nakada MT, Williams J, Muller WA, DeLisser HM (1997). Neutrophil platelet endothelial cell adhesion molecule-1 participates in neutrophil recruitment at inflammatory sites and is down-regulated after leukocyte extravasation. *The Journal of Immunology* 158(10)*:*4872-4878.

Clark SR, Ma AC, Tavener SA, McDonald B, Goodarzi Z, Kelly MM *et al.* (2007). Platelet TLR4 activates neutrophil extracellular traps to ensnare bacteria in septic blood. *Nature medicine* 13(4)*:*463-469.

Cooper PR, Palmer LJ, Chapple IL (2013). Neutrophil extracellular traps as a new paradigm in innate immunity: friend or foe? *Periodontology 2000* 63(1)*:*165-197.

Courtney P, Crockard A, Williamson K, Irvine A, Kennedy R, Bell A (1999). Increased apoptotic peripheral blood neutrophils in systemic lupus erythematosus: relations with disease activity, antibodies to double stranded DNA, and neutropenia. *Annals of the rheumatic diseases* 58(5)*:*309-314.

Dahiya P, Kamal R, Gupta R, Bhardwaj R, Chaudhary K, Kaur S (2013). Reactive oxygen species in periodontitis. *Journal of Indian Society of Periodontology* 17(4)*:*411.

Darveau RP, Tanner A, Page RC (1997). The microbial challenge in periodontitis. *Periodontology 2000* 14(1)*:*12-32.

de Haar SF, Hiemstra PS, van Steenbergen MT, Everts V, Beertsen W (2006). Role of polymorphonuclear leukocyte-derived serine proteinases in defense against Actinobacillus actinomycetemcomitans. *Infection and immunity* 74(9)*:*5284-5291.

de Pablo P, Chapple IL, Buckley CD, Dietrich T (2009). Periodontitis in systemic rheumatic diseases. *Nature Reviews Rheumatology* 5(4)*:*218-224.

de Pablo P, Dietrich T, Chapple IL, Milward M, Chowdhury M, Charles PJ *et al.* (2013). The autoantibody repertoire in periodontitis: a role in the induction of autoimmunity to citrullinated proteins in rheumatoid arthritis? *Annals of the rheumatic diseases:*annrheumdis-2012-202701.

Delbosc S, Alsac J-M, Journe C, Louedec L, Castier Y, Bonnaure-Mallet M *et al.* (2011). Porphyromonas gingivalis participates in pathogenesis of human abdominal aortic aneurysm by neutrophil activation. Proof of concept in rats. *PLoS One* 6(4)*:*e18679.

Delima A, Oates T, Assuma R, Schwartz Z, Cochran D, Amar S *et al.* (2001). Soluble antagonists to interleukin-1 (IL-1) and tumor necrosis factor (TNF) inhibits loss of tissue attachment in experimental periodontitis. *Journal of clinical periodontology* 28(3)*:*233-240.

Delima SL, McBride RK, Preshaw PM, Heasman PA, Kumar PS (2010). Response of subgingival bacteria to smoking cessation. *Journal of clinical microbiology* 48(7)*:*2344-2349.

Demmer RT, Holtfreter B, Desvarieux M, Jacobs DR, Kerner W, Nauck M *et al.* (2012). The Influence of Type 1 and Type 2 Diabetes on Periodontal Disease Progression Prospective results from the Study of Health in Pomerania (SHIP). *Diabetes Care* 35(10)*:*2036-2042.

Dewhirst FE, Chen T, Izard J, Paster BJ, Tanner AC, Yu W-H *et al.* (2010). The human oral microbiome. *Journal of bacteriology* 192(19)*:*5002-5017.

Dias I, Chapple I, Milward M, Grant MM, Hill E, Brown J *et al.* (2013). Sulforaphane restores cellular glutathione levels and reduces chronic periodontitis neutrophil hyperactivity in vitro. *PLoS One* 8(6)*:*e66407.

Dias IH, Matthews JB, Chapple IL, Wright HJ, Dunston CR, Griffiths HR (2011). Activation of the neutrophil respiratory burst by plasma from periodontitis patients is mediated by pro-inflammatory cytokines. *Journal of clinical periodontology* 38(1)*:*1-7.

Ding Y, Haapasalo M, Kerosuo E, Lounatmaa K, Kotiranta A, Sorsa T (1997). Release and activation of human neutrophil matrix metallo-and serine proteinases during phagocytosis of Fusobacterium nucleatum, Porphyromonas gingivalis and Treponema denticola. *Journal of clinical periodontology* 24(4)*:*237-248.

Divaris K, Monda KL, North KE, Olshan AF, Reynolds LM, Hsueh W-C *et al.* (2013). Exploring the genetic basis of chronic periodontitis: a genome-wide association study. *Human molecular genetics* 22(11)*:*2312-2324.

Dix TA, Aikens J (1993). Mechanisms and biological relevance of lipid peroxidation initiation. *Chemical research in toxicology* 6(1)*:*2-18.

Dix TA, Hess KM, Medina MA, Sullivan RW, Tilly SL, Webb TLL (1996). Mechanism of site-selective DNA nicking by the hydrodioxyl (perhydroxyl) radical. *Biochemistry* 35(14)*:*4578-4583.

Doeing DC, Borowicz JL, Crockett ET (2003). Gender dimorphism in differential peripheral blood leukocyte counts in mice using cardiac, tail, foot, and saphenous vein puncture methods. *BMC clinical pathology* 3(1)*:*3.

Dorward DA, Lucas CD, Alessandri AL, Marwick JA, Rossi F, Dransfield I *et al.* (2013). Technical advance: autofluorescence-based sorting: rapid and nonperturbing isolation of ultrapure neutrophils to determine cytokine production. *Journal of leukocyte biology* 94(1)*:*193-202.

Drifte G, Dunn-Siegrist I, Tissières P, Pugin J (2013). Innate Immune Functions of Immature Neutrophils in Patients With Sepsis and Severe Systemic Inflammatory Response Syndrome. *Critical care medicine* 41(3)*:*820-832.

Dwivedi N, Upadhyay J, Neeli I, Khan S, Pattanaik D, Myers L *et al.* (2012). Felty's syndrome autoantibodies bind to deiminated histones and neutrophil extracellular chromatin traps. *Arthritis & Rheumatism* 64(4)*:*982-992.

Dwivedi N, Radic M (2014). Citrullination of autoantigens implicates NETosis in the induction of autoimmunity. *Annals of the rheumatic diseases* 73(3)*:*483-491.

Dwyer M, Shan Q, D'Ortona S, Maurer R, Mitchell R, Olesen H *et al.* (2014). Cystic fibrosis sputum DNA has NETosis characteristics and neutrophil extracellular trap release is regulated by macrophage migration-inhibitory factor. *Journal of innate immunity* 6(6)*:*765-779.

Eberhard J, Grote K, Luchtefeld M, Heuer W, Schuett H, Divchev D *et al.* (2013). Experimental gingivitis induces systemic inflammatory markers in young healthy individuals: a single-subject interventional study. *PLoS One* 8(2)*:*e55265.

Edwards JL, Hansen P (1996). Elevated temperature increases heat shock protein 70 synthesis in bovine two-cell embryos and compromises function of maturing oocytes. *Biology of reproduction* 55(2)*:*341-346.

Eggert F, Drewell L, Bigelow J, Speck J, Goldner M (1991). The pH of gingival crevices and periodontal pockets in children, teenagers and adults. *Archives of oral biology* 36(3)*:*233-238.

Eggleton P, Wang L, Penhallow J, Crawford N, Brown KA (1995). Differences in oxidative response of subpopulations of neutrophils from healthy subjects and patients with rheumatoid arthritis. *Annals of the rheumatic diseases* 54(11)*:*916-923.

Eilers B, Mayer-Scholl A, Walker T, Tang C, Weinrauch Y, Zychlinsky A (2010). Neutrophil antimicrobial proteins enhance Shigella flexneri adhesion and invasion. *Cellular microbiology* 12(8)*:*1134-1143.

El Kebir D, József L, Pan W, Wang L, Filep JG (2009). Bacterial DNA activates endothelial cells and promotes neutrophil adherence through TLR9 signaling. *The Journal of Immunology* 182(7)*:*4386-4394.

Ernst RK, Guina T, Miller SI (1999). How intracellular bacteria survive: surface modifications that promote resistance to host innate immune responses. *Journal of Infectious Diseases* 179(Supplement 2)*:*S326-S330.

Esfahanian V, Shamami MS, Shamami MS (2012). Relationship between osteoporosis and periodontal disease: review of the literature. *Journal of dentistry (Tehran, Iran)* 9(4)*:*256.

Fabbri C, Fuller R, Bonfá E, Guedes LK, D'Alleva PSR, Borba EF (2014). Periodontitis treatment improves systemic lupus erythematosus response to immunosuppressive therapy. *Clinical rheumatology* 33(4)*:*505-509.

Fadeel B, Åhlin A, Henter J-I, Orrenius S, Hampton MB (1998). Involvement of caspases in neutrophil apoptosis: regulation by reactive oxygen species. *Blood* 92(12)*:*4808-4818.

Fan C-Y, Lee S, Cyr DM (2003). Mechanisms for regulation of Hsp70 function by Hsp40. *Cell stress & chaperones* 8(4)*:*309.

Farrera C, Fadeel B (2013). Macrophage clearance of neutrophil extracellular traps is a silent process. *The Journal of Immunology* 191(5)*:*2647-2656.

Fauzi A, Kong N, Chua M, Jeyabalan V, Idris M, Azizah R (2004). Antibodies in systemic lupus antineutrophil cytoplasmic erythematosus: prevalence, disease activity correlations and organ system associations. *Med J Malaysia* 59(3)*:*372-377.

Feng Z, Weinberg A (2006). Role of bacteria in health and disease of periodontal tissues. *Periodontology 2000* 40(1)*:*50-76.

Ferrante A, Thong Y (1980). Optimal conditions for simultaneous purification of mononuclear and polymorphonuclear leucocytes from human blood by the Hypaque-Ficoll method. *Journal of immunological methods* 36(2)*:*109-117.

Firatli E, Tüzün B, Efeoğlu A (1996). Papillon-Lefevre syndrome. Analysis of neutrophil chemotaxis. *Journal of periodontology* 67(6)*:*617-620.

Freitas M, Porto G, Lima JL, Fernandes E (2008). Isolation and activation of human neutrophils in vitro. The importance of the anticoagulant used during blood collection. *Clinical biochemistry* 41(7)*:*570-575.

Fuchs TA, Abed U, Goosmann C, Hurwitz R, Schulze I, Wahn V *et al.* (2007). Novel cell death program leads to neutrophil extracellular traps. *The Journal of cell biology* 176(2)*:*231-241.

Fulop T, Larbi A, Douziech N, Fortin C, Guérard KP, Lesur O *et al.* (2004). Signal transduction and functional changes in neutrophils with aging. *Aging cell* 3(4)*:*217-226.

Furze RC, Rankin SM (2008). Neutrophil mobilization and clearance in the bone marrow. *Immunology* 125(3)*:*281-288.

Gabriel C, McMaster WR, Girard D, Descoteaux A (2010). Leishmania donovani promastigotes evade the antimicrobial activity of neutrophil extracellular traps. *The Journal of Immunology* 185(7)*:*4319-4327.

Ganz T, Selsted ME, Szklarek D, Harwig S, Daher K, Bainton DF *et al.* (1985). Defensins. Natural peptide antibiotics of human neutrophils. *Journal of Clinical Investigation* 76(4)*:*1427.

Garwicz D, Lennartsson A, Jacobsen S, Gullberg U, Lindmark A (2005). Biosynthetic profiles of neutrophil serine proteases in a human bone marrow-derived cellular myeloid differentiation model. *haematologica* 90(1)*:*38-44.

Gennaro R, Zanetti M (2000). Structural features and biological activities of the cathelicidin-derived antimicrobial peptides. *Peptide Science* 55(1)*:*31-49.

Gifford AM, Chalmers JD (2014). The role of neutrophils in cystic fibrosis. *Current opinion in hematology* 21(1)*:*16-22.

Gillenius E, Urban CF (2015). The adhesive protein invasin of Yersinia pseudotuberculosis induces neutrophil extracellular traps via β1 integrins. *Microbes and Infection*.

Glenthoj A, Nickles K, Cowland JB, Borregaard N (2014). Processing of Neutrophil α-Defensins Does Not Rely on Serine Proteases in Vivo. *Blood* 124(21)*:*1400-1400.

Gocke C, Holtfreter B, Meisel P, Grotevendt A, Jablonowski L, Nauck M *et al.* (2014). Abdominal obesity modifies long-term associations between periodontitis and markers of systemic inflammation. *Atherosclerosis* 235(2)*:*351-357.

Gomes DA, Pires JR, Zuza EP, Muscara MN, Herrera BS, Spolidorio LC *et al.* (2009). Myeloperoxidase as inflammatory marker of periodontal disease: experimental study in rats. *Immunological investigations* 38(2)*:*117-122.

González-Juarbe N, Mares CA, Hinojosa CA, Medina JL, Cantwell A, Dube PH *et al.* (2015). Requirement for Serratia marcescens cytolysin in a murine model of hemorrhagic pneumonia. *Infection and immunity* 83(2)*:*614-624.

Gonzalez S, Frydman A (2014). The non-surgical management of a patient with Kostmann syndrome-associated periodontitis: a case report. *Journal of oral science* 56(4)*:*315-318.

Gottenberg J-E, Aucouturier F, Goetz J, Sordet C, Jahn I, Busson M *et al.* (2007). Serum immunoglobulin free light chain assessment in rheumatoid arthritis and primary Sjögren's syndrome. *Annals of the rheumatic diseases* 66(1)*:*23-27.

Gottlieb R, Giesing H, Engler R, Babior B (1995). The acid deoxyribonuclease of neutrophils: a possible participant in apoptosis-associated genome destruction. *Blood* 86(6)*:*2414-2418.

Gould TJ, Vu TT, Swystun LL, Dwivedi DJ, Mai SH, Weitz JI *et al.* (2014). Neutrophil extracellular traps promote thrombin generation through platelet-dependent and platelet-independent mechanisms. *Arteriosclerosis, thrombosis, and vascular biology* 34(9)*:*1977-1984.

Grant MM, Brock GR, Matthews JB, Chapple IL (2010). Crevicular fluid glutathione levels in periodontitis and the effect of non-surgical therapy. *Journal of clinical periodontology* 37(1)*:*17-23.

Grassi F, Cristino S, Toneguzzi S, Piacentini A, Facchini A, Lisignoli G (2004). CXCL12 chemokine up-regulates bone resorption and MMP-9 release by human osteoclasts: CXCL12 levels are increased in synovial and bone tissue of rheumatoid arthritis patients. *Journal of cellular physiology* 199(2)*:*244-251.

Graswinckel J, Van Der Velden U, Van Winkelhoff A, Hoek F, Loos B (2004). Plasma antibody levels in periodontitis patients and controls. *Journal of clinical periodontology* 31(7)*:*562-568.

Grau AJ, Becher H, Ziegler CM, Lichy C, Buggle F, Kaiser C *et al.* (2004). Periodontal disease as a risk factor for ischemic stroke. *Stroke* 35(2)*:*496-501.

Grinberg N, Elazar S, Rosenshine I, Shpigel NY (2008). β-Hydroxybutyrate abrogates formation of bovine neutrophil extracellular traps and bactericidal activity against mammary pathogenic Escherichia coli. *Infection and immunity* 76(6)*:*2802-2807.

Grisham MB, Engerson TD, McCord JM, Jones HP (1985). A comparative study of neutrophil purification and function. *Journal of immunological methods* 82(2)*:*315-320.

Grossi S, Genco R, Machtet E, Ho A, Koch G, Dunford R *et al.* (1995). Assessment of Risk for Periodontal Disease. II. Risk Indicators for Alveolar Bone Loss. *Journal of periodontology* 66(1)*:*23-29.

Grossi SG, Zambon JJ, Ho AW, Koch G, Dunford RG, Machtei EE *et al.* (1994). Assessment of risk for periodontal disease. I. Risk indicators for attachment loss. *Journal of periodontology* 65(3)*:*260-267.

Guimarães-Costa AB, Nascimento MT, Froment GS, Soares RP, Morgado FN, Conceição-Silva F *et al.* (2009). Leishmania amazonensis promastigotes induce and are killed by neutrophil extracellular traps. *Proceedings of the National Academy of Sciences* 106(16)*:*6748-6753.

Guzik K, Skret J, Smagur J, Bzowska M, Gajkowska B, Scott D *et al.* (2011). Cigarette smoke-exposed neutrophils die unconventionally but are rapidly phagocytosed by macrophages. *Cell death & disease* 2(3)*:*e131.

Haffajee AD, Socransky SS (1986). Attachment level changes in destructive periodontal diseases. *Journal of clinical periodontology* 13(5)*:*461-472.

Hajishengallis G (2014). Immunomicrobial pathogenesis of periodontitis: keystones, pathobionts, and host response. *Trends in immunology* 35(1)*:*3-11.

Hakkim A, Fürnrohr BG, Amann K, Laube B, Abed UA, Brinkmann V *et al.* (2010). Impairment of neutrophil extracellular trap degradation is associated with lupus nephritis. *Proceedings of the National Academy of Sciences* 107(21)*:*9813-9818.

Halverson TW, Wilton M, Poon KK, Petri B, Lewenza S (2015). DNA is an antimicrobial component of neutrophil extracellular traps. *PLoS pathogens* 11(1).

Happle C, Germeshausen M, Zeidler C, Welte K, Skokowa J Neutrophil Extracellular Traps (NETs) in Patients with Congenital Neutropenia. Blood2011: AMER SOC Hematology 1900 M Street. NW suite 200, Washington, USA.

Harper L, Cockwell P, Adu D, Savage CO (2001). Neutrophil priming and apoptosis in anti-neutrophil cytoplasmic autoantibody-associated vasculitis1. *Kidney international* 59(5)*:*1729-1738.

Harris PC (2012). Effect of density gradient material upon ex-vivo neutrophil behaviour, and Effect of neutrophil extracellular traps upon the growth and survival of periodontopathogenic bacteria, University of Birmingham.

Hattori H, Subramanian KK, Sakai J, Luo HR (2010). Reactive oxygen species as signaling molecules in neutrophil chemotaxis. *Communicative & integrative biology* 3(3)*:*278-281.

Hazeldine J, Harris P, Chapple IL, Grant M, Greenwood H, Livesey A *et al.* (2014). Impaired neutrophil extracellular trap formation: a novel defect in the innate immune system of aged individuals. *Aging cell* 13(4)*:*690-698.

Hirschfeld J, Dommisch H, Skora P, Horvath G, Latz E, Hoerauf A *et al.* (2015). Neutrophil extracellular trap formation in supragingival biofilms. *International Journal of Medical Microbiology*.

Hochreiter-Hufford A, Ravichandran KS (2013). Clearing the dead: apoptotic cell sensing, recognition, engulfment, and digestion. *Cold Spring Harbor perspectives in biology* 5(1)*:*a008748.

Holzhausen M, Spolidorio LC, Ellen RP, Jobin M-C, Steinhoff M, Andrade-Gordon P *et al.* (2006). Protease-activated receptor-2 activation: a major role in the pathogenesis of Porphyromonas gingivalis infection. *The American journal of pathology* 168(4)*:*1189-1199.

Index M (1996). An encyclopedia of Chemicals, Drugs and Biologicals 12th edition., Merck and Co. *INC, USA:*8697.

Itagaki K, Kaczmarek E, Lee YT, Tang IT, Isal B, Adibnia Y *et al.* (2015). Mitochondrial DNA Released by Trauma Induces Neutrophil Extracellular Traps. *PLoS One* 10(3)*:*e0120549.

Jaillon S, Galdiero MR, Del Prete D, Cassatella MA, Garlanda C, Mantovani A Neutrophils in innate and adaptive immunity. Seminars in immunopathology2013: Springer.

Janke M, Poth J, Wimmenauer V, Giese T, Coch C, Barchet W *et al.* (2009). Selective and direct activation of human neutrophils but not eosinophils by Toll-like receptor 8. *Journal of Allergy and Clinical Immunology* 123(5)*:*1026-1033.

Jeffrey JY, Ruddy MJ, Wong GC, Sfintescu C, Baker PJ, Smith JB *et al.* (2007). An essential role for IL-17 in preventing pathogen-initiated bone destruction: recruitment of neutrophils to inflamed bone requires IL-17 receptor–dependent signals. *Blood* 109(9)*:*3794-3802.

Jenne CN, Wong CH, Zemp FJ, McDonald B, Rahman MM, Forsyth PA *et al.* (2013). Neutrophils recruited to sites of infection protect from virus challenge by releasing neutrophil extracellular traps. *Cell host & microbe* 13(2)*:*169-180.

Ji S, Hyun J, Park E, Lee BL, Kim KK, Choi Y (2007). Susceptibility of various oral bacteria to antimicrobial peptides and to phagocytosis by neutrophils. *Journal of periodontal research* 42(5)*:*410-419.

Kakudate N, Morita M, Kawanami M (2008). Oral health care-specific self-efficacy assessment predicts patient completion of periodontal treatment: a pilot cohort study. *Journal of periodontology* 79(6)*:*1041-1047.

Kantarci A, Oyaizu K, Dyke TEV (2003). Neutrophil-mediated tissue injury in periodontal disease pathogenesis: findings from localized aggressive periodontitis. *Journal of periodontology* 74(1)*:*66-75.

Kaplan MJ, Radic M (2012). Neutrophil extracellular traps: double-edged swords of innate immunity. *The Journal of Immunology* 189(6)*:*2689-2695.

Karlsson A, Nixon JB, McPhail LC (2000). Phorbol myristate acetate induces neutrophil NADPH-oxidase activity by two separate signal transduction pathways: dependent or independent of phosphatidylinositol 3-kinase. *Journal of leukocyte biology* 67(3)*:*396-404.

Kassebaum N, Bernabé E, Dahiya M, Bhandari B, Murray C, Marcenes W (2014). Global Burden of Severe Periodontitis in 1990-2010 A Systematic Review and Meta-regression. *Journal of dental research:*0022034514552491.

Katzmann JA, Clark RJ, Abraham RS, Bryant S, Lymp JF, Bradwell AR *et al.* (2002). Serum reference intervals and diagnostic ranges for free κ and free λ immunoglobulin light chains: relative sensitivity for detection of monoclonal light chains. *Clinical Chemistry* 48(9)*:*1437-1444.

Keshari RS, Jyoti A, Dubey M, Kothari N, Kohli M, Bogra J *et al.* (2012). Cytokines induced neutrophil extracellular traps formation: implication for the inflammatory disease condition. *PLoS One* 7(10)*:*e48111.

Kessenbrock K, Krumbholz M, Schönermarck U, Back W, Gross WL, Werb Z *et al.* (2009). Netting neutrophils in autoimmune small-vessel vasculitis. *Nature medicine* 15(6)*:*623-625.

Khandpur R, Carmona-Rivera C, Vivekanandan-Giri A, Gizinski A, Yalavarthi S, Knight JS *et al.* (2013). NETs are a source of citrullinated autoantigens and stimulate inflammatory responses in rheumatoid arthritis. *Science translational medicine* 5(178)*:*178ra140-178ra140.

Kilsgård O, Andersson P, Malmsten M, Nordin SL, Linge HM, Eliasson M *et al.* (2012). Peptidylarginine deiminases present in the airways during tobacco smoking and inflammation can citrullinate the host defense peptide LL-37, resulting in altered activities. *American journal of respiratory cell and molecular biology* 46(2)*:*240-248.

Kim D, Haynes CL (2012). Neutrophil chemotaxis within a competing gradient of chemoattractants. *Analytical chemistry* 84(14)*:*6070-6078.

Kinane DF (2001). Causation and pathogenesis of periodontal disease. *Periodontology 2000* 25(1)*:*8-20.

Kirchner T, Möller S, Klinger M, Solbach W, Laskay T, Behnen M (2012). The impact of various reactive oxygen species on the formation of neutrophil extracellular traps. *Mediators of inflammation* 2012.

Kjeldsen L, Bjerrum O, Askaa J, Borregaard N (1992). Subcellular localization and release of human neutrophil gelatinase, confirming the existence of separate gelatinase-containing granules. *Biochem J* 287(603-610.

Kobayashi SD, DeLeo FR (2009). Role of neutrophils in innate immunity: a systems biology-level approach. *Wiley Interdisciplinary Reviews: Systems Biology and Medicine* 1(3)*:*309-333.

Kolenbrander PE, Jakubovics NS, Chalmers NI, Palmer Jr RJ, Staffan Kjelleberg K, Givskov M *et al.* (2009). Human oral multi-species biofilms: bacterial communities in health and disease. *The Biofilm Mode of Life: Mechanisms and Adaptations:*175-194.

Kolenbrander PE, Palmer RJ, Periasamy S, Jakubovics NS (2010). Oral multispecies biofilm development and the key role of cell–cell distance. *Nature Reviews Microbiology* 8(7)*:*471-480.

Kowolik MJ, Dowsett SA, Rodriguez J, De La Rosa R M, Eckert GJ (2001). Systemic neutrophil response resulting from dental plaque accumulation. *Journal of periodontology* 72(2)*:*146-151.

Krautgartner WD, Klappacher M, Hannig M, Obermayer A, Hartl D, Marcos V *et al.* (2010). Fibrin mimics neutrophil extracellular traps in SEM. *Ultrastructural pathology* 34(4)*:*226-231.

Krysko DV, D'Herde K, Vandenabeele P (2006). Clearance of apoptotic and necrotic cells and its immunological consequences. *Apoptosis* 11(10)*:*1709-1726.

Kumar V, Sharma A (2010). Neutrophils: Cinderella of innate immune system. *International immunopharmacology* 10(11)*:*1325-1334.

Lacy P (2006). Mechanisms of degranulation in neutrophils. *Allergy Asthma Clin Immunol* 2(3)*:*98-108.

Lakshman R, Finn A (2001). Neutrophil disorders and their management. *Journal of clinical pathology* 54(1)*:*7-19.

Lande R, Ganguly D, Facchinetti V, Frasca L, Conrad C, Gregorio J *et al.* (2011). Neutrophils activate plasmacytoid dendritic cells by releasing self-DNA–peptide complexes in systemic lupus erythematosus. *Science translational medicine* 3(73)*:*73ra19-73ra19.

Laplante AF, Moulin V, Auger FA, Landry J, Li H, Morrow G *et al.* (1998). Expression of heat shock proteins in mouse skin during wound healing. *Journal of Histochemistry & Cytochemistry* 46(11)*:*1291-1301.

Lappann M, Danhof S, Guenther F, Olivares-Florez S, Mordhorst IL, Vogel U (2013). In vitro resistance mechanisms of Neisseria meningitidis against neutrophil extracellular traps. *Molecular microbiology* 89(3)*:*433-449.

Lauth X, von Köckritz-Blickwede M, McNamara CW, Myskowski S, Zinkernagel AS, Beall B *et al.* (2009). M1 protein allows Group A streptococcal survival in phagocyte extracellular traps through cathelicidin inhibition. *Journal of innate immunity* 1(3)*:*202.

Leadbetter EA, Rifkin IR, Hohlbaum AM, Beaudette BC, Shlomchik MJ, Marshak-Rothstein A (2002). Chromatin–IgG complexes activate B cells by dual engagement of IgM and Toll-like receptors. *Nature* 416(6881)*:*603-607.

Lee HJ, Kang IK, Chung CP, Choi SM (1995). The subgingival microflora and gingival crevicular fluid cytokines in refractory periodontitis. *Journal of clinical periodontology* 22(11)*:*885-890.

Leffler J, Martin M, Gullstrand B, Tydén H, Lood C, Truedsson L *et al.* (2012). Neutrophil extracellular traps that are not degraded in systemic lupus erythematosus activate complement exacerbating the disease. *The Journal of Immunology* 188(7)*:*3522-3531.

Ley K (2003). The role of selectins in inflammation and disease. *Trends in molecular medicine* 9(6)*:*263-268.

Li P, Li M, Lindberg MR, Kennett MJ, Xiong N, Wang Y (2010). PAD4 is essential for antibacterial innate immunity mediated by neutrophil extracellular traps. *The Journal of experimental medicine* 207(9)*:*1853-1862.

Li X, Kolltveit KM, Tronstad L, Olsen I (2000). Systemic diseases caused by oral infection. *Clinical microbiology reviews* 13(4)*:*547-558.

Ling MR (2015). Neutrophil function in chronic periodontitis, University of Birmingham.

Lobene R, Soparkar P, Newman M (1982). Use of dental floss. Effect on plaque and gingivitis. *Clinical preventive dentistry* 4(1)*:*5.

Löe H, Theilade E, Jensen SB (1965). Experimental gingivitis in man. *Journal of periodontology* 36(3)*:*177-187.

Löe H (1967). The gingival index, the plaque index and the retention index systems. *Journal of periodontology* 38(6 Part II)*:*610-616.

Löe H, Anerud A, Boysen H, Morrison E (1986). Natural history of periodontal disease in man. *Journal of clinical periodontology* 13(5)*:*431-440.

Loesche W (1976). Chemotherapy of dental plaque infections. *Oral sciences reviews* 9(65-107.

Loesche W, Gusberti F, Mettraux G, Higgins T, Syed S (1982). Relationship between oxygen tension and subgingival bacterial flora in untreated human periodontal pockets. *Infection and immunity* 42(2)*:*659-667.

Loesche WJ, Grossman NS (2001). Periodontal disease as a specific, albeit chronic, infection: diagnosis and treatment. *Clinical microbiology reviews* 14(4)*:*727-752.

Lourbakos A, Chinni C, Thompson P, Potempa J, Travis J, Mackie EJ *et al.* (1998). Cleavage and activation of proteinase-activated receptor-2 on human neutrophils by gingipain-R from Porphyromonas gingivalis. *FEBS letters* 435(1)*:*45-48.

Malachowa N, Kobayashi SD, Freedman B, Dorward DW, DeLeo FR (2013). Staphylococcus aureus leukotoxin GH promotes formation of neutrophil extracellular traps. *The Journal of Immunology* 191(12)*:*6022-6029.

Maqbool M, Vidyadaran S, George E, Ramasamy R (2011). Optimisation of laboratory procedures for isolating human peripheral blood derived neutrophils. *Med J Malaysia* 66(4)*:*297.

Marcos V, Zhou Z, Yildirim AÖ, Bohla A, Hector A, Vitkov L *et al.* (2010). CXCR2 mediates NADPH oxidase-independent neutrophil extracellular trap formation in cystic fibrosis airway inflammation. *Nature medicine* 16(9)*:*1018-1023.

Marsh P (1994). Microbial ecology of dental plaque and its significance in health and disease. *Advances in dental research* 8(2)*:*263-271.

Martin S, Bradley J, Cotter T (1990). HL-60 cells induced to differentiate towards neutrophils subsequently die via apoptosis. *Clinical & Experimental Immunology* 79(3)*:*448-453.

Masure S, Proost P, Damme J, Opdenakker G (1991). Purification and identification of 91-kDa neutrophil gelatinase. *European Journal of Biochemistry* 198(2)*:*391-398.

Matarasso S, Daniele V, Iorio Siciliano V, Mignogna MD, Andreuccetti G, Cafiero C (2009). The effect of recombinant granulocyte colony-stimulating factor on oral and periodontal manifestations in a patient with cyclic neutropenia: a case report. *International journal of dentistry* 2009(

Matthews J, Wright H, Roberts A, Cooper P, Chapple I (2007a). Hyperactivity and reactivity of peripheral blood neutrophils in chronic periodontitis. *Clinical & Experimental Immunology* 147(2)*:*255-264.

Matthews J, Wright H, Roberts A, Ling-Mountford N, Cooper P, Chapple I (2007b). Neutrophil hyper-responsiveness in periodontitis. *Journal of dental research* 86(8)*:*718-722.

Matthews JB, Chen FM, Milward MR, Wright HJ, Carter K, McDonagh A *et al.* (2011). Effect of nicotine, cotinine and cigarette smoke extract on the neutrophil respiratory burst. *Journal of clinical periodontology* 38(3)*:*208-218.

Matthews JB, Chen FM, Milward MR, Ling MR, Chapple IL (2012). Neutrophil superoxide production in the presence of cigarette smoke extract, nicotine and cotinine. *Journal of clinical periodontology* 39(7)*:*626-634.

Menegazzi R, Decleva E, Dri P (2012). Killing by neutrophil extracellular traps: fact or folklore? *Blood* 119(5)*:*1214-1216.

Meng W, Paunel-Gorgulu A, Flohé S, Hoffmann A, Witte I, MacKenzie C *et al.* (2012). Depletion of neutrophil extracellular traps in vivo results in hypersusceptibility to polymicrobial sepsis in mice. *Crit Care* 16(4)*:*R137.

Metcalf D (1991). Control of granulocytes and macrophages: molecular, cellular, and clinical aspects. *science* 254(5031)*:*529-533.

Mettraux G, Gusberti F, Graf H (1984). Oxygen Tension (pO2) in Untreated Human Periodontal Pockets. *Journal of periodontology* 55(9)*:*516-521.

Michlewska S, Dransfield I, Megson IL, Rossi AG (2009). Macrophage phagocytosis of apoptotic neutrophils is critically regulated by the opposing actions of pro-inflammatory and anti-inflammatory agents: key role for TNF-α. *The FASEB Journal* 23(3)*:*844-854.

Miyasaki KT (1991). The neutrophil: mechanisms of controlling periodontal bacteria. *Journal of periodontology* 62(12)*:*761-774.

Morgan PE, Pattison DI, Talib J, Summers FA, Harmer JA, Celermajer DS *et al.* (2011). High plasma thiocyanate levels in smokers are a key determinant of thiol oxidation induced by myeloperoxidase. *Free Radical Biology and Medicine* 51(9)*:*1815-1822.

Mori Y, Yamaguchi M, Terao Y, Hamada S, Ooshima T, Kawabata S (2012). α-Enolase of Streptococcus pneumoniae induces formation of neutrophil extracellular traps. *Journal of Biological Chemistry* 287(13)*:*10472-10481.

Mosely LH, Finseth F (1977). Cigarette smoking: impairment of digital blood flow and wound healing in the hand. *The Hand* 2)*:*97-101.

MousaviJazi M, Naderan A, Ebrahimpoor M, Sadeghipoor M (2013). Association between psychological stress and stimulation of inflammatory responses in periodontal disease. *Journal of dentistry (Tehran, Iran)* 10(1)*:*103.

Moxon E, Kroll J (1990). The role of bacterial polysaccharide capsules as virulence factors. In: Bacterial capsules: Springer, pp. 65-85.

Munafo DB, Johnson JL, Brzezinska AA, Ellis BA, Wood MR, Catz SD (2009). DNase I inhibits a late phase of reactive oxygen species production in neutrophils. *Journal of innate immunity* 1(6)*:*527.

Mydel P, Takahashi Y, Yumoto H, Sztukowska M, Kubica M, Gibson 3rd F *et al.* (2006). Roles of the host oxidative immune response and bacterial antioxidant rubrerythrin during Porphyromonas gingivalis infection. *PLoS Pathog* 2(7)*:*e76-e76.

Nagy P, Jameson GN, Winterbourn CC (2009). Kinetics and mechanisms of the reaction of hypothiocyanous acid with 5-thio-2-nitrobenzoic acid and reduced glutathione. *Chemical research in toxicology* 22(11)*:*1833-1840.

Narasaraju T, Yang E, Samy RP, Ng HH, Poh WP, Liew A-A *et al.* (2011). Excessive neutrophils and neutrophil extracellular traps contribute to acute lung injury of influenza pneumonitis. *The American journal of pathology* 179(1)*:*199-210.

Nauseef WM (2007). Isolation of human neutrophils from venous blood. In: Neutrophil Methods and Protocols: Springer, pp. 15-20.

Neumann A, Völlger L, Berends ET, Molhoek EM, Stapels DA, Midon M *et al.* (2014). Novel Role of the Antimicrobial Peptide LL-37 in the Protection of Neutrophil Extracellular Traps against Degradation by Bacterial Nucleases. *Journal of innate immunity* 6(6)*:*860-868.

Nguyen H, Finkelstein E, Reznick A, Cross C, van der Vliet A (2001). Cigarette smoke impairs neutrophil respiratory burst activation by aldehyde-induced thiol modifications. *Toxicology* 160(1)*:*207-217.

Nicu E, Van der Velden U, Everts V, Van Winkelhoff A, Roos D, Loos B (2007). Hyper-reactive PMNs in FcγRIIa 131 H/H genotype periodontitis patients. *Journal of clinical periodontology* 34(11)*:*938-945.

Nishinaka Y, Arai T, Adachi S, Takaori-Kondo A, Yamashita K (2011). Singlet oxygen is essential for neutrophil extracellular trap formation. *Biochemical and biophysical research communications* 413(1)*:*75-79.

Nordenfelt P, Tapper H (2011). Phagosome dynamics during phagocytosis by neutrophils. *Journal of leukocyte biology* 90(2)*:*271-284.

Nunes P, Demaurex N, Dinauer MC (2013). Regulation of the NADPH oxidase and associated ion fluxes during phagocytosis. *Traffic* 14(11)*:*1118-1131.

Nyström P-O (1998). The systemic inflammatory response syndrome: definitions and aetiology. *Journal of Antimicrobial Chemotherapy* 41(suppl 1)*:*1-7.

Nyvad B, Kilian M (1987). Microbiology of the early colonization of human enamel and root surfaces in vivo. *European Journal of Oral Sciences* 95(5)*:*369-380.

Oh H, Siano B, Diamond S (2008). Neutrophil Isolation Protocol. JoVE. 17.

Ooi CE, Weiss J, Elsbach P, Frangione B, Mannion B (1987). A 25-kDa NH2-terminal fragment carries all the antibacterial activities of the human neutrophil 60-kDa bactericidal/permeability-increasing protein. *Journal of Biological Chemistry* 262(31)*:*14891-14894.

Palmer L, Chapple I, Wright H, Roberts A, Cooper P (2012a). Extracellular deoxyribonuclease production by periodontal bacteria. *Journal of periodontal research* 47(4)*:*439-445.

Palmer L, Cooper P, Ling M, Wright H, Huissoon A, Chapple I (2012b). Hypochlorous acid regulates neutrophil extracellular trap release in humans. *Clinical & Experimental Immunology* 167(2)*:*261-268.

Palmer LJ, Damgaard C, Holmstrup P, Nielsen CH (2015). Influence of complement on neutrophil extracellular trap release induced by bacteria. *Journal of periodontal research*.

Papayannopoulos V, Metzler KD, Hakkim A, Zychlinsky A (2010). Neutrophil elastase and myeloperoxidase regulate the formation of neutrophil extracellular traps. *The Journal of cell biology* 191(3)*:*677-691.

Papayannopoulos V, Staab D, Zychlinsky A (2011). Neutrophil elastase enhances sputum solubilization in cystic fibrosis patients receiving DNase therapy. *PLoS One* 6(12)*:*e28526.

Parker H, Dragunow M, Hampton MB, Kettle AJ, Winterbourn CC (2012). Requirements for NADPH oxidase and myeloperoxidase in neutrophil extracellular trap formation differ depending on the stimulus. *Journal of leukocyte biology* 92(4)*:*841-849.

Paster BJ, Dewhirst FE (2009). Molecular microbial diagnosis. *Periodontology 2000* 51(1)*:*38-44.

Patel S, Kumar S, Jyoti A, Srinag BS, Keshari RS, Saluja R *et al.* (2010). Nitric oxide donors release extracellular traps from human neutrophils by augmenting free radical generation. *Nitric Oxide* 22(3)*:*226-234.

Perera NC, Wiesmüller K-H, Larsen MT, Schacher B, Eickholz P, Borregaard N *et al.* (2013). NSP4 is stored in azurophil granules and released by activated neutrophils as active endoprotease with restricted specificity. *The Journal of Immunology* 191(5)*:*2700-2707.

Perera P-Y, Mayadas TN, Takeuchi O, Akira S, Zaks-Zilberman M, Goyert SM *et al.* (2001). CD11b/CD18 acts in concert with CD14 and Toll-like receptor (TLR) 4 to elicit full lipopolysaccharide and taxol-inducible gene expression. *The Journal of Immunology* 166(1)*:*574-581.

Petit-Bertron A-F, Tabary O, Corvol H, Jacquot J, Clément A, Cavaillon J-M *et al.* (2008). Circulating and airway neutrophils in cystic fibrosis display different TLR expression and responsiveness to interleukin-10. *Cytokine* 41(1)*:*54-60.

Pham CT, Ley TJ (1999). Dipeptidyl peptidase I is required for the processing and activation of granzymes A and B in vivo. *Proceedings of the National Academy of Sciences* 96(15)*:*8627-8632.

Pham CT, Ivanovich JL, Raptis SZ, Zehnbauer B, Ley TJ (2004). Papillon-Lefevre syndrome: correlating the molecular, cellular, and clinical consequences of cathepsin C/dipeptidyl peptidase I deficiency in humans. *The Journal of Immunology* 173(12)*:*7277-7281.

Pillay J, den Braber I, Vrisekoop N, Kwast LM, de Boer RJ, Borghans JA *et al.* (2010). In vivo labeling with 2H2O reveals a human neutrophil lifespan of 5.4 days. *Blood* 116(4)*:*625-627.

Pilsczek FH, Salina D, Poon KK, Fahey C, Yipp BG, Sibley CD *et al.* (2010). A novel mechanism of rapid nuclear neutrophil extracellular trap formation in response to Staphylococcus aureus. *The Journal of Immunology* 185(12)*:*7413-7425.

Pinho MM, Faria-Almeida R, Azevedo E, Conceição Manso M, Martins L (2013). Periodontitis and atherosclerosis: an observational study. *Journal of periodontal research* 48(4)*:*452-457.

Porschen RK, Sonntag S (1974). Extracellular deoxyribonuclease production by anaerobic bacteria. *Applied microbiology* 27(6)*:*1031-1033.

Pütsep K, Carlsson G, Boman HG, Andersson M (2002). Deficiency of antibacterial peptides in patients with morbus Kostmann: an observation study. *The Lancet* 360(9340)*:*1144-1149.

Quigley GA, Hein JW (1962). Comparative cleansing efficiency of manual and power brushing. *The Journal of the American Dental Association* 65(1)*:*26-29.

Ragghianti MS, Greghi SLA, Lauris JRP, Sant'Ana ACP, Passanezi E (2004). Influence of age, sex, plaque and smoking on periodontal conditions in a population from Bauru, Brazil. *Journal of Applied Oral Science* 12(4)*:*273-279.

Ramos-Kichik V, Mondragón-Flores R, Mondragón-Castelán M, Gonzalez-Pozos S, Muñiz-Hernandez S, Rojas-Espinosa O *et al.* (2009). Neutrophil extracellular traps are induced by Mycobacterium tuberculosis. *Tuberculosis* 89(1)*:*29-37.

Ramsay RG, Gonda TJ (2008). MYB function in normal and cancer cells. *Nature Reviews Cancer* 8(7)*:*523-534.

Randers E, Erlandsen E, Pedersen O, Hasling C, Danielsen H (2000). Serum cystatin C as an endogenous parameter of the renal function in patients with normal to moderately impaired kidney function. *Clinical nephrology* 54(3)*:*203-209.

Reeves EP, Lu H, Jacobs HL, Messina CG, Bolsover S, Gabella G *et al.* (2002). Killing activity of neutrophils is mediated through activation of proteases by K+ flux. *Nature* 416(6878)*:*291-297.

Reher VG, Zenóbio EG, Costa FO, Reher P, Soares RV (2007). Nitric oxide levels in saliva increase with severity of chronic periodontitis. *Journal of oral science* 49(4)*:*271-276.

Reilly M, Delanty N, Lawson JA, FitzGerald GA (1996). Modulation of oxidant stress in vivo in chronic cigarette smokers. *Circulation* 94(1)*:*19-25.

Reinhardt RA, Bolton RW, McDonald TL, DuBois LM, Kaidahl WB (1988). In Situ Lymphocyte Subpopulations from Active versus Stable Periodontal Sites. *Journal of periodontology* 59(10)*:*656-670.

Remijsen Q, Berghe TV, Wirawan E, Asselbergh B, Parthoens E, De Rycke R *et al.* (2011). Neutrophil extracellular trap cell death requires both autophagy and superoxide generation. *Cell research* 21(2)*:*290-304.

Rice W, Ganz T, Kinkade JJ, Selsted M, Lehrer R, Parmley R (1987). Defensin-rich dense granules of human neutrophils. *Blood* 70(3)*:*757-765.

Roberts HM, Ling MR, Insall R, Kalna G, Spengler J, Grant MM *et al.* (2015). Impaired neutrophil directional chemotactic accuracy in chronic periodontitis patients. *Journal of clinical periodontology*.

Roberts A, Matthews J, Socransky S, Freestone P, Williams P, Chapple I (2005). Stress and the periodontal diseases: growth responses of periodontal bacteria to Escherichia coli stress-associated autoinducer and exogenous Fe. *Oral microbiology and immunology* 20(3)*:*147-153.

Robinson JM (2008). Reactive oxygen species in phagocytic leukocytes. *Histochemistry and cell biology* 130(2)*:*281-297.

Rocha JD, Nascimento MT, Decote-Ricardo D, Côrte-Real S, Morrot A, Heise N *et al.* (2015). Capsular polysaccharides from Cryptococcus neoformans modulate production of neutrophil extracellular traps (NETs) by human neutrophils. *Scientific reports* 5.

Romanelli R, Mancini S, Laschinger C, Overall CM, Sodek J, McCulloch CA (1999). Activation of neutrophil collagenase in periodontitis. *Infection and immunity* 67(5)*:*2319-2326.

Rosin M, Kramer A, Bradtke D, Richter G, Kocher T (2002). The effect of a SCN–/H2O2 toothpaste compared to a commercially available triclosan-containing toothpaste on oral hygiene and gingival health–a 6-month home-use study. *Journal of clinical periodontology* 29(12)*:*1086-1091.

Roxo-Junior P, Simão H (2014). Chronic granulomatous disease: why an inflammatory disease? *Brazilian Journal of Medical and Biological Research* 47(11)*:*924-928.

Ryder MI, Fujitaki R, Johnson G, Hyun W (1998). Alterations of neutrophil oxidative burst by in vitro smoke exposure: implications for oral and systemic diseases. *Annals of Periodontology* 3(1)*:*76-87.

Sabroe I, Dower SK, Whyte MK (2005). The role of Toll-like receptors in the regulation of neutrophil migration, activation, and apoptosis. *Clinical Infectious Diseases* 41(Supplement 7)*:*S421-S426.

Saffarzadeh M, Juenemann C, Queisser MA, Lochnit G, Barreto G, Galuska SP *et al.* (2012). Neutrophil extracellular traps directly induce epithelial and endothelial cell death: a predominant role of histones. *PLoS One* 7(2)*:*e32366-e32366.

Saffarzadeh M, Preissner KT (2013). Fighting against the dark side of neutrophil extracellular traps in disease: manoeuvres for host protection. *Current opinion in hematology* 20(1)*:*3-9.

Saitoh T, Komano J, Saitoh Y, Misawa T, Takahama M, Kozaki T *et al.* (2012). Neutrophil extracellular traps mediate a host defense response to human immunodeficiency virus-1. *Cell host & microbe* 12(1)*:*109-116.

Sakai J, Li J, Subramanian KK, Mondal S, Bajrami B, Hattori H *et al.* (2012). Reactive oxygen species-induced actin glutathionylation controls actin dynamics in neutrophils. *Immunity* 37(6)*:*1037-1049.

Samanta A, Oppenheim JJ, Matsushima K (1990). Interleukin 8 (monocyte-derived neutrophil chemotactic factor) dynamically regulates its own receptor expression on human neutrophils. *Journal of Biological Chemistry* 265(1)*:*183-189.

Savill J, Wyllie A, Henson J, Walport M, Henson P, Haslett C (1989). Macrophage phagocytosis of aging neutrophils in inflammation. Programmed cell death in the neutrophil leads to its recognition by macrophages. *Journal of Clinical Investigation* 83(3)*:*865.

Schauer U, Stemberg F, Rieger CH, Borte M, Schubert S, Riedel F *et al.* (2003). IgG subclass concentrations in certified reference material 470 and reference values for children and adults determined with the binding site reagents. *Clinical Chemistry* 49(11)*:*1924-1929.

Scheel-Toellner D, Wang K, Craddock R, Webb PR, McGettrick HM, Assi LK *et al.* (2004). Reactive oxygen species limit neutrophil life span by activating death receptor signaling. *Blood* 104(8)*:*2557-2564.

Schenkein HA (2006). Host responses in maintaining periodontal health and determining periodontal disease. *Periodontology 2000* 40(1)*:*77-93.

Scott DA, Krauss JL (2012). Neutrophils in periodontal inflammation. *Frontiers of oral biology* 15(56.

Sengeløv H, Kjeldsen L, Borregaard N (1993). Control of exocytosis in early neutrophil activation. *The Journal of Immunology* 150(4)*:*1535-1543.

Sharma A, Sharma S (2011). Reactive oxygen species and antioxidants in periodontics: a review. *International Journal of Dental Clinics* 3(2).

Short KR, von Köckritz-Blickwede M, Langereis JD, Chew KY, Job ER, Armitage CW *et al.* (2014). Antibodies mediate formation of neutrophil extracellular traps in the middle ear and facilitate secondary pneumococcal otitis media. *Infection and immunity* 82(1)*:*364-370.

Silva T, Garlet G, Fukada S, Silva J, Cunha F (2007). Chemokines in oral inflammatory diseases: apical periodontitis and periodontal disease. *Journal of dental research* 86(4)*:*306-319.

Smit M, Westra J, Vissink A, Doornbos-van der Meer B, Brouwer E, van Winkelhoff AJ (2012). Periodontitis in established rheumatoid arthritis patients: a cross-sectional clinical, microbiological and serological study. *Arthritis Res Ther* 14(5)*:*R222.

Snelgrove RJ, Jackson PL, Hardison MT, Noerager BD, Kinloch A, Gaggar A *et al.* (2010). A critical role for LTA4H in limiting chronic pulmonary neutrophilic inflammation. *science* 330(6000)*:*90-94.

Socransky S, Haffajee A, Cugini M, Smith C, Kent R (1998). Microbial complexes in subgingival plaque. *Journal of clinical periodontology* 25(2)*:*134-144.

Söder B, Nedlich U, Jin LJ (1999). Longitudinal effect of non-surgical treatment and systemic metronidazole for 1 week in smokers and non-smokers with refractory periodontitis: a 5-year study. *Journal of periodontology* 70(7)*:*761-771.

Solomon A (1985). Light chains of human immunoglobulins. *Methods in enzymology* 116(101).

Sørensen OE, Clemmensen SN, Dahl SL, Østergaard O, Heegaard NH, Glenthøj A *et al.* (2014). Papillon-Lefèvre syndrome patient reveals species-dependent requirements for neutrophil defenses. *The Journal of clinical investigation* 124(10)*:*4539.

Springer DJ, Ren P, Raina R, Dong Y, Behr MJ, McEwen BF *et al.* (2010). Extracellular fibrils of pathogenic yeast Cryptococcus gattii are important for ecological niche, murine virulence and human neutrophil interactions. *PLoS One* 5(6)*:*e10978.

Takeuchi O, Hoshino K, Kawai T, Sanjo H, Takada H, Ogawa T *et al.* (1999). Differential roles of TLR2 and TLR4 in recognition of gram-negative and gram-positive bacterial cell wall components. *Immunity* 11(4)*:*443-451.

Takiguchi T, Morizane S, Yamamoto T, Kajita A, Ikeda K, Iwatsuki K (2014). Cathelicidin antimicrobial peptide LL-37 augments interferon-β expression and antiviral activity induced by double-stranded RNA in keratinocytes. *British Journal of Dermatology* 171(3)*:*492-498.

Talib J, Pattison DI, Harmer JA, Celermajer DS, Davies MJ (2012). High plasma thiocyanate levels modulate protein damage induced by myeloperoxidase and perturb measurement of 3-chlorotyrosine. *Free Radical Biology and Medicine* 53(1)*:*20-29.

Tervahartiala T, Konttinen YT, Ingman T, Häyrinen-Immonen R, Ding Y, Sorsa T (1996). Cathepsin G in gingival tissue and crevicular fluid in adult periodontitis. *Journal of clinical periodontology* 23(2)*:*68-75.

Theilade E (1986). The non-specific theory in microbial etiology of inflammatory periodontal diseases. *Journal of clinical periodontology* 13(10)*:*905-911.

Tillack K, Breiden P, Martin R, Sospedra M (2012). T lymphocyte priming by neutrophil extracellular traps links innate and adaptive immune responses. *The Journal of Immunology* 188(7)*:*3150-3159.

Tonetti M, Claffey N (2005). Advances in the progression of periodontitis and proposal of definitions of a periodontitis case and disease progression for use in risk factor research. *Journal of clinical periodontology* 32(s6)*:*210-213.

Tonetti MS (1998). Cigarette smoking and periodontal diseases: etiology and management of disease. *Annals of Periodontology* 3(1)*:*88-101.

Tortorella C, Stella I, Piazzolla G, Simone O, Cappiello V, Antonaci S (2004). Role of defective ERK phosphorylation in the impaired GM-CSF-induced oxidative response of neutrophils in elderly humans. *Mechanisms of ageing and development* 125(8)*:*539-546.

Turesky S, Gilmore ND, Glickman I (1970). Reduced plaque formation by the chloromethyl analogue of victamine C. *Journal of periodontology* 41(1)*:*41.

Urban CF, Reichard U, Brinkmann V, Zychlinsky A (2006). Neutrophil extracellular traps capture and kill Candida albicans yeast and hyphal forms. *Cellular microbiology* 8(4)*:*668-676.

Urban CF, Ermert D, Schmid M, Abu-Abed U, Goosmann C, Nacken W *et al.* (2009). Neutrophil extracellular traps contain calprotectin, a cytosolic protein complex involved in host defense against Candida albicans. *PLoS Pathog* 5(10)*:*e1000639.

Van Bavel CC, Dieker JW, Kroeze Y, Tamboer WP, Voll R, Muller S *et al.* (2011). Apoptosis-induced histone H3 methylation is targeted by autoantibodies in systemic lupus erythematosus. *Annals of the rheumatic diseases* 70(1)*:*201-207.

van Houwelingen AH, Weathington NM, Verweij V, Blalock JE, Nijkamp FP, Folkerts G (2008). Induction of lung emphysema is prevented by L-arginine-threonine-arginine. *The FASEB Journal* 22(9)*:*3403-3408.

Vaughan KR, Stokes L, Prince LR, Marriott HM, Meis S, Kassack MU *et al.* (2007). Inhibition of neutrophil apoptosis by ATP is mediated by the P2Y11 receptor. *The Journal of Immunology* 179(12)*:*8544-8553.

Vitkov L, Klappacher M, Hannig M, Krautgartner W (2009). Extracellular neutrophil traps in periodontitis. *Journal of periodontal research* 44(5)*:*664-672.

Vitkov L, Klappacher M, Hannig M, Krautgartner WD (2010). Neutrophil fate in gingival crevicular fluid. *Ultrastructural pathology* 34(1)*:*25-30.

Vuorte J, Jansson SE, Repo H (2001). Evaluation of red blood cell lysing solutions in the study of neutrophil oxidative burst by the DCFH assay. *Cytometry* 43(4)*:*290-296.

Waddington R, Moseley R, Embery G (2000). Reactive oxygen species: a potential role in the pathogenesis of periodontal diseases. *Oral diseases* 6(3)*:*138-151.

Wagner JG, Roth RA (2000). Neutrophil migration mechanisms, with an emphasis on the pulmonary vasculature. *Pharmacological reviews* 52(3)*:*349-374.

Wahaidi V, Dowsett S, Eckert G, Kowolik M (2009). Neutrophil response to dental plaque by gender and race. *Journal of dental research* 88(8)*:*709-714.

Wahaidi VY, Kowolik MJ, Eckert GJ, Galli DM (2011). Endotoxemia and the host systemic response during experimental gingivitis. *Journal of clinical periodontology* 38(5)*:*412-417.

Wang J-G, Mahmud SA, Nguyen J, Slungaard A (2006). Thiocyanate-dependent induction of endothelial cell adhesion molecule expression by phagocyte peroxidases: a novel HOSCN-specific oxidant mechanism to amplify inflammation. *The Journal of Immunology* 177(12)*:*8714-8722.

Wang Y, Li M, Stadler S, Correll S, Li P, Wang D *et al.* (2009). Histone hypercitrullination mediates chromatin decondensation and neutrophil extracellular trap formation. *The Journal of cell biology* 184(2)*:*205-213.

Wardini AB, Guimarães-Costa AB, Nascimento MT, Nadaes NR, Danelli MG, Mazur C *et al.* (2010). Characterization of neutrophil extracellular traps in cats naturally infected with feline leukemia virus. *Journal of general virology* 91(1)*:*259-264.

Wartha F, Beiter K, Albiger B, Fernebro J, Zychlinsky A, Normark S *et al.* (2007). Capsule and d-alanylated lipoteichoic acids protect Streptococcus pneumoniae against neutrophil extracellular traps. *Cellular microbiology* 9(5)*:*1162-1171.

Wegner N, Wait R, Sroka A, Eick S, Nguyen KA, Lundberg K *et al.* (2010). Peptidylarginine deiminase from Porphyromonas gingivalis citrullinates human fibrinogen and α-enolase: Implications for autoimmunity in rheumatoid arthritis. *Arthritis & Rheumatism* 62(9)*:*2662-2672.

Weiner DJ, Bucki R, Janmey PA (2003). The antimicrobial activity of the cathelicidin LL37 is inhibited by F-actin bundles and restored by gelsolin. *American journal of respiratory cell and molecular biology* 28(6)*:*738-745.

Wells JM, Gaggar A, Blalock JE (2015). MMP generated matrikines. *Matrix Biology*.

Whang YM, Jo U, Sung JS, Ju HJ, Kim HK, Park KH *et al.* (2013). Wnt5a is associated with cigarette smoke-related lung carcinogenesis via protein kinase C. *PLoS One* 8(1)*:*e53012.

Whitchurch CB, Tolker-Nielsen T, Ragas PC, Mattick JS (2002). Extracellular DNA required for bacterial biofilm formation. *science* 295(5559)*:*1487-1487.

White D, Tsakos G, Pitts N, Fuller E, Douglas G, Murray J *et al.* (2012). Adult Dental Health Survey 2009: common oral health conditions and their impact on the population. *British dental journal* 213(11)*:*567-572.

Wright HJ, Matthews JB, Chapple IL, Ling-Mountford N, Cooper PR (2008). Periodontitis associates with a type 1 IFN signature in peripheral blood neutrophils. *The Journal of Immunology* 181(8)*:*5775-5784.

Wright HL, Moots RJ, Edwards SW (2014). The multifactorial role of neutrophils in rheumatoid arthritis. *Nature Reviews Rheumatology* 10(10)*:*593-601.

Wright LM, Maloney W, Yu X, Kindle L, Collin-Osdoby P, Osdoby P (2005). Stromal cell-derived factor-1 binding to its chemokine receptor CXCR4 on precursor cells promotes the chemotactic recruitment, development and survival of human osteoclasts. *Bone* 36(5)*:*840-853.

Wyatt T, Heires A, Sanderson S, Floreani A (1999). Protein kinase C activation is required for cigarette smoke–enhanced C5a-mediated release of interleukin-8 in human bronchial epithelial cells. *American journal of respiratory cell and molecular biology* 21(2)*:*283-288.

Xu Y, Loison F, Luo HR (2010). Neutrophil spontaneous death is mediated by down-regulation of autocrine signaling through GPCR, PI3Kγ, ROS, and actin. *Proceedings of the National Academy of Sciences* 107(7)*:*2950-2955.

Yamamoto A, Taniuchi S, Tsuji S, KOBAYASHI MH, Kobayashi Y (2002). Role of reactive oxygen species in neutrophil apoptosis following ingestion of heat-killed Staphylococcus aureus. *Clinical & Experimental Immunology* 129(3)*:*479-484.

Yamauchi K, Tomita M, Giehl T, Ellison Rr (1993). Antibacterial activity of lactoferrin and a pepsin-derived lactoferrin peptide fragment. *Infection and immunity* 61(2)*:*719-728.

Yeh T-M, Chang H-C, Liang C-C, Wu J-J, Liu M-F (2003). Deoxyribonuclease-inhibitory antibodies in systemic lupus erythematosus. *Journal of biomedical science* 10(5)*:*544-551.

Yost CC, Cody MJ, Harris ES, Thornton NL, McInturff AM, Martinez ML *et al.* (2009). Impaired neutrophil extracellular trap (NET) formation: a novel innate immune deficiency of human neonates. *Blood* 113(25)*:*6419-6427.

Yousefi S, Mihalache C, Kozlowski E, Schmid I, Simon H (2009). Viable neutrophils release mitochondrial DNA to form neutrophil extracellular traps. *Cell Death & Differentiation* 16(11)*:*1438-1444.

Yu L, DeLeo FR, Biberstine-Kinkade KJ, Renee J, Nauseef WM, Dinauer MC (1999). Biosynthesis of Flavocytochrome b 558 gp91 phox IS SYNTHESIZED AS A 65-kDa PRECURSOR (p65) IN THE ENDOPLASMIC RETICULUM. *Journal of Biological Chemistry* 274(7)*:*4364-4369.

Yu Y, Su K (2013). Neutrophil extracellular traps and systemic lupus erythematosus. *Journal of clinical & cellular immunology* 4(139).

Zambon J, Grossi S, Machtei E, Ho A, Dunford R, Genco R (1996). Cigarette Smoking Increases the Risk for Subgingival Infection With Periodontal Pathogens. *Journal of periodontology* 67(10s)*:*1050-1054.

APPENDIX

I. ROS and NET production in response to live and dead bacteria

To determine whether neutrophil activation differs between live and heat-killed bacterial stimuli, ROS and NET production were quantified in response to stimulation with 4 bacterial species. Live and heat-killed bacteria were assayed in parallel at the same concentration ($1x10^8$ and MOI of 1000). Total ROS production quantified by enhanced luminol chemiluminescence was significantly higher in cells stimulated with heat-killed bacteria. This was statistically significant following stimulation with *C. rectus, F. nucleatum poly* and *S. aureus* compared with live bacteria (2way ANOVA and Bonferroni post-tests $*p<0.05$, $****p<0.0001$, $*p<0.05$, respectively, n=3) (Figure Ia). Quantification of NET-DNA with Sytox green demonstrated that live bacteria induced elevated NET release compared with dead bacteria after 4 hours, however this was not statistically significant (2way ANOVA $p>0.05$, n=3) (Figure Ib).

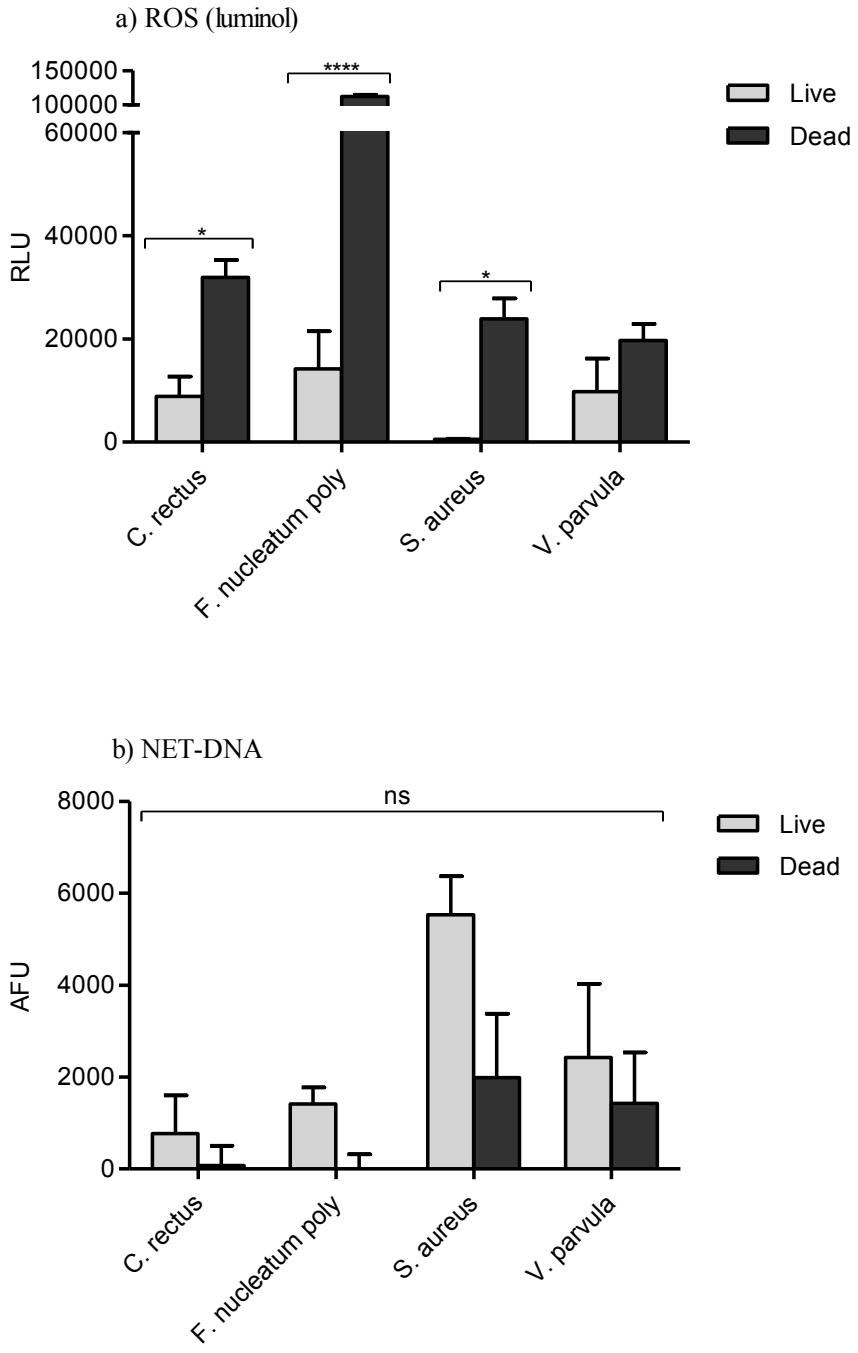

Figure I: ROS and NET production in response to live and dead bacteria
Live and heat-killed bacteria (both at $1x10^8$ and MOI of 1000) were employed as neutrophil stimuli. (a) Total ROS production measured by luminol enhanced chemiluminescence. Data is presented as RLU (relative light units). (b) Quantification of NET-DNA with Sytox green. Data is presented as AFU (arbitrary fluorescence units). Statistical significance calculated using 2way ANOVA and Bonferroni post-tests (*$p<0.05$, ****$p<0.0001$ ns=not significant). Data expressed as mean ± SEM (n=3 in triplicate).

II. NET killing preliminary assays

NET localisation to plastic-ware

To determine the location of NETs post stimulation, NETs were fluorometrically quantified by digestion assay Sytox green staining under three different conditions:

1. The supernatant was carefully aspirated off and the NETs in the supernatant were quantified with MNase digestion and Sytox green staining in a fresh plate.
2. The addition of fresh RPMI to selected wells, which was mixed by pipetting and quantified in the same plate.
3. NETs were quantified in the same well without the addition of fresh media but subjected to mixing by pipetting.

These preliminary experiments indicated that NETs adhere to the culture well surface, as there was no significant difference between the number of NETs quantified in the well with or without the addition of fresh media (1way ANOVA $p>0.05$, n=2). However there were significantly fewer NETs present in the well supernatant if removed from the well prior to the addition of MNase (1way ANOVA, ****$p<0.0001$, n=2). These findings would allow for the media to be aspirated off prior to the addition of live bacteria to the well in future killing assays (Figure IIa). This data was also corroborated by neutrophil and NET visualisation analysis, whereby 50nM PMA-stimulated neutrophils present in a 24-well plate were incubated for 3 hours, after which the supernatant was removed and the well contents visualised under bright field microscopy or by fluorometric analysis following Sytox green straining (Figure IIb).

Bacteria incubated with penicillin-streptomycin

Treatment of bacteria with increasing concentrations of penicillin-streptomycin (pen-strep) was employed as a positive control for bacterial growth inhibition. *S. sanguinis* (representative graph) was incubated with PBS (negative control) or pen-strep (concentrations ranging from 0.125-8.0µg/ml) for 1 hour prior to diluting the bacterial suspension and inoculating agar plates for the enumeration of colonies 24 hours later. A concentration dependent decrease in bacterial growth was observed as a result of pen-strep treatment, relative to the PBS control. This was statistically significant at 8.0µg/ml (Kruskal-Wallis and Dunn's post-tests $*p<0.05$, n=3) (Figure IIc).

a)

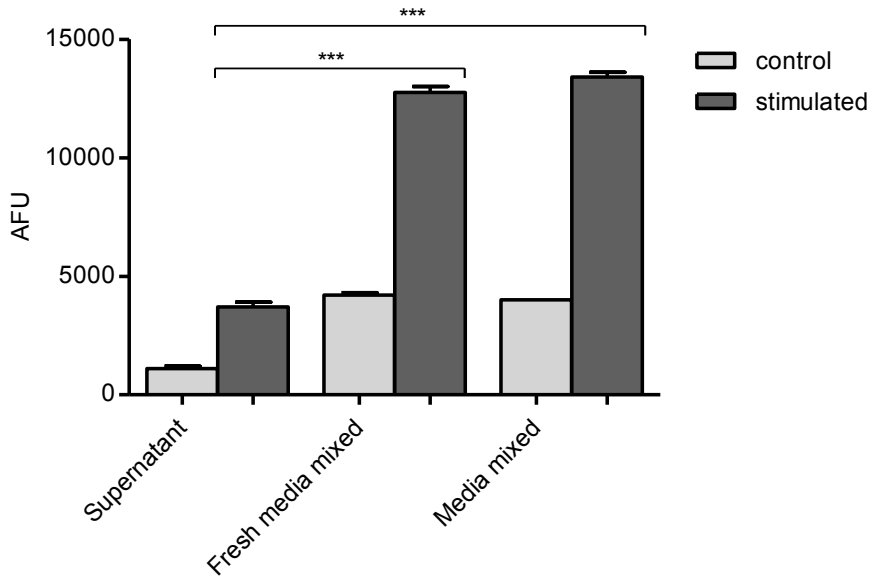

b)

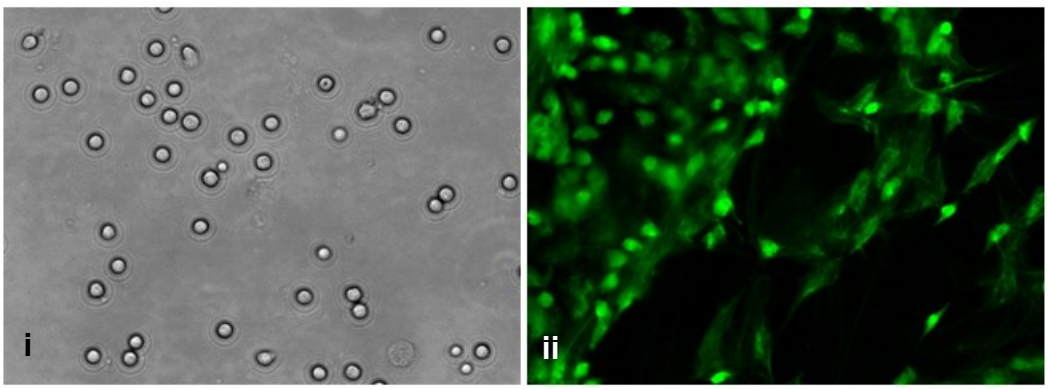

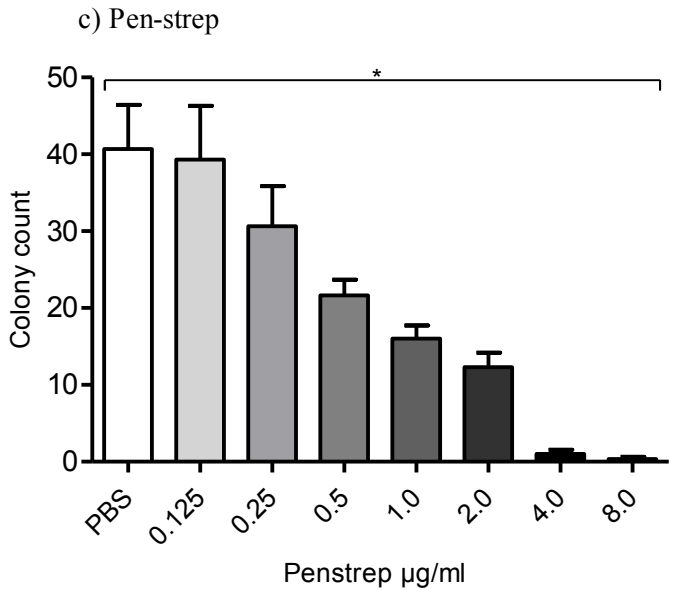

Figure II: NET killing preliminary experiments
(a) Neutrophils were stimulated for NET production (0.75mM HOCl for 3 hours) in a 24-well plate and the NETs fluorometrically quantified (Sytox green) under different experimental conditions. NETs were quantified in: 1) the supernatant carefully removed from the well; 2) in the well following the careful removal of the supernatant and the addition of fresh media which was mixed by pipetting; and 3) in the well where the supernatant had been mixed by pipetting. Statistical significance was calculated using 1way ANOVA (***$p<0.001$). Data presented as AFU (arbitrary fluorescence units) and expressed as mean ± SEM (n=2 in triplicate). (b) Microscopic analysis by stimulating neutrophils to produce NETs (50nM PMA for 3 hours) and removing the supernatant. Adherent neutrophils were visualised under (i) brightfield and (ii) following the addition of Sytox green stain. Representative images of 2 experiments. (c) Bacteria (representative graph showing *S. sanguinis*) incubated with PBS (negative control) or pen-strep (concentrations ranging from 0.125-8.0µg/ml) for 1 hour prior to inoculating agar plates to determine the effect on colony counts 24 hours later. Statistical significance calculated using Kruskal-Wallis and Dunn's post-tests (*$p<0.05$). Data presented as colony counts and expressed as mean ± SEM (n=3).

III. Validation of the quantification of NET-bound components

NET-bound components (NE, MPO and CG) were quantified following stimulation with PMA (50nM) to serve as a DNA-independent measure of NET release and to distinguish DNA release by necrosis from NETosis. NETs were washed in a 24-well plate (2x in PBS) to ensure the quantification of neutrophil granule components associated with NET structures, and not components concurrently released during neutrophil activation. To validate the assumption that wash steps enable only the quantification of NET bound components, preliminary experiments compared the quantification of commercially available MPO (0.5U/ml) in the supernatants of unwashed and washed wells. MPO was significantly higher (OD_{540nm}) in unwashed wells, compared with washed (Mann-Whitney *$p=0.028$, n=3). Similar observations were observed for the quantification of NE and CG (data not shown). These preliminary results confirm that 2 wash steps are sufficient to remove components in the supernatants and quantify only components associated with NETs (Figure III).

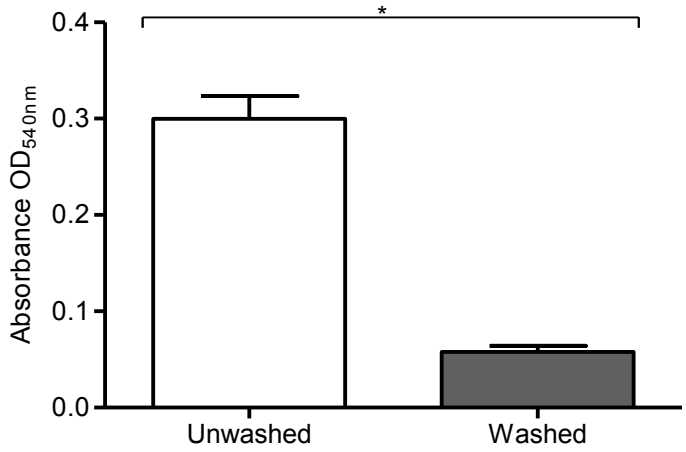

Figure III: Validation of the quantification of NET-bound components
Commercially available MPO (0.5U/ml) was quantified in the supernatants of unwashed and washed wells (2x PBS). MPO was significantly higher (OD_{540nm}) in unwashed wells (2x PBS wash steps), compared with washed (Mann-Whitney *$p=0.028$). Data presented as OD_{540nm} and expressed as mean ± SEM (n=3 in duplicate).

IV. Gram stains of bacteria

A. viscosus (43146)
Gram positive
Short rods

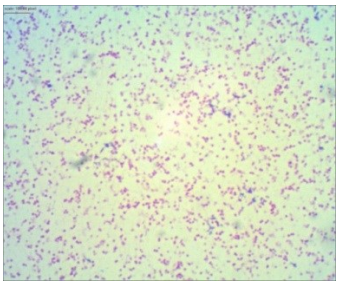

A. actinomycetemcomitans b (43718)
Gram negative
Rods/ovoid

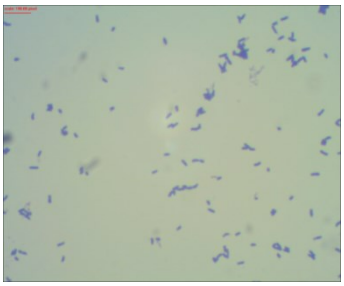

Pro. acnes (11827)
Gram positive
Short rods

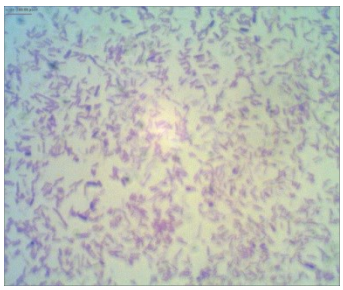

Sel. noxia (43541)
Gram negative
Short rods/crescents

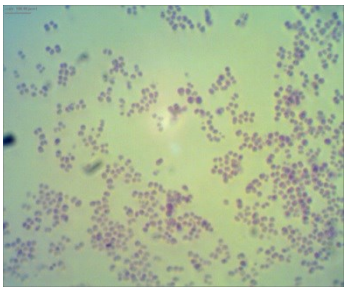

V. parvula (10790)
Gram negative
Cocci

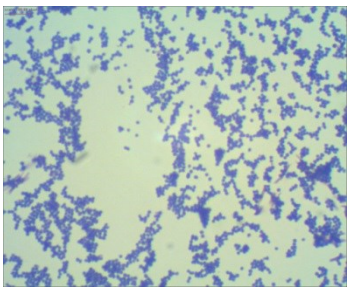

S. sanguinis (10556)
Gram positive
Cocci/ovoid

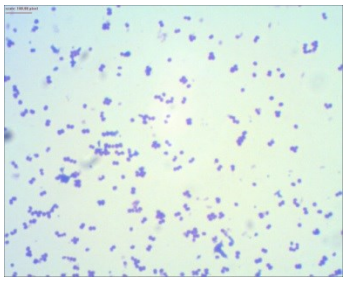

S. oralis (35037)
Gram positive
Cocci/ovoid

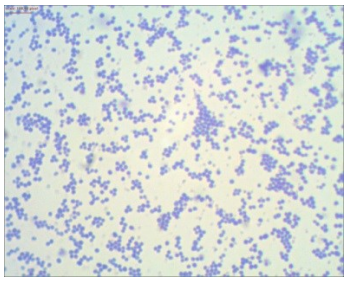

S. intermedius (27335)
Gram positive
Cocci/ovoid

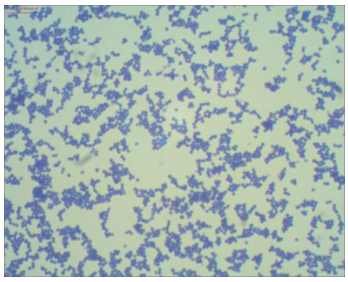

S. anginosus (33397)
Gram positive
Cocci/ovoid

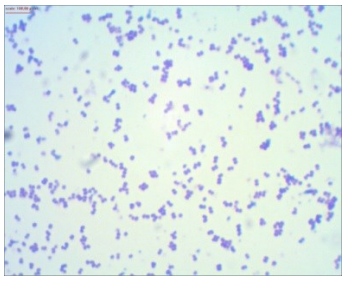

S. gordonii (10558)
Gram positive
Cocci/ovoid

C. gingivalis (33624[27])
Gram negative
Long rods

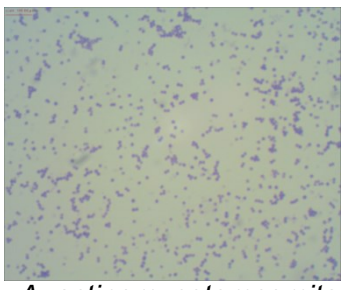

A. actinomycetemcomitans a (29523)
Gram negative
Rods/ovoid

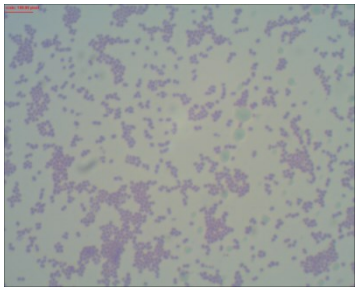

C. sput (33612[4])
Gram negative
Ovoid/rods

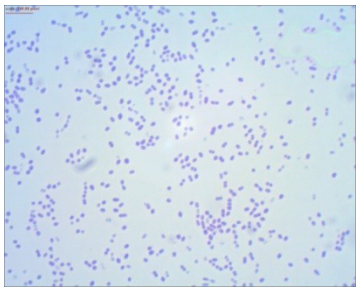

S. constellatus (27823[M32b])
Gram positive
Cocci/ovoid

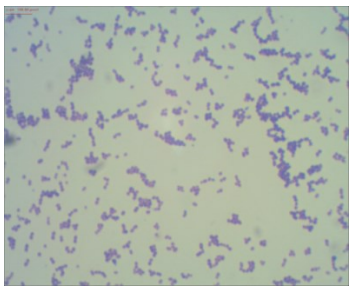

C. rectus (33238[371])
Gram negative
Ovoid/rods

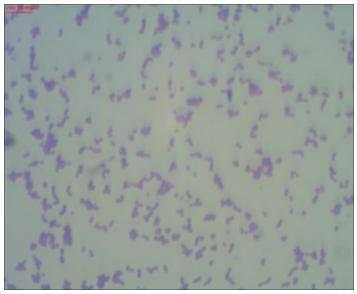

C. showae (51146)
Gram negative
Ovoid/rods

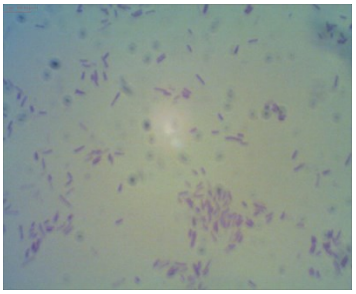

F. nucleatum nuc (25586)
Gram negative
Rods

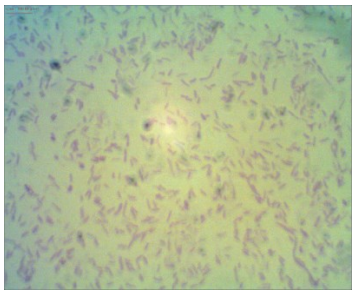

F. nucleatum poly (10953)
Gram negative
Rods

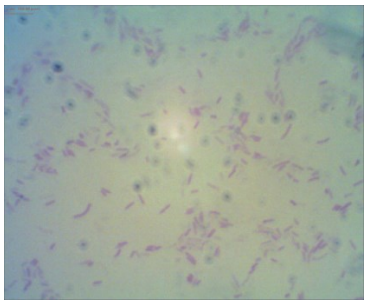

P. gingivalis (W83)
Gram negative
Rods

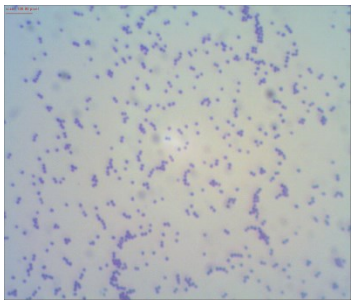

S. aureus (9144)
Gram positive
Cocci

Figure IV: Gram stains of bacterial cultures

Bacterial species were confirmed by Gram staining and analysis of bacteria morphology. Gram-negative bacteria stained-pink and Gram-positive bacteria stained blue. Cell morphologies included cocci (spherical), ovoid or rods (bacilli). Bacteria ATCC numbers are provided.

V. Comparisons between free light chain detection in plasma and serum samples

The assay employed for the detection of FLCs carried out by The Binding Site is validated in serum samples (Katzmann *et al.,* 2002). To validate this technique in plasma samples for subsequent analysis of chronic periodontitis plasma samples, kappa and lambda FLCs were quantified in plasma and serum samples from the same individuals in parallel (n=30). No significant difference was observed in the quantification of kappa (unpaired t-test $p=0.58$) or lambda (unpaired t-test $p=0.28$) FLCs in plasma and serum samples. Based on these results, FLCs were quantified in plasma samples using the same technique currently used by The Binding Site for the quantification of FLC in serum samples (Figure V).

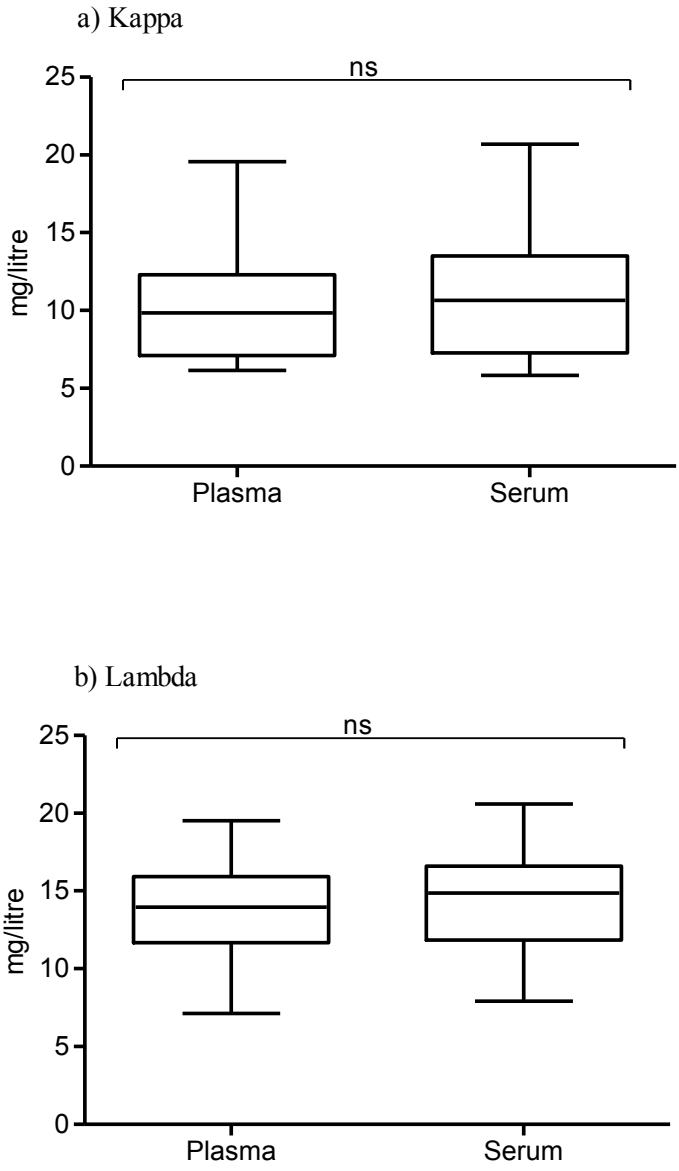

Figure V: Comparison between free light detection in plasma and serum samples
(a) Kappa and (b) lambda FLCs were quantified in plasma and serum from the same individuals (n=30). No significant difference was observed in the quantification of kappa (*p=0.58*) or lambda (*p=0.28*) FLCs in plasma and serum samples (analysed by unpaired t-test). Data presented as mg/l and expressed as mean ± SEM (n=30).

VI. Collection and storage of NET supernatants

To store NET supernatants for subsequent assays investigating the effect of NETs on neutrophil responses and H400 epithelial cell growth, NETs were collected and stored at different temperatures. Storage conditions included 20°C, 37°C, 4°C, -20°C and -80°C (slow freezing by 1°C/minute or snap freezing with liquid nitrogen). The effectiveness of the storage method was determined by comparing the number of NETs (NET-DNA) quantified in the supernatant with Sytox green before and after storage for 24 hours. Results are presented as raw AFU data, as well as a ratio of the number of NETs quantified prior to storage. No significant differences were observed in the number of NETs quantified between the storage conditions compared with NET quantification results prior to storage (2way ANOVA $p>0.05$, n=5) (Figure VIa). Data expressed as a ratio of NET quantification results prior to storage demonstrated that the number of NETs quantified in the supernatant decreased as a result of storage at some temperatures, however this did not reach statistical significance (2way ANOVA $p>0.05$, n=5). Quantification of NET-DNA in supernatants stored at -80°C by snap freezing in liquid nitrogen was the most representative of the NETs prior to storage, evidenced by the smallest ratio change. Based on these findings, all NET supernatants were stored at -80°C by snap freezing prior to subsequent assays (Figure VIb).

a) NET quantification

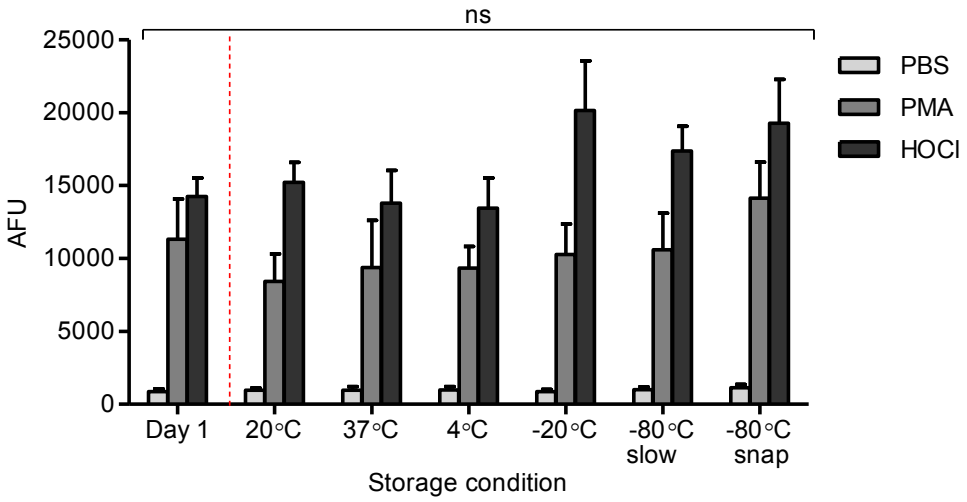

b) NET quantification expressed as a ratio

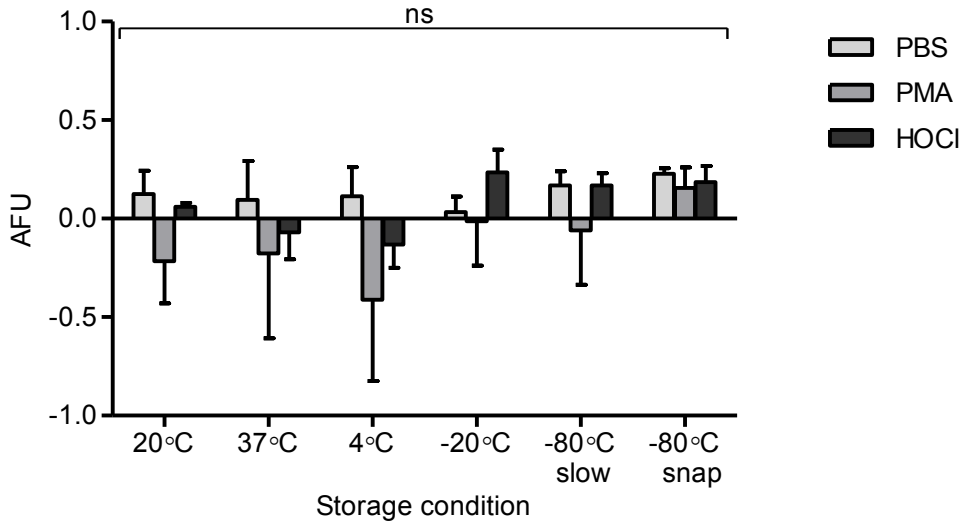

Figure VI: NET supernatant storage
NETs were stored at different temperatures (20°C, 37°C, 4°C, -20°C and -80°C [slow freezing by 1°C/minute or snap freezing with liquid nitrogen]). The effectiveness of the storage method was determined by comparing the number of NETs before and after storage for 24 hours. (a) NETs quantified by comparing AFU (arbitrary fluorescence units) values. (b) NET quantification expressed as a ratio of the number of NETs quantified prior to. Statistical significance calculated using 2way ANOVA (ns=not significant). Data expressed as mean ± SEM (n=5 in triplicate).

VII. H400 cell counting

Preliminary experiments compared *in situ* and trypsinised cell counts of H400 epithelial cells. *In situ* cell counts involved counting the cells comprising the monolayer adhered to the bottom of the flask. Trypsinised counts were performed by discarding the supernatants from the flask and washing in PBS, followed by the addition of T-EDTA for 10 mins at room temperature. The cell suspension was transferred to a fresh universal tube, centrifuged and re-suspended in cell culture media for subsequent cell counts. Cell counts were compared at 2, 3, 4 and 5 days after seeding flasks at $2x10^5$. Results demonstrated that higher cell counts were achieved when cells were counted *in situ* compared with trypsinised cells. However, both methods demonstrated comparable shaped growth curves, with similar standard deviations. *In situ* cell counts may be less accurate, as the monolayer confluency may not be consistent across the entire flask. Furthermore, to seed cells in a 96-well plate for subsequent NET supernatant assays, the cells will require trypsinising as they will not remain in the flask. Therefore, all future counts for assays involving H400s and NET supernatants relied on trypsinised counts (Figure VII).

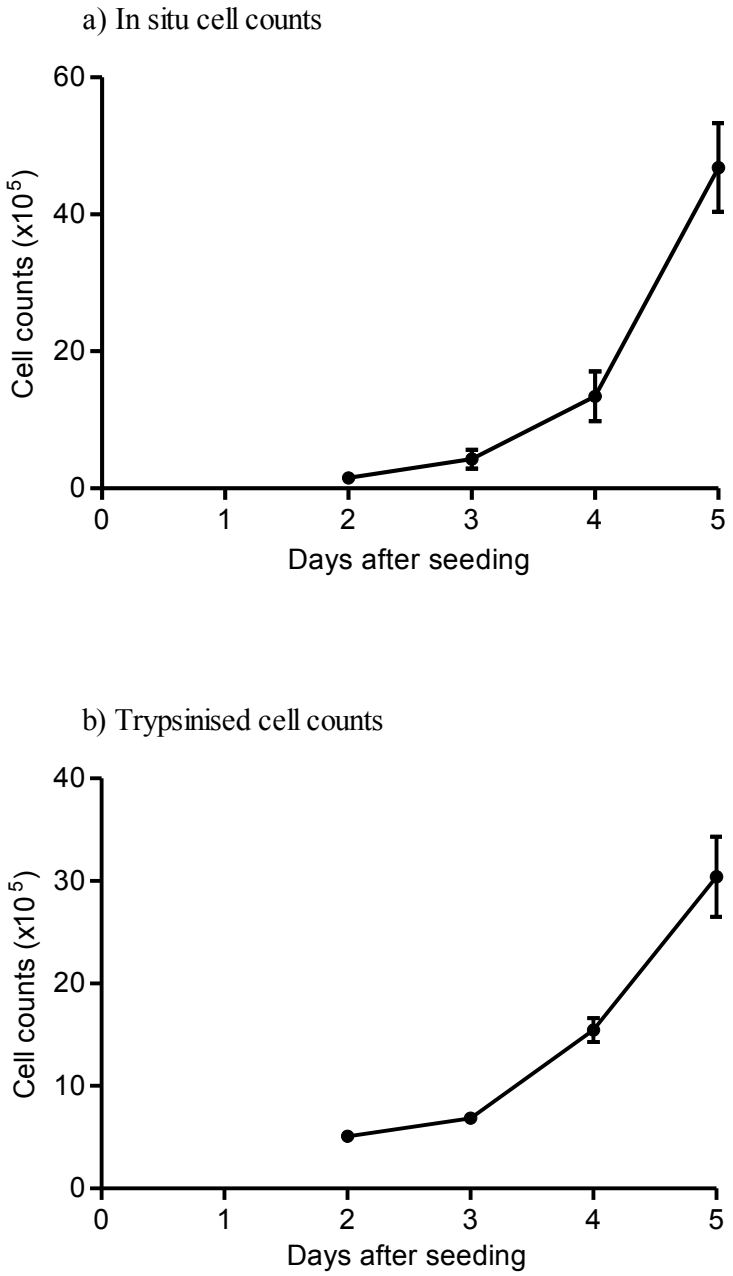

Figure VII: H400 cell counting
Preliminary experiments compared (a) *in situ* and (b) trypsinised cell counts of H400 epithelial cells. Cell counts were compared at 2, 3, 4 and 5 days after seeding flasks at $2x10^5$. Results are representative of a single experiment, data expressed as the mean ± Std Dev.

VIII. Effect of cigarette smoke extract and cigarette smoke extract components on the fluorometric quantification of calf thymus DNA

As it has previously been found that CSE inhibits luminol and isoluminol enhanced-chemiluminescence (Matthews *et al.,* 2011), preliminary studies were undertaken to establish whether CSE interferes with the NET quantification assay with Sytox green. CSE (1%, 5%, 10%) incubated with calf thymus DNA for 4 hours did not significantly affect the fluorometric quantification of calf thymus DNA (1way ANOVA *p=0.98*, n=5*).* The same preliminary experiments were employed to determine whether CSE components affect the quantification of NET-DNA. Nicotine (1µg/ml, 5µg/ml, 10µg/ml), cotinine (1µg/ml, 5µg/ml, 10µg/ml) and SCN- (50µM, 100µM, 150µM) also had no inhibitory effect on NET quantification (1way ANOVA *p=0.99, p=0.98, p=0.99* for nicotine, cotinine and SCN-, respectively, n=5). Based on these results, neutrophils were not washed following a 30 min pre-treatment with CSE or CSE components in subsequent assays (Figure VIII).

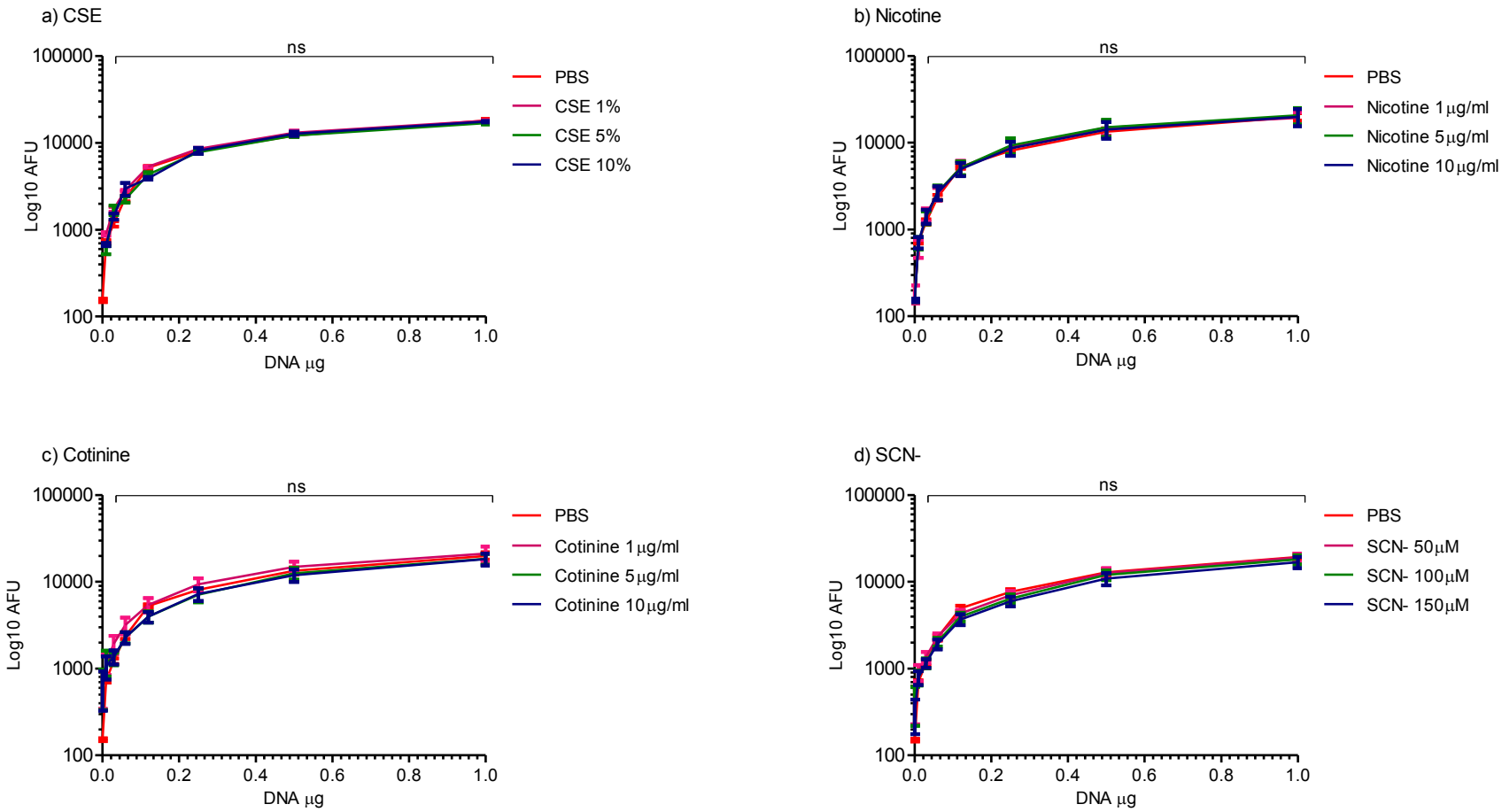

Figure VIII: Effect of cigarette smoke extract and cigarette smoke extract components on the fluorometric quantification of calf thymus DNA

Calf thymus DNA at increasing concentrations (µg) was incubated with PBS (negative control), CSE, nicotine, cotinine or SCN- for 4 hours. Post-incubation DNA was quantified fluorometrically with Sytox green. Statistical significance was calculated using 1way ANOVA (ns=not significant). Data are presented as Log10 AFU (arbitrary fluorescence units) and are expressed as mean ± SEM (n=5 in triplicate).

IX. Isolation of neutrophil RNA

The amount and purity of RNA isolated from treated neutrophils was determined by measuring the absorbance and the ratio of absorbance at 260/280nm. Pure RNA has a 260/280nm absorbance of 2.1, thus a value between 1.8-2.0nm is considered to be pure (Sambrook et al., 1989; Manchester 1996). Adequate amounts (µg/ml) of RNA were measured for each sample, and based on the amount of RNA in each sample, samples were equally pooled across the treatment conditions (n=10 biological repeats per treatment condition) (Table IX a&b).

Table IX: Quantity and purity of RNA

The amount and purity of isolated neutrophil RNA was determined by measuring the absorbance and the ratio of absorbance at 260/280nm.

a)

Sample No.	PBS		CSE 1%		CSE 5%		CSE 10%	
	RNA µg/ml	260nm/280nm ratio	RNA µg/ml	260nm/280nm ratio	RNA µg/ml	260nm/280nm ratio	RNA µg/ml	260nm/280nm ratio
1	28.6	1.43	42.30	1.33	31.6	1.57	29.3	1.69
2	31.9	1.99	54.90	1.40	32.5	1.61	28.2	1.7
3	36.6	1.55	32.00	1.75	45.7	1.50	59.3	1.80
4	55.0	1.60	31.08	1.90	29.6	1.15	31.3	1.70
5	31.1	1.55	29.30	1.46	50.4	1.33	51.6	120
6	33.1	1.29	33.50	1.30	54.5	1.19	43.1	1.25
7	31.9	1.84	34.70	1.51	46.2	1.41	38.1	1.65
8	33.5	1.62	49.80	1.12	33.9	1.18	54.5	1.23
9	31.9	1.84	47.30	1.62	25.6	1.67	34.6	1.51
10	45.1	1.21	33.70	1.89	57.0	1.24	32.4	1.58

b)

Sample No.	PBS		SCN^- 50µM		SCN^- 100µM		SCN^- 150µM	
	RNA µg/ml	260nm/280nm ratio	RNA µg/ml	260nm/280nm ratio	RNA µg/ml	260nm/280nm ratio	RNA µg/ml	260nm/280nm ratio
1	38.1	1.66	54.1	1.50	57.5	1.33	47.2	1.69
2	32.8	1.73	56.9	1.65	59.0	1.62	49.5	1.72
3	42.9	1.71	54.6	1.66	56.5	1.59	41.9	1.69
4	66.3	1.56	55.7	1.48	36.8	1.41	20.8	1.87
5	42.6	1.85	55.6	1.51	43.8	1.59	51.1	1.76
6	52.0	1.82	42.4	1.94	36.9	1.55	48.0	1.80
7	32.0	1.49	49.0	1.65	28.0	1.76	31.0	1.71
8	29.5	1.71	45.8	1.39	38.4	1.70	24.6	1.70
9	41.7	1.45	39.6	1.30	59.7	1.80	35.8	1.81
10	47.6	1.47	29.3	1.58	26.2	1.74	36.5	1.69

X. Determination of stable housekeeping genes

Preliminary assays determined the melt curves, amplification and efficiency of reference genes and the genes of interest. Target gene expression was determined by calculating fold changes in gene expression as a ratio of a reference housekeeping gene. The most appropriate housekeeper gene was determined by analysis of crossing point (CP) data with statistical algorithm BestKeeper (Pfaffl *et al.*, 2004). CP data indicates the number at which the fluorescence generation crosses the threshold and thus a sufficient number of amplicons have been produced (Rasmussen 2001). BestKeeper expression indicates that all candidate housekeeping genes had standard deviations lower than 1, suggesting they were all viable housekeeping genes for the study of these cells. However, YWHAZ had the lowest standard deviation (0.45) and was therefore considered the most stable of the reference genes tests. Based on these results, the YWHAZ housekeeping gene was considered the most consistent and therefore used as the reference against which to quantify the expression of genes of interest (Table X).

Table X: Comparison of housekeeping genes.
Analysis of 4 candidate housekeeping genes (HKG) used crossing point (CP) data. Abbreviations: SD (standard deviation), coefficient of variance % of CP (the coefficient of variance expressed as a percentage on the CP level), minimum/maximum [x-fold] (the extreme values of expression levels expressed as an absolute x-fold over- or under-regulation coefficient). Pfaffl *et al.,* 2004, Rasmussen 2001.

CP data of housekeeping Genes				
	GAPDH HKG 1	**YWHAZ HKG 2**	**HPRT1 HKG 3**	**RPL13 HKG 4**
Number of samples	4	4	4	4
Geometric mean of CP	29.50	27.36	32.40	25.58
Arithmetic mean of CP	29.52	27.36	32.41	25.59
Minimum CP	27.99	26.96	31.73	24.94
Maximum CP	30.87	28.27	33.72	26.46
SD of CP	0.79	0.45	0.65	0.56
coefficient of variance (% of CP)	2.66	1.66	2.02	2.20
minimum [x-fold]	-2.48	-1.31	-1.58	-1.49
maximum [x-fold]	2.28	1.85	2.45	1.73
Std Dev of absolute regulation coefficients	1.60	1.31	1.48	1.40

XI. RNA expression of cigarette smoke extract treated neutrophils relative to other reference genes

Neutrophil RNA expression of NF-κB, HSP40, IL-8, P-47^{phox}, P-67^{phox} and GP-91^{phox} was quantified by RT-PCR following CSE treatment (1%, 5%, 10%). Data are expressed as a ratio of the reference genes, GADPH, HPTY1 and RPL13, and RNA expression of cells treated with PBS (negative control) were normalised to 1.

GADPH

In response to CSE treatment, HSP40 expression increased and this was statistically significant at concentrations of 5% and 10% CSE (2way ANOVA and Bonferroni post-tests ****$p<0.0001$ for 5% and 10%, n=10 biological repeats, n=3 technical repeats) (Figure XIa).

HPTY1

In response to CSE treatment, HSP40 expression increased and this was statistically significant at concentrations of 5% and 10% CSE (2way ANOVA and Bonferroni post-tests ****$p<0.0001$ for 5% and 10%, n=10 biological repeats, n=3 technical repeats). Other non-significant trends included decreases in P-67^{phox} and GP-91^{phox} expression (Figure XIb).

RPL13

In response to CSE treatment, HSP40 expression increased and this was statistically significant at concentrations of 5% and 10% CSE (2way ANOVA and Bonferroni post-tests **$p<0.01$, ****$p<0.0001$ for 5% and 10%, respectively, n=10 biological repeats, n=3 technical repeats). Other non-significant trends included a CSE-concentration dependent decrease in NF-κB and decreased GP-91^{phox} expression (Figure XIc).

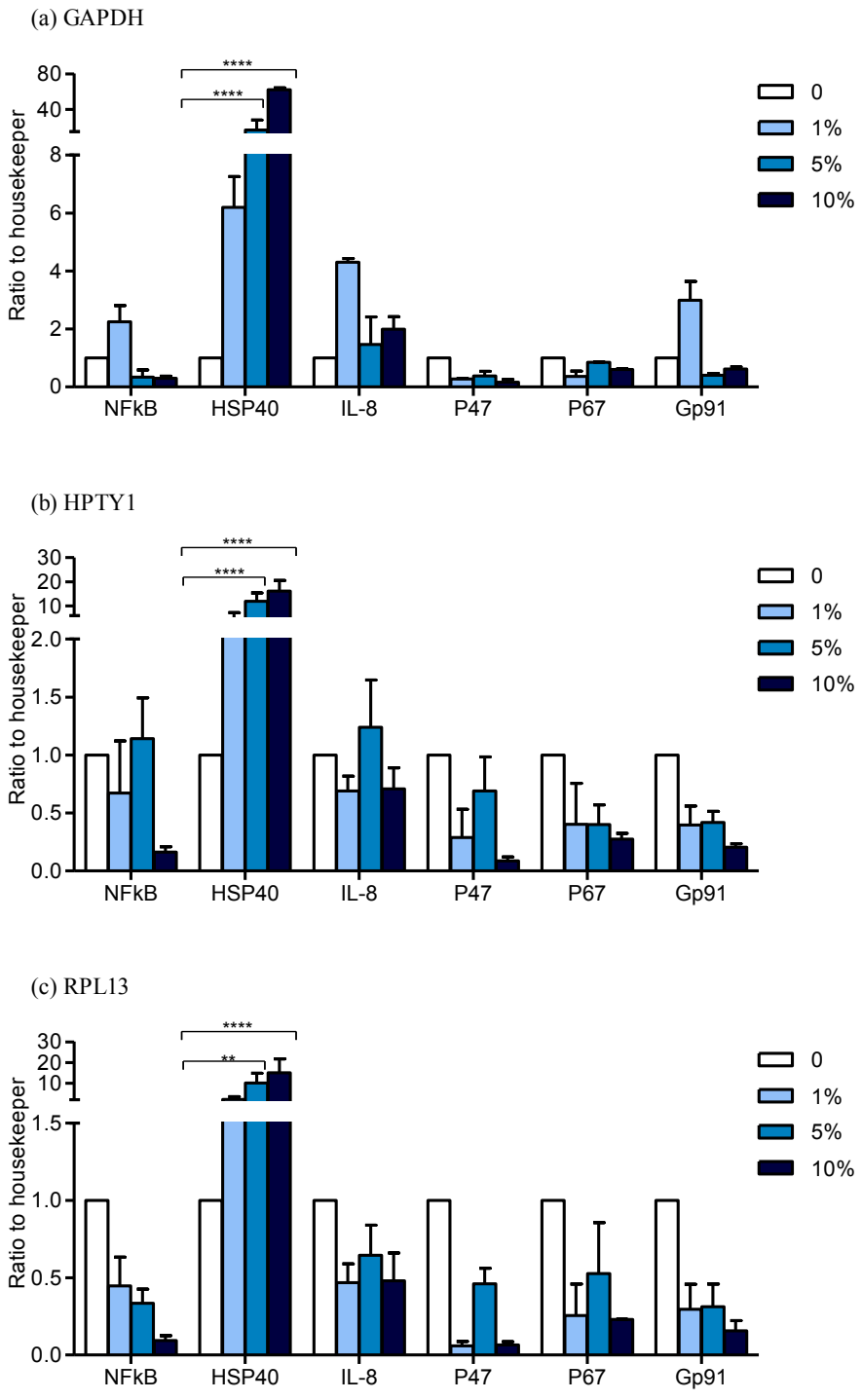

Figure XI: RNA expression of CSE treated neutrophils relative to other reference genes
Data are expressed as a ratio of the reference gene and RNA expression of cells treated with PBS (negative control) was normalised to 1. RNA expression as a ratio of reference gene (a) GAPDH, (b) HPTY1, (c) RPL13. Statistical significance calculated using 2way ANOVA and Bonferroni post-tests (***p<0.01,* *****p<0.0001*). Data is expressed as mean ± SEM (n=10 pooled biological repeats and n=3 technical repeats).

XII. RNA expression of thiocyanate treated neutrophils relative to other reference genes

Neutrophil RNA expression of NF-κB, HSP40, IL-8, P-47^{phox}, P-67^{phox} and GP-91^{phox} was quantified by real time PCR following SCN- treatment (1%, 5% or 10%). Data are expressed as a ratio of the reference genes, GADPH, HPTY1 and RPL13, and RNA expression of cells treated with PBS (negative control) were normalised to 1.

GADPH

In response to all concentrations of SCN- treatment, HSP40 expression significantly increased (2way ANOVA and Bonferroni multiple comparisons tests ****$p<0.0001$ for 50µM and 100µM, $p<0.05$ for 150µM, n=3 technical repeats). The expression of P-67^{phox} increased following 50µM SCN- treatment (2way ANOVA and Bonferroni multiple comparisons tests *$p<0.05$, n=10 biological repeats, n=3 technical repeats). SCN- treatment at all concentrations was found to have an inhibitory effect on the expression of GP-91^{phox}; however this was not statistically significant (Figure XIIa).

HPTY1

In response to all concentrations of SCN- treatment, HSP40 expression increased and this was statistically significant at concentrations of 50µM and 150µM SCN- (2way ANOVA and Bonferroni post-tests ****$p<0.0001$ for 50µM and 150µM, n=3 technical repeats). The expression of P-47^{phox} increased following treatment with 150µM SCN- (2way ANOVA and Bonferroni multiple comparisons tests ****$p<0.0001$, n=10 biological repeats, n=3 technical repeats). SCN- treatment at all concentrations was found to increase P-67^{phox} expression and was statistically significant at 100µM and 150µM SCN- (2way ANOVA and Bonferroni multiple comparisons tests **$p<0.01$, ****$p<0.0001$ for 100µM and 150µM SCN-, respectively, n=10 biological repeats, n=3 technical repeats) (Figure XIIb).

RPL13

In response to SCN- treatment, HSP40 expression significantly increased and this was statistically significant at concentrations of 50µM and 100µM SCN- (2way ANOVA and Bonferroni post-tests $^{**}p<0.01$, $^{***}p<0.001$ for 50µM and 100µM SCN-, respectively, n=10 biological repeats, n=3 technical repeats). P-67^{phox} expression increased following treatment with 100µM SCN- (2way ANOVA and Bonferroni post-tests $^{****}p<0.0001$, n=10 biological repeats, n=3 technical repeats). Decreased GP-91^{phox} expression was also observed in response to all concentrations of SCN-, however this was not statistically significant (Figure XIIc).

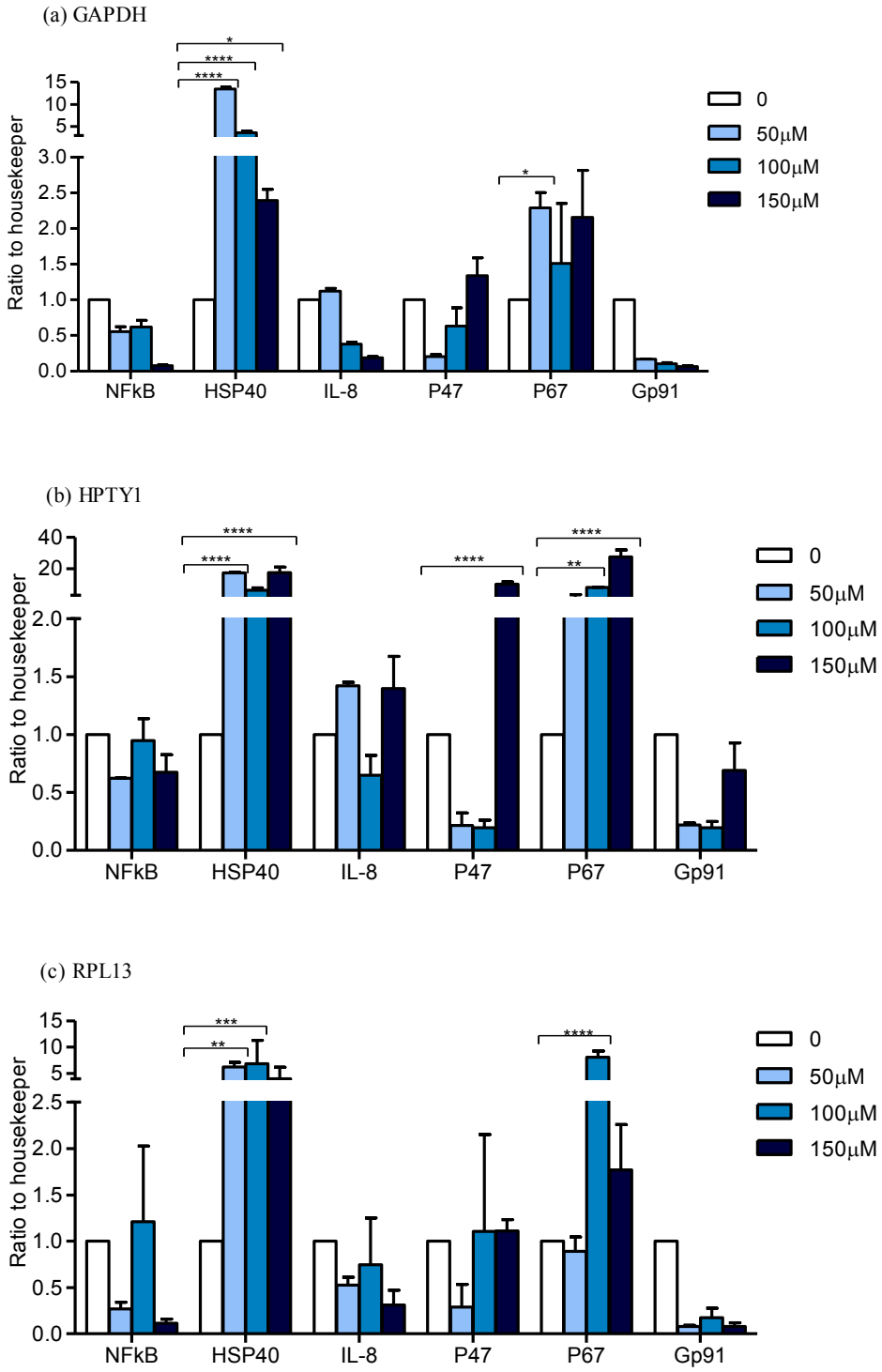

Figure XII: RNA expression of thiocyanate treated neutrophils relative to other reference genes

Data are expressed as a ratio of the reference gene and RNA expression of cells treated with PBS (negative control) was normalised to 1. RNA expression as a ratio of reference gene (a) GAPDH, (b) HPTY1, (c) RPL13. Statistical significance calculated using 2way ANOVA and Bonferroni post-tests (*$p<0.05$, **$p<0.01$, ****$p<0.0001$). Data is expressed as mean ± SEM (n=10 pooled biological repeats and n=3 technical repeats).